# N-cadherin: Regulation, Role and Therapeutic Targeting in Multiple Myeloma

**Krzysztof Marek Mrozik**

Myeloma Research Laboratory
Faculty of Health and Medical Sciences
Adelaide Medical School
The University of Adelaide
&
Cancer Theme
South Australian Health and Medical Research Institute
(SAHMRI)



A thesis submitted to the University of Adelaide
for the degree of Doctor of Philosophy
May 2018

# Table of Contents

# Abstract

Multiple myeloma (MM) is a largely incurable haematological malignancy characterised by the clonal proliferation of neoplastic immunoglobulin-producing plasma cells (PCs) within the bone marrow (BM). Previous studies from our laboratory, and those of others, have shown that gene and protein expression of the homophilic cell-cell adhesion and signalling molecule, N-cadherin, is up-regulated in PCs in approximately 50% of newly-diagnosed MM patients. Notably, increased expression of N-cadherin is associated with inferior prognosis in these patients. In this thesis, bioinformatic and *in vitro* analyses were performed to determine the mechanisms responsible for the up-regulation of N-cadherin expression in MM. The histone methyltransferase MMSET, universally dysregulated in the 10-15% of MM patients which harbour the chromosomal translocation t(4;14), was a positive regulator of *CDH2* expression in human MM cell lines, suggesting it is a key driver of in N-cadherin expression in $t(4;14)^{+}$ MM. Several additional candidate molecules and pathways (e.g. miR-190 and IL-6/JAK2/STAT3 signalling) were also identified which may represent previously unknown, MMSET-independent regulators of N-cadherin expression in $t(4;14)^{-}$ MM.

The development, progression and relapse of MM is underpinned by the trafficking, or dissemination, of MM PCs from one tumour site to distant BM sites via the circulation. Previous studies suggest that inhibition of MM PC adhesion to the endothelium may represent a potential therapeutic modality to prevent the extravasation and dissemination of MM PCs. In this thesis, pre-treatment of C57Bl/KaLwRij mice with the cyclic pentapeptide N-cadherin antagonist ADH-1 inhibited tumour development following intravenous injection of 5TGM1 MM PCs. This effect was not seen in mice treated with ADH-1 after tumour establishment, suggesting that N-cadherin plays a role in the extravasation and BM homing of MM PCs. In support of this, N-cadherin was found to mediate the adhesion of MM PCs to endothelial cells (ECs), which represents a key step in the extravasation of circulating MM PCs. These studies suggest that ADH-1 may be clinically useful in the prevention of MM PC dissemination, thereby delaying disease progression and relapse.

In addition to its role in MM pathogenesis, N-cadherin is critical in the regulation of vascular integrity and permeability. Recently, studies have shown that

perturbation of N-cadherin function disrupts established EC-EC and EC-mural cell junctions resulting in increased permeability of the EC barrier to macromolecules *in vitro* and *in vivo*. This thesis describes the identification of a small molecule peptidomimetic of ADH-1, LCRF-0006, as a novel vascular disrupting agent which enhances vascular permeability *in vitro* and *in vivo*, and synergistically increases the efficacy of the anti-MM agent bortezomib in C57Bl/KaLwRij mice with established MM disease. To this end, LCRF-0006 may be clinically useful in increasing the depth of MM tumour response to bortezomib, which is currently used in MM patients as induction therapy, maintenance therapy, and in the relapse setting. In addition, we speculate that the potential ability of LCRF-0006 to augment the enhanced permeability and retention (EPR) effect could be utilised to increase the delivery, and therefore anti-cancer efficacy, of various therapeutic agents in MM and other cancers in the clinical setting.

# Declaration

I certify that this work contains no material which has been accepted for the award of any other degree or diploma in my name in any university or other tertiary institution and, to the best of my knowledge and belief, contains no material previously published or written by another person, except where due reference has been made in the text. In addition, I certify that no part of this work will, in the future, be used in a submission in my name for any other degree or diploma in any university or other tertiary institution without the prior approval of the University of Adelaide and where applicable, any partner institution responsible for the joint award of this degree.

I acknowledge that copyright of published works contained within this thesis resides with the copyright holder(s) of those works.

I also give permission for the digital version of my thesis to be made available on the web, via the University's digital research repository, the Library Search and also through web search engines, unless permission has been granted by the University to restrict access for a period of time.

I acknowledge the support I have received for my research through the provision of an Australian Government Research Training Program Scholarship.

Signed

29/5/18

Krzysztof Marek Mrozik

# Acknowledgements

To say I felt like the day I completed my PhD would never arrive is an understatement. Yet, here I am looking back over the past 5 years with a sense of achievement, happiness and relief knowing that I've finally made it. The completion of this thesis would not have been possible without the support of many truly wonderful colleagues, friends and family which I'm so fortunate to have.

Firstly, I'd like to thank my incredible supervisors Prof. Andrew Zannettino and Dr Kate Vandyke. Thanks to Prof. Andrew Zannettino for giving me the opportunity to undertake my PhD studies in the Myeloma Research Laboratory, and for his wonderful mentorship and unwavering support and encouragement over the course of my PhD studies. Thank you for always making yourself available to discuss my work and for your unbridled enthusiasm and optimism. Thank you so much to Dr Kate Vandyke for her constant guidance and support, and having a knowledgeable answer to everything I asked her. Thank you especially for your tremendously insightful and hard work in reviewing my thesis. You have both been wonderful during this stressful time and I am very grateful.

I also thank A/Prof. Orest Blaschuk for sharing his invaluable expertise in the field of cadherin biology and critically reviewing this thesis. Visiting A/Prof. Orest Blaschuk at McGill University and his visits to Adelaide are highlights of my PhD experience. Thank you very much to A/Prof. Orest Blaschuk and Dr Arkadii Vaisburg for providing critical reagents for the project and assistance with drug formulation.

A big thank you to the PhD Eagles; Dr Chee Man Cheong, Jia Ng and Ankit Dutta for their friendship, support, coffee runs, lunch-time chats, outings and generally sharing in the PhD experience and making it an enjoyable one. A special thank you to Dr Chee Man Cheong for her assistance throughout my candidature, especially in helping me on my big mouse experiment days even when she was busy with her own experiments and thesis writing.

I'd also like to thank Dr Duncan Hewett and Dr Jacqueline Noll for their friendship, encouragement and assistance during my candidature. The chats about weekend sports, kids and generally having a laugh have been very enjoyable.

Thank you to all other past and present members of the Myeloma Research Laboratory (Dr Stephen Fitter, Dr Sally Martin, Dr Peter Diamond, Dr Melissa Cantley, Dr Bill Panagopoulos, Mary Matthews, Anna Melville, Sharon Paton, Vicki Wilczek, Rosa Harmer, Natasha Friend (Strong), Kimberley Clark, Mara Zeissig, Pawanrat (Queenie) Tangseefa, Khatora Opperman and Alanah Bradey) and the Mesenchymal Stem Cell Laboratory (Prof. Stan Gronthos, Dr Dimitrios Cakouros (a.k.a. The Stud), Dr Esther Camp-Dotlic, Dr Agnes Arthur, Dr Danijela Menicanin, Dr Sarah Hemming, Dr Thao Nguyen, Dr Kim Hynes, Sandra Isenmann, Chee Ho H'ng and Clara Pribadi) for their support and assistance throughout my candidature and for being a fantastic group of people to work with. This experience would not have been the same without you all.

I would also like to acknowledge the assistance of animal facility and flow cytometry staff at both SAHMRI and SA Pathology and thank Jim Manavis and Sophie Kogoj for assistance with histological processing of tissues.

Thank you to all of my friends, especially Mark, Andrew, Aaron, Daniel, Daniel, John and Anthony for their support, encouragement and understanding during this time. The catch-ups, chats, outings and banter throughout the course of my PhD have certainly helped me smile and have some fun during this time.

A big thank you to my parents for all the love and support they have provided thoughout the past 5 years. Thank you for all the times you have looked after Alina and Lukas, cooked and done the gardening just to let me concentrate on my studies. Thank you for always being there and for being fantastic parents. This would not have been possible without you both. Thank you also to my sister Alinka, brother-in-law Darek and nephews Sebastian and Aleksander for your love and support during this time. I also thank Ciocia Andziu for her love and encouragement and for her understanding in why I haven't visited her as often as I would have liked to.

I’d also like to thank Lauren's parents who travelled from Melbourne countless times over the course of my PhD to look after Alina and Lukas, and generally helping us manage the craziness that our household has been over the past 5 years. This would have been impossible without you both. Thank you to Sarah, Andrea, Brendan, Dan and Raphaela for your love and support and my apologies for my infrequent trips to visit you in Melbourne. I also thank all of you for providing Lauren with the love and support she has needed while I've devoted my mental and physical capacity to finishing this PhD.

Finally, the biggest thank you goes to my wife Lauren and my beautiful children, Alina and Lukas. Your love, support, encourgement, patience and understanding has been incredible and is something for which I will forever be grateful. The past 5 years have been quite difficult and crazy at times, and I know that you have all had to sacrifice so much along the way. Thank you for riding all the bumps along the journey with me, especially when the light at the end of the tunnel probably still seemed so far away. I don't think I can ever truly make it up to you all but I know that we have so many wonderful things to look forward in the future as a family. I can't wait to be the Tata and husband that I wish I could have been for so long now. I love you all so much.

Thank you.

# Abbreviations

| | |
|---|---|
| aa | amino acid |
| ALL | acute lymphoblastic leukaemia |
| α-MEM | α-modified Eagle's medium |
| AML | acute myeloid leukaemia |
| ANOVA | analysis of variance |
| AP | alkaline phosphatase |
| ASCT | autologous stem cell transplant |
| Bad | Bcl2-associated agonist of cell death |
| Bcl-2 | B-cell lymphoma 2 |
| BCR-ABL | breakpoint cluster region-Abelson kinase |
| BLI | bioluminescence imaging |
| BM | bone marrow |
| BMEC | bone marrow endothelial cell |
| BMSC | bone marrow stromal cell |
| B-Myb | myb-related protein B |
| BTBD3 | Broad-complex, Tramtrak, Bric-a-brac (Pox virus and zinc finger) (BTB [POZ]) domain-containing 3 |
| BTF3 | basic transcription factor 3 |
| CB | compact bone |
| CCL | chemokine (C-C motif) ligand |
| Cdc42 | cell division cycle 42 |
| CD | cluster of designation |
| CDI | coefficient of drug interaction |
| CLL | chronic lymphocytic leukaemia |
| CML | chronic myeloid leukaemia |
| CTC | circulating tumour cell |
| CXCL | chemokine (C-X-C motif) ligand |
| DMEM | Dulbecco's modified Eagle's medium |
| DMSO | dimethyl sulphoxide |
| E-box | enhancer box |
| EC | endothelial cell |
| EC1 | extracellular domain 1 |

| | |
|---|---|
| EC2 | extracellular domain 2 |
| EC4 | extracellular domain 4 |
| ECL | enhanced chemiluminescence |
| ECM | extracellular matrix |
| EDTA | ethylenediaminetetraacetic acid |
| EGF | epidermal growth factor |
| EMT | epithelial-to-mesenchymal transition |
| EPR | enhanced permeability and retention |
| ERK | extracellular signal-related kinase |
| EV | empty vector |
| FAK | focal adhesion kinase |
| FCS | foetal calf serum |
| FDR | false discovery rate |
| Fer | tyrosine-protein kinase Fer |
| FGF | fibroblast growth factor |
| FGFR | fibroblast growth factor receptor |
| FISH | fluorescent in situ hybridization |
| FITC | fluorescein isothiocyanate |
| FOXP3 | forkhead box protein P3 |
| GEO | Gene Expression Omnibus |
| GFP | green fluorescent protein |
| GIST | gastrointestinal stromal tumours |
| GSEA | gene set enrichment analysis |
| Gy | gray |
| HEPES | 4-(2-hydroxyethyl)-1-piperazineethanesulfonic acid |
| His-Ala-Val (HAV) | histidine-alanine-valine |
| HGF | hepatocyte growth factor |
| HMCL | human MM cell line |
| HR | hazard ratio |
| HSC | haematopoietic stem cell |
| HUVEC | human umbilical vein endothelial cells |
| ICAM-1 | intercellular adhesion molecule 1 |
| $IC_{50}$ | inhibitory concentration, 50% |
| IGF-1 | insulin-like growth factor 1 |

| | |
|---|---|
| IL-6 | interleukin-6 |
| IL6ST | interleukin-6 signal transducer |
| i.p. | intraperitoneal |
| i.v. | intravenous |
| IMDM | Iscove's Modified Dulbecco's Medium |
| ISS | multiple myeloma International Staging System |
| kDa | kilodalton |
| JAK2 | Janus kinase 2 |
| JNK | Jun N-terminal kinase |
| Lef | lymphoid enhancer-binding factor |
| LFA-1 | lymphocyte function-associated antigen 1 (integrin alpha-L) |
| LIMMA | Linear Models for Microarray Data |
| Lin | lineage |
| LSC | leukaemic stem cell |
| luc | luciferase |
| MAPK | mitogen-activated protein kinase |
| Mcl-1 | induced myeloid leukemia cell differentiation protein Mcl-1 |
| MGUS | monoclonal gammopathy of undetermined significance |
| MDCK | Madin-Darby canine kidney |
| miRNA (miR) | microRNA |
| MM | multiple myeloma |
| MMP9 | matrix metalloproteinase-9 |
| MMSET | multiple myeloma SET domain |
| mRNA | messenger ribonucleic acid |
| MSC | mesenchymal stromal cell |
| MUC-4 | mucin-4 |
| NF-κB | nuclear factor of k light polypeptide gene enhancer in B-cells |
| NOD/SCID | nonobese diabetic/severe combined immunodeficiency |
| OB | osteoblast |
| OP | osteoprogenitor |
| OS | overall survival |

| | |
|---|---|
| Pak1 | p21-activated kinase-1 |
| PBS | phosphate-buffered saline |
| PC | plasma cell |
| PE | phycoerythrin |
| PFA | paraformaldehyde |
| PFS | progression-free survival |
| PI3K | phosphoinositide 3-kinase |
| photons/s (p/s) | photons per second |
| PSGL-1 | P-selectin glycoprotein ligand 1 |
| PTEN | phosphatase and tensin homologue |
| PTP1B | tyrosine-protein phosphatase non-receptor type 1 |
| PVDF | polyvinylidene fluoride |
| PyVmT | polyoma virus middle T antigen |
| qPCR | quantitative polymerase chain reaction |
| Rac | Ras-related C3 botulinum toxin substrate 1 |
| RANKL | receptor activator of nuclear factor-kB |
| RhoA | Ras homolog gene family, member A |
| RMA | Robust Multi-array Average |
| RPMI-1640 | Roswell Park Memorial Institute 1640 |
| SATB2 | special AT-rich sequence-binding protein 2 |
| SD | standard deviation |
| SET | Su(var)3-9, Enhancer-of-zeste and Trithorax domain |
| 7-AAD | 7-aminoactinomycin D |
| SEM | standard error of the mean |
| shRNA | short hairpin RNA |
| siRNA | small interfering RNA |
| Smad | small mothers against decapentaplegic homologues |
| S1PL | sphingosine-1-phosphate lyase 1 |
| sr | steradian |
| Src | proto-oncogene tyrosine-protein kinase Src |
| STAT3 | signal transducer and activator of transcription 3 |
| TCF | T-cell-specific transcription factor |
| TGF-β1 | transforming growth factor-β1 |
| TKO | targeted knock-out |

| | |
|---|---|
| TNF-α | tumour necrosis factor-α |
| Trp | tryptophan |
| 2-HP-b-CD | 2-hydroxypropyl-β-cyclodextrin |
| UTR | untranslated region |
| var.1 | variant 1 |
| var.6 | variant 6 |
| VCAM-1 | vascular cell adhesion protein 1 |
| VLA-4 | very late antigen-4 (α4β1 integrin) |
| v/v | volume per volume |
| Wnt | wingless-type mouse mammary tumour virus integration type family member |
| WST-1 | 4-[3-(4-iodophenyl)-2-(4-nitophenyl)-2H-5-tetrazolio]-1,3-benzene disulphonate |
| ZNF622 | zinc finger protein 622 |

# Publications

***Scientific Manuscripts***

1. **Mrozik K.M.**, Blaschuk O.W., Cheong C.M., Zannettino A.C.W., Vandyke K. (2018). N-cadherin in cancer metastasis, its emerging role in haematological malignancies and potential as a therapeutic target in cancer. *Manuscript submitted to BMC Cancer*.

2. **Mrozik K.M.**, Blaschuk O.W., Cheong C.M., Hewett. D.R., Noll J.E., Opperman K.S., Zannettino A.C.W., Vandyke K. (2018). LCRF-0006 is a novel vascular disrupting agent which synergistically enhances tumour response to bortezomib in a pre-clinical mouse model of established multiple myeloma. *Manuscript in preparation*.

3. **Mrozik K.M.**, Cheong C.M., Hewett. D.R., Zannettino A.C.W., Vandyke K. (2018). The identification of novel mechanisms of N-cadherin regulation in $t(4;14)^{+}$ and $t(4;14)^{-}$ multiple myeloma. *Manuscript in preparation*.

4. Cheong C.M., **Mrozik K.M.**, Kok C.H., Hewett D.R., Panagopoulos V., Noll J.E., Lee O.L., Gronthos S., Zannettino A.C.W, Vandyke K. (2018). TWIST1 promotes tumour migration and dissemination in multiple myeloma. *Manuscript in preparation*.

5. Vandyke K., Zeissig M.N., Hewett D.R., Martin S.K., **Mrozik K.M.**, Cheong C.M., Diamond P., To L.B., Gronthos S., Peet D.J., Croucher P.I., Zannettino A.C.W. (2017). HIF-2α promotes dissemination of plasma cells in multiple myeloma by regulating CXCL12/CXCR4 and CCR1. *Cancer Research*, 77(20):5452-5463.

6. **Mrozik K.M.**, Cheong C.M., Hewett D.R, Chow A.W., Blaschuk O.W., Zannettino A.C.W, Vandyke K. (2015). Therapeutic targeting of N-cadherin is an effective treatment for multiple myeloma. *British Journal of Haematology*, 171(3):387-99.

7. Noll J.E., Vandyke K., Hewett D.R., **Mrozik K.M.**, Bala R.J., Williams S.A., Kok C.H., Zannettino A.C.W. (2015). PTTG1 expression is associated with hyperproliferative disease and poor prognosis in multiple myeloma. *Journal of Hematology & Oncology*, 6;8:106.

***Conference Proceedings***

1. **Mrozik K.M.**, Blaschuk O.W., Cheong C.M., Hewett D.R., Noll J.E., Opperman K.S., Vandyke K., Zannettino A.C.W. (2018). The novel vascular disruption agent LCRF-0006 synergistically enhances response to bortezomib to inhibit the progression of multiple myeloma. *ASMR SA Scientific Meeting 2018*. Adelaide, Australia, June 2018. Oral presentation.

2. **Mrozik K.M.**, Cheong C.M., Hewett D.R., Chow A.W.S, Blaschuk O.W., Vandyke K., Zannettino A.C.W. (2016). N-cadherin is a therapeutic target in multiple myeloma. *Inaugural National Myeloma Workshop 2016*. Yarra Valley, Australia, September 2016. Oral presentation.

3. **Mrozik K.M.**, Cheong C.M., Hewett D.R., Chow A.W., Blaschuk O.W., Vandyke K., Zannettino A.C.W. (2016). N-cadherin is a therapeutic target in multiple myeloma. *ASMR SA Scientific Meeting 2016*. Adelaide, Australia, June 2016. Oral presentation.

4. **Mrozik K.M.**, Cheong C.M., Hewett D.R., Kok C.H., Chow A.W.S., Blaschuk O.W., Licht J.D., Zannettino A.C.W., Vandyke K. (2015). N-cadherin is a therapeutic target in t(4;14)-positive multiple myeloma. *15$^{th}$ International Myeloma Workshop*, Rome, Italy, September 2015. Poster presentation.

5. **Mrozik K.M.**, Cheong C.M., Hewett D.R., Kok C.H., Heatley S., Chow A.W.S., Blaschuk O.W., Zannettino A.C.W., Vandyke K. (2015). Therapeutic targeting of N-cadherin is an effective treatment for multiple myeloma. *ASMR SA Scientific Meeting 2015*. Adelaide, Australia, June 2015. Oral presentation.

6. Vandyke K., **Mrozik K.M.**, Cheong C.M., Chow A.W.S, Kok C.H., Blaschuk O.W., Licht J.D., Zannettino A.C.W. (2014) Identification of an epithelial-to-mesenchymal transition (EMT)-like programme in t(4;14)-positive multiple myeloma reveals novel targets for therapeutic intervention. *American Society for Hematology 56th Annual Meeting*. San Francisco, USA, December 2014. Oral presentation.

7. **Mrozik K.M.**, Vandyke K., Cheong C.M., Chow A.S., To L.B., Zannettino A.C.W. (2014). Targeted inhibition of N-cadherin as a therapeutic modality for multiple myeloma. *HAA Annual Scientific Meeting 2014*. Perth, Australia, October 2014. Poster presentation.

8. Cheong C.M., **Mrozik K.M.**, Kok C.H., Licht J.D., Zannettino A.C.W., Vandyke K. (2014). Epithelial-to-mesenchymal transition (EMT) is a key feature of t(4;14)-positive multiple myeloma. *HAA Annual Scientific Meeting 2014*. Perth, Australia, October 2014. Poster presentation.

9. **Mrozik K.M.**, Vandyke K., Chow A.W.S., To L.B., Zannettino A.C.W. Targeted inhibition of N-cadherin as a therapeutic modality for multiple myeloma. *ASMR SA Scientific Meeting 2014*. Adelaide, Australia, June 2014. Oral presentation.

10. **Mrozik K.M.**, Vandyke K., Chow A.W.S., To L.B., Zannettino A.C.W. (2013). The Role of N-Cadherin in Multiple Myeloma. *Frontiers in Skeletal Biology Symposium*. Sydney, Australia, November 2013. Oral presentation.

"Chance favors the prepared mind"

*- Louis Pasteur, 1854*

This thesis is dedicated to my family;
for their love, support and patience.

Chapter 1

# Introduction

# Statement of Authorship

| | |
|---|---|
| Title of Paper | N-cadherin in cancer metastasis, its emerging role in haematological malignancies and potential as a therapeutic target in cancer |
| Publication Status | ☐ Published ☐ Accepted for Publication<br>☐ Submitted for Publication ☑ Unpublished and Unsubmitted work written in manuscript style |
| Publication Details | **Mrozik K.M.**, Blaschuk O.W., Cheong, C.M., Zannettino A.C.W., Vandyke K. Manuscript in preparation. |

## Principal Author

| | | | |
|---|---|---|---|
| Name of Principal Author (Candidate) | Krzysztof Marek Mrozik | | |
| Contribution to the Paper | Primary reviewer of literature and author of manuscript<br>Conceptualisation of manuscript | | |
| Overall percentage (%) | 80% | | |
| Certification: | This paper reports on original research I conducted during the period of my Higher Degree by Research candidature and is not subject to any obligations or contractual agreements with a third party that would constrain its inclusion in this thesis. I am the primary author of this paper. | | |
| Signature | | Date | 15/02/18 |

## Co-Author Contributions

By signing the Statement of Authorship, each author certifies that:
the candidate's stated contribution to the publication is accurate (as detailed above);
permission is granted for the candidate in include the publication in the thesis; and
the sum of all co-author contributions is equal to 100% less the candidate's stated contribution.

| | | | |
|---|---|---|---|
| Name of Co-Author | Orest W. Blaschuk | | |
| Contribution to the Paper | Critical review of manuscript | | |
| Signature | | Date | 12/02/18 |

| | | | |
|---|---|---|---|
| Name of Co-Author | Chee M. Cheong | | |
| Contribution to the Paper | Critical review of manuscript | | |
| Signature | | Date | 14/02/18 |

| | | | |
|---|---|---|---|
| Name of Co-Author | Andrew C.W. Zannettino | | |
| Contribution to the Paper | Conceptualisation and critical review of manuscript | | |
| Signature | | Date | 14/02/18 |

| | | | |
|---|---|---|---|
| Name of Co-Author | Kate Vandyke | | |
| Contribution to the Paper | Conceptualisation and critical review of manuscript | | |
| Signature | | Date | 15/02/18 |

**N-cadherin in cancer metastasis, its emerging role in haematological malignancies and potential as a therapeutic target in cancer.**

Krzysztof M. Mrozik[1,2], Orest W. Blaschuk[3], Chee M. Cheong[1,2], Andrew C.W. Zannettino[1,2,4*], Kate Vandyke[1,2*]

Author Affiliations:

1. Myeloma Research Laboratory, Adelaide Medical School, Faculty of Health and Medical Sciences, The University of Adelaide, Adelaide, Australia
2. Cancer Theme, South Australian Health and Medical Research Institute, Adelaide, Australia
3. Division of Urology, Department of Surgery, McGill University, Montreal, Canada
4. Centre for Cancer Biology, University of South Australia, Adelaide, Australia

* co-senior authors

Keywords:

N-cadherin, cancer, metastasis, haematological malignancies, regulation, therapeutic target

## 1.1 Abstract

In many types of solid tumours, the aberrant expression of the cell adhesion molecule N-cadherin is a hallmark of epithelial-to-mesenchymal transition, resulting in the acquisition of an aggressive tumour phenotype. This transition endows tumour cells with the capacity to escape from the confines of the primary tumour and metastasise to secondary sites. In this review, we will discuss how N-cadherin actively promotes the metastatic behaviour of tumour cells, including its involvement in critical signalling pathways which mediate these events. In addition, we will explore the emerging role of N-cadherin in haematological malignancies, including bone marrow homing and microenvironmental protection to chemotherapeutic agents. Finally, we will discuss the evidence that N-cadherin may be a viable therapeutic target to inhibit cancer metastasis and increase tumour cell sensitivity to existing anti-cancer therapies.

## 1.2 Introduction

Cancer metastasis is a leading cause of cancer-related mortality. The metastasis of cancer cells within primary tumours is characterised by localised invasion into the surrounding microenvironment, entry into the vasculature and subsequent spread to permissive distant organs (reviewed in Valastyan & Weinberg, 2011 and Friedl & Alexander, 2011).[1,2] In many epithelial cancers, metastasis is facilitated by the genetic reprogramming and transitioning of cancer cells from a non-motile, epithelial phenotype into a migratory, mesenchymal-like phenotype, a process known as epithelial-to-mesenchymal transition (EMT) (reviewed in Thiery *et al*., 2009 and De Craene & Berx, 2013).[3,4] A common feature of EMT is the loss of epithelial cadherin (E-cadherin) expression and the concomitant up-regulation or *de novo* expression of neural cadherin (N-cadherin). This so-called "cadherin switch" is associated with increased migratory and invasive behaviour (reviewed in Wheelock *et al*., 2008 and Gheldof & Berx, 2013)[5,6] and inferior patient prognosis.[7-10] A major consequence of E-cadherin down-regulation is the loss of stable epithelial cell-cell adhesive junctions, apico-basal cell polarity and epithelial tissue structure, thereby facilitating the release of cancer cells from the primary tumour site (reviewed in Kourtidis *et al*., 2017 and Perl *et al*., 1998)[11,12]. In contrast to the migration-suppressive role of E-cadherin, N-cadherin endows tumour cells with enhanced migratory and invasive capacity, irrespective of E-cadherin expression (reviewed in Hazan *et al*., 2004).[13] Thus, the acquisition of N-cadherin appears to be a critical step in epithelial cancer metastasis and disease progression.

In this review, we will discuss how N-cadherin promotes the metastatic behaviour of tumour cells by directly mediating cell-cell adhesion, and by its involvement in modulating critical signalling pathways implicated in metastatic events. In addition, we will discuss the emerging relevance of N-cadherin in haematological malignancies, namely leukaemias and multiple myeloma. Finally, we will review the emerging evidence that N-cadherin may be a viable therapeutic target to inhibit cancer metastasis and overcome chemotherapeutic resistance.

## 1.3 Structure and formation of the N-cadherin adhesive complex

N-cadherin is a calcium-dependent adhesion molecule which directly mediates homotypic and heterotypic cellular interactions, thereby facilitating cell-cell recognition

and sorting. N-cadherin is a classical type I cadherin consisting of 5 extracellular domains linked to a functional intracellular domain. The engagement between N-cadherin monomers on opposing cells occurs by reciprocal insertion of a Trp residue side-chain on its first extracellular domain (EC1) into the hydrophobic pocket of the partner N-cadherin EC1 (*trans* adhesion). In addition, the stabilization of N-cadherin-mediated adhesion requires the interaction, or clustering, of adjacent monomers on the surface of the same cell, involving the His-Ala-Val (HAV) sequence on EC1 and a recognition sequence on the second extracellular domain (EC2) of the lateral N-cadherin monomer (*cis* adhesion).[14-16] The membrane expression and lateral clustering of N-cadherin is dependent upon p120 catenin, which localizes N-cadherin at cholesterol-rich microdomains.[17,18] The initial ligation of N-cadherin extracellular domains triggers the activation of the Rho GTPase family member Rac, which stimulates localized actin filament assembly and the formation of membrane protrusions at points of cell-cell contact (reviewed in Yap & Kovacs, 2003 and Ratheesh *et al*., 2013).[19,20] The subsequent activation of the Rho GTPase family member RhoA, at the expense of Rac function, facilitates the maturation of N-cadherin-based cell-cell junctions by triggering the sequestration of β-catenin to the cadherin intracellular domain.[21,22] β-catenin serves as a critical link to α-catenin which accumulates at nascent cell-cell junctions and suppresses actin branching. In addition, α-catenin facilitates the anchorage of the N-cadherin-catenin complex to the actin cytoskeleton via actin-binding proteins such as cortactin and α-actinin, thereby promoting the maturation of cell-cell contacts (reviewed in Niessen *et al*., 2011 and Pokutta & Weis, 2007)[23,24] (Figure 1.1). The stability of the N-cadherin-catenin complex is highly dependent on the phosphorylation status of N-cadherin and the associated catenins, which is regulated by tyrosine kinases, such as Fer and Src, and the tyrosine phosphatase PTP1B (reviewed by McLachlan & Yap, 2007 and Lilien & Balsamo, 2005).[25,26]

## 1.4 The functional role of N-cadherin in solid tumour metastasis

In the normal physiological setting, N-cadherin plays a functional role in a variety of cell types including neuronal cells, myocytes, endothelial cells, stromal cells and osteoblasts.[21,27-31] While N-cadherin is typically absent, or expressed at low levels, in normal epithelial cells, the aberrant expression of N-cadherin in cancer cells is a well-documented feature of disease progression in many epithelial malignancies.[32-35] In a

**Figure 1.1. Schematic representation of the N-cadherin-catenin adhesive complex.** The extracellular domains of N-cadherin monomers engage in *trans* and *cis* interactions with partner monomers, facilitated by p120-catenin (p120), resulting in a lattice-like arrangement. Interactions occur via a reciprocal insertion of tryptophan side-chains (in *trans*) and the HAV adhesion motif (in *cis*) (inset). Activation of RhoA sequesters β-catenin (β-cat) and results in accumulation of α-catenin (α-cat) to the N-cadherin intracellular domain. This promotes anchorage of the N-cadherin-catenin complex to the actin cytoskeleton via actin-binding proteins, thereby stabilizing cell-cell contacts. Initial ligation of N-cadherin extracellular domains also triggers PI3K/Akt signalling which inactivates the pro-apoptotic protein Bad, resulting in activation of the anti-apoptotic protein Bcl-2.

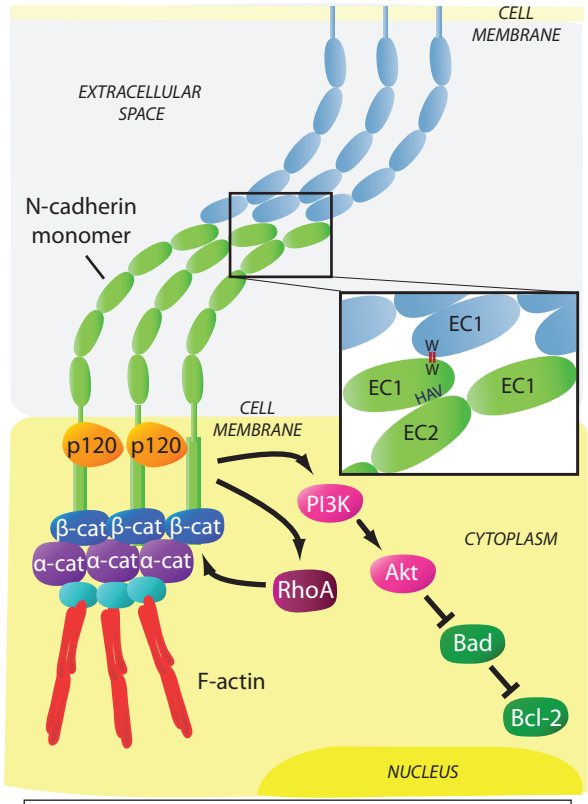


W = tryptophan; ▬ = tryptophan side-chain; HAV = histidine-alanine-valine; ⬬ = actin-binding proteins

similar manner, studies have shown that the up-regulation of N-cadherin is also a feature of melanoma progression.[36-38] Whilst the aberrant expression of N-cadherin in epithelial tissues is not considered to be oncogenic, or a promoter of solid tumour growth[39-41], the up-regulated expression of N-cadherin expression in cancer is widely associated with cancer aggressiveness. Indeed, many studies have demonstrated a significant correlation between elevated N-cadherin levels in epithelial, and some non-epithelial solid tumours, and clinicopathologic features such as increased localised tumour invasion and distant metastasis, and inferior patient prognosis. Multivariate analyses have also identified that elevated N-cadherin expression is independently associated with inferior patient prognosis in several epithelial malignancies including prostate, lung and bladder cancer[7,8,42-76] (Table 1.1). The aggressive phenotype and inferior prognosis associated with up-regulated N-cadherin expression in solid tumours is also supported by a recent meta-analysis incorporating patients with various epithelial malignancies.[77]

Beyond the prognostic implications of aberrant N-cadherin expression, the relationship between N-cadherin and metastasis is not merely associative. Indeed, there is a wealth of evidence that increased N-cadherin expression endows tumour cells with a greater capacity to migrate. In addition to directly mediating cancer cell adhesion to a variety of cell types within tumour host microenvironments, including stromal cells, endothelial cells and osteoblasts[29,78-81], early studies identified that increased N-cadherin expression enhances the migratory and invasive capacity of multiple tumour cell types *in vitro*.[80,82-84] N-cadherin has also been shown to promote the capacity of melanoma cells to undergo *in vitro* trans-endothelial migration.[85,86] The ability of N-cadherin to promote epithelial tumour metastasis *in vivo* was initially demonstrated using the MCF-7 breast cancer cell line, following injection into the mammary fat pad of nude mice. In contrast to wild-type cells, MCF-7 cells ectopically expressing N-cadherin formed tumour metastases in several organs including the liver, pancreas and lymph nodes.[78] Similarly, N-cadherin expression in the mammary epithelium in the transgenic PyVmT murine breast cancer model resulted in a three-fold increase in the number of pulmonary metastatic foci without affecting the onset or growth of the primary tumour.[40] Using an orthotopic mouse model of pancreatic cancer, the over-expression of N-cadherin in BxPC-3 cells increased the formation of disseminated tumour nodules throughout the abdominal cavity and induced the formation of N-cadherin-expressing lung micro-metastases.[84] Consistent with these findings, enforced expression of N-cadherin in

## Table 1.1. Association of increased N-cadherin expression in cancer with clinicopathologic features and survival

| Cancer type | Cohort information & treatment details | No. of patients | N-cadherin detection method | Association with clinico-pathologic features | Association with survival | Reference |
|---|---|---|---|---|---|---|
| **Epithelial cancers** | | | | | | |
| **Breast cancer** | Pre-metastatic; resected | 574 | IHC | High grade & LN metastasis | Shorter PFS (U) | [42] |
| | Early-stage invasive | 1902 | IHC | Earlier development of distant metastasis | n/a | [43] |
| | Primary inoperable and LN negative | 275 | IHC | n.s. | Shorter OS (U) | [44] |
| | Invasive; no prior therapy | 94 | IHC | High grade, late stage & LN metastasis | n/a | [45] |
| **Prostate cancer** | Clinically localized; radical prostatectomy | 104 | IHC | Poor differentiation, seminal vesicle invasion & pelvic LN metastasis | Shorter time to biochemical failure (U), clinical recurrence (M) & skeletal metastasis (U) | [8] |
| | Castration-resistant; transurethral resection | 26 | IHC | Higher Gleason score & metastasis | n/a | [46] |
| | Localized; no therapy prior to radical prostatectomy | 157 | IHC | Later stage, higher PSA & Gleason score, seminal vesicle invasion and LN metastasis | n/a | [47] |
| | Blood from cancer follow-up patients | 179 | Serum ELISA (sN-cad) | Higher PSA | n/a | [48] |
| | Radical prostatectomy, metformin-treated | 49 | IHC | n/a | Increased recurrence | [49] |
| **Lung cancer** | No therapy prior to surgery (adenocarcinoma & squamous cell carcinoma) | 68 | IHC | Higher TNM stage & poor differentiation | Shorter OS (M) | [50] |
| | Primary adenocarcinoma; no therapy prior to surgery | 147 | IHC | n/a | Shorter OS (M) | [51] |
| | Surgical resection of adenocarcinoma; no prior therapy | 57 | qPCR | LN metastasis | n/a | [52] |
| | No post-operative surgery | 186 | IHC | Higher TNM stage & metastasis | n/a | [53] |
| | Blood collected prior to or up to 3 weeks after platinum-based therapy (adenocarcinoma & squamous cell carcinoma) | 43 | IF (on CTCs) | n/a | Shorter PFS | [54] |
| **Urothelial cancers** | Radical cystecomy with pelvic LN dissection, clinically non-metastatic bladder cancer | 433 | IHC | Higher clinical & pathologic tumour stage, LN metastasis & LN stage, lymphovascular invasion | Shorter RFS (M), OS (U) & cancer-specific survival (U) | [55] |
| | Invasive bladder cancer undergoing radical cystectomy; no prior treatment | 30 | qPCR | n/a | Shorter OS | [56] |
| | Transurethral resection of non-muscle-invasive bladder cancer | 115 | IHC | Higher incidence of intravesical recurrence | Shorter intravesical RFS (M) | [57] |
| | Clinically-localized upper urinary tract carcinoma undergoing nephroureterectomy; cisplatin-based therapy in late-stage patients | 59 | IHC | n/a | Intravesical and extravesical RFS (M) | [58] |
| **Liver cancer** | Resection of hepatocellular carcinoma | 100 | IHC | Higher histologic grade, multifocal tuimours & vascular invasion | Shorter disease-free and OS | [59] |
| | Surgical resection of hepatocellular carcinoma | 57 | IHC | n.s. | Increased recurrence-rate within 2 years of resection | [60] |
| | Surgical resection of intrahepatic cholangiocarcinoma (no prior therapy); adjuvant therapy in patients with recurrence | 96 | IHC | Higher recurrence of vascular invasion | Shorter OS | [61] |
| **Head & neck cancer** | Surgical specimen of HNSCC, patients are +/- LN metastasis | 119 | IHC | Greater tumour size, higher clinical stage & LN metastasis | Shorter OS (M) | [62] |

**Table 1.1. Association of increased N-cadherin expression in cancer with clinicopathologic features and survival (continued)**

| Cancer type | Cohort information & treatment details | No. of patients | N-cadherin detection method | Association with clinico-pathologic features | Association with survival | Reference |
|---|---|---|---|---|---|---|
| **Epithelial cancers** | | | | | | |
| **Head & neck cancer (continued)** | Blood collected following HNSCC resection (laryngeal, oropharyngeal & oral cancer) | 10 | IF (on CTCs) | n/a | Shorter OS | [63] |
| | Radical surgery for laryngeal cancer; adjuvant therapy in 60% of cases | 50 | IHC | Higher grade | Increased relapse | [64] |
| | Nasopharyngeal cancer | 122 | IHC | LN involvement, distant metastasis & later clinical stage | Shorter OS (nuclear N-cadherin) | [65] |
| **Gastrointestinal tract cancer** | Colorectal cancer; no therapy prior to surgery | 37 | qPCR | Local invasion, Dukes staging & vascular invasion | n/a | [66] |
| | Colorectal cancer; no therapy prior to surgery | 102 | IHC | Larger tumour size, poor differentiation, tumour invasion, LN metastasis & distant metastasis | Shorter OS (M) & shorter disease-free survival | [67] |
| | Colon carcinoma; no therapy prior to surgery | 90 | IHC | Greater depth of tumour invasion & higher TNM stage | n/a | [68] |
| | Gastric cancer surgery with LN metastasis; no prior therapy | 89 | IHC (on LN) | LN involvement, higher pathological stage, lymphatic invasion & venous invasion | Shorter OS | [69] |
| | Curative surgery for gastric adenocarcinoma; no prior therapy, stage II patients received adjuvant therapy | 146 | IHC | Hematogenous recurrence | Shorter survival | [70] |
| **Renal cancer** | Blood collected from metastatic renal cell carcinoma patients with prior nephrectomy and therapy | 14 | IF (on CTCs; also CK-) | n/a | Shorter PFS | [71] |
| **Ovarian cancer** | Surgical specimens of high-grade serous carcinoma | 167 | IHC | n/a | Shorter PFS and OS (U) | [72] |
| **Gallbladder cancer** | Adenocarcinoma (+/- surgery) | 80 | IHC | Poor differentiation, larger tumour size, TNM stage, invasion & LN metastasis | Shorter OS (M) | [73] |
| | Squamous cell/adenosquamous carcinoma (+/- surgery) | 46 | IHC | Larger tumour size, invasion and LN metastasis | Shorter OS (M) | [73] |
| **Non-epithelial solid cancers** | | | | | | |
| **Melanoma** | Removal of primary melanoma, various stages of disease | 394 | IHC | Increased Breslow thickness | Distant metastasis-free survival (M; p = 0.13) | [7] |
| **Sarcoma** | Surgical resection of osteosarcoma | 107 | qPCR | Later stage and distant metastasis | Shorter survival | [74] |
| | Blood collected from a variety of bone & soft tissue sarcoma patients | 73 | Serum ELISA (sN-cad) | Larger tumour size & higher grade | Shorter disease-free survival (M) & OS (U) | [75] |
| **Haematological malignancies** | | | | | | |
| **Multiple myeloma** | Blood collected from newly-diagnosed patients; no prior therapy | 84 | Serum ELISA (sN-cad) | n/a | Shorter PFS and OS | [76] |
| | Bone marrow aspirate from newly-diagnosed patients; no prior therapy | 14 | qPCR (on $CD38^+/CD138^+$ tumour cells) | n/a | Shorter PFS | [76] |

All clinicopathologic and survival data shown is positively associated with increased N-cadherin expression. All data is statistically significant ($P < 0.05$), unless otherwise indicated. Abbreviations: PFS (progression-free survival), RFS (recurrence-free survival), OS (overall survival), U (univariate analysis), M (multivariate analysis), IHC (immunohistochemistry), qPCR (quantitative PCR), IF (immunofluorescence), ELISA (enzyme-linked immunosorbent assay), sN-cad (soluble N-cadherin), PSA (prostate specific antigen), LN (lymph node), TNM (tumour, node and metastases), CTCs (circulating tumour cells), CK (cytokeratin), n/a (not applicable), n.s. (not significant).

androgen-responsive prostate cancer cells promoted invasion of underlying muscle and lymph node metastasis following subcutaneous injection in castrated mice.[87] Moreover, the ability of melanoma cells to extravasate (a key step in the metastatic cascade) and form lung metastases following intravenous injection in NOD/SCID mice was attenuated following N-cadherin knock-down in tumour cells.[88]

To appreciate how N-cadherin, a *bona fide* cell adhesion molecule, may actively promote cancer cell migration, it is important to consider that the N-cadherin-catenin complex is situated at the cross-roads of cell adhesion and activation of pro-metastatic signalling cascades, in both a physical and functional context. Notably, the adhesive function and migration-related signalling capacity of N-cadherin can occur simultaneously, or as antagonistic events, adding further complexity to its role in cancer metastasis. In the following section, we describe three key mechanisms by which N-cadherin has been shown to actively promote the migratory capacity of tumour cells: facilitation of collective cell migration, augmentation of fibroblast growth factor-receptor (FGFR) signalling and modulation of canonical Wnt signalling.

### 1.4.1 N-cadherin promotes collective cell migration

While the mesenchymal phenotype of carcinoma cells, that have undergone EMT, promotes the migration of individual cancer cells, the localised invasion and metastasis of epithelial tumour cells is also facilitated by their ability to migrate as sheets, clusters or strands, a process known as collective cell migration (reviewed in Clark & Vignjevic, 2015 and Friedl & Alexander, 2011).[2,89] Collectively migrating groups of cells maintain adhesive interconnectivity, collective cell polarity and co-ordinated cytoskeletal activity, resulting in a 'leader-follower'-type cell arrangement which promotes more directional and efficient migration than that of an individual migrating cell (reviewed in Mayor & Etienne-Manneville, 2016 and Etienne-Manneville, 2014).[90,91] Several studies have demonstrated the importance of N-cadherin in collective cell migration in cancer. For instance, N-cadherin has been shown to promote the ability of lung or ovarian cancer cells to form aggregates and collectively invade three-dimensional (3D) collagen matrices or penetrate peritoneal mesothelium-like cell layers *in vitro*.[92,93] Similarly, studies in transformed canine kidney epithelial cells (MDCK cells) have shown that N-cadherin promotes aggregate formation which allows directional collective cell migration in a 3D collagen matrix. In these cells, deletion of the entire N-cadherin intracellular domain, or the β-catenin binding domain alone, resulted in greater

individual cell detachment and migration from cell clusters, highlighting the importance of the N-cadherin-actin cytoskeleton interaction in collective cell migration. Moreover, over-expression of an N-cadherin mutant in which the extracellular domain was fused to the anti-binding domain of α-catenin hindered the movement of follower cells, demonstrating that dynamic N-cadherin-actin linkage is required for efficient collective cell migration.[94]

In addition to maintaining multi-cellular aggregates of tumour cells, studies in N-cadherin-expressing non-tumour cells demonstrate that N-cadherin also promotes collective cell migration by polarizing Rho-family GTPase signalling (e.g. Rac1 and cdc42), known to play an important role in the co-ordination of cytoskeletal remodelling in collectively migrating cells (reviewed in Ridley, 2015 and Combedazou *et al*., 2017).[95,96] For example, models of arterial smooth muscle wound-healing and neural crest migration have shown that the asymmetric distribution of N-cadherin-mediated cell-cell adhesion at the lateral and posterior aspects of leader cells promotes directional cell alignment and increased cdc42 and Rac1 activity and protrusion formation at the free leading cell edge, resulting in enhanced migration.[97,98] Mechanistically, studies in mouse embryonic fibroblasts have demonstrated that N-cadherin-adhesive complexes at the rear of cells suppress localized integrin-α5 activity, thereby polarizing integrin and Rac activity towards the free leading edge of the cell.[99] Indeed, functional inhibition of N-cadherin in transformed mammary cells has been shown to reduce integrin-α5-dependent cell migration on fibronectin *in vitro*.[100] In a similar manner, silencing of N-cadherin expression in melanoma cells perturbs α2β1-integrin-dependent collagen matrix invasion *in vitro*.[101] Reciprocally, integrin signalling at focal adhesions has been shown to regulate the ability of HeLa cells to engage in N-cadherin-based connections and to promote collective cell migration.[102] Given that integrins play an important role in the activation of Rho signalling (reviewed in Moreno-Layseca & Streuli, 2014 and Grande-Garcia *et al*., 2005)[103,104], it is plausible that N-cadherin may polarize Rho-family GTPase signalling *via* intercommunication with integrins, thereby promoting the collective migration of cancer cells (Figure 1.2A).

### 1.4.2 N-cadherin augments fibroblast growth factor receptor signalling

Functional interaction between the extracellular domains of N-cadherin and receptor-tyrosine kinase FGFRs was first recognised as a mechanism by which N-cadherin promoted axonal outgrowth of rat cerebellar neuronal cells. These studies identified that

**Figure 1.2. Schematic representation of cell signalling events modulated by increased N-cadherin expression in the context of cell migration.** In addition to mediating cellular aggregation, N-cadherin may facilitate the collective migration of tumour cells by excluding focal adhesions and Rac1 activity, and promoting RhoA activity, at sites of N-cadherin-mediated cell-cell contact. The asymmetric distribution of N-cadherin adhesive complexes polarizes integrin function and Rac1 activity towards the free edges of cells, thereby directing focal adhesion and lamellipodia formation away from the cell cluster and promoting cell migration. Similar to Rac1, N-cadherin-mediated cell-cell adhesion promotes cdc42 activity at the free edges of cells, resulting in filipodia formation (**A**). Functional interaction between the extracellular domains of N-cadherin and FGFR-1 potentiates FGF-2-activated FGFR-1 signalling by attenuating ligand-induced receptor internalisation. The resulting augmentation of down-stream MAPK-ERK and PI3K-Akt signalling pathways promotes the metastatic behaviour of cancer cells by increasing the production of invasion-facilitating molecules such as MMPs (**B**). N-cadherin-mediated adhesive complexes and Wnt/β-catenin signalling are thought to compete for the same cellular pool of β-catenin. While N-cadherin sequesters β-catenin from the nucleus, the N-cadherin adhesive complex provides a reservoir of β-catenin which, upon Wnt activation, becomes available for nuclear translocation and TCF/LEF-mediated gene transcription (eg. *CD44* and MMP genes), resulting in the loss of N-cadherin-mediated cellular adhesion in cancer cells (**C**).

A Polarization of Rho family GTPase signalling

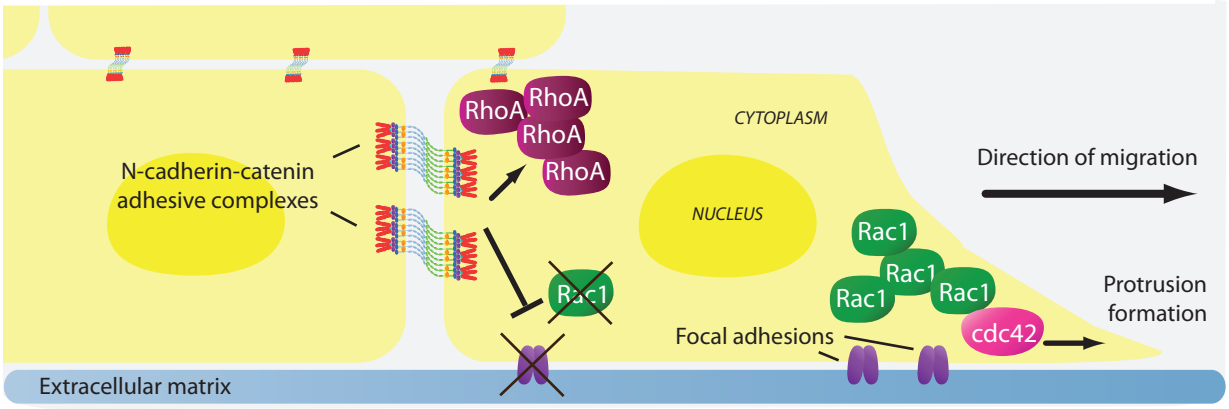


B Augmentation of FGFR signalling

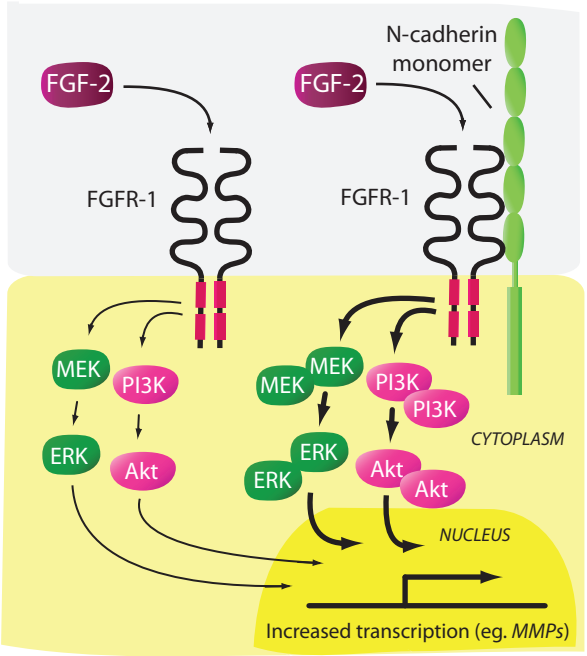


C Modulation of canonical Wnt signalling

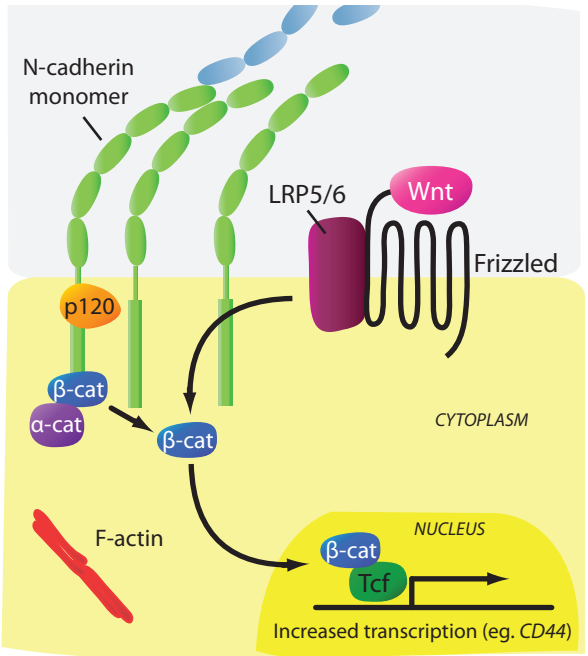

the fourth extracellular domain of N-cadherin (EC4) trans-activated FGFRs to promote neurite outgrowth independent of FGF ligands, suggesting that N-cadherin can act as a surrogate ligand of FGFRs.[28,105] Notably, the physical interaction of N-cadherin and FGFRs has also been shown in breast and pancreatic cancer cells.[106-109] Evidence that FGFR played a functional role in N-cadherin-mediated cancer metastasis was initially demonstrated in breast cancer cells, whereby FGFR inhibition reduced the migratory capacity of N-cadherin-expressing human breast cancer cells, but not N-cadherin-negative cells.[83] In addition, FGF-2 increased the invasiveness of N-cadherin-expressing MCF-7 human breast cancer cells, but not control MCF-7 cells.[78] To this end, it has been shown that N-cadherin potentiates FGF-2-activated FGFR-1 signalling by attenuating ligand-induced FGFR-1 internalisation, thereby stabilising FGFR-1 expression.[106,108] In turn, the sustained activation of the down-stream MAPK-ERK signalling pathway results in increased production of the extracellular matrix (ECM)-degrading enzyme matrix metalloproteinase-9 (MMP-9) and enhanced breast cancer cell invasiveness.[78,106] In line with these findings, the over-expression of N-cadherin in mammary epithelium in transgenic mouse models of breast cancer resulted in an increased propensity for lung metastasis, compared with control mice.[40,110] Examination of tumour cell isolates from these mice showed that N-cadherin potentiates breast cancer cell migration and invasion in an FGFR-dependent manner.[40] These studies suggested that the ability of N-cadherin-FGFR interactions to promote breast cancer metastasis may also involve activation of phosphatidylinositide-3 kinase (PI3K)/Akt signalling via Akt2[110] (Figure 1.2B).

Two lines of evidence suggest that N-cadherin-FGFR-1 interactions promote the invasive behaviour in both collectively migrating and individual cancer cells. Firstly, N-cadherin-FGFR-1 interactions have been shown to occur over most of the cell membrane, but are excluded from sites of cell-cell adhesion, suggesting that the interaction is independent of N-cadherin-mediated cellular adhesion.[107] Secondly, blocking antibodies directed at the FGFR-1-interacting domain of N-cadherin (EC4) have been shown to inhibit N-cadherin-mediated migration, but not N-cadherin-mediated aggregation, of human breast cancer cells.[111] Thus, it would appear that N-cadherin-mediated cell-cell adhesion and N-cadherin-mediated cell migration *via* FGFR-1 are independent and mutually exclusive events. Further studies are warranted to identify whether N-cadherin potentiates FGFR-1 signalling in cancers other than breast and pancreatic cancer.

### 1.4.3 N-cadherin modulates canonical Wnt signalling

In addition to stabilising cadherin-mediated cell-cell adhesion, β-catenin plays a central role in the canonical Wnt signalling pathway. Canonical Wnt signalling promotes the cytoplasmic accumulation and nuclear translocation of β-catenin which activates T cell factor/lymphoid enhancer factor (TCF/LEF)-mediated transcription of gene targets (reviewed in Murillo-Garzón & Kypta, 2017, Valenta *et al.*, 2012 and Klaus & Birchmeier, 2008)[112-114] including genes which promote tumour cell invasion and metastasis (e.g. MMPs and CD44).[115-121] It has been proposed that cadherins and the canonical Wnt signalling pathway may compete for the same cellular pool of β-catenin, with cadherins sequestering β-catenin from the nucleus, thereby attenuating Wnt signalling.[122,123] Indeed, enforced expression of N-cadherin in colon carcinoma cells resulted in the relocation of nuclear β-catenin to the plasma membrane and attenuated LEF-responsive trans-activation.[124] Alternatively, studies suggest that the N-cadherin-β-catenin complex may provide a stable pool of β-catenin which is available for TCF/LEF-mediated gene transcription in cancer cells.[86,125] To this end, disruption of N-cadherin-mediated adhesion in leukaemic cells was found to increase TCF/LEF reporter activity.[126] Thus, given β-catenin is essential in the stabilization of N-cadherin-mediated cellular adhesion (discussed earlier), it is feasible that the ability of N-cadherin to modulate TCF/LEF-mediated gene transcription may play an important role in individual cell migration, at the expense of collective cell migration (Figure 1.2C).

The ability of N-cadherin to modulate canonical Wnt signalling has been shown to play a role in the trans-endothelial migration of cancer cells, a key process in the metastatic cascade (reviewed in van Zijl *et al.*, 2011).[127] Studies in melanoma cells have shown that while β-catenin co-localizes with N-cadherin during the initial stages of endothelial cell adhesion, the activation of the tyrosine kinase Src phosphorylates the N-cadherin cytoplasmic domain, leading to the dissociation of the N-cadherin-β-catenin complex.[128] β-catenin is then translocated to the nucleus during trans-endothelial migration and activates TCF/LEF-mediated gene transcription, resulting in up-regulation of the diapedesis-promoting adhesion molecule CD44.[86,129-131] In line with these *in vitro* findings, N-cadherin knock-down in human melanoma cells has been shown to reduce lung nodule formation following intravenous injection in immuno-compromised mice.[88] While N-cadherin-expressing tumour cells have been detected in the circulation of patients with various epithelial cancers[54,63,71], a role for N-cadherin in the trans-endothelial migration of epithelial cancer cells has not yet been demonstrated.

## 1.5 The emerging role of N-cadherin in haematological malignancies

We have thus far summarised the functional role and clinical implications of aberrant N-cadherin expression in the context of solid tumour metastasis. There is now emerging evidence suggesting that N-cadherin plays a role in haematological malignancies, including leukaemia and multiple myeloma (MM). These cancers account for approximately 10% of all cancer cases and are typically characterized by the abnormal proliferation of malignant white blood cells within the bone marrow (BM) and the presence of tumour cells within the circulation. Specialised compartments, or 'niches', within the BM microenvironment play critical roles in housing and maintaining pools of quiescent haematopoietic stem cells (HSCs), and in regulating HSC self-renewal and differentiation.[132,133] Notably, N-cadherin is expressed by various cell types associated with the HSC niche, including osteoblasts and stromal cells in the endosteal niche, and endothelial cells and pericytes in the perivascular niche.[30,134-136] In the following section, we discuss the potential implications of aberrant N-cadherin expression in haematological cancer cells; namely, BM homing and the BM microenvironmental protection to chemotherapeutic agents.

### 1.5.1 Leukaemia

Leukaemias are thought to arise by the malignant transformation of HSCs into leukaemic stem cells (LSCs) which occupy and modify BM HSC niches.[137-140] Adhesive interactions between LSCs and the BM microenvironment activate signalling cascades which contribute to LSC self-renewal and survival, and the capacity to evade the cytotoxic effects of chemotherapeutic agents.[141, 142] Indeed, therapeutic targeting of adhesion molecules to disrupt interactions with the niche represents a potential strategy to eliminate LSCs.[143]

Studies have demonstrated that N-cadherin is expressed in a subpopulation of primitive HSCs[30], although its precise role within the HSC niche in normal haematopoiesis is controversial. To this end, the over-expression of N-cadherin in HSCs has been shown to increase HSC lodgement to BM endosteal surfaces in irradiated mice, enhance HSC self-renewal following serial BM transplantation and promote HSC quiescence *in vitro*.[144] However, other studies have reported that deletion of N-cadherin in HSCs or osteoblastic cells has no effect on haematopoiesis or HSC quiescence, self-renewal or long-term repopulating activity.[31,134, 145]

While these studies suggest that N-cadherin is not essential for the maintenance of the HSC niche, emerging evidence implicates N-cadherin in the function of the LSC niche. Studies have reported that N-cadherin is expressed on primitive sub-populations of leukaemic cells including patient-derived $CD34^+$ $CD38^-$ chronic myeloid leukaemia (CML) cells and $CD34^+$ $CD38^-$ $CD123^+$ acute myeloid leukaemia (AML) cells, suggesting that N-cadherin is a marker of LSCs.[125,146,147] Similar to solid tumours, N-cadherin is thought to facilitate engagement of leukaemic cancer cells with cells of the surrounding microenvironment. For example, treatment of primary human $CD34^+$ CML cells with the N-cadherin blocking antibody GC-4 significantly reduced their adhesion to human BM stromal cells.[125] Similarly, GC-4 treatment of a BCR-ABL-positive mouse acute lymphoblastic leukaemia (ALL) cell line was found to inhibit their ability to adhere to mouse fibroblasts.[148] Pre-clinical mouse models also suggest that N-cadherin may promote BM homing, engraftment and self-renewal of AML cells *in vivo*.[149,150] Thus, N-cadherin represents a potential target to inhibit LSC interactions with the BM microenvironment.

#### 1.5.1.1 *N-cadherin-mediated cell adhesive interactions promote microenvironmental protection of leukaemic cells to chemotherapeutic agents*

Adhesive interactions between leukaemic cells and cells of the BM microenvironment confers sub-populations of leukaemic cells with resistance to chemotherapy, leading to disease relapse.[151,152] As such, there is growing interest in targeting molecules involved in leukaemic cell-BMSC interactions to enhance leukaemic sensitivity to chemotherapy.[125,153] The role of N-cadherin in the microenvironmental protection of leukaemic cells to chemotherapeutic agents was first demonstrated in studies showing that N-cadherin expression was associated with resistance to treatment with a farnesyltransferase inhibitor in the murine lymphoblastic leukaemia cell line, B-1, when grown in co-culture with fibroblasts. Enforced N-cadherin expression in B-1 cells also conferred farnesyltransferase inhibitor-resistance when grown in the presence of fibroblasts.[148] Notably, these findings are in line with reports showing that N-cadherin is up-regulated in solid tumour cancer cells resistant to chemotherapeutic agents[154-157] and androgen deprivation therapy.[46,158] Direct demonstration that N-cadherin-mediated cell-cell adhesion facilitated microenvironmental protection of leukaemic cells to chemotherapy was provided in co-culture experiments with primary human $CD34^+$ CML cells and BMSCs. Disruption of CML cell-BMSC adhesion, using an N-cadherin

antagonist peptide (containing the HAV sequence) or the N-cadherin function-blocking antibody GC-4 increased CML cell sensitivity to the tyrosine kinase inhibitor imatinib.[125,126] An association between response to chemotherapy and LSC expression of N-cadherin has also been reported in AML patients. To this end, patients exhibiting a higher proportion of N-cadherin-expressing BM-derived $CD34^+$ $CD38^-$ $CD123^+$ LSCs at diagnosis were less responsive to induction chemotherapy.[146] While the precise mechanism by which N-cadherin-mediated adhesion confers drug-resistance in leukaemic cells is unclear, studies in solid tumour cells suggest that N-cadherin-mediated adhesion increases activity of the anti-apoptotic protein Bcl-2, by PI3K-Akt-mediated inactivation of the pro-apoptotic protein Bad.[80,155,159]

### 1.5.2 Multiple myeloma

Multiple myeloma (MM), preceded by a benign precursor condition called monoclonal gammopathy of undetermined significance (MGUS), is a haematological malignancy characterised by the uncontrolled proliferation of transformed immunoglobulin-producing plasma cells (PCs) within the BM. Clinical manifestations of MM include osteolytic bone lesions, hypercalcaemia, renal insufficiency and anaemia. While the introduction of so-called 'novel' anti-MM agents (e.g. the immunomodulatory drugs thalidomide and lenalidomide, and the proteasome inhibitor bortezomib) have significantly improved the overall survival prospects of MM patients over the past 10-15 years, the long-term management of MM patients following disease relapse and progression remains a major challenge.[160-164] Nevertheless, the identification of MM patients who are likely to experience rapid disease relapse is paramount to the success of therapeutically managing these patients in order to maximise their survival prospects.[162] Notably, studies in our laboratory have demonstrated that stratification of newly-diagnosed MM patients based on plasma N-cadherin levels identifies a subset of individuals (> 6ng/ml plasma N-cadherin) with increased risk of earlier death, irrespective of disease stage, tumour burden or poor cytogenetic features.[76] Moreover, data from our group, and others, suggest that N-cadherin gene and protein expression is elevated in $CD138^+$ BM-derived PCs in approximately 50% of newly-diagnosed MM patients compared with BM PCs from healthy individuals, and is associated with poor prognosis[76,81] (Table 1.1). Notably, the expression of the N-cadherin gene, *CDH2*, is up-regulated in MM patients harbouring the high-risk t(4;14)(p16;q32) translocation. This translocation encompasses 15-20% of all MM patients and is characterised by the

dysregulated expression of the histone methyltransferase MMSET.[81,165-167] Through yet to be defined mechanisms, *CDH2* expression is also up-regulated in more than 50% of MM patients in the hyperdiploidy-related sub-group.[81]

#### 1.5.2.1 *N-cadherin mediates cell-cell adhesion between MM PCs and the BM microenvironment*

Adhesive interactions between MM PCs and the BM microenvironment are critical in the permissiveness of the BM to the development of MM disease. These include cell-cell interactions which support MM PC growth and resistance to chemotherapeutic agents, and promote the inhibition of osteoblast differentiation, thereby contributing to MM PC-mediated bone loss (reviewed in Noll *et al.*, 2012 and Katz, 2010).[168,169] In addition to endothelial cell adhesion, *in vitro* studies have demonstrated that N-cadherin mediates the adhesion of human MM PCs to osteoblasts and stromal cells, which constitute the endosteal MM niche.[81,170] In a functional context, N-cadherin-mediated adhesion between MM PCs and pre-osteoblastic cells has been shown to inhibit osteoblast differentiation, suggesting that N-cadherin may contribute to MM-related bone loss in the clinical setting.[81] Mechanistically, studies have demonstrated that N-cadherin inhibits osteoblast function and impedes bone formation *in vivo* by negative regulation of canonical Wnt signalling in bone cells.[171-174] Studies have also shown that treatment of human MM PC lines in co-culture with stromal cells or osteoblasts with the N-cadherin blocking antibody GC-4 induced a significant expansion of MM PCs *in vitro*.[170] Thus, it has been proposed N-cadherin may maintain the proliferative quiescence of MM PC in contact with cells of the endosteal MM niche.[170] In light of the role of N-cadherin in mediating leukaemic cell resistance to chemotherapeutic agents, these findings may provide a rationale to investigate whether N-cadherin-mediated adhesion potentiates chemotherapeutic resistance in MM.

## 1.6 The regulation of N-cadherin expression in cancer

A range of extracellular stimuli implicated in cancer pathogenesis have been shown to increase N-cadherin gene and protein expression in cancer cells including transforming growth factor β1 (TGF-β1)[175-178], ligands for receptor tyrosine kinases (epidermal growth factor [EGF][179-181], insulin-like growth factor 1 [IGF-1][182-184] and hepatocyte growth factor [HGF][185,186]), C-X-C and C-C chemokines (CXCL12[187,188], CCL21[189,190

and CCL18[191]), cytokines (receptor activator of nuclear factor κB [NF-κB] ligand [RANKL][192,193] and interleukin 6 [IL-6][88,194,195]), Wnt3a[157], ECM proteins[196,197] and hypoxia.[198-201] These stimuli up-regulate N-cadherin expression by activating a number of intracellular signalling cascades including, but not limited to, canonical and non-canonical TGF-β1[175,177,202,203], Wnt/β-catenin[157,188,201,204], PI3K/Akt[205-207], NF-κB[193,199], Janus kinase 2/signal transducer and activator of transcription 3 (JAK2/STAT3)[88,180,184,195,205] and c-Jun N-terminal kinase (JNK)[84,177,197,208,209] signalling pathways. The expression of N-cadherin has also been shown to be up-regulated by oncogenic transcription factors, histone-modifying enzymes and glycoproteins including SET (activator of JNK signalling)[209-211], BTF3 (JAK/STAT3)[212-214], SATB2 (Wnt/β-catenin)[215,216], FOXP3 (Wnt/β-catenin)[217-219] and MUC-4 (JNK signalling).[108,220] In turn, these signalling pathways orchestrate the activation of classical EMT-associated transcription factors Twist1[88,178,179,184,193,196,199] and Slug[68,176,195,208,209], which are well-established positive regulators of N-cadherin expression in cancer cells. In some cancers, the up-regulation of N-cadherin may also be potentiated by the EMT-associated transcription factor Snail, following the activation of PI3K/Akt and MAPK signalling.[37,185,221] In addition, the dysregulated expression of the histone methyltransferase MMSET appears to play a major role in the up-regulation of N-cadherin expression in prostate cancer and MM[81,166,167] (Figure 1.3). Notably, *in vitro* and *in vivo* studies have also demonstrated that N-cadherin expression is increased in prostate cancer cells following androgen deprivation, and suppressed following androgen re-introduction, suggesting N-cadherin may be negatively regulated by androgens.[46,87,158] Here, we discuss some of the key transcriptional regulators of N-cadherin gene expression, and the negative regulation of N-cadherin expression by microRNAs, in cancer cells.

### 1.6.1 Twist1

The basic helix-loop-helix transcription factor Twist1 is well-established as a central regulator of EMT and its expression is extensively associated with cancer metastasis.[222-227] In addition to Twist1 positively correlating with N-cadherin expression in clinical samples of various cancers[50,228,229], over-expression and knock-down studies have demonstrated that Twist1 positively regulates N-cadherin expression *in vitro* in melanoma cells and in a number of epithelial cancers.[37,50,196,226,230,231] Mechanistically, Twist1 has been shown to directly regulate transcription of the N-cadherin gene, *CDH2*,

**Figure 1.3. A schematic overview of N-cadherin regulatory mechanisms in cancer.** A multitude of extracellular stimuli implicated in cancer pathogenesis (shown in purple) activate numerous intracellular signalling pathways (green). In turn, these pathways converge to up-regulate classical EMT-related transcription factors (orange) which increase N-cadherin expression. Whether transcription factors intrinsically associated with these signalling pathways (eg. c-Jun, TCF/LEF, p50/p65 and STAT3) up-regulate N-cadherin independent of Twist1, Slug and Snail, is not known. It is also unknown whether Slug- and Snail-induced N-cadherin expression is independent of Twist1. Several microRNAs (maroon) also directly regulate N-cadherin expression in cancer. For simplicity, not all extracellular stimuli, transcription regulators, microRNAs (e.g. targeting Twist1, Slug or Smads), intracellular signalling pathways (including the involvement of the PI3K/Akt module in mediating these pathways) and cross-regulation of these signalling cascades, are shown.

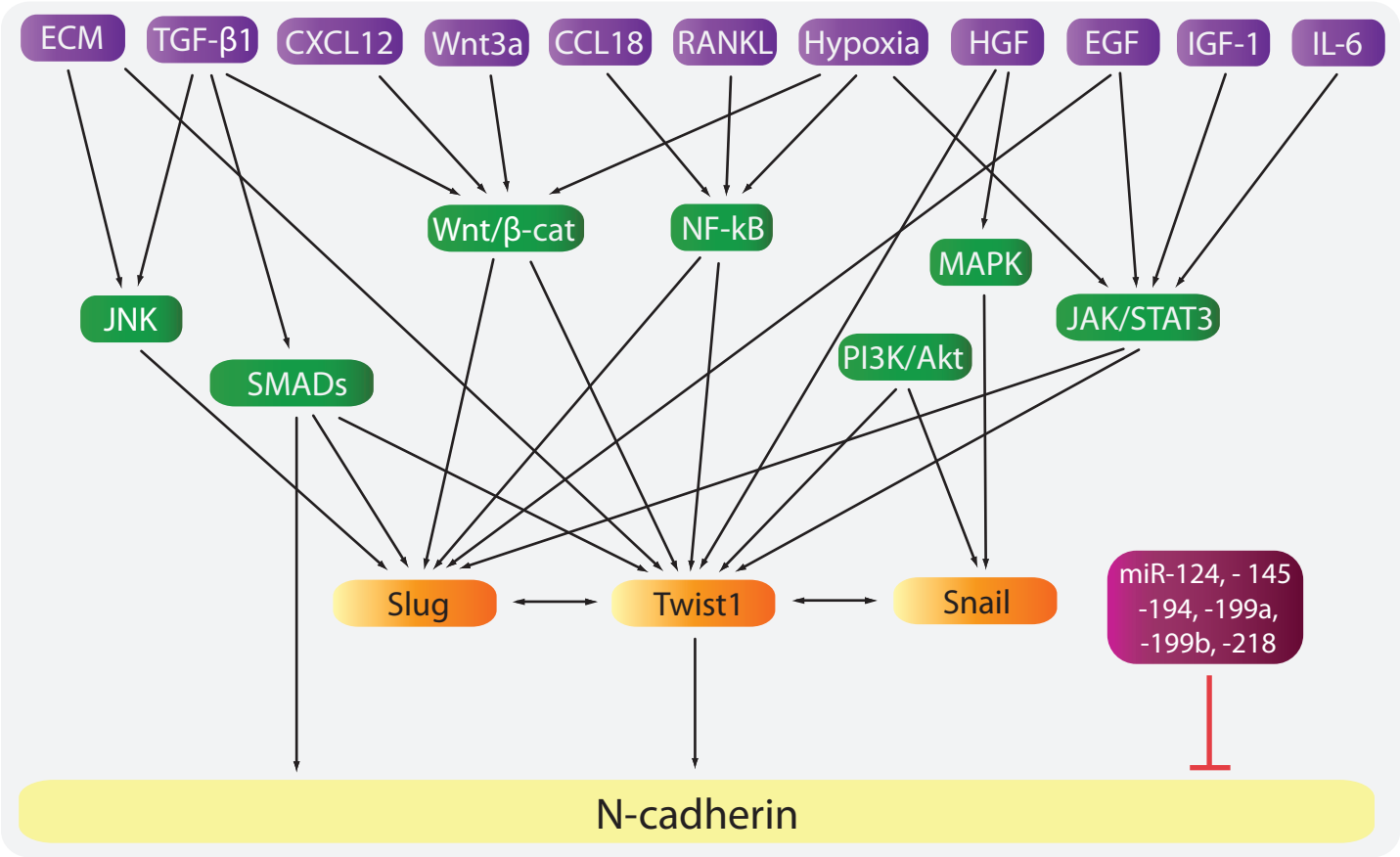
ECM
TGF-β1
CXCL12
Wnt3a
CCL18
RANKL
Hypoxia
HGF
EGF
IGF-1
IL-6
Wnt/β-cat
NF-kB
MAPK
JNK
JAK/STAT3
PI3K/Akt
SMADs
Slug
Twist1
Snail
miR-124, - 145
-194, -199a,
-199b, -218
N-cadherin

through binding to an E-box within the first intron of *CDH2*. Twist1-mediated regulation of N-cadherin expression may be dependent on adhesion to ECM proteins, as both the nuclear accumulation of Twist1 and subsequent expression of N-cadherin was strongly up-regulated in PC-3 prostate cancer cells following adhesion to fibronectin.[196] Thus, tumour cell attachment to ECM proteins may play an important role in Twist1-driven induction of N-cadherin in cancer cells. In prostate cancer cells, Twist1 also indirectly potentiates TGF-β1-mediated N-cadherin up-regulation by activation of the metastasis-associated protein clusterin.[178,232]

### 1.6.2 Slug

Slug is a member of the Snail family of transcription factors and putatively behaves as a transcriptional repressor.[233] However, while it is well established that Slug induces EMT by directly repressing E-cadherin gene transcription[234,235], over-expression and knock-down studies in a variety of epithelial and non-epithelial cancer cells have demonstrated that Slug positively regulates N-cadherin expression *in vitro*.[62,236-239] Up-regulation of Slug is also associated with increased N-cadherin expression in clinical samples of bladder and head and neck cancer.[62,237] While it is unknown whether Slug directly activates *CDH2* gene transcription, Slug has been shown to positively regulate Twist1 expression[236], suggesting that Twist1 may mediate Slug-induced up-regulation of N-cadherin expression. Moreover, Twist1 positively regulates Slug expression[240], implying a Twist1-Slug positive feedback loop may further potentiate the up-regulation of N-cadherin in cancer cells.

### 1.6.3 Smads

Smads, the intracellular effecter proteins of canonical TGF-β signalling which control gene transcription[241], are important mediators of TGF-β-driven up-regulation of N-cadherin expression in cancer. Notably, Smad complexes have been shown to bind to the *CDH2* promoter and activate *CDH2* transcription in lung cancer and immortalised pancreatic epithelial cells *in vitro*.[175,242] Knock-down of Smad3 or Smad4, or inhibition of Smad2 and Smad3 phosphorylation, has also been shown to prevent the induction of *CDH2* transcription in response to TGF-β in lung, ovarian and prostate cancer cell lines.[175,243] Studies suggest that Smads may also indirectly promote N-cadherin expression in cancer cells by up-regulating the expression of Twist1, Slug or Snail.[242-244]

### 1.6.4 MicroRNAs

MicroRNAs (miRs) are small (~22 nucleotide long) single-stranded non-coding RNAs which mediate post-transcriptional gene silencing and are widely implicated in cancer-associated EMT (reviewed in Fabbri *et al*., 2007 and Ceppi & Peter, 2014).[245,246] To date, studies have identified several miRs that are down-regulated in epithelial cancer tissues, when compared with corresponding normal epithelium, and which suppress N-cadherin expression and metastasis. These include miR-218, miR-194, miR-199a, miR-199b, miR-145 and miR-124 which directly target *CDH2* transcripts and down-regulate N-cadherin expression in various solid tumours.[52,59,74,247-254] The expression of a number of these miRs is also inversely associated with N-cadherin levels in human cancer tissue samples[52,74,247,253,254] (Figure 1.3).

Studies in cancer cell lines have also identified a number of miRs which indirectly down-regulate N-cadherin expression by targeting Twist1 (miR-106b, miR-720)[230,255], Slug (miR-140)[256] and Smad gene transcripts (miR-125b, miR-34a and miR-136).[257-259] These miRs are down-regulated in cancer tissues, compared with normal tissues, and suppress cancer cell invasiveness.[230,255-261] Additionally, studies using clinical colorectal cancer specimens identified two miRs, miR-135b and miR-210, which indirectly up-regulate N-cadherin expression by targeting the FOXN3 gene, a transcriptional repressor of *CDH2*. Expression of these miRs, in conjunction with down-regulation of miR-218, was associated with elevated N-cadherin levels and metastasis in colorectal cancer.[247] Recent studies have also shown that miR-181a positively regulates N-cadherin in prostate cancer cells, potentially by targeting PTEN, a PI3K/Akt pathway inhibitor and tumour suppressor.[262,263]

## 1.7 N-cadherin as a therapeutic target in cancer

As N-cadherin is widely implicated in cancer metastasis, the utility of N-cadherin antagonists as therapeutic drugs is being investigated in the oncology setting. Notably, N-cadherin-targeting agents have been shown to inhibit cell adhesion and to modulate cell signalling. Interestingly, studies have also shown that N-cadherin-targeting agents affect both tumour cells and tumour-associated vasculature. Here, we describe the current repertoire of N-cadherin antagonists that have displayed efficacy as anti-cancer agents *in vivo*.

### 1.7.1 Monoclonal antibodies

Several monoclonal antibodies directed against N-cadherin have been investigated for their ability to block N-cadherin-dependent tumour migration and invasion *in vitro* and metastasis *in vivo*. The mouse monoclonal antibody, designated GC-4, binds to the EC1 domain of N-cadherin monomers and subsequently blocks N-cadherin-mediated adhesion.[30,81,264,265] GC-4 has been shown to suppress N-cadherin-mediated Akt signalling[56,159], and inhibit the migration and invasion of melanoma, bladder, ovarian and breast cancer cells *in vitro*.[56,78,86,92] *In vivo*, pre-treatment of AML cells with GC-4 has been shown to inhibit BM homing of circulating tumour cells.[149] Thus, treatment with GC-4 may by therapeutically relevant in the context of limiting the metastatic dissemination of tumour cells in melanoma and haematological malignancies, where N-cadherin plays a role in trans-endothelial migration and BM homing of circulating tumour cells.[81,86,149] Additionally, GC-4-mediated blocking of N-cadherin engagement between human $CD34^+$ CML cells and stromal cells increased tumour cell sensitivity to imatinib, demonstrating a potential therapeutic strategy to overcome tyrosine kinase inhibitor resistance.[126] Two additional monoclonal antibodies, 1H7 (targeting N-cadherin EC1-3) and 2A9 (targeting N-cadherin EC4), have shown efficacy in a subcutaneous xenograft prostate cancer mouse model, whereby both antibodies reduced the growth of established tumours and inhibited localised muscle invasion and distant lymph node metastasis.[87]

### 1.7.2 ADH-1

The lateral clustering of N-cadherin monomers is essential in the stabilization and maturation of nascent N-cadherin-mediated adhesive junctions between neighbouring cells.[14,16] Peptides containing the classical cadherin HAV motif are likely to complete with the *cis* adhesive interface of N-cadherin on EC1, thereby inhibiting the lateral clustering of N-cadherin monomers.[266] On the basis that a HAV motif located on FGFR-1 is required for FGF-2 binding[107], it is feasible that ADH-1 may also inhibit FGFR signalling. The cyclization of first-generation linear peptides harbouring the HAV sequence led to the development of a more stable cyclic pentapetide called ADH-1 (N-Ac-CHAVC-$NH_2$) which similarly inhibited N-cadherin-dependent function.[267] *In vitro*, ADH-1 has been shown to induce apoptosis in a range of tumour cell types, and inhibits tumour cell migration at sub-cytotoxic concentrations, with cell sensitivity proportional to relative N-cadherin expression.[268-270] The efficacy of ADH-1 to inhibit

primary tumour growth has been demonstrated in a number of pre-clinical mouse models including pancreatic, breast, colon, ovarian and lung cancer.[268,271] Notably, ADH-1 has also been identified as a vascular disrupting agent, suggesting the compound may have effects on both tumour cells and tumour-associated vasculature.[271,272] In phase I clinical trials, ADH-1 was shown to have an acceptable toxicity profile with no maximum tolerated dose achieved. ADH-1 treatment was associated with disease control in approximately 25% of patients with advanced chemotherapy-refractory solid tumours, independent of tumour N-cadherin expression status.[273,274]

The therapeutic efficacy of ADH-1 as an anti-cancer agent has been most extensively evaluated in the melanoma setting. Pre-clinical studies suggest that ADH-1 synergistically enhances melanoma tumour response to melphalan.[275,276] These studies showed that ADH-1 enhances the permeability of tumour vasculature and increases melphalan delivery to the tumour microenvironment, as evidenced by increased formation of melphalan-DNA adducts in tumours. However, the combinatorial effects of ADH-1 and melphalan were not replicated in phase I/II clinical trials.[277,278] In contrast to other tumour settings, studies have also suggested that ADH-1 may stimulate tumour growth in some mouse models of melanoma.[275,276] These effects were associated with activation of pro-growth and survival intracellular signalling pathways including Akt signalling and the down-stream mTOR signalling pathway *in vitro* and *in vivo*.[276] These data suggest that ADH-1 may act as an N-cadherin agonist in certain tumour contexts. However, to date, ADH-1-mediated activation of tumour cell proliferation and signalling has not been reported in the clinical setting.

## 1.8 Concluding remarks and future perspectives

The up-regulation or '*de novo*' expression of N-cadherin has significant negative implications in metastasis-related cancer relapse and progression, as well as overall survival of cancer patients. In addition to its prognostic significance in cancer, N-cadherin actively promotes the metastatic capacity of tumour cells. Here, we have described three distinct mechanisms by which N-cadherin endows tumour cells with increased migratory capacity: facilitation of collective cell migration, augmentation of FGFR-1 signalling and modulation of canonical Wnt signalling. Unfortunately, our understanding of how N-cadherin influences cancer cell metastasis, and tumorigenesis

in general, remains incomplete. Studies in cardiomyocytes, stromal cells and epithelial cancer-like cells have ascribed focal adhesion-like properties to N-cadherin including mechano-transduction and traction-force transmission.[279-282] Indeed, whether a 'traction and propulsion'-type system, *via* homotypic N-cadherin mediated cell-cell contacts, is utilised by cancer cells to facilitate migration is intriguing and warrants further investigation. Moreover, there is an emerging body of evidence demonstrating that N-cadherin is expressed and is functionally relevant in the context of numerous haematological malignancies including lymphoblastic and myelogenous leukaemias, and MM. Notably, studies suggest that N-cadherin facilitates engagement of LSCs with the tumour microenvironment and promotes chemotherapeutic resistance of leukaemic cells. On the basis of observations in epithelial cancers, N-cadherin may mediate drug resistance in leukaemic cells, at least in part, by activation of the pro-survival protein Bcl-2[87,155,159], or modulation of Sonic Hedgehog signalling[283], widely implicated in cancer stem cell function and maintenance.[284] Interestingly, N-cadherin expression is induced in solid tumour cells resistant to standard chemotherapeutic agents including tyrosine kinase inhibitors.[154-157] However, it remains to be determined whether N-cadherin functionally contributes to microenvironmental cell adhesion mediated-drug resistance in these cancers.

Given the established role of N-cadherin in cancer, N-cadherin is continually being investigated as a therapeutic target. To date, peptides and mouse monoclonal antibodies have demonstrated some efficacy in the pre-clinical setting, by inhibiting cancer metastasis, enhancing cancer cell sensitivity to chemotherapeutic agents and delaying castration resistance in prostate cancer. However, the challenge remains to develop N-cadherin antagonists which are effective anti-cancer agents in the clinical setting. The humanization of N-cadherin blocking antibodies such as GC-4 may represent one such approach to utilize N-cadherin as a therapeutic target. Moreover, the development of next-generation N-cadherin-targeting small molecules with enhanced stability over existing peptide inhibitors show promise as potent inhibitors of N-cadherin function.[285-287] It remains to be seen whether these compounds have efficacy as anti-cancer agents in solid tumours and in haematological malignancies. Undoubtedly, further exploration of N-cadherin as a therapeutic target to inhibit metastasis and overcome chemotherapeutic resistance is warranted.

## 1.9 References

1. Valastyan S, Weinberg RA. Tumor metastasis: molecular insights and evolving paradigms. *Cell*. 2011; 147(2):275-292.

2. Friedl P, Alexander S. Cancer invasion and the microenvironment: plasticity and reciprocity. *Cell*. 2011; 147(5):992-1009.

3. Thiery JP, Acloque H, Huang RY, Nieto MA. Epithelial-mesenchymal transitions in development and disease. *Cell*. 2009; 139(5):871-890.

4. De Craene B, Berx G. Regulatory networks defining EMT during cancer initiation and progression. *Nat Rev Cancer*. 2013; 13(2):97-110.

5. Wheelock MJ, Shintani Y, Maeda M, Fukumoto Y, Johnson KR. Cadherin switching. *J Cell Sci*. 2008; 121(Pt 6):727-735.

6. Gheldof A, Berx G. Cadherins and epithelial-to-mesenchymal transition. *Prog Mol Biol Transl Sci*. 2013; 116:317-336.

7. Lade-Keller J, Riber-Hansen R, Guldberg P, Schmidt H, Hamilton-Dutoit SJ, Steiniche T. E- to N-cadherin switch in melanoma is associated with decreased expression of phosphatase and tensin homolog and cancer progression. *Br J Dermatol*. 2013; 169(3):618-628.

8. Gravdal K, Halvorsen OJ, Haukaas SA, Akslen LA. A switch from E-cadherin to N-cadherin expression indicates epithelial to mesenchymal transition and is of strong and independent importance for the progress of prostate cancer. *Clin Cancer Res*. 2007; 13(23):7003-7011.

9. Araki K, Shimura T, Suzuki H, Tsutsumi S, Wada W, Yajima T, Kobayahi T, Kubo N, Kuwano H. E/N-cadherin switch mediates cancer progression via TGF-beta-induced epithelial-to-mesenchymal transition in extrahepatic cholangiocarcinoma. *Br J Cancer*. 2011; 105(12):1885-1893.

10. Aleskandarany MA, Negm OH, Green AR, Ahmed MA, Nolan CC, Tighe PJ, Ellis IO, Rakha EA. Epithelial mesenchymal transition in early invasive breast cancer: an immunohistochemical and reverse phase protein array study. *Breast Cancer Res Treat*. 2014; 145(2):339-348.

11. Kourtidis A, Lu R, Pence LJ, Anastasiadis PZ. A central role for cadherin signaling in cancer. *Exp Cell Res*. 2017; 358(1):78-85.

12. Perl AK, Wilgenbus P, Dahl U, Semb H, Christofori G. A causal role for E-cadherin in the transition from adenoma to carcinoma. *Nature*. 1998; 392(6672):190-193.

13. Hazan RB, Qiao R, Keren R, Badano I, Suyama K. Cadherin switch in tumor progression. *Ann N Y Acad Sci*. 2004; 1014:155-163.

14. Harrison OJ, Jin X, Hong S, Bahna F, Ahlsen G, Brasch J, Wu Y, Vendome J, Felsovalyi K, Hampton CM *et al*. The extracellular architecture of adherens junctions revealed by crystal structures of type I cadherins. *Structure*. 2011; 19(2):244-256.

15. Shapiro L, Fannon AM, Kwong PD, Thompson A, Lehmann MS, Grubel G, Legrand JF, Als-Nielsen J, Colman DR, Hendrickson WA. Structural basis of cell-cell adhesion by cadherins. *Nature*. 1995; 374(6520):327-337.

16. Yap AS, Brieher WM, Pruschy M, Gumbiner BM. Lateral clustering of the adhesive ectodomain: a fundamental determinant of cadherin function. *Curr Biol*. 1997; 7(5):308-315.

17. Taulet N, Comunale F, Favard C, Charrasse S, Bodin S, Gauthier-Rouviere C. N-cadherin/p120 catenin association at cell-cell contacts occurs in cholesterol-rich membrane domains and is required for RhoA activation and myogenesis. *J Biol Chem*. 2009; 284(34):23137-23145.

18. Davis MA, Ireton RC, Reynolds AB. A core function for p120-catenin in cadherin turnover. *J Cell Biol*. 2003; 163(3):525-534.

19. Yap AS, Kovacs EM. Direct cadherin-activated cell signaling: a view from the plasma membrane. *J Cell Biol*. 2003; 160(1):11-16.

20. Ratheesh A, Priya R, Yap AS. Coordinating Rho and Rac: the regulation of Rho GTPase signaling and cadherin junctions. *Prog Mol Biol Transl Sci*. 2013; 116:49-68.

21. Charrasse S, Meriane M, Comunale F, Blangy A, Gauthier-Rouviere C. N-cadherin-dependent cell-cell contact regulates Rho GTPases and beta-catenin localization in mouse C2C12 myoblasts. *J Cell Biol*. 2002; 158(5):953-965.

22. Comunale F, Causeret M, Favard C, Cau J, Taulet N, Charrasse S, Gauthier-Rouviere C. Rac1 and RhoA GTPases have antagonistic functions during N-cadherin-dependent cell-cell contact formation in C2C12 myoblasts. *Biol Cell*. 2007; 99(9):503-517.

23. Niessen CM, Leckband D, Yap AS. Tissue organization by cadherin adhesion molecules: dynamic molecular and cellular mechanisms of morphogenetic regulation. *Physiol Rev*. 2011; 91(2):691-731.

24. Pokutta S, Weis WI. Structure and mechanism of cadherins and catenins in cell-cell contacts. *Annu Rev Cell Dev Biol*. 2007; 23:237-261.

25. McLachlan RW, Yap AS. Not so simple: the complexity of phosphotyrosine signaling at cadherin adhesive contacts. *J Mol Med (Berl)*. 2007; 85(6):545-554.

26. Lilien J, Balsamo J. The regulation of cadherin-mediated adhesion by tyrosine phosphorylation/dephosphorylation of beta-catenin. *Curr Opin Cell Biol*. 2005; 17(5):459-465.

27. Navarro P, Ruco L, Dejana E. Differential localization of VE- and N-cadherins in human endothelial cells: VE-cadherin competes with N-cadherin for junctional localization. *J Cell Biol*. 1998; 140(6):1475-1484.

28. Williams EJ, Furness J, Walsh FS, Doherty P. Activation of the FGF receptor underlies neurite outgrowth stimulated by L1, N-CAM, and N-cadherin. *Neuron*. 1994; 13(3):583-594.

29. Hazan RB, Kang L, Whooley BP, Borgen PI. N-cadherin promotes adhesion between invasive breast cancer cells and the stroma. *Cell Adhes Commun*. 1997; 4(6):399-411.

30. Puch S, Armeanu S, Kibler C, Johnson KR, Muller CA, Wheelock MJ, Klein G. N-cadherin is developmentally regulated and functionally involved in early hematopoietic cell differentiation. *J Cell Sci*. 2001; 114(Pt 8):1567-1577.

31. Bromberg O, Frisch BJ, Weber JM, Porter RL, Civitelli R, Calvi LM. Osteoblastic N-cadherin is not required for microenvironmental support and regulation of hematopoietic stem and progenitor cells. *Blood*. 2012; 120(2):303-313.

32. Tomita K, van Bokhoven A, van Leenders GJ, Ruijter ET, Jansen CF, Bussemakers MJ, Schalken JA. Cadherin switching in human prostate cancer progression. *Cancer Res*. 2000; 60(13):3650-3654.

33. Choi Y, Lee HJ, Jang MH, Gwak JM, Lee KS, Kim EJ, Kim HJ, Lee HE, Park SY. Epithelial-mesenchymal transition increases during the progression of in situ to invasive basal-like breast cancer. *Hum Pathol*. 2013; 44(11):2581-2589.

34. Lascombe I, Clairotte A, Fauconnet S, Bernardini S, Wallerand H, Kantelip B, Bittard H. N-cadherin as a novel prognostic marker of progression in superficial urothelial tumors. *Clin Cancer Res*. 2006; 12(9):2780-2787.

35. Nakajima S, Doi R, Toyoda E, Tsuji S, Wada M, Koizumi M, Tulachan SS, Ito D, Kami K, Mori T *et al*. N-cadherin expression and epithelial-mesenchymal transition in pancreatic carcinoma. *Clin Cancer Res*. 2004; 10(12 Pt 1):4125-4133.

36. Hsu MY, Wheelock MJ, Johnson KR, Herlyn M. Shifts in cadherin profiles between human normal melanocytes and melanomas. *J Investig Dermatol Symp Proc*. 1996; 1(2):188-194.

37. Hao L, Ha JR, Kuzel P, Garcia E, Persad S. Cadherin switch from E- to N-cadherin in melanoma progression is regulated by the PI3K/PTEN pathway through Twist and Snail. *Br J Dermatol*. 2012; 166(6):1184-1197.

38. Watson-Hurst K, Becker D. The role of N-cadherin, MCAM and beta3 integrin in melanoma progression, proliferation, migration and invasion. *Cancer Biol Ther*. 2006; 5(10):1375-1382.

39. Knudsen KA, Sauer C, Johnson KR, Wheelock MJ. Effect of N-cadherin misexpression by the mammary epithelium in mice. *J Cell Biochem*. 2005; 95(6):1093-1107.

40. Hulit J, Suyama K, Chung S, Keren R, Agiostratidou G, Shan W, Dong X, Williams TM, Lisanti MP, Knudsen K *et al*. N-cadherin signaling potentiates mammary tumor metastasis via enhanced extracellular signal-regulated kinase activation. *Cancer Res*. 2007; 67(7):3106-3116.

41. Su Y, Li J, Shi C, Hruban RH, Radice GL. N-cadherin functions as a growth suppressor in a model of K-ras-induced PanIN. *Oncogene*. 2016; 35(25):3335-3341.

42. Saadatmand S, de Kruijf EM, Sajet A, Dekker-Ensink NG, van Nes JG, Putter H, Smit VT, van de Velde CJ, Liefers GJ, Kuppen PJ. Expression of cell adhesion molecules and prognosis in breast cancer. *Br J Surg*. 2013; 100(2):252-260.

43. Aleskandarany MA, Soria D, Green AR, Nolan C, Diez-Rodriguez M, Ellis IO, Rakha EA. Markers of progression in early-stage invasive breast cancer: a predictive immunohistochemical panel algorithm for distant recurrence risk stratification. *Breast Cancer Res Treat*. 2015; 151(2):325-333.

44. Bock C, Kuhn C, Ditsch N, Krebold R, Heublein S, Mayr D, Doisneau-Sixou S, Jeschke U. Strong correlation between N-cadherin and CD133 in breast cancer: role of both markers in metastatic events. *J Cancer Res Clin Oncol*. 2014; 140(11):1873-1881.

45. Ning Q, Liu C, Hou L, Meng M, Zhang X, Luo M, Shao S, Zuo X, Zhao X. Vascular endothelial growth factor receptor-1 activation promotes migration and invasion of breast cancer cells through epithelial-mesenchymal transition. *PLoS One*. 2013; 8(6):e65217.

46. Jennbacken K, Tesan T, Wang W, Gustavsson H, Damber JE, Welen K. N-cadherin increases after androgen deprivation and is associated with metastasis in prostate cancer. *Endocr Relat Cancer*. 2010; 17(2):469-479.

47. Drivalos A, Chrisofos M, Efstathiou E, Kapranou A, Kollaitis G, Koutlis G, Antoniou N, Karanastasis D, Dimopoulos MA, Bamias A. Expression of alpha5-integrin, alpha7-integrin, Epsilon-cadherin, and N-cadherin in localized prostate cancer. *Urol Oncol*. 2016; 34(4):165 e111-168.

48. Derycke L, De Wever O, Stove V, Vanhoecke B, Delanghe J, Depypere H, Bracke M. Soluble N-cadherin in human biological fluids. *Int J Cancer*. 2006; 119(12):2895-2900.

49. Ge R, Wang Z, Wu S, Zhuo Y, Otsetov AG, Cai C, Zhong W, Wu CL, Olumi AF. Metformin represses cancer cells via alternate pathways in N-cadherin expressing vs. N-cadherin deficient cells. *Oncotarget*. 2015; 6(30):28973-28987.

50. Hui L, Zhang S, Dong X, Tian D, Cui Z, Qiu X. Prognostic significance of twist and N-cadherin expression in NSCLC. *PLoS One*. 2013; 8(4):e62171.

51. Xu J, Lv W, Hu Y, Wang L, Wang Y, Cao J, Hu J. Wnt3a Expression Is Associated with Epithelial-Mesenchymal Transition and Impacts Prognosis of Lung Adenocarcinoma Patients. *J Cancer*. 2017; 8(13):2523-2531.

52. Mo D, Yang D, Xiao X, Sun R, Huang L, Xu J. MiRNA-145 suppresses lung adenocarcinoma cell invasion and migration by targeting N-cadherin. *Biotechnol Lett*. 2017; 39(5):701-710.

53. Yang Z, Wang H, Xia L, Oyang L, Zhou Y, Zhang B, Chen X, Luo X, Liao Q, Liang J. Overexpression of PAK1 Correlates with Aberrant Expression of EMT Markers and Poor Prognosis in Non-Small Cell Lung Cancer. *J Cancer*. 2017; 8(8):1484-1491.

54. Nel I, Jehn U, Gauler T, Hoffmann AC. Individual profiling of circulating tumor cell composition in patients with non-small cell lung cancer receiving platinum based treatment. *Transl Lung Cancer Res*. 2014; 3(2):100-106.

55. Abufaraj M, Haitel A, Moschini M, Gust K, Foerster B, Ozsoy M, D'Andrea D, Karakiewicz PI, Roupret M, Briganti A *et al*. Prognostic Role of N-cadherin Expression in Patients With Invasive Bladder Cancer. *Clin Genitourin Cancer*. 2017.

56. Wallerand H, Cai Y, Wainberg ZA, Garraway I, Lascombe I, Nicolle G, Thiery JP, Bittard H, Radvanyi F, Reiter RR. Phospho-Akt pathway activation and inhibition depends on N-cadherin or phospho-EGFR expression in invasive human bladder cancer cell lines. *Urol Oncol*. 2010; 28(2):180-188.

57. Muramaki M, Miyake H, Terakawa T, Kumano M, Sakai I, Fujisawa M. Expression profile of E-cadherin and N-cadherin in non-muscle-invasive bladder cancer as a novel predictor of intravesical recurrence following transurethral resection. *Urol Oncol*. 2012; 30(2):161-166.

58. Muramaki M, Miyake H, Terakawa T, Kusuda Y, Fujisawa M. Expression profile of E-cadherin and N-cadherin in urothelial carcinoma of the upper urinary tract is associated with disease recurrence in patients undergoing nephroureterectomy. *Urology*. 2011; 78(6):1443 e1447-1412.

59. Zhou SJ, Liu FY, Zhang AH, Liang HF, Wang Y, Ma R, Jiang YH, Sun NF. MicroRNA-199b-5p attenuates TGF-beta1-induced epithelial-mesenchymal transition in hepatocellular carcinoma. *Br J Cancer*. 2017; 117(2):233-244.

60. Seo DD, Lee HC, Kim HJ, Min HJ, Kim KM, Lim YS, Chung YH, Lee YS, Suh DJ, Yu E *et al*. Neural cadherin overexpression is a predictive marker for early postoperative recurrence in hepatocellular carcinoma patients. *J Gastroenterol Hepatol*. 2008; 23(7 Pt 1):1112-1118.

61. Yao X, Wang X, Wang Z, Dai L, Zhang G, Yan Q, Zhou W. Clinicopathological and prognostic significance of epithelial mesenchymal transition-related protein expression in intrahepatic cholangiocarcinoma. *Onco Targets Ther*. 2012; 5:255-261.

62. Zhang J, Cheng Q, Zhou Y, Wang Y, Chen X. Slug is a key mediator of hypoxia induced cadherin switch in HNSCC: correlations with poor prognosis. *Oral Oncol*. 2013; 49(11):1043-1050.

63. Weller P, Nel I, Hassenkamp P, Gauler T, Schlueter A, Lang S, Dountsop P, Hoffmann AC, Lehnerdt G. Detection of circulating tumor cell subpopulations in patients with head and neck squamous cell carcinoma (HNSCC). *PLoS One*. 2014; 9(12):e113706.

64. Mezi S, Chiappetta C, Carletti R, Nardini A, Cortesi E, Orsi E, Piesco G, Di Gioia C. Clinical significance of epithelial-to-mesenchymal transition in laryngeal carcinoma: Its role in the different subsites. *Head Neck*. 2017; 39(9):1806-1818.

65. Luo WR, Wu AB, Fang WY, Li SY, Yao KT. Nuclear expression of N-cadherin correlates with poor prognosis of nasopharyngeal carcinoma. *Histopathology*. 2012; 61(2):237-246.

66. Ye Z, Zhou M, Tian B, Wu B, Li J. Expression of lncRNA-CCAT1, E-cadherin and N-cadherin in colorectal cancer and its clinical significance. *Int J Clin Exp Med*. 2015; 8(3):3707-3715.

67. Yan X, Yan L, Liu S, Shan Z, Tian Y, Jin Z. N-cadherin, a novel prognostic biomarker, drives malignant progression of colorectal cancer. *Mol Med Rep*. 2015; 12(2):2999-3006.

68. Liu CC, Cai DL, Sun F, Wu ZH, Yue B, Zhao SL, Wu XS, Zhang M, Zhu XW, Peng ZH *et al*. FERMT1 mediates epithelial-mesenchymal transition to promote colon cancer metastasis via modulation of beta-catenin transcriptional activity. *Oncogene*. 2017; 36(13):1779-1792.

69. Okubo K, Uenosono Y, Arigami T, Yanagita S, Matsushita D, Kijima T, Amatatsu M, Uchikado Y, Kijima Y, Maemura K *et al*. Clinical significance of altering epithelial-mesenchymal transition in metastatic lymph nodes of gastric cancer. *Gastric Cancer*. 2017; 20(5):802-810.

70. Kamikihara T, Ishigami S, Arigami T, Matsumoto M, Okumura H, Uchikado Y, Kita Y, Kurahara H, Kijima Y, Ueno S *et al*. Clinical implications of N-cadherin expression in gastric cancer. *Pathol Int*. 2012; 62(3):161-166.

71. Nel I, Gauler TC, Bublitz K, Lazaridis L, Goergens A, Giebel B, Schuler M, Hoffmann AC. Circulating Tumor Cell Composition in Renal Cell Carcinoma. *PLoS One*. 2016; 11(4):e0153018.

72. Quattrocchi L, Green AR, Martin S, Durrant L, Deen S. The cadherin switch in ovarian high-grade serous carcinoma is associated with disease progression. *Virchows Arch*. 2011; 459(1):21-29.

73. Yi S, Yang ZL, Miao X, Zou Q, Li J, Liang L, Zeng G, Chen S. N-cadherin and P-cadherin are biomarkers for invasion, metastasis, and poor prognosis of gallbladder carcinomas. *Pathol Res Pract*. 2014; 210(6):363-368.

74. Han K, Zhao T, Chen X, Bian N, Yang T, Ma Q, Cai C, Fan Q, Zhou Y, Ma B. microRNA-194 suppresses osteosarcoma cell proliferation and metastasis in vitro and in vivo by targeting CDH2 and IGF1R. *Int J Oncol*. 2014; 45(4):1437-1449.

75. Niimi R, Matsumine A, Iino T, Nakazora S, Nakamura T, Uchida A, Sudo A. Soluble Neural-cadherin as a novel biomarker for malignant bone and soft tissue tumors. *BMC Cancer*. 2013; 13(1):309.

76. Vandyke K, Chow AW, Williams SA, To LB, Zannettino AC. Circulating N-cadherin levels are a negative prognostic indicator in patients with multiple myeloma. *Br J Haematol*. 2013; 161(4):499-507.

77. Luo Y, Yu T, Zhang Q, Fu Q, Hu Y, Xiang M, Peng H, Zheng T, Lu L, Shi H. Up-regulated N-cadherin expression is associated with poor prognosis in epithelial-derived solid tumors: a meta-analysis. *Eur J Clin Invest*. 2018.

78. Hazan RB, Phillips GR, Qiao RF, Norton L, Aaronson SA. Exogenous expression of N-cadherin in breast cancer cells induces cell migration, invasion, and metastasis. *J Cell Biol*. 2000; 148(4):779-790.

79. Nalla AK, Estes N, Patel J, Rao JS. N-cadherin mediates angiogenesis by regulating monocyte chemoattractant protein-1 expression via PI3K/Akt signaling in prostate cancer cells. *Exp Cell Res*. 2011; 317(17):2512-2521.

80. Li G, Satyamoorthy K, Herlyn M. N-cadherin-mediated intercellular interactions promote survival and migration of melanoma cells. *Cancer Res*. 2001; 61(9):3819-3825.

81. Groen RW, de Rooij MF, Kocemba KA, Reijmers RM, de Haan-Kramer A, Overdijk MB, Aalders L, Rozemuller H, Martens AC, Bergsagel PL *et al*. N-cadherin-mediated interaction with multiple myeloma cells inhibits osteoblast differentiation. *Haematologica*. 2011; 96(11):1653-1661.

82. Islam S, Carey TE, Wolf GT, Wheelock MJ, Johnson KR. Expression of N-cadherin by human squamous carcinoma cells induces a scattered fibroblastic phenotype with disrupted cell-cell adhesion. *J Cell Biol*. 1996; 135(6 Pt 1):1643-1654.

83. Nieman MT, Prudoff RS, Johnson KR, Wheelock MJ. N-cadherin promotes motility in human breast cancer cells regardless of their E-cadherin expression. *J Cell Biol*. 1999; 147(3):631-644.

84. Shintani Y, Hollingsworth MA, Wheelock MJ, Johnson KR. Collagen I promotes metastasis in pancreatic cancer by activating c-Jun NH(2)-terminal kinase 1 and up-regulating N-cadherin expression. *Cancer Res*. 2006; 66(24):11745-11753.

85. Sandig M, Voura EB, Kalnins VI, Siu CH. Role of cadherins in the transendothelial migration of melanoma cells in culture. *Cell Motil Cytoskeleton*. 1997; 38(4):351-364.

86. Qi J, Chen N, Wang J, Siu CH. Transendothelial migration of melanoma cells involves N-cadherin-mediated adhesion and activation of the beta-catenin signaling pathway. *Mol Biol Cell*. 2005; 16(9):4386-4397.

87. Tanaka H, Kono E, Tran CP, Miyazaki H, Yamashiro J, Shimomura T, Fazli L, Wada R, Huang J, Vessella RL *et al*. Monoclonal antibody targeting of N-cadherin inhibits prostate cancer growth, metastasis and castration resistance. *Nat Med*. 2010; 16(12):1414-1420.

88. Na YR, Lee JS, Lee SJ, Seok SH. Interleukin-6-induced Twist and N-cadherin enhance melanoma cell metastasis. *Melanoma Res*. 2013; 23(6):434-443.

89. Clark AG, Vignjevic DM. Modes of cancer cell invasion and the role of the microenvironment. *Curr Opin Cell Biol*. 2015; 36:13-22.

90. Mayor R, Etienne-Manneville S. The front and rear of collective cell migration. *Nat Rev Mol Cell Biol*. 2016; 17(2):97-109.

91. Etienne-Manneville S. Neighborly relations during collective migration. *Curr Opin Cell Biol*. 2014; 30:51-59.

92. Klymenko Y, Kim O, Loughran E, Yang J, Lombard R, Alber M, Stack MS. Cadherin composition and multicellular aggregate invasion in organotypic models of epithelial ovarian cancer intraperitoneal metastasis. *Oncogene*. 2017; 36(42):5840-5851.

93. Kuriyama S, Yoshida M, Yano S, Aiba N, Kohno T, Minamiya Y, Goto A, Tanaka M. LPP inhibits collective cell migration during lung cancer dissemination. *Oncogene*. 2016; 35(8):952-964.

94. Shih W, Yamada S. N-cadherin-mediated cell-cell adhesion promotes cell migration in a three-dimensional matrix. *J Cell Sci*. 2012; 125(Pt 15):3661-3670.

95. Ridley AJ. Rho GTPase signalling in cell migration. *Curr Opin Cell Biol*. 2015; 36:103-112.

96. Combedazou A, Gayral S, Colombie N, Fougerat A, Laffargue M, Ramel D. Small GTPases orchestrate cell-cell communication during collective cell movement. *Small GTPases*. 2017:0.

97. Sabatini PJ, Zhang M, Silverman-Gavrila R, Bendeck MP, Langille BL. Homotypic and endothelial cell adhesions via N-cadherin determine polarity and regulate migration of vascular smooth muscle cells. *Circ Res*. 2008; 103(4):405-412.

98. Theveneau E, Marchant L, Kuriyama S, Gull M, Moepps B, Parsons M, Mayor R. Collective chemotaxis requires contact-dependent cell polarity. *Dev Cell*. 2010; 19(1):39-53.

99. Ouyang M, Lu S, Kim T, Chen CE, Seong J, Leckband DE, Wang F, Reynolds AB, Schwartz MA, Wang Y. N-cadherin regulates spatially polarized signals through

distinct p120ctn and beta-catenin-dependent signalling pathways. *Nat Commun*. 2013; 4:1589.

100. Wasil LR, Shair KH. Epstein-Barr virus LMP1 induces focal adhesions and epithelial cell migration through effects on integrin-alpha5 and N-cadherin. *Oncogenesis*. 2015; 4:e171.

101. Siret C, Terciolo C, Dobric A, Habib MC, Germain S, Bonnier R, Lombardo D, Rigot V, Andre F. Interplay between cadherins and alpha2beta1 integrin differentially regulates melanoma cell invasion. *Br J Cancer*. 2015; 113(10):1445-1453.

102. Yano H, Mazaki Y, Kurokawa K, Hanks SK, Matsuda M, Sabe H. Roles played by a subset of integrin signaling molecules in cadherin-based cell-cell adhesion. *J Cell Biol*. 2004; 166(2):283-295.

103. Moreno-Layseca P, Streuli CH. Signalling pathways linking integrins with cell cycle progression. *Matrix Biol*. 2014; 34:144-153.

104. Grande-Garcia A, Echarri A, Del Pozo MA. Integrin regulation of membrane domain trafficking and Rac targeting. *Biochem Soc Trans*. 2005; 33(Pt 4):609-613.

105. Williams EJ, Williams G, Howell FV, Skaper SD, Walsh FS, Doherty P. Identification of an N-cadherin motif that can interact with the fibroblast growth factor receptor and is required for axonal growth. *J Biol Chem*. 2001; 276(47):43879-43886.

106. Suyama K, Shapiro I, Guttman M, Hazan RB. A signaling pathway leading to metastasis is controlled by N-cadherin and the FGF receptor. *Cancer Cell*. 2002; 2(4):301-314.

107. Sanchez-Heras E, Howell FV, Williams G, Doherty P. The fibroblast growth factor receptor acid box is essential for interactions with N-cadherin and all of the major isoforms of neural cell adhesion molecule. *J Biol Chem*. 2006; 281(46):35208-35216.

108. Rachagani S, Macha MA, Ponnusamy MP, Haridas D, Kaur S, Jain M, Batra SK. MUC4 potentiates invasion and metastasis of pancreatic cancer cells through stabilization of fibroblast growth factor receptor 1. *Carcinogenesis*. 2012; 33(10):1953-1964.

109. Cavallaro U, Niedermeyer J, Fuxa M, Christofori G. N-CAM modulates tumour-cell adhesion to matrix by inducing FGF-receptor signalling. *Nat Cell Biol*. 2001; 3(7):650-657.

110. Qian X, Anzovino A, Kim S, Suyama K, Yao J, Hulit J, Agiostratidou G, Chandiramani N, McDaid HM, Nagi C *et al*. N-cadherin/FGFR promotes metastasis through epithelial-to-mesenchymal transition and stem/progenitor cell-like properties. *Oncogene*. 2014; 33(26):3411-3421.

111. Kim JB, Islam S, Kim YJ, Prudoff RS, Sass KM, Wheelock MJ, Johnson KR. N-Cadherin extracellular repeat 4 mediates epithelial to mesenchymal transition and increased motility. *J Cell Biol*. 2000; 151(6):1193-1206.

112. Murillo-Garzon V, Kypta R. WNT signalling in prostate cancer. *Nat Rev Urol*. 2017; 14(11):683-696.

113. Valenta T, Hausmann G, Basler K. The many faces and functions of beta-catenin. *Embo J*. 2012; 31(12):2714-2736.

114. Klaus A, Birchmeier W. Wnt signalling and its impact on development and cancer. *Nat Rev Cancer*. 2008; 8(5):387-398.

115. Qi J, Yu Y, Akilli Ozturk O, Holland JD, Besser D, Fritzmann J, Wulf-Goldenberg A, Eckert K, Fichtner I, Birchmeier W. New Wnt/beta-catenin target genes promote experimental metastasis and migration of colorectal cancer cells through different signals. *Gut*. 2016; 65(10):1690-1701.

116. Stein U, Arlt F, Walther W, Smith J, Waldman T, Harris ED, Mertins SD, Heizmann CW, Allard D, Birchmeier W *et al*. The metastasis-associated gene S100A4 is a novel target of beta-catenin/T-cell factor signaling in colon cancer. *Gastroenterology*. 2006; 131(5):1486-1500.

117. Zeilstra J, Joosten SP, Dokter M, Verwiel E, Spaargaren M, Pals ST. Deletion of the WNT target and cancer stem cell marker CD44 in Apc(Min/+) mice attenuates intestinal tumorigenesis. *Cancer Res*. 2008; 68(10):3655-3661.

118. Crawford HC, Fingleton BM, Rudolph-Owen LA, Goss KJ, Rubinfeld B, Polakis P, Matrisian LM. The metalloproteinase matrilysin is a target of beta-catenin transactivation in intestinal tumors. *Oncogene*. 1999; 18(18):2883-2891.

119. Chen L, Li M, Li Q, Wang CJ, Xie SQ. DKK1 promotes hepatocellular carcinoma cell migration and invasion through beta-catenin/MMP7 signaling pathway. *Mol Cancer*. 2013; 12:157.

120. Lowy AM, Clements WM, Bishop J, Kong L, Bonney T, Sisco K, Aronow B, Fenoglio-Preiser C, Groden J. beta-Catenin/Wnt signaling regulates expression of the membrane type 3 matrix metalloproteinase in gastric cancer. *Cancer Res*. 2006; 66(9):4734-4741.

121. Takahashi M, Tsunoda T, Seiki M, Nakamura Y, Furukawa Y. Identification of membrane-type matrix metalloproteinase-1 as a target of the beta-catenin/Tcf4 complex in human colorectal cancers. *Oncogene*. 2002; 21(38):5861-5867.

122. Heuberger J, Birchmeier W. Interplay of cadherin-mediated cell adhesion and canonical Wnt signaling. *Cold Spring Harb Perspect Biol*. 2010; 2(2):a002915.

123. Nelson WJ, Nusse R. Convergence of Wnt, beta-catenin, and cadherin pathways. *Science*. 2004; 303(5663):1483-1487.

124. Sadot E, Simcha I, Shtutman M, Ben-Ze'ev A, Geiger B. Inhibition of beta-catenin-mediated transactivation by cadherin derivatives. *Proc Natl Acad Sci U S A*. 1998; 95(26):15339-15344.

125. Zhang B, Li M, McDonald T, Holyoake TL, Moon RT, Campana D, Shultz L, Bhatia R. Microenvironmental protection of CML stem and progenitor cells from tyrosine kinase inhibitors through N-cadherin and Wnt-beta-catenin signaling. *Blood*. 2013; 121(10):1824-1838.

126. Eiring AM, Khorashad JS, Anderson DJ, Yu F, Redwine HM, Mason CC, Reynolds KR, Clair PM, Gantz KC, Zhang TY *et al*. beta-Catenin is required for intrinsic but not extrinsic BCR-ABL1 kinase-independent resistance to tyrosine kinase inhibitors in chronic myeloid leukemia. *Leukemia*. 2015; 29(12):2328-2337.

127. van Zijl F, Krupitza G, Mikulits W. Initial steps of metastasis: cell invasion and endothelial transmigration. *Mutat Res*. 2011; 728(1-2):23-34.

128. Qi J, Wang J, Romanyuk O, Siu CH. Involvement of Src family kinases in N-cadherin phosphorylation and beta-catenin dissociation during transendothelial migration of melanoma cells. *Mol Biol Cell*. 2006; 17(3):1261-1272.

129. Zhang P, Fu C, Bai H, Song E, Dong C, Song Y. CD44 variant, but not standard CD44 isoforms, mediate disassembly of endothelial VE-cadherin junction on metastatic melanoma cells. *FEBS Lett*. 2014; 588(24):4573-4582.

130. Kang SA, Hasan N, Mann AP, Zheng W, Zhao L, Morris L, Zhu W, Zhao YD, Suh KS, Dooley WC *et al*. Blocking the adhesion cascade at the premetastatic niche for prevention of breast cancer metastasis. *Mol Ther*. 2015; 23(6):1044-1054.

131. Zen K, Liu DQ, Guo YL, Wang C, Shan J, Fang M, Zhang CY, Liu Y. CD44v4 is a major E-selectin ligand that mediates breast cancer cell transendothelial migration. *PLoS One*. 2008; 3(3):e1826.

132. Adams GB, Scadden DT. The hematopoietic stem cell in its place. *Nat Immunol*. 2006; 7(4):333-337.

133. Wilson A, Trumpp A. Bone-marrow haematopoietic-stem-cell niches. *Nat Rev Immunol*. 2006; 6(2):93-106.

134. Greenbaum AM, Revollo LD, Woloszynek JR, Civitelli R, Link DC. N-cadherin in osteolineage cells is not required for maintenance of hematopoietic stem cells. *Blood*. 2012; 120(2):295-302.

135. Paik JH, Skoura A, Chae SS, Cowan AE, Han DK, Proia RL, Hla T. Sphingosine 1-phosphate receptor regulation of N-cadherin mediates vascular stabilization. *Genes Dev*. 2004; 18(19):2392-2403.

136. Tillet E, Vittet D, Feraud O, Moore R, Kemler R, Huber P. N-cadherin deficiency impairs pericyte recruitment, and not endothelial differentiation or sprouting, in embryonic stem cell-derived angiogenesis. *Exp Cell Res*. 2005; 310(2):392-400.

137. Lapidot T, Sirard C, Vormoor J, Murdoch B, Hoang T, Caceres-Cortes J, Minden M, Paterson B, Caligiuri MA, Dick JE. A cell initiating human acute myeloid leukaemia after transplantation into SCID mice. *Nature*. 1994; 367(6464):645-648.

138. Petzer AL, Eaves CJ, Lansdorp PM, Ponchio L, Barnett MJ, Eaves AC. Characterization of primitive subpopulations of normal and leukemic cells present in the blood of patients with newly diagnosed as well as established chronic myeloid leukemia. *Blood*. 1996; 88(6):2162-2171.

139. Colmone A, Amorim M, Pontier AL, Wang S, Jablonski E, Sipkins DA. Leukemic cells create bone marrow niches that disrupt the behavior of normal hematopoietic progenitor cells. *Science*. 2008; 322(5909):1861-1865.

140. Schepers K, Pietras EM, Reynaud D, Flach J, Binnewies M, Garg T, Wagers AJ, Hsiao EC, Passegue E. Myeloproliferative neoplasia remodels the endosteal bone marrow niche into a self-reinforcing leukemic niche. *Cell Stem Cell*. 2013; 13(3):285-299.

141. Wang X, Huang S, Chen JL. Understanding of leukemic stem cells and their clinical implications. *Mol Cancer*. 2017; 16(1):2.

142. Zhou HS, Carter BZ, Andreeff M. Bone marrow niche-mediated survival of leukemia stem cells in acute myeloid leukemia: Yin and Yang. *Cancer Biol Med*. 2016; 13(2):248-259.

143. Jin L, Hope KJ, Zhai Q, Smadja-Joffe F, Dick JE. Targeting of CD44 eradicates human acute myeloid leukemic stem cells. *Nat Med*. 2006; 12(10):1167-1174.

144. Hosokawa K, Arai F, Yoshihara H, Iwasaki H, Hembree M, Yin T, Nakamura Y, Gomei Y, Takubo K, Shiama H *et al*. Cadherin-based adhesion is a potential target for niche manipulation to protect hematopoietic stem cells in adult bone marrow. *Cell Stem Cell*. 2010; 6(3):194-198.

145. Kiel MJ, Acar M, Radice GL, Morrison SJ. Hematopoietic stem cells do not depend on N-cadherin to regulate their maintenance. *Cell Stem Cell*. 2009; 4(2):170-179.

146. Zhi L, Wang M, Rao Q, Yu F, Mi Y, Wang J. Enrichment of N-Cadherin and Tie2-bearing CD34+/CD38-/CD123+ leukemic stem cells by chemotherapy-resistance. *Cancer Lett*. 2010; 296(1):65-73.

147. Qiu S, Jia Y, Xing H, Yu T, Yu J, Yu P, Tang K, Tian Z, Wang H, Mi Y *et al*. N-Cadherin and Tie2 positive CD34(+)CD38(-)CD123(+) leukemic stem cell populations can develop acute myeloid leukemia more effectively in NOD/SCID mice. *Leuk Res*. 2014; 38(5):632-637.

148. Zhang B, Groffen J, Heisterkamp N. Increased resistance to a farnesyltransferase inhibitor by N-cadherin expression in Bcr/Abl-P190 lymphoblastic leukemia cells. *Leukemia*. 2007; 21(6):1189-1197.

149. Marjon KD, Termini CM, Karlen KL, Saito-Reis C, Soria CE, Lidke KA, Gillette JM. Tetraspanin CD82 regulates bone marrow homing of acute myeloid leukemia by modulating the molecular organization of N-cadherin. *Oncogene*. 2016; 35(31):4132-4140.

150. Zhi L, Gao Y, Yu C, Zhang Y, Zhang B, Yang J, Yao Z. N-Cadherin Aided in Maintaining the Characteristics of Leukemic Stem Cells. *Anat Rec (Hoboken)*. 2016; 299(7):990-998.

151. Jacamo R, Chen Y, Wang Z, Ma W, Zhang M, Spaeth EL, Wang Y, Battula VL, Mak PY, Schallmoser K *et al*. Reciprocal leukemia-stroma VCAM-1/VLA-4-dependent activation of NF-kappaB mediates chemoresistance. *Blood*. 2014; 123(17):2691-2702.

152. Kurtova AV, Balakrishnan K, Chen R, Ding W, Schnabl S, Quiroga MP, Sivina M, Wierda WG, Estrov Z, Keating MJ *et al*. Diverse marrow stromal cells protect CLL cells from spontaneous and drug-induced apoptosis: development of a reliable and reproducible system to assess stromal cell adhesion-mediated drug resistance. *Blood*. 2009; 114(20):4441-4450.

153. Hsieh YT, Gang EJ, Geng H, Park E, Huantes S, Chudziak D, Dauber K, Schaefer P, Scharman C, Shimada H *et al*. Integrin alpha4 blockade sensitizes drug resistant pre-B acute lymphoblastic leukemia to chemotherapy. *Blood*. 2013; 121(10):1814-1818.

154. Latifi A, Abubaker K, Castrechini N, Ward AC, Liongue C, Dobill F, Kumar J, Thompson EW, Quinn MA, Findlay JK *et al*. Cisplatin treatment of primary and metastatic epithelial ovarian carcinomas generates residual cells with mesenchymal stem cell-like profile. *J Cell Biochem*. 2011; 112(10):2850-2864.

155. Yamauchi M, Yoshino I, Yamaguchi R, Shimamura T, Nagasaki M, Imoto S, Niida A, Koizumi F, Kohno T, Yokota J *et al*. N-cadherin expression is a potential survival mechanism of gefitinib-resistant lung cancer cells. *Am J Cancer Res*. 2011; 1(7):823-833.

156. Zhang X, Liu G, Kang Y, Dong Z, Qian Q, Ma X. N-cadherin expression is associated with acquisition of EMT phenotype and with enhanced invasion in erlotinib-resistant lung cancer cell lines. *PLoS One*. 2013; 8(3):e57692.

157. Wu Y, Ginther C, Kim J, Mosher N, Chung S, Slamon D, Vadgama JV. Expression of Wnt3 activates Wnt/beta-catenin pathway and promotes EMT-like phenotype in trastuzumab-resistant HER2-overexpressing breast cancer cells. *Mol Cancer Res*. 2012; 10(12):1597-1606.

158. Sun Y, Wang BE, Leong KG, Yue P, Li L, Jhunjhunwala S, Chen D, Seo K, Modrusan Z, Gao WQ *et al*. Androgen deprivation causes epithelial-mesenchymal transition in the prostate: implications for androgen-deprivation therapy. *Cancer Res*. 2012; 72(2):527-536.

159. Tran NL, Adams DG, Vaillancourt RR, Heimark RL. Signal transduction from N-cadherin increases Bcl-2. Regulation of the phosphatidylinositol 3-kinase/Akt pathway by homophilic adhesion and actin cytoskeletal organization. *J Biol Chem*. 2002; 277(36):32905-32914.

160. Kumar SK, Dispenzieri A, Lacy MQ, Gertz MA, Buadi FK, Pandey S, Kapoor P, Dingli D, Hayman SR, Leung N *et al*. Continued improvement in survival in multiple

myeloma: changes in early mortality and outcomes in older patients. *Leukemia*. 2014; 28(5):1122-1128.

161. Blimark CH, Turesson I, Genell A, Ahlberg L, Bjorkstrand B, Carlson K, Forsberg K, Juliusson G, Linder O, Mellqvist UH *et al*. Outcome and survival of myeloma patients diagnosed 2008-2015. Real world data on 4904 patients from the Swedish Myeloma Registry (SMR). *Haematologica*. 2017.

162. Lonial S, Boise LH, Kaufman J. How I treat high-risk myeloma. *Blood*. 2015; 126(13):1536-1543.

163. Moreau P. How I treat myeloma with new agents. *Blood*. 2017; 130(13):1507-1513.

164. Chim CS, Kumar SK, Orlowski RZ, Cook G, Richardson PG, Gertz MA, Giralt S, Mateos MV, Leleu X, Anderson KC. Management of relapsed and refractory multiple myeloma: novel agents, antibodies, immunotherapies and beyond. *Leukemia*. 2018; 32(2):252-262.

165. Dring AM, Davies FE, Fenton JA, Roddam PL, Scott K, Gonzalez D, Rollinson S, Rawstron AC, Rees-Unwin KS, Li C *et al*. A global expression-based analysis of the consequences of the t(4;14) translocation in myeloma. *Clin Cancer Res*. 2004; 10(17):5692-5701.

166. Lauring J, Abukhdeir AM, Konishi H, Garay JP, Gustin JP, Wang Q, Arceci RJ, Matsui W, Park BH. The multiple myeloma associated MMSET gene contributes to cellular adhesion, clonogenic growth, and tumorigenicity. *Blood*. 2008; 111(2):856-864.

167. Ezponda T, Popovic R, Shah MY, Martinez-Garcia E, Zheng Y, Min DJ, Will C, Neri A, Kelleher NL, Yu J *et al*. The histone methyltransferase MMSET/WHSC1 activates TWIST1 to promote an epithelial-mesenchymal transition and invasive properties of prostate cancer. *Oncogene*. 2012; 32(23):2882-2890.

168. Noll JE, Williams SA, Purton LE, Zannettino AC. Tug of war in the haematopoietic stem cell niche: do myeloma plasma cells compete for the HSC niche? *Blood Cancer J*. 2012; 2:e91.

169. Katz BZ. Adhesion molecules--The lifelines of multiple myeloma cells. *Seminars in cancer biology*. 2010; 20(3):186-195.

170. Sadler NM, Harris BR, Metzger BA, Kirshner J. N-cadherin impedes proliferation of the multiple myeloma cancer stem cells. *American journal of blood research*. 2013; 3(4):271-285.

171. Fontana F, Hickman-Brecks CL, Salazar VS, Revollo L, Abou-Ezzi G, Grimston SK, Jeong SY, Watkins M, Fortunato M, Alippe Y *et al*. N-cadherin Regulation of Bone Growth and Homeostasis Is Osteolineage Stage-Specific. *J Bone Miner Res*. 2017; 32(6):1332-1342.

172. Hay E, Laplantine E, Geoffroy V, Frain M, Kohler T, Muller R, Marie PJ. N-cadherin interacts with axin and LRP5 to negatively regulate Wnt/beta-catenin signaling, osteoblast function, and bone formation. *Mol Cell Biol*. 2009; 29(4):953-964.

173. Hay E, Nouraud A, Marie PJ. N-cadherin negatively regulates osteoblast proliferation and survival by antagonizing Wnt, ERK and PI3K/Akt signalling. *PLoS One*. 2009; 4(12):e8284.

174. Hay E, Buczkowski T, Marty C, Da Nascimento S, Sonnet P, Marie PJ. Peptide-based mediated disruption of N-cadherin-LRP5/6 interaction promotes Wnt signaling and bone formation. *J Bone Miner Res*. 2012; 27(9):1852-1863.

175. Yang H, Wang L, Zhao J, Chen Y, Lei Z, Liu X, Xia W, Guo L, Zhang HT. TGF-beta-activated SMAD3/4 complex transcriptionally upregulates N-cadherin expression in non-small cell lung cancer. *Lung Cancer*. 2015; 87(3):249-257.

176. Qi Y, Wang N, He Y, Zhang J, Zou H, Zhang W, Gu W, Huang Y, Lian X, Hu J *et al*. Transforming growth factor-beta1 signaling promotes epithelial-mesenchymal transition-like phenomena, cell motility, and cell invasion in synovial sarcoma cells. *PLoS One*. 2017; 12(8):e0182680.

177. Park MK, You HJ, Lee HJ, Kang JH, Oh SH, Kim SY, Lee CH. Transglutaminase-2 induces N-cadherin expression in TGF-beta1-induced epithelial mesenchymal transition via c-Jun-N-terminal kinase activation by protein phosphatase 2A down-regulation. *Eur J Cancer*. 2013; 49(7):1692-1705.

178. Shiota M, Zardan A, Takeuchi A, Kumano M, Beraldi E, Naito S, Zoubeidi A, Gleave ME. Clusterin mediates TGF-beta-induced epithelial-mesenchymal transition and metastasis via Twist1 in prostate cancer cells. *Cancer Res*. 2012; 72(20):5261-5272.

179. Cho KH, Choi MJ, Jeong KJ, Kim JJ, Hwang MH, Shin SC, Park CG, Lee HY. A ROS/STAT3/HIF-1alpha signaling cascade mediates EGF-induced TWIST1 expression and prostate cancer cell invasion. *Prostate*. 2014; 74(5):528-536.

180. Colomiere M, Ward AC, Riley C, Trenerry MK, Cameron-Smith D, Findlay J, Ackland L, Ahmed N. Cross talk of signals between EGFR and IL-6R through JAK2/STAT3 mediate epithelial-mesenchymal transition in ovarian carcinomas. *Br J Cancer*. 2009; 100(1):134-144.

181. Xu Z, Jiang Y, Steed H, Davidge S, Fu Y. TGFbeta and EGF synergistically induce a more invasive phenotype of epithelial ovarian cancer cells. *Biochem Biophys Res Commun*. 2010; 401(3):376-381.

182. Liao G, Wang M, Ou Y, Zhao Y. IGF-1-induced epithelial-mesenchymal transition in MCF-7 cells is mediated by MUC1. *Cell Signal*. 2014; 26(10):2131-2137.

183. Li C, Li J, Wu D, Han G. The involvement of survivin in insulin-like growth factor 1-induced epithelial-mesenchymal transition in gastric cancer. *Tumour Biol*. 2016; 37(1):1091-1096.

184. Takeuchi A, Shiota M, Beraldi E, Thaper D, Takahara K, Ibuki N, Pollak M, Cox ME, Naito S, Gleave ME *et al*. Insulin-like growth factor-I induces CLU expression through Twist1 to promote prostate cancer growth. *Mol Cell Endocrinol*. 2014; 384(1-2):117-125.

185. Nagai T, Arao T, Furuta K, Sakai K, Kudo K, Kaneda H, Tamura D, Aomatsu K, Kimura H, Fujita Y *et al*. Sorafenib inhibits the hepatocyte growth factor-mediated epithelial mesenchymal transition in hepatocellular carcinoma. *Molecular cancer therapeutics*. 2011; 10(1):169-177.

186. Koefinger P, Wels C, Joshi S, Damm S, Steinbauer E, Beham-Schmid C, Frank S, Bergler H, Schaider H. The cadherin switch in melanoma instigated by HGF is mediated through epithelial-mesenchymal transition regulators. *Pigment Cell Melanoma Res*. 2011; 24(2):382-385.

187. Shan S, Lv Q, Zhao Y, Liu C, Sun Y, Xi K, Xiao J, Li C. Wnt/beta-catenin pathway is required for epithelial to mesenchymal transition in CXCL12 over expressed breast cancer cells. *Int J Clin Exp Pathol*. 2015; 8(10):12357-12367.

188. Hu TH, Yao Y, Yu S, Han LL, Wang WJ, Guo H, Tian T, Ruan ZP, Kang XM, Wang J *et al*. SDF-1/CXCR4 promotes epithelial-mesenchymal transition and progression of colorectal cancer by activation of the Wnt/beta-catenin signaling pathway. *Cancer Lett*. 2014; 354(2):417-426.

189. Zhang L, Wang D, Li Y, Liu Y, Xie X, Wu Y, Zhou Y, Ren J, Zhang J, Zhu H *et al*. CCL21/CCR7 Axis Contributed to CD133+ Pancreatic Cancer Stem-Like Cell Metastasis via EMT and Erk/NF-kappaB Pathway. *PLoS One*. 2016; 11(8):e0158529.

190. Li F, Zou Z, Suo N, Zhang Z, Wan F, Zhong G, Qu Y, Ntaka KS, Tian H. CCL21/CCR7 axis activating chemotaxis accompanied with epithelial-mesenchymal transition in human breast carcinoma. *Med Oncol*. 2014; 31(9):180.

191. Wang H, Liang X, Li M, Tao X, Tai S, Fan Z, Wang Z, Cheng B, Xia J. Chemokine (CC motif) ligand 18 upregulates Slug expression to promote stem-cell like features by activating the mammalian target of rapamycin pathway in oral squamous cell carcinoma. *Cancer Sci*. 2017; 108(8):1584-1593.

192. Song FN, Duan M, Liu LZ, Wang ZC, Shi JY, Yang LX, Zhou J, Fan J, Gao Q, Wang XY. RANKL promotes migration and invasion of hepatocellular carcinoma cells via NF-kappaB-mediated epithelial-mesenchymal transition. *PLoS One*. 2014; 9(9):e108507.

193. Tsubaki M, Komai M, Fujimoto S, Itoh T, Imano M, Sakamoto K, Shimaoka H, Takeda T, Ogawa N, Mashimo K *et al*. Activation of NF-kappaB by the RANKL/RANK system up-regulates snail and twist expressions and induces epithelial-to-mesenchymal transition in mammary tumor cell lines. *J Exp Clin Cancer Res*. 2013; 32:62.

194. Yamada D, Kobayashi S, Wada H, Kawamoto K, Marubashi S, Eguchi H, Ishii H, Nagano H, Doki Y, Mori M. Role of crosstalk between interleukin-6 and

transforming growth factor-beta 1 in epithelial-mesenchymal transition and chemoresistance in biliary tract cancer. *Eur J Cancer*. 2013; 49(7):1725-1740.

195. Wu YS, Chung I, Wong WF, Masamune A, Sim MS, Looi CY. Paracrine IL-6 signaling mediates the effects of pancreatic stellate cells on epithelial-mesenchymal transition via Stat3/Nrf2 pathway in pancreatic cancer cells. *Biochim Biophys Acta*. 2017; 1861(2):296-306.

196. Alexander NR, Tran NL, Rekapally H, Summers CE, Glackin C, Heimark RL. N-cadherin gene expression in prostate carcinoma is modulated by integrin-dependent nuclear translocation of Twist1. *Cancer Res*. 2006; 66(7):3365-3369.

197. Shintani Y, Fukumoto Y, Chaika N, Svoboda R, Wheelock MJ, Johnson KR. Collagen I-mediated up-regulation of N-cadherin requires cooperative signals from integrins and discoidin domain receptor 1. *J Cell Biol*. 2008; 180(6):1277-1289.

198. Zhang L, Huang G, Li X, Zhang Y, Jiang Y, Shen J, Liu J, Wang Q, Zhu J, Feng X *et al*. Hypoxia induces epithelial-mesenchymal transition via activation of SNAI1 by hypoxia-inducible factor -1alpha in hepatocellular carcinoma. *BMC Cancer*. 2013; 13:108.

199. Cheng ZX, Sun B, Wang SJ, Gao Y, Zhang YM, Zhou HX, Jia G, Wang YW, Kong R, Pan SH *et al*. Nuclear factor-kappaB-dependent epithelial to mesenchymal transition induced by HIF-1alpha activation in pancreatic cancer cells under hypoxic conditions. *PLoS One*. 2011; 6(8):e23752.

200. Azimi I, Petersen RM, Thompson EW, Roberts-Thomson SJ, Monteith GR. Hypoxia-induced reactive oxygen species mediate N-cadherin and SERPINE1 expression, EGFR signalling and motility in MDA-MB-468 breast cancer cells. *Sci Rep*. 2017; 7(1):15140.

201. Zhao JH, Luo Y, Jiang YG, He DL, Wu CT. Knockdown of beta-Catenin through shRNA cause a reversal of EMT and metastatic phenotypes induced by HIF-1alpha. *Cancer investigation*. 2011; 29(6):377-382.

202. Brandl M, Seidler B, Haller F, Adamski J, Schmid RM, Saur D, Schneider G. IKK(alpha) controls canonical TGF(ss)-SMAD signaling to regulate genes expressing SNAIL and SLUG during EMT in panc1 cells. *J Cell Sci*. 2010; 123(Pt 24):4231-4239.

203. Al-Azayzih A, Gao F, Somanath PR. P21 activated kinase-1 mediates transforming growth factor beta1-induced prostate cancer cell epithelial to mesenchymal transition. *Biochim Biophys Acta*. 2015; 1853(5):1229-1239.

204. Shin S, Im HJ, Kwon YJ, Ye DJ, Baek HS, Kim D, Choi HK, Chun YJ. Human steroid sulfatase induces Wnt/beta-catenin signaling and epithelial-mesenchymal transition by upregulating Twist1 and HIF-1alpha in human prostate and cervical cancer cells. *Oncotarget*. 2017; 8(37):61604-61617.

205. Liu XL, Zhang XT, Meng J, Zhang HF, Zhao Y, Li C, Sun Y, Mei QB, Zhang F, Zhang T. ING5 knockdown enhances migration and invasion of lung cancer cells by

inducing EMT via EGFR/PI3K/Akt and IL-6/STAT3 signaling pathways. *Oncotarget*. 2017; 8(33):54265-54276.

206. Li B, Xu WW, Lam AKY, Wang Y, Hu HF, Guan XY, Qin YR, Saremi N, Tsao SW, He QY *et al*. Significance of PI3K/AKT signaling pathway in metastasis of esophageal squamous cell carcinoma and its potential as a target for anti-metastasis therapy. *Oncotarget*. 2017; 8(24):38755-38766.

207. Meng J, Zhang XT, Liu XL, Fan L, Li C, Sun Y, Liang XH, Wang JB, Mei QB, Zhang F *et al*. WSTF promotes proliferation and invasion of lung cancer cells by inducing EMT via PI3K/Akt and IL-6/STAT3 signaling pathways. *Cell Signal*. 2016; 28(11):1673-1682.

208. Yoon C, Cho SJ, Chang KK, Park DJ, Ryeom SW, Yoon SS. Role of Rac1 Pathway in Epithelial-to-Mesenchymal Transition and Cancer Stem-like Cell Phenotypes in Gastric Adenocarcinoma. *Mol Cancer Res*. 2017; 15(8):1106-1116.

209. Mody HR, Hung SW, Naidu K, Lee H, Gilbert CA, Hoang TT, Pathak RK, Manoharan R, Muruganandan S, Govindarajan R. SET contributes to the epithelial-mesenchymal transition of pancreatic cancer. *Oncotarget*. 2017; 8(40):67966-67979.

210. Cristobal I, Rincon R, Manso R, Carames C, Zazo S, Madoz-Gurpide J, Rojo F, Garcia-Foncillas J. Deregulation of the PP2A inhibitor SET shows promising therapeutic implications and determines poor clinical outcome in patients with metastatic colorectal cancer. *Clin Cancer Res*. 2015; 21(2):347-356.

211. Christensen DJ, Chen Y, Oddo J, Matta KM, Neil J, Davis ED, Volkheimer AD, Lanasa MC, Friedman DR, Goodman BK *et al*. SET oncoprotein overexpression in B-cell chronic lymphocytic leukemia and non-Hodgkin lymphoma: a predictor of aggressive disease and a new treatment target. *Blood*. 2011; 118(15):4150-4158.

212. Zhang DZ, Chen BH, Zhang LF, Cheng MK, Fang XJ, Wu XJ. Basic Transcription Factor 3 Is Required for Proliferation and Epithelial-Mesenchymal Transition via Regulation of FOXM1 and JAK2/STAT3 Signaling in Gastric Cancer. *Oncol Res*. 2017; 25(9):1453-1462.

213. Liu Q, Zhou JP, Li B, Huang ZC, Dong HY, Li GY, Zhou K, Nie SL. Basic transcription factor 3 is involved in gastric cancer development and progression. *World J Gastroenterol*. 2013; 19(28):4495-4503.

214. Wang CJ, Franbergh-Karlson H, Wang DW, Arbman G, Zhang H, Sun XF. Clinicopathological significance of BTF3 expression in colorectal cancer. *Tumour Biol*. 2013; 34(4):2141-2146.

215. Yu W, Ma Y, Shankar S, Srivastava RK. SATB2/beta-catenin/TCF-LEF pathway induces cellular transformation by generating cancer stem cells in colorectal cancer. *Sci Rep*. 2017; 7(1):10939.

216. Xu HY, Fang W, Huang ZW, Lu JC, Wang YQ, Tang QL, Song GH, Kang Y, Zhu XJ, Zou CY *et al*. Metformin reduces SATB2-mediated osteosarcoma stem cell-

like phenotype and tumor growth via inhibition of N-cadherin/NF-kB signaling. *Eur Rev Med Pharmacol Sci*. 2017; 21(20):4516-4528.

217. Yang S, Liu Y, Li MY, Ng CSH, Yang SL, Wang S, Zou C, Dong Y, Du J, Long X *et al*. FOXP3 promotes tumor growth and metastasis by activating Wnt/beta-catenin signaling pathway and EMT in non-small cell lung cancer. *Mol Cancer*. 2017; 16(1):124.

218. Wang X, Lang M, Zhao T, Feng X, Zheng C, Huang C, Hao J, Dong J, Luo L, Li X *et al*. Cancer-FOXP3 directly activated CCL5 to recruit FOXP3(+)Treg cells in pancreatic ductal adenocarcinoma. *Oncogene*. 2017; 36(21):3048-3058.

219. Song JJ, Zhao SJ, Fang J, Ma D, Liu XQ, Chen XB, Wang Y, Cheng B, Wang Z. Foxp3 overexpression in tumor cells predicts poor survival in oral squamous cell carcinoma. *BMC Cancer*. 2016; 16:530.

220. Ponnusamy MP, Lakshmanan I, Jain M, Das S, Chakraborty S, Dey P, Batra SK. MUC4 mucin-induced epithelial to mesenchymal transition: a novel mechanism for metastasis of human ovarian cancer cells. *Oncogene*. 2010; 29(42):5741-5754.

221. Zhao X, Yu D, Yang J, Xue K, Liu Y, Jin C. Knockdown of Snail inhibits epithelial-mesenchymal transition of human laryngeal squamous cell carcinoma Hep-2 cells through the vitamin D receptor signaling pathway. *Biochem Cell Biol*. 2017; 95(6):672-678.

222. Malek R, Gajula RP, Williams RD, Nghiem B, Simons BW, Nugent K, Wang H, Taparra K, Lemtiri-Chlieh G, Yoon AR *et al*. TWIST1-WDR5-Hottip Regulates Hoxa9 Chromatin to Facilitate Prostate Cancer Metastasis. *Cancer Res*. 2017; 77(12):3181-3193.

223. Nam EH, Lee Y, Moon B, Lee JW, Kim S. Twist1 and AP-1 cooperatively upregulate integrin alpha5 expression to induce invasion and the epithelial-mesenchymal transition. *Carcinogenesis*. 2015; 36(3):327-337.

224. Weiss MB, Abel EV, Mayberry MM, Basile KJ, Berger AC, Aplin AE. TWIST1 is an ERK1/2 effector that promotes invasion and regulates MMP-1 expression in human melanoma cells. *Cancer Res*. 2012; 72(24):6382-6392.

225. Yang WH, Lan HY, Huang CH, Tai SK, Tzeng CH, Kao SY, Wu KJ, Hung MC, Yang MH. RAC1 activation mediates Twist1-induced cancer cell migration. *Nat Cell Biol*. 2012; 14(4):366-374.

226. Yang J, Mani SA, Donaher JL, Ramaswamy S, Itzykson RA, Come C, Savagner P, Gitelman I, Richardson A, Weinberg RA. Twist, a master regulator of morphogenesis, plays an essential role in tumor metastasis. *Cell*. 2004; 117(7):927-939.

227. Fu J, Qin L, He T, Qin J, Hong J, Wong J, Liao L, Xu J. The TWIST/Mi2/NuRD protein complex and its essential role in cancer metastasis. *Cell Res*. 2011; 21(2):275-289.

228. Niu RF, Zhang L, Xi GM, Wei XY, Yang Y, Shi YR, Hao XS. Up-regulation of Twist induces angiogenesis and correlates with metastasis in hepatocellular carcinoma. *J Exp Clin Cancer Res*. 2007; 26(3):385-394.

229. Ding J, Zhang Z, Pan Y, Liao G, Zeng L, Chen S. Expression and significance of twist, E-cadherin, and N-cadherin in gastrointestinal stromal tumors. *Dig Dis Sci*. 2012; 57(9):2318-2324.

230. Dong P, Kaneuchi M, Watari H, Sudo S, Sakuragi N. MicroRNA-106b modulates epithelial-mesenchymal transition by targeting TWIST1 in invasive endometrial cancer cell lines. *Mol Carcinog*. 2014; 53(5):349-359.

231. Yang Z, Zhang X, Gang H, Li X, Li Z, Wang T, Han J, Luo T, Wen F, Wu X. Up-regulation of gastric cancer cell invasion by Twist is accompanied by N-cadherin and fibronectin expression. *Biochem Biophys Res Commun*. 2007; 358(3):925-930.

232. Lenferink AE, Cantin C, Nantel A, Wang E, Durocher Y, Banville M, Paul-Roc B, Marcil A, Wilson MR, O'Connor-McCourt MD. Transcriptome profiling of a TGF-beta-induced epithelial-to-mesenchymal transition reveals extracellular clusterin as a target for therapeutic antibodies. *Oncogene*. 2010; 29(6):831-844.

233. Phillips S, Kuperwasser C. SLUG: Critical regulator of epithelial cell identity in breast development and cancer. *Cell Adh Migr*. 2014; 8(6):578-587.

234. Bolos V, Peinado H, Perez-Moreno MA, Fraga MF, Esteller M, Cano A. The transcription factor Slug represses E-cadherin expression and induces epithelial to mesenchymal transitions: a comparison with Snail and E47 repressors. *J Cell Sci*. 2003; 116(Pt 3):499-511.

235. Hajra KM, Chen DY, Fearon ER. The SLUG zinc-finger protein represses E-cadherin in breast cancer. *Cancer Res*. 2002; 62(6):1613-1618.

236. Ferrari-Amorotti G, Chiodoni C, Shen F, Cattelani S, Soliera AR, Manzotti G, Grisendi G, Dominici M, Rivasi F, Colombo MP *et al*. Suppression of invasion and metastasis of triple-negative breast cancer lines by pharmacological or genetic inhibition of slug activity. *Neoplasia*. 2014; 16(12):1047-1058.

237. Wu K, Zeng J, Zhou J, Fan J, Chen Y, Wang Z, Zhang T, Wang X, He D. Slug contributes to cadherin switch and malignant progression in muscle-invasive bladder cancer development. *Urol Oncol*. 2013; 31(8):1751-1760.

238. Shirley SH, Greene VR, Duncan LM, Torres Cabala CA, Grimm EA, Kusewitt DF. Slug expression during melanoma progression. *Am J Pathol*. 2012; 180(6):2479-2489.

239. Yang J, Eddy JA, Pan Y, Hategan A, Tabus I, Wang Y, Cogdell D, Price ND, Pollock RE, Lazar AJ *et al*. Integrated proteomics and genomics analysis reveals a novel mesenchymal to epithelial reverting transition in leiomyosarcoma through regulation of slug. *Mol Cell Proteomics*. 2010; 9(11):2405-2413.

240. Casas E, Kim J, Bendesky A, Ohno-Machado L, Wolfe CJ, Yang J. Snail2 is an essential mediator of Twist1-induced epithelial mesenchymal transition and metastasis. *Cancer Res*. 2011; 71(1):245-254.

241. Derynck R, Zhang YE. Smad-dependent and Smad-independent pathways in TGF-beta family signalling. *Nature*. 2003; 425(6958):577-584.

242. Kang Y, Ling J, Suzuki R, Roife D, Chopin-Laly X, Truty MJ, Chatterjee D, Wang H, Thomas RM, Katz MH *et al*. SMAD4 regulates cell motility through transcription of N-cadherin in human pancreatic ductal epithelium. *PLoS One*. 2014; 9(9):e107948.

243. Wu Y, Fu Y, Zheng L, Lin G, Ma J, Lou J, Zhu H, He Q, Yang B. Nutlin-3 inhibits epithelial-mesenchymal transition by interfering with canonical transforming growth factor-beta1-Smad-Snail/Slug axis. *Cancer Lett*. 2014; 342(1):82-91.

244. Takano S, Kanai F, Jazag A, Ijichi H, Yao J, Ogawa H, Enomoto N, Omata M, Nakao A. Smad4 is essential for down-regulation of E-cadherin induced by TGF-beta in pancreatic cancer cell line PANC-1. *J Biochem*. 2007; 141(3):345-351.

245. Fabbri M, Ivan M, Cimmino A, Negrini M, Calin GA. Regulatory mechanisms of microRNAs involvement in cancer. *Expert Opin Biol Ther*. 2007; 7(7):1009-1019.

246. Ceppi P, Peter ME. MicroRNAs regulate both epithelial-to-mesenchymal transition and cancer stem cells. *Oncogene*. 2014; 33(3):269-278.

247. Mudduluru G, Abba M, Batliner J, Patil N, Scharp M, Lunavat TR, Leupold JH, Oleksiuk O, Juraeva D, Thiele W *et al*. A Systematic Approach to Defining the microRNA Landscape in Metastasis. *Cancer Res*. 2015; 75(15):3010-3019.

248. Sher YP, Wang LJ, Chuang LL, Tsai MH, Kuo TT, Huang CC, Chuang EY, Lai LC. ADAM9 up-regulates N-cadherin via miR-218 suppression in lung adenocarcinoma cells. *PLoS One*. 2014; 9(4):e94065.

249. Meng Z, Fu X, Chen X, Zeng S, Tian Y, Jove R, Xu R, Huang W. miR-194 is a marker of hepatic epithelial cells and suppresses metastasis of liver cancer cells in mice. *Hepatology*. 2010; 52(6):2148-2157.

250. Bao C, Li Y, Huan L, Zhang Y, Zhao F, Wang Q, Liang L, Ding J, Liu L, Chen T *et al*. NF-kappaB signaling relieves negative regulation by miR-194 in hepatocellular carcinoma by suppressing the transcription factor HNF-1alpha. *Sci Signal*. 2015; 8(387):ra75.

251. Suzuki T, Mizutani K, Minami A, Nobutani K, Kurita S, Nagino M, Shimono Y, Takai Y. Suppression of the TGF-beta1-induced protein expression of SNAI1 and N-cadherin by miR-199a. *Genes Cells*. 2014; 19(9):667-675.

252. Zhou M, Wang S, Hu L, Liu F, Zhang Q, Zhang D. miR-199a-5p suppresses human bladder cancer cell metastasis by targeting CCR7. *BMC Urol*. 2016; 16(1):64.

253. Gao P, Xing AY, Zhou GY, Zhang TG, Zhang JP, Gao C, Li H, Shi DB. The molecular mechanism of microRNA-145 to suppress invasion-metastasis cascade in gastric cancer. *Oncogene*. 2013; 32(4):491-501.

254. Ma T, Zhao Y, Wei K, Yao G, Pan C, Liu B, Xia Y, He Z, Qi X, Li Z *et al*. MicroRNA-124 Functions as a Tumor Suppressor by Regulating CDH2 and Epithelial-Mesenchymal Transition in Non-Small Cell Lung Cancer. *Cell Physiol Biochem*. 2016; 38(4):1563-1574.

255. Li LZ, Zhang CZ, Liu LL, Yi C, Lu SX, Zhou X, Zhang ZJ, Peng YH, Yang YZ, Yun JP. miR-720 inhibits tumor invasion and migration in breast cancer by targeting TWIST1. *Carcinogenesis*. 2014; 35(2):469-478.

256. Li W, Jiang G, Zhou J, Wang H, Gong Z, Zhang Z, Min K, Zhu H, Tan Y. Down-regulation of miR-140 induces EMT and promotes invasion by targeting Slug in esophageal cancer. *Cell Physiol Biochem*. 2014; 34(5):1466-1476.

257. Zhou JN, Zeng Q, Wang HY, Zhang B, Li ST, Nan X, Cao N, Fu CJ, Yan XL, Jia YL *et al*. MicroRNA-125b attenuates epithelial-mesenchymal transitions and targets stem-like liver cancer cells through small mothers against decapentaplegic 2 and 4. *Hepatology*. 2015; 62(3):801-815.

258. Qiao P, Li G, Bi W, Yang L, Yao L, Wu D. microRNA-34a inhibits epithelial mesenchymal transition in human cholangiocarcinoma by targeting Smad4 through transforming growth factor-beta/Smad pathway. *BMC Cancer*. 2015; 15:469.

259. Yang Y, Liu L, Cai J, Wu J, Guan H, Zhu X, Yuan J, Chen S, Li M. Targeting Smad2 and Smad3 by miR-136 suppresses metastasis-associated traits of lung adenocarcinoma cells. *Oncol Res*. 2013; 21(6):345-352.

260. Liang YJ, Wang QY, Zhou CX, Yin QQ, He M, Yu XT, Cao DX, Chen GQ, He JR, Zhao Q. MiR-124 targets Slug to regulate epithelial-mesenchymal transition and metastasis of breast cancer. *Carcinogenesis*. 2013; 34(3):713-722.

261. Chen S, Chen X, Xiu YL, Sun KX, Zhao Y. Inhibition of Ovarian Epithelial Carcinoma Tumorigenesis and Progression by microRNA 106b Mediated through the RhoC Pathway. *PLoS One*. 2015; 10(5):e0125714.

262. Liang J, Li X, Li Y, Wei J, Daniels G, Zhong X, Wang J, Sfanos K, Melamed J, Zhao J *et al*. LEF1 targeting EMT in prostate cancer invasion is mediated by miR-181a. *Am J Cancer Res*. 2015; 5(3):1124-1132.

263. Li H, Zhang P, Sun X, Sun Y, Shi C, Liu H, Liu X. MicroRNA-181a regulates epithelial-mesenchymal transition by targeting PTEN in drug-resistant lung adenocarcinoma cells. *Int J Oncol*. 2015; 47(4):1379-1392.

264. Volk T, Volberg T, Sabanay I, Geiger B. Cleavage of A-CAM by endogenous proteinases in cultured lens cells and in developing chick embryos. *Dev Biol*. 1990; 139(2):314-326.

265. Harrison OJ, Corps EM, Berge T, Kilshaw PJ. The mechanism of cell adhesion by classical cadherins: the role of domain 1. *J Cell Sci*. 2005; 118(Pt 4):711-721.

266. Blaschuk OW. N-cadherin antagonists as oncology therapeutics. *Philosophical transactions of the Royal Society of London Series B, Biological sciences*. 2015; 370(1661):20140039.

267. Williams E, Williams G, Gour BJ, Blaschuk OW, Doherty P. A novel family of cyclic peptide antagonists suggests that N-cadherin specificity is determined by amino acids that flank the HAV motif. *J Biol Chem*. 2000; 275(6):4007-4012.

268. Shintani Y, Fukumoto Y, Chaika N, Grandgenett PM, Hollingsworth MA, Wheelock MJ, Johnson KR. ADH-1 suppresses N-cadherin-dependent pancreatic cancer progression. *Int J Cancer*. 2008; 122(1):71-77.

269. Li H, Price DK, Figg WD. ADH1, an N-cadherin inhibitor, evaluated in preclinical models of angiogenesis and androgen-independent prostate cancer. *Anticancer Drugs*. 2007; 18(5):563-568.

270. Lammens T, Swerts K, Derycke L, De Craemer A, De Brouwer S, De Preter K, Van Roy N, Vandesompele J, Speleman F, Philippe J *et al*. N-cadherin in neuroblastoma disease: expression and clinical significance. *PLoS One*. 2012; 7(2):e31206.

271. Kelland L. Drug evaluation: ADH-1, an N-cadherin antagonist targeting cancer vascularization. *Curr Opin Mol Ther*. 2007; 9(1):86-91.

272. Erez N, Zamir E, Gour BJ, Blaschuk OW, Geiger B. Induction of apoptosis in cultured endothelial cells by a cadherin antagonist peptide: involvement of fibroblast growth factor receptor-mediated signalling. *Exp Cell Res*. 2004; 294(2):366-378.

273. Perotti A, Sessa C, Mancuso A, Noberasco C, Cresta S, Locatelli A, Carcangiu ML, Passera K, Braghetti A, Scaramuzza D *et al*. Clinical and pharmacological phase I evaluation of Exherin (ADH-1), a selective anti-N-cadherin peptide in patients with N-cadherin-expressing solid tumours. *Ann Oncol*. 2009; 20(4):741-745.

274. Yarom N, Stewart D, Malik R, Wells J, Avruch L, Jonker DJ. Phase I clinical trial of Exherin (ADH-1) in patients with advanced solid tumors. *Current clinical pharmacology*. 2013; 8(1):81-88.

275. Augustine CK, Yoshimoto Y, Gupta M, Zipfel PA, Selim MA, Febbo P, Pendergast AM, Peters WP, Tyler DS. Targeting N-cadherin enhances antitumor activity of cytotoxic therapies in melanoma treatment. *Cancer Res*. 2008; 68(10):3777-3784.

276. Turley RS, Tokuhisa Y, Toshimitsu H, Lidsky ME, Padussis JC, Fontanella A, Deng W, Augustine CK, Beasley GM, Davies MA *et al*. Targeting N-cadherin increases vascular permeability and differentially activates AKT in melanoma. *Ann Surg*. 2015; 261(2):368-377.

277. Beasley GM, McMahon N, Sanders G, Augustine CK, Selim MA, Peterson B, Norris R, Peters WP, Ross MI, Tyler DS. A phase 1 study of systemic ADH-1 in combination with melphalan via isolated limb infusion in patients with locally advanced in-transit malignant melanoma. *Cancer*. 2009; 115(20):4766-4774.

278. Beasley GM, Riboh JC, Augustine CK, Zager JS, Hochwald SN, Grobmyer SR, Peterson B, Royal R, Ross MI, Tyler DS. Prospective multicenter phase II trial of systemic ADH-1 in combination with melphalan via isolated limb infusion in patients with advanced extremity melanoma. *J Clin Oncol*. 2011; 29(9):1210-1215.

279. Cosgrove BD, Mui KL, Driscoll TP, Caliari SR, Mehta KD, Assoian RK, Burdick JA, Mauck RL. N-cadherin adhesive interactions modulate matrix mechanosensing and fate commitment of mesenchymal stem cells. *Nat Mater*. 2016; 15(12):1297-1306.

280. Ganz A, Lambert M, Saez A, Silberzan P, Buguin A, Mege RM, Ladoux B. Traction forces exerted through N-cadherin contacts. *Biol Cell*. 2006; 98(12):721-730.

281. Chopra A, Tabdanov E, Patel H, Janmey PA, Kresh JY. Cardiac myocyte remodeling mediated by N-cadherin-dependent mechanosensing. *Am J Physiol Heart Circ Physiol*. 2011; 300(4):H1252-1266.

282. Lee E, Ewald ML, Sedarous M, Kim T, Weyers BW, Truong RH, Yamada S. Deletion of the cytoplasmic domain of N-cadherin reduces, but does not eliminate, traction force-transmission. *Biochem Biophys Res Commun*. 2016; 478(4):1640-1646.

283. Su Y, Li J, Witkiewicz AK, Brennan D, Neill T, Talarico J, Radice GL. N-cadherin haploinsufficiency increases survival in a mouse model of pancreatic cancer. *Oncogene*. 2012; 31(41):4484-4489.

284. Cochrane CR, Szczepny A, Watkins DN, Cain JE. Hedgehog Signaling in the Maintenance of Cancer Stem Cells. *Cancers (Basel)*. 2015; 7(3):1554-1585.

285. Burden-Gulley SM, Gates TJ, Craig SE, Lou SF, Oblander SA, Howell S, Gupta M, Brady-Kalnay SM. Novel peptide mimetic small molecules of the HAV motif in N-cadherin inhibit N-cadherin-mediated neurite outgrowth and cell adhesion. *Peptides*. 2009; 30(12):2380-2387.

286. Devemy E, Blaschuk OW. Identification of a novel N-cadherin antagonist. *Peptides*. 2008; 29(11):1853-1861.

287. Doro F, Colombo C, Alberti C, Arosio D, Belvisi L, Casagrande C, Fanelli R, Manzoni L, Parisini E, Piarulli U *et al*. Computational design of novel peptidomimetic inhibitors of cadherin homophilic interactions. *Org Biomol Chem*. 2015; 13(9):2570-2573.

Chapter 2

# Therapeutic targeting of N-cadherin is an effective treatment for multiple myeloma

# Statement of Authorship

| | |
|---|---|
| Title of Paper | Therapeutic targeting of N-cadherin is an effective treatment for multiple myeloma |
| Publication Status | ☑ Published ☐ Accepted for Publication<br>☐ Submitted for Publication ☐ Unpublished and Unsubmitted work written in manuscript style |
| Publication Details | **Mrozik K.M.**, Cheong C.M., Hewett D.R., Chow A.W.S., Blaschuk O.W., Zannettino A.C.W., Vandyke K.<br>British Journal of Haematology, 2015, 171, 387–399 |

## Principal Author

| | | | |
|---|---|---|---|
| Name of Principal Author (Candidate) | Krzysztof Marek Mrozik | | |
| Contribution to the Paper | Primary author of manuscript<br>Designed and performed experiments<br>Data analysis and interpretation | | |
| Overall percentage (%) | 80% | | |
| Certification: | This paper reports on original research I conducted during the period of my Higher Degree by Research candidature and is not subject to any obligations or contractual agreements with a third party that would constrain its inclusion in this thesis. I am the primary author of this paper. | | |
| Signature | | Date | 15/02/18 |

## Co-Author Contributions

By signing the Statement of Authorship, each author certifies that:
the candidate's stated contribution to the publication is accurate (as detailed above);
permission is granted for the candidate in include the publication in the thesis; and
the sum of all co-author contributions is equal to 100% less the candidate's stated contribution.

| | | | |
|---|---|---|---|
| Name of Co-Author | Chee M. Cheong | | |
| Contribution to the Paper | Assisted with experiments | | |
| Signature | | Date | 14/02/18 |

| | | | |
|---|---|---|---|
| Name of Co-Author | Duncan R. Hewett | | |
| Contribution to the Paper | Critical review of manuscript<br>Assisted with experiments | | |
| Signature | | Date | 14/02/17 |

| | | | |
|---|---|---|---|
| Name of Co-Author | Annie W.S. Chow | | |
| Contribution to the Paper | Assisted with experiments | | |
| Signature | On behalf of A.W.S Chow | Date | 15/02/18 |

| | | | |
|---|---|---|---|
| Name of Co-Author | Orest W. Blaschuk | | |
| Contribution to the Paper | Critical review of manuscript | | |
| Signature | | Date | 12/02/18 |

| | | | |
|---|---|---|---|
| Name of Co-Author | Andrew C.W. Zannettino | | |
| Contribution to the Paper | Conceptualisation and critical review of manuscript<br>Experimental design | | |
| Signature | | Date | 14/02/18 |

| | | | |
|---|---|---|---|
| Name of Co-Author | Kate Vandyke | | |
| Contribution to the Paper | Conceptualisation and critical review of manuscript<br>Experimental design<br>Assisted with experiments | | |
| Signature | | Date | 15/02/18 |

**Therapeutic targeting of N-cadherin is an effective treatment for multiple myeloma**

Krzysztof M. Mrozik[1,2], Chee M. Cheong[1,2], Duncan R. Hewett[1,2], Annie W.S. Chow[1], Orest W. Blaschuk[3], Andrew C.W. Zannettino[1,2,4*], Kate Vandyke[1,2*]

Author Affiliations:

1. Myeloma Research Laboratory, Adelaide Medical School, Faculty of Health and Medical Sciences, The University of Adelaide, Adelaide, Australia
2. Cancer Theme, South Australian Health and Medical Research Institute, Adelaide, Australia
3. Division of Urology, Department of Surgery, McGill University, Montreal, Canada
4. Centre for Cancer Biology, University of South Australia, Adelaide, Australia

* co-senior authors

Running title:

Therapeutic targeting of N-cadherin is an effective treatment for MM

Keywords:

N-cadherin, multiple myeloma, adhesion, extravasation, ADH-1

## 2.1 Abstract

Elevated expression of the cell adhesion molecule N-cadherin (*CDH2*) is associated with poor prognosis in newly-diagnosed multiple myeloma (MM) patients. In this study, we investigated whether targeting of N-cadherin represents a potential treatment for the ~50% of MM patients with elevated N-cadherin. Initially, we stably knocked-down N-cadherin in the mouse MM plasma cell (PC) line 5TGM1 to assess the functional role of N-cadherin in MM pathogenesis. When compared with 5TGM1-scramble-shRNA cells, 5TGM1-*Cdh2*-shRNA cells had significantly reduced adhesion to bone marrow endothelial cells. However, N-cadherin knock-down did not affect 5TGM1 cell proliferation or adhesion to bone marrow stromal cells. In the C57BL/KaLwRij murine MM model, mice intravenously inoculated with 5TGM1-*Cdh2*-shRNA cells showed significantly decreased tumour burden after four weeks, compared with animals bearing 5TGM1-scramble-shRNA cells. Finally, the N-cadherin antagonist ADH-1 had no effect on tumour burden in the established disease setting, whereas up-front ADH-1 treatment resulted in significantly reduced tumour burden after four weeks. Our findings demonstrate that N-cadherin may play a key role in the extravasation of circulating MM PCs promoting bone marrow homing. Moreover, these studies suggest that N-cadherin may represent a viable therapeutic target to prevent the dissemination of MM PCs and delay MM disease progression.

## 2.2 Introduction

Multiple myeloma (MM) is an incurable haematological malignancy characterized by the clonal proliferation of immunoglobulin-producing plasma cells (PCs) within the bone marrow (BM).[1] Despite recent advances in therapeutics and improvements in overall survival rates, the prognosis of patients with intermediate to high-risk MM remains relatively poor.[2] During MM disease progression, MM PCs egress from the localized BM microenvironment, enter the circulation and disseminate to distal medullary sites.[3] MM PC extravasation and BM homing is a multi-step process requiring attachment to the BM endothelial lumen, trans-endothelial migration and colonisation within the new stromal microenvironment. These processes are mediated by stromal cell-derived chemokines, which promote MM PC migration, as well as dynamic adhesive interactions.[4-6] MM PCs express several adhesion molecules which mediate the physical interactions between PCs and the cellular (endothelial and stromal cells) and acellular (extracellular matrix proteins) components of the BM microenvironment. Previous studies have implicated the adhesion molecules CD44, VLA-4 and PSGL-1 in the attachment of MM PCs to BM endothelial cells (BMECs).[7-9] Studies have also demonstrated that functional blocking of CD44 and PSGL-1 inhibits MM PC extravasation and BM homing *in vivo*.[8,9] Moreover, interactions between adhesion molecules expressed by MM PCs and their cognate adhesion partners activate numerous signal transduction cascades and positive feed-back loops which promote MM PC growth, survival, migration and resistance to chemotherapeutic agents.[10-12] Given that malignant transformation of normal PCs is often associated with the dysregulated expression of adhesion molecules[13,14], the targeting of adhesion molecules represents an attractive therapeutic modality for MM.

N-cadherin (encoded by the gene *CDH2*) is a calcium-binding, single pass transmembrane glycoprotein expressed by a variety of cell types including neuronal, smooth muscle and endothelial cells.[15-19] N-cadherin is a homophilic cell adhesion molecule that plays an important role in embryogenesis, morphogenesis and cancer pathogenesis.[20] N-cadherin consists of 5 extracellular domains and mediates cell-cell binding through the reciprocal insertion of a Trp2 side chain located near the N-terminus of the first extracellular domain (EC1) into the hydrophobic pocket of the apposed partner EC1 domain. Lateral clustering of N-cadherin through EC1 and the second extracellular domain (EC2) further strengthens the adhesive interaction.[19,21-24]

The cadherin cytoplasmic domain is functionally linked to the actin cytoskeleton via β-catenin, α-catenin and p120 catenin, which also stabilizes the adhesive contacts.[25] Additionally, N-cadherin is implicated in the activation of several signal transduction pathways including MAPK-ERK (via cross-talk with FGF receptor) and PI3K/Akt, and signalling via Rho family GTPases, which regulates cell survival, proliferation, migration and differentiation.[26-29] Sequestration of β-catenin to the plasma membrane by N-cadherin may also modulate β-catenin/TCF-dependent transcription of canonical Wnt-signalling gene targets.[26,30] In the context of cancer, studies have shown that N-cadherin mediates binding between tumour cells and stromal cells[28,31,32], osteoblasts[33] and endothelial cells.[34,35] Studies have also shown that N-cadherin promotes the survival, migration, invasion and metastatic capacity of solid tumour cell lines.[28,34,36,37] N-cadherin expression is up-regulated during tumour cell epithelial-to-mesenchymal transition (EMT) which involves a loss of cell polarity and an increase in dynamic cellular interactions, and consequently promotes tumour cell migration and dissemination.[28,35,38-40]. Indeed, aberrant expression of N-cadherin is strongly associated with highly aggressive forms of epithelial malignancies including breast, prostate, bladder and pancreatic cancer.[41-45] Notably, the disulphide-linked N-cadherin antagonist ADH-1 (N-Ac-CHAVC-$NH_2$) has been shown to inhibit tumour growth in pre-clinical models of pancreatic cancer and, when used in combination with melphalan, limits melanoma tumour growth.[19,46,47] Moreover, phase I and II clinical trials with ADH-1 have demonstrated disease control, and improved initial responses to melphalan, in some patients with advanced solid tumours.[48-51]

Our recent studies[52], and those of others[33], have shown that N-cadherin gene expression is up-regulated in PCs in approximately 50% of newly-diagnosed MM patients. In addition, we have recently demonstrated that circulating N-cadherin levels, which correlate with membrane N-cadherin expression in MM PCs, are up-regulated in approximately 30% of newly diagnosed MM patients. Moreover, these patients have decreased progression-free and overall survival compared with patients with normal circulating N-cadherin levels demonstrating that N-cadherin is a negative prognostic indicator in patients with MM.[52] Previous studies have implicated N-cadherin in BM homing of MM PCs and in MM PC-osteoblast interactions.[33] In this study, we investigated the effect of N-cadherin knock-down on MM PC behaviour *in vitro* using the murine MM PC line 5TGM1. Furthermore, utilising the C57BL/KaLwRij murine model of MM, we also assessed whether targeting of N-cadherin by knock-down or

pharmacological inhibition with ADH-1 is a potential therapeutic modality for the treatment of MM.

## 2.3 Methods

### 2.3.1 Mouse tissue and PC isolation

C57BL/KaLwRij mice, originally kindly provided by Andrew Spencer (Monash University, Clayton, Australia) were bred and housed at the SA Pathology Animal Care Facility (Adelaide, Australia). All procedures were performed with approval of the SA Pathology and University of Adelaide Animal Ethics Committees. Brain tissue from C57BL/KaLwRij mice was snap frozen in liquid nitrogen and homogenised in TRIzol® (Life Technologies, Carlsbad, CA). Murine BM PCs and BM stromal cells (BMSCs) were isolated from C57BL/KaLwRij mice as previously described.[53,54] Briefly, mouse femora and tibiae were excised, the bone marrow was flushed and the bones were crushed prior to isolation of MSC cultures.[53] The BM mononuclear fraction was isolated by Ficoll density gradient separation and the cells were blocked with 110µg/mL murine gamma globulin (Jackson Laboratories, Bar Harbor, ME, USA) and stained with rat anti-mouse CD138 (R & D Systems, Minneapolis, MN) followed by goat anti-rat IgG PE (Southern Biotech, Birmingham, AL). $CD138^+$ BM PCs were then isolated by flow cytometry (FACSAria II, BD Biosciences, San Jose, CA) and total RNA was isolated from sorted cells using an RNAqueous Micro kit (Life Technologies).

### 2.3.2 Cell culture

All cell culture reagents were sourced from Sigma-Aldrich (St Louis, MO, USA), unless otherwise stated. All media were supplemented with 2mM L-glutamine, 100U/ml penicillin, 100µg/ml streptomycin, 1mM sodium pyruvate and 10mM HEPES buffer, unless otherwise specified. The mouse MM PC line 5TGM1 was maintained in Iscove's modified Dulbecco's medium (IMDM) with 20% foetal calf serum (FCS; Thermo Fisher Scientific, Waltham, MA, USA) and supplements. The human BM endothelial cell (BMEC) line TrHBMEC[55] was maintained in M199 medium with 20% FCS and supplemented with 0.1% sodium bicarbonate, 1x MEM Non-Essential Amino Acids, 100U/ml penicillin, 100ug/ml streptomycin, 1mM sodium pyruvate and 10mM HEPES buffer, 50µg/ml endothelial cell growth factor (BD Biosciences) and 100U/ml heparin. C57BL/KaLwRij BMSCs were maintained in alpha-modified Eagle’s medium (α-MEM) with 10% FCS, 100mM L-ascorbate-2-phosphate and supplements.

### 2.3.3 Generation of a 5TGM1 N-cadherin (*Cdh2*) shRNA cell line

The pFIV-H1-mCherry vector was created by excising the GFP cassette from pFIV-H1-GFP (System Biosciences, Mountain View, CA) using XbaI and SalI and replacing it with the mCherry cassette from pMSCV-mCherry. To generate stable knock-down cell lines, an RNA duplex targeting mouse *Cdh2* (AAGGATGTGCACGAAGGACAG)[56] was cloned into pFIV-H1-mCherry. A scrambled sequence (AAGCCACGGCCATAGAAGGCA) was used as a control. Following lentiviral infection of 5TGM1-luc cells (expressing a dual GFP and luciferase reporter construct)[54,57], GFP and mCherry-expressing cells were sorted by FACS using a Beckman Coulter Epics AltraHyperSort (Beckman Coulter, Miami, FL, USA) and single cell clones were generated. A pool of 3 clonal 5TGM1-*Cdh2*-shRNA lines was used for subsequent *in vitro* and *in vivo* assays.

### 2.3.4 Quantitative PCR

Total RNA was isolated using TRIzol® and cDNA was synthesised using Superscript® III First-Strand Synthesis System (Life Technologies). Quantitative real-time PCR (qPCR) was performed using a Rotor-Gene (QIAGEN, Valencia, CA, USA) using primers for *Cdh2* (Fwd 5'-ATCACTACTATTGCCGTTTTGG-3'; Rev 5'-CTCCGGCTCTTGAGGTAACA-3') and *Actb* (Fwd 5'-GATCATTGCTCCTCCTGAGC-3'; Rev 5'-GTCATAGTCCGCCTAGAAGCAT-3').

### 2.3.5 Western blotting

Whole cell lysates were prepared and polyacrylamide gel electrophoresis was performed as described previously.[54] Following transfer, the polyvinylidinedifluoride (PVDF) membrane was incubated in blocking buffer (2.5% ECL Blocking Agent [GE Healthcare, Little Chalfont, Buckinghamshire] in 0.1% Tween 20 Tris-buffered saline) for 2 hours at room temperature. The PVDF membrane was then probed overnight at 4°C with a monoclonal rabbit anti-mouse N-cadherin antibody (Millipore; Billerica, MA, USA) diluted 1:10,000 in blocking buffer. Primary antibody binding was detected by incubating membranes with an alkaline phosphatase (AP)-conjugated anti-rabbit IgG (Millipore) diluted 1:2500 in blocking buffer for 1 hour at room temperature. Proteins were visualised with ECL detection reagent (GE Healthcare) on a Typhoon FLA 7000 (GE Healthcare).

To ensure equal loading of total protein, the membrane was stripped using Western Blot Recycling kit (Alpha Diagnostic International Inc., San Antonio, TX, USA) and probed for 1 hour at room temperature with rat anti-α-tubulin (Abcam; Cambridge, UK) at 200ng/ml in blocking buffer. The membrane was then incubated for 1 hour at room temperature with AP-conjugated anti-rat IgG (Millipore; diluted 1:5000) and proteins visualised with ECL detection reagent. N-cadherin levels were quantitated and normalised to α-tubulin levels using ImageQuant TL Software (GE Healthcare).

### 2.3.6 Proliferation assays

For WST-1 assays, 5TGM1 cells were plated at $1x10^5$ cells/ml in triplicate in phenol red-free IMDM containing 20% FCS and supplements using a 96-well plate. Relative cell numbers were assessed over 3 days using WST-1 (Roche, Basel, Switzerland) as per manufacturer's instructions.

To assess cell numbers by bioluminescence imaging (BLI), 5TGM1 cells were plated at $5x10^4$/ml in triplicate in IMDM using black clear-bottomed 96-well plates (Corning Life Science, New York, USA). For proliferation assays in co-culture, BMSCs were irradiated at 30 Gy and seeded at $1.5x10^5$/ml in black clear-bottomed 96-well plates 24 hours prior to the addition of the 5TGM1 cells. After 3 days, firefly D-luciferin (Biosynth AG, Staad, Switzerland) was added to wells with a final concentration of 150ng/ml and incubated for 20 mins at 37°C. Bioluminescence (photons/sec) was measured and analysed using the Xenogen IVIS 100 (Caliper Life Sciences, Hopkinton, MA, USA) and Living Image software (PerkinElmer, Waltham, MA). Absolute cell numbers were calculated using a standard curve.

5TGM1-scramble-shRNA cells and 5TGM1-*Cdh2*-shRNA cells displayed equivalent levels of basal mitochondrial dehydrogenase activity (WST-1 assay) and bioluminescence, allowing for direct comparison between the cell lines (data not shown).

### 2.3.7 Adhesion assays

Adhesion under static conditions was performed as previously described.[57] For adhesion to cell monolayers, non-irradiated BMSCs or BMECs were plated at $1x10^5$/ml 24 hours prior to adhesion assay. 5TGM1 cells were added at $1x10^6$/ml in triplicate and incubated at 37°C. After 10 minutes, non-adherent 5TGM1 cells were gently removed by aspiration followed by 3 washes with IMDM with 20% FCS and supplements and cell

number was quantitated by BLI as described above. For adhesion to N-cadherin-Fc, 96-well plates were coated with 10μg/ml recombinant human N-cadherin-Fc (R&D Systems, Northeast Minneapolis, MN, USA) or human IgG-Fc fragment (Rockland Immunochemicals, Limerick, PA, USA) for 2 hours at 37°C. After blocking wells with 1% BSA in IMDM for 2 hours at 37°C, 5TGM1 cells were added at $1x10^6$/ml in triplicate and incubated at 37°C. After 2 hours, non-adherent 5TGM1 cells were gently removed by aspiration and 1 wash with IMDM with 20% FCS and supplements and adherent cells were quantitated by BLI. The percentage of 5TGM1 cells adherent to cell monolayers or N-cadherin-Fc was calculated relative to total cell input, following subtraction of the untreated or IgG-Fc controls, respectively.

Adhesion under shear stress was performed using a parallel plate flow chamber assay (GlycoTech, Gaithersburg, MD, USA).[58] Non-irradiated BMECs were seeded at $6x10^4/cm^2$ ($5x10^5$ cells in total) in 35mm dishes (Corning) 24 hours prior to the adhesion assay. BMECs were stimulated with 5ng/ml TNF-α for 4 hours prior to the assay. Using a syringe pump (New Era Pump Systems, Farmingdale, NY, USA), a total of $6x10^6$ 5TGM1 cells in IMDM with 2% FCS and supplements were pre-warmed to 37°C and were perfused across BMECs at 2 dynes/$cm^2$ (1.25ml/min using a 10mm gasket window width) to mimic physiologic shear forces within the vasculature.[59,60] After flushing away non-adherent cells with IMDM + 2% FCS with supplements, the average number of adherent 5TGM1 cells was enumerated over 7 fields of view. 5TGM1 cells were visualized using an inverted microscope and digital video recorder (Olympus, Tokyo, Japan).

### 2.3.8 Trans-well and trans-endothelial migration assays

Migration assays were performed using trans-wells (8 μm polycarbonate membrane; Costar) in a 24-well plate with a FCS concentration gradient (0% and 20% in upper and lower chambers, respectively), as previously described.[57] For trans-well migration assays, 5TGM1 cells ($1x10^5$ per trans-well) were seeded in triplicate trans-wells in IMDM with supplements and cell migration towards IMDM with 20% FCS and supplements was assessed after 24 hours. For trans-endothelial migration assays, $1x10^4$ BMECs were plated per trans-well and were allowed to adhere for 24 hours. 5TGM1 cells ($5x10^5$ per trans-well) were then added to triplicate trans-wells and cell migration to the lower chamber was assessed after 8 hours. The number of migrated cells was

enumerated using an inverted microscope and digital camera (Olympus) and ImageJ software (http://imagej.nih.gov/ij/).

### 2.3.9 Gelatine zymography

To assess matrix metalloproteinase 9 (MMP9) activity, 5TGM1 cells were cultured at $2x10^5$/ml in a 6-well plate and conditioned media was collected after 3 days. Conditioned media (20µl) was run on a gelatine-sodium dodecyl sulphate-polyacrylamide gel (30% acrylamide and 1% gelatine) as previously described.[61] The gel was incubated overnight in MMP9 activation buffer (1.25% Triton X-100, 10mM Tris-HCl, 5mM $CaCl_2$, 1µM $ZnCl_2$) at 37°C. The gel was then stained with 0.25% Coomassie Blue in de-stain solution (50% (v/v) methanol and 10% (v/v) acetic acid in water) for 2 hours and de-stained for 2 hours. Clear zones were imaged on a Typhoon FLA 7000.

### 2.3.10 Animal studies

C57BL/KaLwRij mice (6-8 weeks old) were inoculated with $5x10^5$ 5TGM1-scramble-shRNA cells or 5TGM1-*Cdh2*-shRNA cells in 100µl phosphate-buffered saline (PBS) via tail vein injection as previously described.[54,62] After 2, 3 and 4 weeks, mice were intraperitoneally administered 150mg/kg firefly D-luciferin (diluted in PBS; 100µl volume), bioluminescence was measured after 10 mins using the Xenogen IVIS 100 system and total body MM tumour burden was assessed using Living Image software. Total body MM tumour burden, as assessed by BLI at 4 weeks, closely correlates with serum paraprotein levels as an independent measure of MM tumour burden ($n$ = 34 mice; $P < 0.0001$, $R^2 = 0.7874$; supplementary Fig. 1).

For N-cadherin inhibition studies with the N-cadherin antagonist ADH-1[19], 6–8-week-old C57BL/KaLwRij mice were inoculated with $5x10^5$ parental 5TGM1-luc cells in 100µl phosphate-buffered saline (PBS) via tail vein injection. Mice were intraperitoneally injected once daily with either the N-cadherin antagonist ADH-1 (N-Ac-CHAVC-$NH_2$) (100mg/kg/day in PBS; CanPeptide, Pointe-Claire, Canada) or PBS vehicle alone, commencing immediately prior to 5TGM1 cell injection (up-front treatment group) or 1 week after 5TGM1 cell injection (delayed treatment group) for the duration of the experiment. Tumour burden was assessed 2, 3 and 4 weeks following tumour inoculation using BLI.

### 2.3.11 Statistical analyses

Statistical analyses were performed using GraphPad Prism 6. *In vitro* assays were analysed using a paired *t* test or two-way ANOVA. Tumour burden was analysed using a two-way ANOVA with Bonferroni's multiple comparisons test. The correlation between total body MM tumour burden, as assessed by BLI and serum paraprotein levels, was analysed by Pearson correlation.

## 2.4 Results

### 2.4.1 N-cadherin expression in 5TGM1 cell lines

The expression of the N-cadherin gene, *Cdh2*, in 5TGM1 cells was assessed by qPCR. While *Cdh2* was not expressed in normal murine BM PCs, *Cdh2* expression in 5TGM1 cells was approximately 5-fold higher than in mouse positive control cells (brain tissue and BMSCs) (Figure 2.1A). Expression of *CDH2* was also detected in human BMECs (data not shown). C57BL/KaLwRij mouse-derived BMSC and human BMECs also exhibited considerable expression of N-cadherin protein (Figure 2.1B). Following stable 5TGM1 *Cdh2*-shRNA knock-down, expression of N-cadherin protein was reduced by 60%, as assessed by Western blot, when compared with 5TGM1-scramble-shRNA control cells (Figure 2.1B).

### 2.4.2 5TGM1 cell proliferation and adhesion to BMSCs is unaffected by N-cadherin knock-down

Basal proliferation of 5TGM1 cells following N-cadherin shRNA-mediated knock-down was unaffected, relative to 5TGM1-scramble-shRNA cells, over a 3 day time course as shown using a WST-1 assay (scramble-shRNA: 1.55 ± 0.14 A450 [mean ± SD]; *Cdh2*-shRNA: 1.51 ± 0.14; after 3 days; $P = 0.99$) (Figure 2.2A). Similarly, there was no difference between 5TGM1-scramble-shRNA and 5TGM1-*Cdh2*-shRNA cell numbers after 3 days of culture, as assessed by BLI (scramble-shRNA: 60.86 ± 11.00 [$x10^3$] cells/well; *Cdh2*-shRNA: 50.82 ± 8.66; $P = 0.22$) (Figure 2.2B). Given that C57BL/KaLwRij mouse-derived BMSCs express abundant N-cadherin (Figure 2.1A,B) and that MM PC interactions with stromal cells are important in cell survival and drug resistance in MM[63,64], we assessed the effect of N-cadherin knock-down on 5TGM1 cell proliferation in co-culture with BMSCs and on adhesion to confluent BMSC monolayers. We found no difference in 5TGM1 cell numbers, as assessed by BLI, between 5TGM1-scramble-shRNA and 5TGM1-*Cdh2*-shRNA cells after 3 days of co-culture with BMSCs (scramble-shRNA: 41.84 ± 6.33 [$x10^3$] cells/well; *Cdh2*-shRNA 32.92 ± 2.50; $P = 0.20$) (Figure 2.2C). In addition, there was no difference in the adhesion of 5TGM1-scramble-shRNA cells and 5TGM1-*Cdh2*-shRNA cells to BMSC monolayers (scramble-shRNA: 46.9 ± 1.7% adherence [mean ± SD]; *Cdh2*-shRNA: 44.7 ± 2.3%; $P = 0.13$) (Figure 2.3A).

**Figure 2.1. N-cadherin expression in C57BL/KaLwRij mouse tissues and 5TGM1 cell lines.** 5TGM1 cells express high levels of *Cdh2* compared with positive control C57BL/KaLwRij mouse-derived brain tissue and BMSCs, and negative control C57BL/KaLwRij PCs, as shown by qPCR. Data was normalised to *Actb* expression. Graph depicts mean ± SD of 2 independent experiments (**A**). C57BL/KaLwRij mouse BMSCs and human BMECs express N-cadherin protein as shown by Western blot. Levels of N-cadherin protein is reduced by 60% in 5TGM1-*Cdh2*-shRNA cells compared with 5TGM1-scramble-shRNA cells. α-tubulin was used as a loading control (**B**).

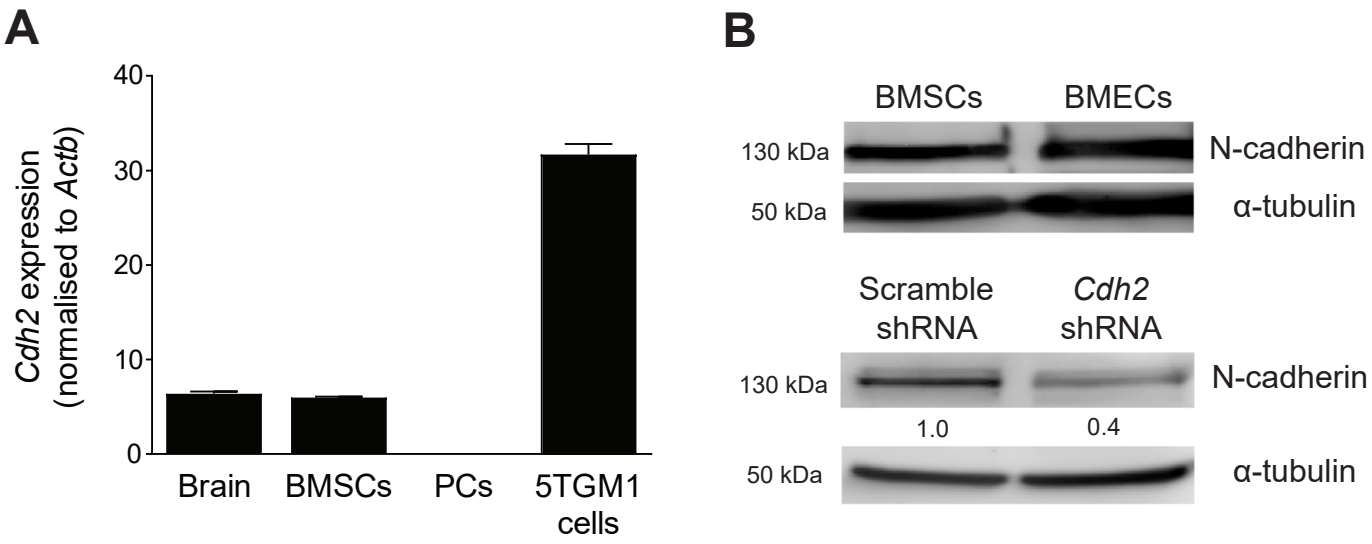
A
Cdh2 expression (normalised to Actb)
40
30
20
10
0
Brain
BMSCs
PCs
5TGM1 cells
B
BMSCs
BMECs
130 kDa
N-cadherin
50 kDa
α-tubulin
Scramble shRNA
Cdh2 shRNA
130 kDa
N-cadherin
1.0
0.4
50 kDa
α-tubulin

**Figure 2.2. N-cadherin does not affect the proliferation of 5TGM1 cells *in vitro*.** Basal proliferation of 5TGM1-*Cdh2*-shRNA cells is no different from that of 5TGM1-scramble-shRNA cells after 3 days as assessed by WST-1 assay (**A**) and BLI (**B**). Graphs depict mean ± SEM of 3 and 5 independent experiments, respectively. shRNA-mediated N-cadherin knockdown has no effect on proliferation of 5TGM1 cells in co-culture with C57BL/KaLwRij mouse-derived BMSCs as assessed by bioluminescence imaging after 3 days. Graph depicts mean ± SEM of 4 independent experiments (**C**).

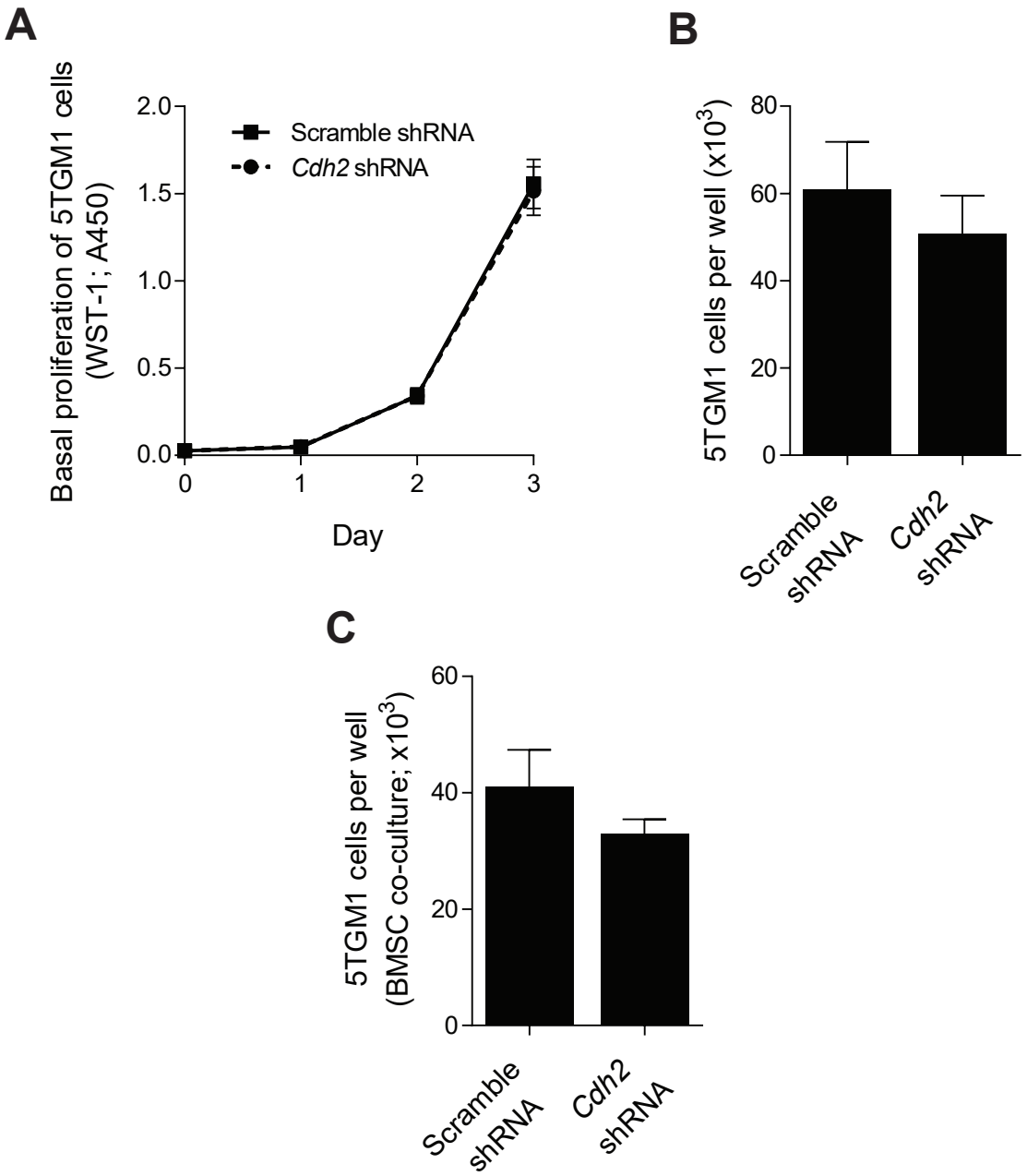
A
Basal proliferation of 5TGM1 cells (WST-1; A450)
2.0
1.5
1.0
0.5
0.0
0
1
2
3
Day
Scramble shRNA
Cdh2 shRNA
B
5TGM1 cells per well (x10^3)
80
60
40
20
0
Scramble shRNA
Cdh2 shRNA
C
5TGM1 cells per well (BMSC co-culture; x10^3)
60
40
20
0
Scramble shRNA
Cdh2 shRNA

**Figure 2.3. N-cadherin expression modulates the adhesive capacity of 5TGM1 cells to BMECs *in vitro*.** Adhesion of 5TGM1-*Cdh2*-shRNA cells to monolayers of C57BL/KaLwRij BMSCs is no different from that of 5TGM1-scramble-shRNA cells after 10 minutes. Graph depicts mean ± range of 2 independent experiments (**A**). Adhesion of 5TGM1-*Cdh2*-shRNA cells to immobilised N-cadherin-Fc (10µg/ml) after 2 hours is significantly inhibited compared with 5TGM1-scramble-shRNA cells. Graph depicts mean ± range of 2 independent experiments (**B**). 5TGM1-*Cdh2*-shRNA cells adhere significantly less to monolayers of BMECs compared with 5TGM1-scramble-shRNA cells after 10 minutes in a static adhesion assay (**C**) or under 2 dynes/cm$^2$ of shear stress (**D**). Graphs depict mean ± SEM of 4 and 3 independent experiments, respectively. * $P < 0.05$ ** $P < 0.01$ (paired *t* test).

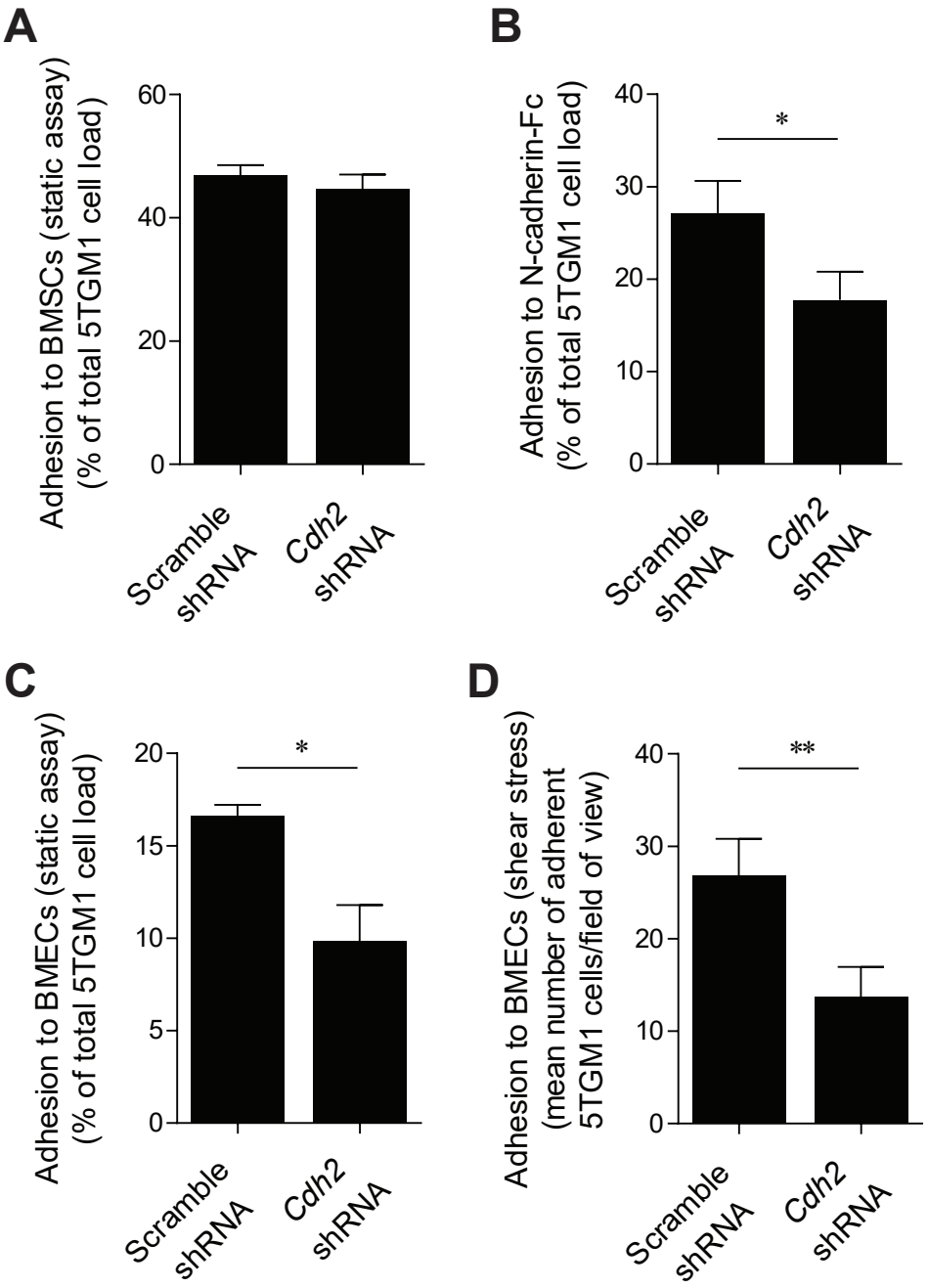
A
Adhesion to BMSCs (static assay)
(% of total 5TGM1 cell load)
60
40
20
0
Scramble shRNA
Cdh2 shRNA
B
Adhesion to N-cadherin-Fc
(% of total 5TGM1 cell load)
40
30
20
10
0
*
Scramble shRNA
Cdh2 shRNA
C
Adhesion to BMECs (static assay)
(% of total 5TGM1 cell load)
20
15
10
5
0
*
Scramble shRNA
Cdh2 shRNA
D
Adhesion to BMECs (shear stress)
(mean number of adherent
5TGM1 cells/field of view)
40
30
20
10
0
**
Scramble shRNA
Cdh2 shRNA

### 2.4.3 N-cadherin knock-down reduces 5TGM1 cell adhesion to BMECs

A crucial step in the extravasation and BM homing of circulating MM PCs is their adhesion to BMECs.[65] As BMECs express abundant N-cadherin (Figure 2.1B) and N-cadherin has been implicated in the adhesion of tumour cells to endothelial cells[28,34], the role of N-cadherin in the adhesion of 5TGM1 cells to BMECs was assessed. Initially, we confirmed N-cadherin-mediated binding in 5TGM1 cells by assessing adhesion to immobilised N-cadherin-Fc. Compared with 5TGM1-scramble-shRNA cells, 5TGM1-*Cdh2*-shRNA cells displayed a reduced capacity to adhere to N-cadherin-Fc (scramble-shRNA: 27.2 ± 3.5% adherence [mean ± range]; *Cdh2*-shRNA: 17.8 ± 3.1%; $P < 0.05$) (Figure 2.3B).

Subsequently, we assessed 5TGM1 cell adhesion to BMECs under static conditions and under shear stress, representative of physiological flow in blood vessels. Compared with 5TGM1-scramble-shRNA cells, 5TGM1-*Cdh2*-shRNA cell adhesion to BMECs was significantly reduced (scramble-shRNA: 16.61 ± 0.61% adherence [mean ± SEM]; *Cdh2*-shRNA: 9.85 ± 1.95%; $P < 0.05$) (Figure 2.3C). Using a parallel plate flow chamber, we assessed the ability of 5TGM1 cells to adhere to confluent monolayers of BMECs under 2 dynes/cm$^2$ of shear stress. Compared with 5TGM1-scramble-shRNA cells, 5TGM1-*Cdh2*-shRNA cells displayed a reduced capacity to adhere to BMECs under shear stress (scramble-shRNA: 26.81 ± 3.99 cells/field of view [mean ± SEM]; *Cdh2*-shRNA: 13.69 ± 3.28; $P < 0.01$) (Figure 2.3D).

### 2.4.4 Trans-endothelial migration of 5TGM1 cells is unaffected by N-cadherin knock-down

Following adhesion to BM endothelium, MM PCs penetrate the endothelial basement membrane and extravasate into the BM microenvironment.[65] We assessed the functional role of N-cadherin in 5TGM1 cell migration using a FCS concentration gradient as a chemoattractant. We found no difference in basal migration of 5TGM1-scramble-shRNA cells and 5TGM1-*Cdh2*-shRNA cells across a transwell membrane, after 24 hours (scramble-shRNA: 252.3 ± 21.2 cells/well [mean ± SEM]; *Cdh2*-shRNA: 321.3 ± 84.1 cells/well; $P = 0.56$) (Figure 2.4A). Furthermore, the ability of 5TGM1-*Cdh2*-shRNA cells to migrate through a monolayer of BMECs was unchanged relative to 5TGM1-scramble-shRNA cells (scramble-shRNA: 830.7 ± 134.4 cells/well [mean ± range]; *Cdh2*-shRNA: 717 ± 111 cells/well; $P = 0.72$) (Figure 2.4B).

**Figure 2.4. N-cadherin does not affect the migration of 5TGM1 cells *in vitro*.** Migration of 5TGM1 cells through trans-wells or through BMECs is unaffected by N-cadherin shRNA. 5TGM1 cells ($1x10^5$) were seeded into the upper chamber of trans-wells and migration to the bottom chamber was assessed after 24 hours. Graph depicts mean ± SEM of 3 independent experiments (**A**). 5TGM1 cells ($5x10^5$) were seeded onto a confluent monolayer of BMECs established on trans-well membranes (upper chamber) and trans-endothelial migration to the bottom chamber was assessed after 8 hours. Graph depicts mean ± range of 2 independent experiments (**B**).

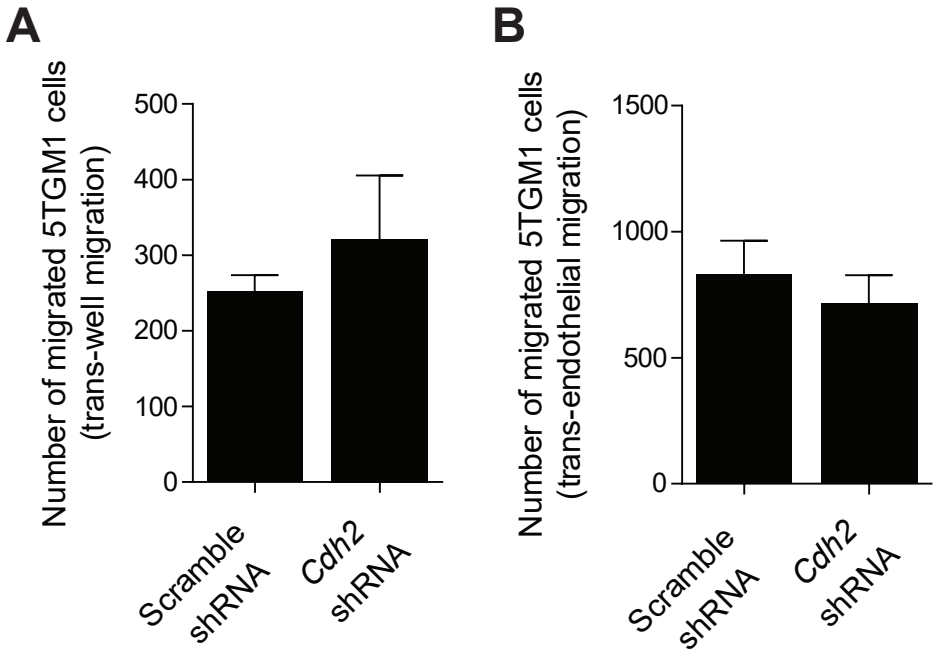
A
Number of migrated 5TGM1 cells
(trans-well migration)
500
400
300
200
100
0
Scramble shRNA
Cdh2 shRNA
B
Number of migrated 5TGM1 cells
(trans-endothelial migration)
1500
1000
500
0
Scramble shRNA
Cdh2 shRNA

MM PC extravasation is dependent on the production of proteolytic enzymes such as matrix metalloprotease 9 (MMP9) to degrade the endothelial basement membrane [66]. We found no difference in the MMP9 activity of 5TGM1 cells following N-cadherin knock-down compared to control 5TGM1 cells (data not shown).

### 2.4.5 Targeting of N-cadherin reduces total body tumour burden in a C57BL/KalwRij murine model of MM

To investigate whether therapeutic targeting of N-cadherin may represent a novel treatment modality for MM patients with high N-cadherin expression, we utilised the 5TGM1-C57BL/KaLwRij murine model of MM. In this model, following intravenous injection, circulating 5TGM1 tumour cells home to the BM and establish at multiple sites throughout the skeleton. Initially, we investigated the effect of N-cadherin knock-down in 5TGM1 cells on MM development *in vivo*. Total body tumour burden in mice inoculated with 5TGM1-*Cdh2*-shRNA cells was reduced by 73.1%, compared with mice inoculated with 5TGM1-scramble-shRNA cells (scramble-shRNA: $1.99x10^6 \pm 0.46x10^6$ photons per second [photons/s]; *Cdh2*-shRNA: $0.54x10^6 \pm 0.15x10^6$ photons/s; $P < 0.0001$), after 4 weeks ($n = 5$ mice/group; Figure 2.5A).

In order to investigate the effectiveness of the N-cadherin inhibition in suppressing MM establishment and disease progression *in vivo*, the effects of the N-cadherin antagonist ADH-1 were assessed in C57BL/KaLwRij mice bearing parental 5TGM1-luc cells, which express abundant N-cadherin. C57BL/KaLwRij mice were treated with ADH-1 (100mg/kg/day) or PBS vehicle control commencing immediately prior to inoculation with 5TGM1-luc cells (up-front treatment group) or one week after parental 5TGM1-luc cell inoculation (delayed treatment group). ADH-1 did not cause adverse effects, as assessed by weight loss or change in physical appearance. The total body tumour burden in the ADH-1 up-front treatment group ($2.09x10^6 \pm 0.43x10^6$ photons/s) was reduced by 68.6% compared with mice treated with PBS vehicle alone ($6.67x10^6 \pm 0.21x10^6$ photons/s) as assessed by BLI after 4 weeks ($n$ = 10-11 mice/group; $P < 0.01$) (Figure 2.5B). In contrast, there was no reduction in total body tumour burden in the delayed ADH-1 treatment group ($1.59x10^7 \pm 0.43x10^7$ photons/s) compared with mice treated with PBS vehicle alone ($1.46x10^7 \pm 0.13x10^7$ photons/s) after 4 weeks ($n$ = 6-7 mice/group) (Figure 2.5C).

**Figure 2.5. Targeting of N-cadherin reduces total body MM tumour burden in C57BL/KaLwRij mice after 4 weeks.** C57BL/KalwRij mice bearing 5TGM1-*Cdh2*-shRNA cells had significantly reduced overall tumour burden compared with 5TGM1-scramble-shRNA cell-bearing C57BL/KalwRij mice after four weeks, as shown by BLI. Graph depicts mean ± SEM. $n$ = 5 mice/group (**A**). Daily treatment of C57BL/KalwRij mice with 100mg/kg/day ADH-1 commencing pre-5TGM1 cell injection significantly reduced overall tumour burden after 4 weeks compared with C57BL/KalwRij mice treated with PBS vehicle alone, as measured by BLI. Graph depicts mean ± SEM. $n$ = 10 and 11 PBS-treated and ADH-1-treated mice, respectively (**B**). Daily treatment of C57BL/KaLwRij mice with 100mg/kg/day ADH-1 commencing 1 week post-5TGM1 cell injection did not reduce overall tumour burden after 4 weeks compared with C57BL/KaLwRij mice treated with PBS vehicle alone, as measured by BLI. Graph depicts mean ± SEM. $n$ = 6 and 7 PBS-treated and ADH-1-treated mice, respectively (**C**). ** $P < 0.01$ **** $P < 0.0001$ (two-way ANOVA with Bonferroni's multiple comparisons test). BLI images of one representative animal from each group over the 4 weeks of each experiment are also shown.

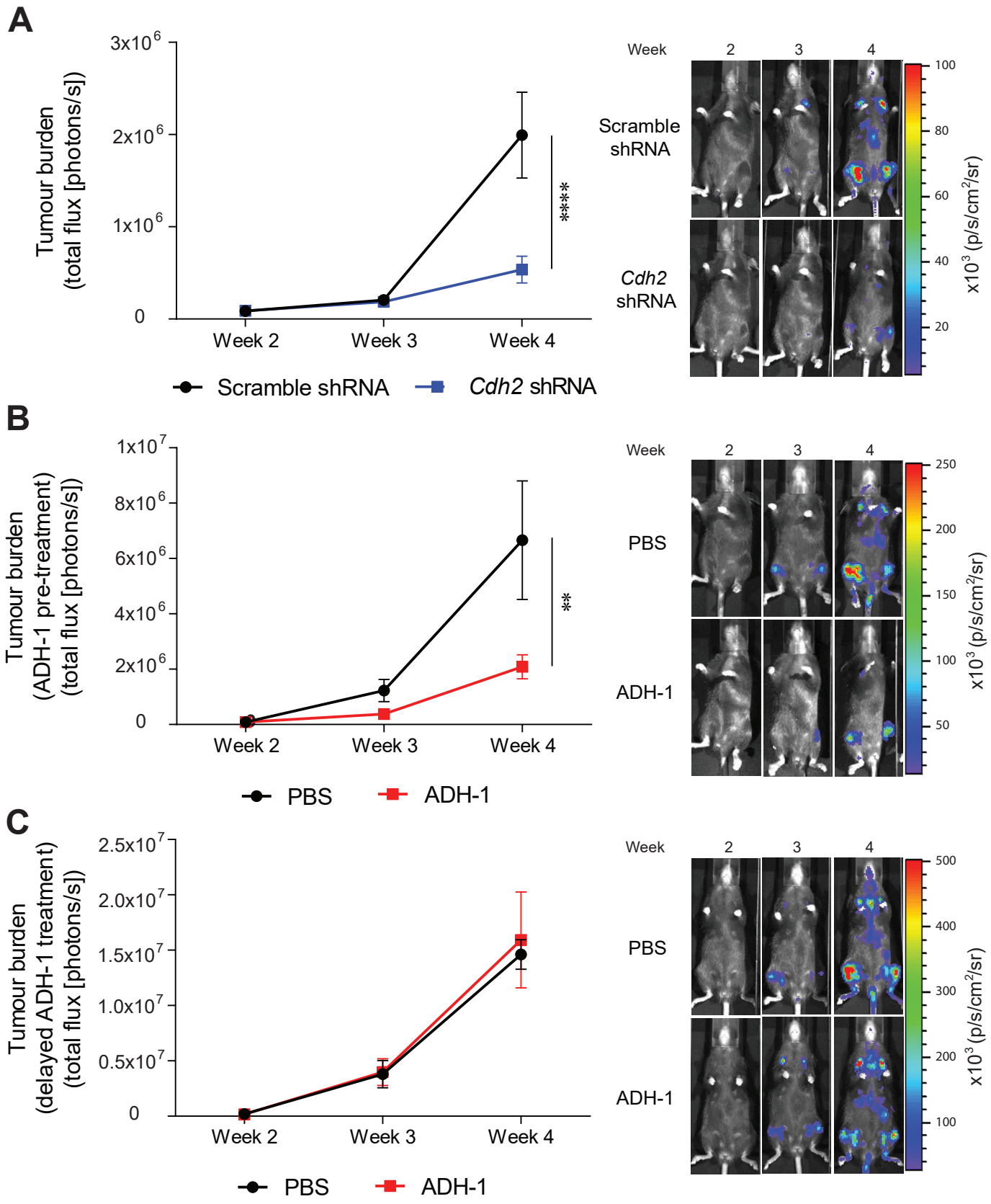
A
Tumour burden (total flux [photons/s])
3x10^6
2x10^6
1x10^6
0
Week 2
Week 3
Week 4
****
Scramble shRNA
Cdh2 shRNA
Week
2
3
4
Scramble shRNA
Cdh2 shRNA
100
80
60
40
20
x10^3 (p/s/cm^2/sr)
B
Tumour burden (ADH-1 pre-treatment) (total flux [photons/s])
1x10^7
8x10^6
6x10^6
4x10^6
2x10^6
0
Week 2
Week 3
Week 4
**
PBS
ADH-1
Week
2
3
4
PBS
ADH-1
250
200
150
100
50
x10^3 (p/s/cm^2/sr)
C
Tumour burden (delayed ADH-1 treatment) (total flux [photons/s])
2.5x10^7
2.0x10^7
1.5x10^7
1.0x10^7
0.5x10^7
0
Week 2
Week 3
Week 4
PBS
ADH-1
Week
2
3
4
PBS
ADH-1
500
400
300
200
100
x10^3 (p/s/cm^2/sr)

## 2.5 Discussion

Approximately 30% of newly diagnosed MM patients display elevated levels of circulating N-cadherin, which correlate with membrane N-cadherin expression in MM PCs. Notably, these patients have significantly worse progression-free and overall survival compared with patients with normal circulating N-cadherin levels, demonstrating that elevated N-cadherin confers a poor prognosis in MM.[52] Previous studies have also shown that N-cadherin plays a functional role in MM PC biology and behaviour such as BM homing, osteoblast interactions and, in certain contexts, proliferation.[33,67] In this study, our findings suggest that N-cadherin plays an important role in the pathogenesis of MM *in vivo* by mediating MM PC adhesion to BMECs, a crucial step in the extravasation of circulating MM PCs and subsequent establishment within the BM microenvironment. Notably, this is the first pre-clinical study to target N-cadherin as a potential therapeutic modality in MM. The C57BL/KaLwRij murine model of MM was utilised as it replicates many of the clinical and histopathological features characteristic of human MM disease.[68,69] The N-cadherin-expressing murine 5TGM1 MM PC line is highly aggressive following intravenous inoculation into C57BL/KaLwRij mice resulting in extensive tumour burden in the spleen and throughout the skeleton after four weeks.[54,70] Importantly, knock-down of N-cadherin in 5TGM1 cells and up-front administration of the N-cadherin antagonist ADH-1 significantly decreased total body MM tumour burden after four weeks compared with control animals.

Following intravenous inoculation into C57BL/KaLwRij mice, 5TGM1 cells extravasate, home to, and establish within BM microenvironment leading to the formation of multiple tumour foci throughout the axial and appendicular skeleton within four weeks.[54] In this study, knock-down of N-cadherin in 5TGM1 cells resulted in a significant reduction in overall tumour burden in C57BL/KaLwRij mice demonstrating the functional role of N-cadherin in MM development *in vivo*. Pre-clinical studies have previously shown that targeting N-cadherin using the antagonist ADH-1 alone, or in combination with other chemotherapeutics, significantly inhibited the growth of pancreatic tumours and melanoma, respectively.[46,47] ADH-1 is a disulfide-linked cyclic pentapeptide harbouring the His-Ala-Val (HAV) motif, found in the EC1 domain of type I classical cadherins, including N-cadherin.[19] Previous studies have demonstrated that synthetic linear and cyclic peptides containing the HAV motif are potent N-

cadherin antagonists, inhibiting N-cadherin-dependent neurite outgrowth and myoblast fusion, retarding Schwann cell and smooth muscle cell migration and inducing endothelial cell apoptosis *in vitro*.[15,16,71-73] We investigated the effect of ADH-1 on MM pathogenesis using the C57BL/KaLwRij murine model. Notably, daily administration of 5TGM1 cell-inoculated C57BL/KaLwRij mice with ADH-1 significantly reduced overall tumour burden demonstrating that N-cadherin function in MM development can be pharmaceutically inhibited *in vivo*. By commencing ADH-1 treatment of tumour-bearing C57BL/KaLwRij mice before and (one week) after 5TGM1 cell inoculation, we were able to assess the functional role of N-cadherin in BM homing of circulating MM PCs (ADH-1 up-front treatment) and intramedullary growth (delayed ADH-1 treatment) *in vivo*. In contrast to up-front ADH-1 treatment, delayed ADH-1 administration did not reduce total body tumour burden in C57BL/KaLwRij mice suggesting that N-cadherin is particularly important in the BM homing of MM PCs. Notably, our findings are consistent with previous observations in which N-cadherin knock-down in NCI-H929 MM PCs reduced their capacity to home to the BM following intravenous inoculation into Rag-2$^{-/-}\gamma c^{-/-}$ mice.[33] Moreover, this is in line with evidence demonstrating the efficacy of N-cadherin inhibition in limiting metastasis in pre-clinical solid tumour models.[34,36]

We assessed the functional role of N-cadherin in 5TGM1 cells using a series of *in vitro* assays addressing individual aspects of MM PC behaviour, which contribute to MM development *in vivo*. Previous over-expression and knock-down studies have demonstrated that the proliferation of tumour and non-tumour cell lines can be either inhibited or promoted by N-cadherin in a cell context-specific manner.[34,74,75] In our study, N-cadherin knock-down did not affect the proliferation of 5TGM1 cells under basal growth conditions or in co-culture with N-cadherin-expressing BMSCs *in vitro*, suggesting that N-cadherin-mediated homotypic binding (between 5TGM1 cells) and heterotypic binding (between 5TGM1 and BMSCs) does not appear to play a crucial role in 5TGM1 cell proliferation. These results are consistent with previous findings which showed that N-cadherin knock-down had no effect on basal proliferation of the human MM PC line NCI-H929.[33] Moreover, there was no difference in the proliferation of N-cadherin-positive and negative human MM PC lines when cultured on immobilized N-cadherin-Fc.[33] In contrast to these results, Sadler et al. found that the N-cadherin blocking antibody GC-4 increased the proliferation of N-cadherin-expressing human MM cell lines when co-cultured with BMSCs or osteoblasts.[67] However, the

interpretation of these results is complicated by the fact that while GC-4 blocks cell-cell binding[67], it has also been shown to stimulate the adhesion and spreading of tumour cells[76], suggesting that the antibody may behave as an agonist. To this end, while GC-4 may promote cell proliferation, our *in vitro* data supports previous data suggesting that N-cadherin knock-down does not affect the proliferation of MM cell lines either basally or in the presence of BMSCs.

Stromal cells constitute the majority of the non-hematopoietic cellular compartment within the BM microenvironment and are essential in providing pro-growth and survival cues to MM PCs.[63,64,77] Studies using an N-cadherin blocking antibody have previously shown that N-cadherin mediates the adhesion of breast cancer and melanoma cell lines to stromal cells and dermal fibroblasts, respectively.[28,31] In addition, studies using the N-cadherin antagonist ADH-1 have shown a role for N-cadherin in the adhesion of CML progenitor cells to BMSCs.[78] In contrast, our study shows that N-cadherin knock-down did not affect the ability of 5TGM1 cells to adhere to BMSCs. This finding is discordant with previous studies which reported that N-cadherin knock-down or blocking with antibody decreased the adhesion of human MM PC lines to murine fibroblast cells.[33] However, while our studies were performed in medium containing several divalent cations, the aforementioned study conducted adhesion assays in the presence of calcium only, that is, in the absence of other divalent cations that are required for integrin-mediated adhesion.[79-81] Our findings therefore suggest that other adhesion interactions, such as VLA-4-VCAM-1/fibronectin and LFA-1-ICAM-1, are potentially more important than N-cadherin-mediated binding in 5TGM1 cell adhesion to BMSCs.

The BM-homing cascade of MM PCs involves adhesion to the BM endothelium, trans-endothelial migration and establishment within the local BM microenvironment.[65] Studies have previously established the importance of N-cadherin in mediating haematopoietic and tumour cell interactions with endothelial cells. For example, an N-cadherin blocking antibody prevented the adhesion of neutrophil granulocytes to endothelial cells.[82] Additionally, enforced expression of N-cadherin in MCF-7 breast cancer cells promoted adhesion to human umbilical vein endothelial cells (HUVECs), while antibody-mediated N-cadherin blocking impeded the adhesion of melanoma cells to HUVECs.[28,34] Furthermore, previous studies have shown that N-cadherin accumulates at the initial heterotypic contact sites between melanoma cells and endothelial cells, suggesting a role in adhesion.[18,35,83,84] In the current study, we found

that N-cadherin knock-down significantly reduced the adhesion of 5TGM1 cells to monolayers of BMECs under static conditions and under shear stress, representative of physiological stress encountered within the vasculature. Given that N-cadherin knock-down reduced the ability of 5TGM1 cells to adhere to endothelial cells, it may impede the ability of 5TGM1 cells to undergo trans-endothelial migration. N-cadherin knock-down or blocking with antibody in melanoma cell lines has previously been shown to decrease trans-endothelial migration without affecting adhesion to endothelial cells, suggesting a specific role of N-cadherin in diapedesis.[35,84] However, consistent with previous studies using NCI-H929 MM PCs[33], N-cadherin knock-down did not affect trans-endothelial migration of 5TGM1 cells in this study. Taken together, these data suggest that N-cadherin knockdown may decrease tumour homing *in vivo* by inhibiting MM cell adhesion to endothelial cells, and therefore arrest of the tumour cells in the vasculature, without affecting the rate of the subsequent diapedesis.

Our findings demonstrate that N-cadherin is an important mediator of MM PC adhesive interactions with the BM endothelium, a crucial step in the BM homing cascade. We propose a mechanism whereby functional inhibition of N-cadherin prevents the extravasation of circulating MM PCs, which subsequently inhibits homing and colonization within the BM microenvironment. From a therapeutic perspective, our findings suggest that targeting of N-cadherin with ADH-1 may be of particular benefit in MM patients with high N-cadherin expression and, hence, high-risk disease. Further studies are warranted to examine the effectiveness of ADH-1 as a maintenance therapy in order to inhibit the ability of MM PCs to disseminate to multiple BM sites. Our results also encourage the examination of orally available ADH-1 peptidomimetics[19] for their ability to suppress MM disease. To this end, therapeutic targeting of N-cadherin may be a novel approach in delaying disease progression and relapse and improving overall survival in MM patients with aggressive disease.

## 2.6 Acknowledgements

This research was supported by a grant from the Cancer Australia Priority-driven Collaborative Cancer Research Scheme, co-funded by the Leukaemia Foundation. Kate Vandyke was supported by a fellowship from the Multiple Myeloma Research Foundation and by a Mary Overton Early Career Research Fellowship (Royal Adelaide Hospital).

## 2.7 References

1. Kyle RA, Rajkumar SV. Multiple myeloma. *N Engl J Med*. 2004; 351(18):1860-1873.

2. Bergsagel PL, Mateos MV, Gutierrez NC, Rajkumar SV, San Miguel JF. Improving overall survival and overcoming adverse prognosis in the treatment of cytogenetically high-risk multiple myeloma. *Blood*. 2013; 121(6):884-892.

3. Ghobrial IM. Myeloma as a model for the process of metastasis: implications for therapy. *Blood*. 2012; 120(1):20-30.

4. Alsayed Y, Ngo H, Runnels J, Leleu X, Singha UK, Pitsillides CM, Spencer JA, Kimlinger T, Ghobrial JM, Jia X *et al*. Mechanisms of regulation of CXCR4/SDF-1 (CXCL12)-dependent migration and homing in multiple myeloma. *Blood*. 2007; 109(7):2708-2717.

5. Vande Broek I, Asosingh K, Vanderkerken K, Straetmans N, Van Camp B, Van Riet I. Chemokine receptor CCR2 is expressed by human multiple myeloma cells and mediates migration to bone marrow stromal cell-produced monocyte chemotactic proteins MCP-1, -2 and -3. *Br J Cancer*. 2003; 88(6):855-862.

6. Katz BZ. Adhesion molecules--The lifelines of multiple myeloma cells. *Seminars in cancer biology*. 2010; 20(3):186-195.

7. Okada T, Hawley RG, Kodaka M, Okuno H. Significance of VLA-4-VCAM-1 interaction and CD44 for transendothelial invasion in a bone marrow metastatic myeloma model. *Clin Exp Metastasis*. 1999; 17(7):623-629.

8. Asosingh K, Gunthert U, De Raeve H, Van Riet I, Van Camp B, Vanderkerken K. A unique pathway in the homing of murine multiple myeloma cells: CD44v10 mediates binding to bone marrow endothelium. *Cancer Res*. 2001; 61(7):2862-2865.

9. Azab AK, Quang P, Azab F, Pitsillides C, Thompson B, Chonghaile T, Patton JT, Maiso P, Monrose V, Sacco A *et al*. P-selectin glycoprotein ligand regulates the interaction of multiple myeloma cells with the bone marrow microenvironment. *Blood*. 2012; 119(6):1468-1478.

10. Hideshima T, Mitsiades C, Tonon G, Richardson PG, Anderson KC. Understanding multiple myeloma pathogenesis in the bone marrow to identify new therapeutic targets. *Nat Rev Cancer*. 2007; 7(8):585-598.

11. Chauhan D, Uchiyama H, Akbarali Y, Urashima M, Yamamoto K, Libermann TA, Anderson KC. Multiple myeloma cell adhesion-induced interleukin-6 expression in bone marrow stromal cells involves activation of NF-kappa B. *Blood*. 1996; 87(3):1104-1112.

12. Hazlehurst LA, Damiano JS, Buyuksal I, Pledger WJ, Dalton WS. Adhesion to fibronectin via beta1 integrins regulates p27kip1 levels and contributes to cell adhesion mediated drug resistance (CAM-DR). *Oncogene*. 2000; 19(38):4319-4327.

13. Helfrich MH, Livingston E, Franklin IM, Soutar RL. Expression of adhesion molecules in malignant plasma cells in multiple myeloma: comparison with normal plasma cells and functional significance. *Blood reviews*. 1997; 11(1):28-38.

14. Van Riet I, Van Camp B. The involvement of adhesion molecules in the biology of multiple myeloma. *Leuk Lymphoma*. 1993; 9(6):441-452.

15. Doherty P, Rowett LH, Moore SE, Mann DA, Walsh FS. Neurite outgrowth in response to transfected N-CAM and N-cadherin reveals fundamental differences in neuronal responsiveness to CAMs. *Neuron*. 1991; 6(2):247-258.

16. Wilby MJ, Muir EM, Fok-Seang J, Gour BJ, Blaschuk OW, Fawcett JW. N-Cadherin inhibits Schwann cell migration on astrocytes. *Mol Cell Neurosci*. 1999; 14(1):66-84.

17. Blindt R, Bosserhoff AK, Dammers J, Krott N, Demircan L, Hoffmann R, Hanrath P, Weber C, Vogt F. Downregulation of N-cadherin in the neointima stimulates migration of smooth muscle cells by RhoA deactivation. *Cardiovasc Res*. 2004; 62(1):212-222.

18. Salomon D, Ayalon O, Patel-King R, Hynes RO, Geiger B. Extrajunctional distribution of N-cadherin in cultured human endothelial cells. *J Cell Sci*. 1992; 102 ( Pt 1):7-17.

19. Blaschuk OW. N-cadherin antagonists as oncology therapeutics. *Philosophical transactions of the Royal Society of London Series B, Biological sciences*. 2015; 370(1661):20140039.

20. Derycke LD, Bracke ME. N-cadherin in the spotlight of cell-cell adhesion, differentiation, embryogenesis, invasion and signalling. *Int J Dev Biol*. 2004; 48(5-6):463-476.

21. Boggon TJ, Murray J, Chappuis-Flament S, Wong E, Gumbiner BM, Shapiro L. C-cadherin ectodomain structure and implications for cell adhesion mechanisms. *Science*. 2002; 296(5571):1308-1313.

22. Harrison OJ, Jin X, Hong S, Bahna F, Ahlsen G, Brasch J, Wu Y, Vendome J, Felsovalyi K, Hampton CM *et al*. The extracellular architecture of adherens junctions revealed by crystal structures of type I cadherins. *Structure*. 2011; 19(2):244-256.

23. Chen CP, Posy S, Ben-Shaul A, Shapiro L, Honig BH. Specificity of cell-cell adhesion by classical cadherins: Critical role for low-affinity dimerization through beta-strand swapping. *Proc Natl Acad Sci U S A*. 2005; 102(24):8531-8536.

24. Bunse S, Garg S, Junek S, Vogel D, Ansari N, Stelzer EH, Schuman E. Role of N-cadherin cis and trans interfaces in the dynamics of adherens junctions in living cells. *PLoS One*. 2013; 8(12):e81517.

25. Pokutta S, Weis WI. Structure and mechanism of cadherins and catenins in cell-cell contacts. *Annu Rev Cell Dev Biol*. 2007; 23:237-261.

26. Niessen CM, Leckband D, Yap AS. Tissue organization by cadherin adhesion molecules: dynamic molecular and cellular mechanisms of morphogenetic regulation. *Physiol Rev*. 2011; 91(2):691-731.

27. Suyama K, Shapiro I, Guttman M, Hazan RB. A signaling pathway leading to metastasis is controlled by N-cadherin and the FGF receptor. *Cancer Cell*. 2002; 2(4):301-314.

28. Li G, Satyamoorthy K, Herlyn M. N-cadherin-mediated intercellular interactions promote survival and migration of melanoma cells. *Cancer Res*. 2001; 61(9):3819-3825.

29. Charrasse S, Meriane M, Comunale F, Blangy A, Gauthier-Rouviere C. N-cadherin-dependent cell-cell contact regulates Rho GTPases and beta-catenin localization in mouse C2C12 myoblasts. *J Cell Biol*. 2002; 158(5):953-965.

30. Moon RT, Bowerman B, Boutros M, Perrimon N. The promise and perils of Wnt signaling through beta-catenin. *Science*. 2002; 296(5573):1644-1646.

31. Hazan RB, Kang L, Whooley BP, Borgen PI. N-cadherin promotes adhesion between invasive breast cancer cells and the stroma. *Cell Adhes Commun*. 1997; 4(6):399-411.

32. Tran NL, Nagle RB, Cress AE, Heimark RL. N-Cadherin expression in human prostate carcinoma cell lines. An epithelial-mesenchymal transformation mediating adhesion withStromal cells. *Am J Pathol*. 1999; 155(3):787-798.

33. Groen RW, de Rooij MF, Kocemba KA, Reijmers RM, de Haan-Kramer A, Overdijk MB, Aalders L, Rozemuller H, Martens AC, Bergsagel PL *et al*. N-cadherin-mediated interaction with multiple myeloma cells inhibits osteoblast differentiation. *Haematologica*. 2011; 96(11):1653-1661.

34. Hazan RB, Phillips GR, Qiao RF, Norton L, Aaronson SA. Exogenous expression of N-cadherin in breast cancer cells induces cell migration, invasion, and metastasis. *J Cell Biol*. 2000; 148(4):779-790.

35. Qi J, Chen N, Wang J, Siu CH. Transendothelial migration of melanoma cells involves N-cadherin-mediated adhesion and activation of the beta-catenin signaling pathway. *Mol Biol Cell*. 2005; 16(9):4386-4397.

36. Tanaka H, Kono E, Tran CP, Miyazaki H, Yamashiro J, Shimomura T, Fazli L, Wada R, Huang J, Vessella RL *et al*. Monoclonal antibody targeting of N-cadherin inhibits prostate cancer growth, metastasis and castration resistance. *Nat Med*. 2010; 16(12):1414-1420.

37. Nieman MT, Prudoff RS, Johnson KR, Wheelock MJ. N-cadherin promotes motility in human breast cancer cells regardless of their E-cadherin expression. *J Cell Biol*. 1999; 147(3):631-644.

38. Sengupta S, Jana S, Biswas S, Mandal PK, Bhattacharyya A. Cooperative involvement of NFAT and SnoN mediates transforming growth factor-beta (TGF-beta)

induced EMT in metastatic breast cancer (MDA-MB 231) cells. *Clin Exp Metastasis*. 2013.

39. Ezponda T, Popovic R, Shah MY, Martinez-Garcia E, Zheng Y, Min DJ, Will C, Neri A, Kelleher NL, Yu J *et al*. The histone methyltransferase MMSET/WHSC1 activates TWIST1 to promote an epithelial-mesenchymal transition and invasive properties of prostate cancer. *Oncogene*. 2012; 32(23):2882-2890.

40. Araki K, Shimura T, Suzuki H, Tsutsumi S, Wada W, Yajima T, Kobayahi T, Kubo N, Kuwano H. E/N-cadherin switch mediates cancer progression via TGF-beta-induced epithelial-to-mesenchymal transition in extrahepatic cholangiocarcinoma. *Br J Cancer*. 2011; 105(12):1885-1893.

41. Nagi C, Guttman M, Jaffer S, Qiao R, Keren R, Triana A, Li M, Godbold J, Bleiweiss IJ, Hazan RB. N-cadherin expression in breast cancer: correlation with an aggressive histologic variant--invasive micropapillary carcinoma. *Breast Cancer Res Treat*. 2005; 94(3):225-235.

42. Tomita K, van Bokhoven A, van Leenders GJ, Ruijter ET, Jansen CF, Bussemakers MJ, Schalken JA. Cadherin switching in human prostate cancer progression. *Cancer Res*. 2000; 60(13):3650-3654.

43. Gravdal K, Halvorsen OJ, Haukaas SA, Akslen LA. A switch from E-cadherin to N-cadherin expression indicates epithelial to mesenchymal transition and is of strong and independent importance for the progress of prostate cancer. *Clin Cancer Res*. 2007; 13(23):7003-7011.

44. Lascombe I, Clairotte A, Fauconnet S, Bernardini S, Wallerand H, Kantelip B, Bittard H. N-cadherin as a novel prognostic marker of progression in superficial urothelial tumors. *Clin Cancer Res*. 2006; 12(9):2780-2787.

45. Nakajima S, Doi R, Toyoda E, Tsuji S, Wada M, Koizumi M, Tulachan SS, Ito D, Kami K, Mori T *et al*. N-cadherin expression and epithelial-mesenchymal transition in pancreatic carcinoma. *Clin Cancer Res*. 2004; 10(12 Pt 1):4125-4133.

46. Shintani Y, Fukumoto Y, Chaika N, Grandgenett PM, Hollingsworth MA, Wheelock MJ, Johnson KR. ADH-1 suppresses N-cadherin-dependent pancreatic cancer progression. *Int J Cancer*. 2008; 122(1):71-77.

47. Augustine CK, Yoshimoto Y, Gupta M, Zipfel PA, Selim MA, Febbo P, Pendergast AM, Peters WP, Tyler DS. Targeting N-cadherin enhances antitumor activity of cytotoxic therapies in melanoma treatment. *Cancer Res*. 2008; 68(10):3777-3784.

48. Yarom N, Stewart D, Malik R, Wells J, Avruch L, Jonker DJ. Phase I clinical trial of Exherin (ADH-1) in patients with advanced solid tumors. *Current clinical pharmacology*. 2013; 8(1):81-88.

49. Perotti A, Sessa C, Mancuso A, Noberasco C, Cresta S, Locatelli A, Carcangiu ML, Passera K, Braghetti A, Scaramuzza D *et al*. Clinical and pharmacological phase I

evaluation of Exherin (ADH-1), a selective anti-N-cadherin peptide in patients with N-cadherin-expressing solid tumours. *Ann Oncol*. 2009; 20(4):741-745.

50. Beasley GM, McMahon N, Sanders G, Augustine CK, Selim MA, Peterson B, Norris R, Peters WP, Ross MI, Tyler DS. A phase 1 study of systemic ADH-1 in combination with melphalan via isolated limb infusion in patients with locally advanced in-transit malignant melanoma. *Cancer*. 2009; 115(20):4766-4774.

51. Beasley GM, Riboh JC, Augustine CK, Zager JS, Hochwald SN, Grobmyer SR, Peterson B, Royal R, Ross MI, Tyler DS. Prospective multicenter phase II trial of systemic ADH-1 in combination with melphalan via isolated limb infusion in patients with advanced extremity melanoma. *J Clin Oncol*. 2011; 29(9):1210-1215.

52. Vandyke K, Chow AW, Williams SA, To LB, Zannettino AC. Circulating N-cadherin levels are a negative prognostic indicator in patients with multiple myeloma. *Br J Haematol*. 2013; 161(4):499-507.

53. Arthur A, Panagopoulos RA, Cooper L, Menicanin D, Parkinson IH, Codrington JD, Vandyke K, Zannettino AC, Koblar SA, Sims NA *et al*. EphB4 enhances the process of endochondral ossification and inhibits remodeling during bone fracture repair. *J Bone Miner Res*. 2013; 28(4):926-935.

54. Noll JE, Hewett DR, Williams SA, Vandyke K, Kok C, To LB, Zannettino AC. SAMSN1 is a tumor suppressor gene in multiple myeloma. *Neoplasia*. 2014; 16(7):572-585.

55. Schweitzer KM, Vicart P, Delouis C, Paulin D, Drager AM, Langenhuijsen MM, Weksler BB. Characterization of a newly established human bone marrow endothelial cell line: distinct adhesive properties for hematopoietic progenitors compared with human umbilical vein endothelial cells. *Lab Invest*. 1997; 76(1):25-36.

56. Wei CJ, Francis R, Xu X, Lo CW. Connexin43 associated with an N-cadherin-containing multiprotein complex is required for gap junction formation in NIH3T3 cells. *J Biol Chem*. 2005; 280(20):19925-19936.

57. Cheong CM, Chow AW, Fitter S, Hewett DR, Martin SK, Williams SA, To LB, Zannettino AC, Vandyke K. Tetraspanin 7 (TSPAN7) expression is upregulated in multiple myeloma patients and inhibits myeloma tumour development in vivo. *Exp Cell Res*. 2015; 332(1):24-38.

58. Bonder CS, Clark SR, Norman MU, Johnson P, Kubes P. Use of CD44 by CD4+ Th1 and Th2 lymphocytes to roll and adhere. *Blood*. 2006; 107(12):4798-4806.

59. DeGrendele HC, Estess P, Picker LJ, Siegelman MH. CD44 and its ligand hyaluronate mediate rolling under physiologic flow: a novel lymphocyte-endothelial cell primary adhesion pathway. *J Exp Med*. 1996; 183(3):1119-1130.

60. Perry MA, Granger DN. Role of CD11/CD18 in shear rate-dependent leukocyte-endothelial cell interactions in cat mesenteric venules. *J Clin Invest*. 1991; 87(5):1798-1804.

61. Diamond P, Labrinidis A, Martin SK, Farrugia AN, Gronthos S, To LB, Fujii N, O'Loughlin PD, Evdokiou A, Zannettino AC. Targeted disruption of the CXCL12/CXCR4 axis inhibits osteolysis in a murine model of myeloma-associated bone loss. *J Bone Miner Res*. 2009; 24(7):1150-1161.

62. Gan ZY, Fitter S, Vandyke K, To LB, Zannettino AC, Martin SK. The effect of the dual PI3K and mTOR inhibitor BEZ235 on tumour growth and osteolytic bone disease in multiple myeloma. *Eur J Haematol*. 2014.

63. Damiano JS, Cress AE, Hazlehurst LA, Shtil AA, Dalton WS. Cell adhesion mediated drug resistance (CAM-DR): role of integrins and resistance to apoptosis in human myeloma cell lines. *Blood*. 1999; 93(5):1658-1667.

64. Dalton WS. The tumor microenvironment: focus on myeloma. *Cancer treatment reviews*. 2003; 29 Suppl 1:11-19.

65. Vande Broek I, Vanderkerken K, Van Camp B, Van Riet I. Extravasation and homing mechanisms in multiple myeloma. *Clin Exp Metastasis*. 2008; 25(4):325-334.

66. Asosingh K, Menu E, Van Valckenborgh E, Vande Broek I, Van Riet I, Van Camp B, Vanderkerken K. Mechanisms involved in the differential bone marrow homing of CD45 subsets in 5T murine models of myeloma. *Clin Exp Metastasis*. 2002; 19(7):583-591.

67. Sadler NM, Harris BR, Metzger BA, Kirshner J. N-cadherin impedes proliferation of the multiple myeloma cancer stem cells. *American journal of blood research*. 2013; 3(4):271-285.

68. Vanderkerken K, De Raeve H, Goes E, Van Meirvenne S, Radl J, Van Riet I, Thielemans K, Van Camp B. Organ involvement and phenotypic adhesion profile of 5T2 and 5T33 myeloma cells in the C57BL/KaLwRij mouse. *Br J Cancer*. 1997; 76(4):451-460.

69. Radl J, Croese JW, Zurcher C, Van den Enden-Vieveen MH, de Leeuw AM. Animal model of human disease. Multiple myeloma. *Am J Pathol*. 1988; 132(3):593-597.

70. Oyajobi BO, Munoz S, Kakonen R, Williams PJ, Gupta A, Wideman CL, Story B, Grubbs B, Armstrong A, Dougall WC *et al*. Detection of myeloma in skeleton of mice by whole-body optical fluorescence imaging. *Molecular cancer therapeutics*. 2007; 6(6):1701-1708.

71. Mege RM, Goudou D, Diaz C, Nicolet M, Garcia L, Geraud G, Rieger F. N-cadherin and N-CAM in myoblast fusion: compared localisation and effect of blockade by peptides and antibodies. *J Cell Sci*. 1992; 103 ( Pt 4):897-906.

72. Lyon CA, Koutsouki E, Aguilera CM, Blaschuk OW, George SJ. Inhibition of N-cadherin retards smooth muscle cell migration and intimal thickening via induction of apoptosis. *Journal of vascular surgery*. 2010; 52(5):1301-1309.

73. Erez N, Zamir E, Gour BJ, Blaschuk OW, Geiger B. Induction of apoptosis in cultured endothelial cells by a cadherin antagonist peptide: involvement of fibroblast growth factor receptor-mediated signalling. *Exp Cell Res*. 2004; 294(2):366-378.

74. Kamei J, Toyofuku T, Hori M. Negative regulation of p21 by beta-catenin/TCF signaling: a novel mechanism by which cell adhesion molecules regulate cell proliferation. *Biochem Biophys Res Commun*. 2003; 312(2):380-387.

75. Li K, He W, Lin N, Wang X, Fan QX. Downregulation of N-cadherin expression inhibits invasiveness, arrests cell cycle and induces cell apoptosis in esophageal squamous cell carcinoma. *Cancer investigation*. 2010; 28(5):479-486.

76. Maes D, Bracke M, Ost P. An immobilized antibody targeting N-cadherin facilitates spread of N-cadherin-positive tumour cells. *Anticancer research*. 2012; 32(11):4755-4757.

77. Arnulf B, Lecourt S, Soulier J, Ternaux B, Lacassagne MN, Crinquette A, Dessoly J, Sciaini AK, Benbunan M, Chomienne C *et al*. Phenotypic and functional characterization of bone marrow mesenchymal stem cells derived from patients with multiple myeloma. *Leukemia*. 2007; 21(1):158-163.

78. Zhang B, Li M, McDonald T, Holyoake TL, Moon RT, Campana D, Shultz L, Bhatia R. Microenvironmental protection of CML stem and progenitor cells from tyrosine kinase inhibitors through N-cadherin and Wnt-beta-catenin signaling. *Blood*. 2013; 121(10):1824-1838.

79. Slordahl TS, Hov H, Holt RU, Baykov V, Syversen T, Sundan A, Waage A, Borset M. Mn2+ regulates myeloma cell adhesion differently than the proadhesive cytokines HGF, IGF-1, and SDF-1alpha. *Eur J Haematol*. 2008; 81(6):437-447.

80. Dransfield I, Cabanas C, Craig A, Hogg N. Divalent cation regulation of the function of the leukocyte integrin LFA-1. *J Cell Biol*. 1992; 116(1):219-226.

81. Gailit J, Ruoslahti E. Regulation of the fibronectin receptor affinity by divalent cations. *J Biol Chem*. 1988; 263(26):12927-12932.

82. Strell C, Lang K, Niggemann B, Zaenker KS, Entschladen F. Surface molecules regulating rolling and adhesion to endothelium of neutrophil granulocytes and MDA-MB-468 breast carcinoma cells and their interaction. *Cellular and molecular life sciences : CMLS*. 2007; 64(24):3306-3316.

83. Navarro P, Ruco L, Dejana E. Differential localization of VE- and N-cadherins in human endothelial cells: VE-cadherin competes with N-cadherin for junctional localization. *J Cell Biol*. 1998; 140(6):1475-1484.

84. Sandig M, Voura EB, Kalnins VI, Siu CH. Role of cadherins in the transendothelial migration of melanoma cells in culture. *Cell Motil Cytoskeleton*. 1997; 38(4):351-364.

**Supplementary Figure 2.1. Positive correlation between total body MM tumour burden assessed by BLI and serum paraprotein levels after 4 weeks.** Serum paraprotein levels are presented as a percentage of total serum protein. $n$ = 34 MM tumour-bearing C57BL/KaLwRij mice. **** $P < 0.0001$, R squared = 0.7874 (Pearson correlation).

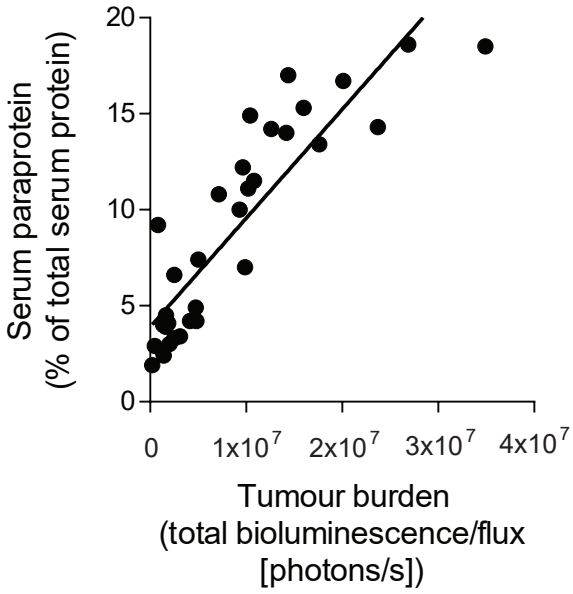
Serum paraprotein
(% of total serum protein)
20
15
10
5
0
0
1x10^7
2x10^7
3x10^7
4x10^7
Tumour burden
(total bioluminescence/flux
[photons/s])

Chapter 3

# LCRF-0006 is a novel vascular disrupting agent which synergistically enhances tumour response to bortezomib in a pre-clinical model of multiple myeloma

# Statement of Authorship

| | |
|---|---|
| Title of Paper | LCRF-0006 is a novel vascular disrupting agent which synergistically enhances tumour response to bortezomib in a pre-clinical mouse model of established multiple myeloma |
| Publication Status | ☐ Published ☐ Accepted for Publication<br>☐ Submitted for Publication ☑ Unpublished and Unsubmitted w ork w ritten in manuscript style |
| Publication Details | **Mrozik K.M.**, Blaschuk O.W., Cheong C.M., Hewett D.R., Noll J.E., Opperman K.S., Zannettino A.C.W., Vandyke K.<br>Manuscript in preparation. |

## Principal Author

| | | | |
|---|---|---|---|
| Name of Principal Author (Candidate) | Krzysztof Marek Mrozik | | |
| Contribution to the Paper | Conceptualisation and primary author of manuscript<br>Designed and performed experiments<br>Data analysis and interpretation | | |
| Overall percentage (%) | 80% | | |
| Certification: | This paper reports on original research I conducted during the period of my Higher Degree by Research candidature and is not subject to any obligations or contractual agreements with a third party that would constrain its inclusion in this thesis. I am the primary author of this paper. | | |
| Signature | | Date | 15/02/18 |

## Co-Author Contributions

By signing the Statement of Authorship, each author certifies that:
the candidate's stated contribution to the publication is accurate (as detailed above);
permission is granted for the candidate in include the publication in the thesis; and
the sum of all co-author contributions is equal to 100% less the candidate's stated contribution.

| | | | |
|---|---|---|---|
| Name of Co-Author | Orest W. Blaschuk | | |
| Contribution to the Paper | Critical review of manuscript | | |
| Signature | | Date | 12/02/18 |

| | | | |
|---|---|---|---|
| Name of Co-Author | Chee M. Cheong | | |
| Contribution to the Paper | Assisted with experiments | | |
| Signature | | Date | 14/02/18 |

| Name of Co-Author | Duncan R. Hewett | | |
|---|---|---|---|
| Contribution to the Paper | Critical review of manuscript<br>Assisted with experiments | | |
| Signature | | Date | 14/02/18 |

| Name of Co-Author | Jacqueline E. Noll | | |
|---|---|---|---|
| Contribution to the Paper | Assisted with experiments | | |
| Signature | | Date | 14/02/18 |

| Name of Co-Author | Khatora S. Opperman | | |
|---|---|---|---|
| Contribution to the Paper | Assisted with experiments | | |
| Signature | | Date | 14/02/18 |

| Name of Co-Author | Kate Vandyke | | |
|---|---|---|---|
| Contribution to the Paper | Conceptualisation and critical review of manuscript<br>Experimental design | | |
| Signature | | Date | 15/02/18 |

| Name of Co-Author | Andrew C.W. Zannettino | | |
|---|---|---|---|
| Contribution to the Paper | Conceptualisation and critical review of manuscript<br>Experimental design | | |
| Signature | | Date | 14/02/18 |

**LCRF-0006 is a novel vascular disrupting agent which synergistically enhances tumour response to bortezomib in a pre-clinical model of multiple myeloma**

Krzysztof M. Mrozik[1,2], Orest W. Blaschuk[3], Chee M. Cheong[1,2], Duncan R. Hewett[1,2], Jacqueline E. Noll[1,2], Khatora S. Opperman[1,2], Kate Vandyke[1,2*], Andrew C.W. Zannettino[1,2,4*].

Author Affiliations:

1. Myeloma Research Laboratory, Adelaide Medical School, Faculty of Health and Medical Sciences, The University of Adelaide, Adelaide, Australia
2. Cancer Theme, South Australian Health and Medical Research Institute, Adelaide, Australia
3. Division of Urology, Department of Surgery, McGill University, Montreal, Canada
4. Centre for Cancer Biology, University of South Australia, Adelaide, Australia

* co-senior authors

Running title:

LCRF-0006 synergistically enhances MM tumour response to bortezomib

Keywords:

N-cadherin, endothelial cell, permeability, multiple myeloma, tumour-associated vasculature, bortezomib

## 3.1 Abstract

N-cadherin is a homophilic cell-cell adhesion molecule which plays a critical role in maintaining vascular stability and modulating endothelial barrier permeability. Previous studies have demonstrated that the N-cadherin antagonist peptide ADH-1 enhances chemotherapeutic drug delivery to the tumour microenvironment by increasing vascular permeability to macromolecules, thereby enhancing tumour response. In the current study, we evaluated a synthetic small molecule peptidomimetic of ADH-1, LCRF-0006, as a novel vascular disrupting agent. We demonstrate that LCRF-0006 displays rapid, transient and reversible effects on endothelial cell junctions and increases vascular permeability *in vitro* and *in vivo*. Using a well-established C57Bl/KaLwRij/5TGM1 mouse model of multiple myeloma (MM) disease, LCRF-0006 synergised with the anti-MM agent bortezomib, significantly inhibiting MM tumour progression and leading to regression of disease in 100% of mice (co-efficient of drug interaction < 0.7). Moreover, LCRF-0006 and bortezomib synergistically induced 5TGM1 MM plasma cell apoptosis *in vitro* (co-efficient of drug interaction < 0.7). Our findings suggest the potential clinical utility of LCRF-0006 in a combinatorial approach to significantly increase bortezomib efficacy in MM.

## 3.2 Introduction

The structural integrity and permeability of the vascular endothelial barrier plays an essential role in the supply of nutrients and the maintenance of fluid balance in tissues.[1] Endothelial barrier stability is tightly controlled and maintained through adhesive interactions between neighbouring endothelial cells (ECs), as well as between ECs and adjacent mural cells (pericytes and smooth muscle cells).[2,3] In addition to molecules that mediate tight junctions between ECs (eg, occludin and claudins), the adhesive interactions in blood vessels involve N-cadherin and VE-cadherin, which mediate calcium-dependent, adherens junction-type cell-cell adhesion and inhibit EC proliferation and apoptosis by the activation of intracellular signalling cascades.[3-8] While VE-cadherin is the major cadherin expressed at established EC-EC junctions, N-cadherin is diffusely expressed on the EC surface and is thought to facilitate adhesion in nascent EC-EC junctions.[9-12] In addition, studies have proposed that N-cadherin may co-ordinate endothelial junction maturation by controlling VE-cadherin expression.[13] N-cadherin also plays a major role in the recruitment and adhesion of mural cells to ECs on the abluminal surface of blood vessels, which facilitates the remodelling, maturation and stabilisation of vascular networks.[5,6,14-16] Notably, recent studies have shown that perturbation of N-cadherin function can also disrupt established EC-EC and EC-mural cell junctions, thereby destabilising vascular integrity.[17,18]

Tumour-associated vasculature, essential to cancer cell growth, survival and metastasis, is widely recognised and investigated as a potential anti-cancer therapeutic target.[19,20] In comparison to normal vasculature, tumour-associated vasculature is relatively immature and structurally abnormal, characterised by gaps between adjacent ECs and loosely-attached or absent pericytes, resulting in a weakened endothelial barrier.[21-27] These characteristics are also thought to endow tumour-associated vasculature with greater sensitivity to vascular-disrupting agents, compared with normal vasculature.[28,29] The importance of N-cadherin in establishing and maintaining vascular stability suggests that inhibition of N-cadherin function is a potential mechanism to disrupt tumour vasculature. In support of this, perturbation of N-cadherin function has been shown to increase vascular permeability to macromolecules *in vitro* and *in vivo*.[17,18] Indeed, treatment of confluent human umbilical vein-derived EC monolayers with the cyclic pentapeptide N-cadherin inhibitor ADH-1 increased permeability to FITC-conjugated dextran *in vitro*.[17] Additionally, ADH-1 treatment in a rat melanoma

xenograft model increased the permeability of the tumour vasculature to Evans blue dye and increased delivery of the chemotherapeutic melphalan to the tumour microenvironment.[17] In support of these findings, a Phase I/II clinical trial found that intravenous ADH-1 treatment, in combination with isolated limb intravenous infusion of melphalan improved initial response rates in patients with advanced melanoma, when compared with melphalan alone. Notably, 60% of patients receiving the combination therapy achieved a partial response or greater, compared with 40% of patients receiving melphalan alone. However, the combination did not improve time to disease progression, compared with melphalan alone.[30,31] While preliminary, these data suggest that therapeutic targeting of N-cadherin may increase chemotherapeutic drug delivery to the tumour microenvironment and enhance tumour response.

Synthetic small molecule mimetics of peptide drugs may offer increased therapeutic efficacy in comparison to their peptide counterparts, due to enhanced proteolytic stability, bio-availability and potency.[32,33] LCRF-0006 (compound number 35 in patent US 7,446,120 B2[34]) was originally identified as a potential ADH-1 mimetic in a screen of compounds with three-dimensional structures that were similar to the HAV sequence-containing region of ADH-1 (Figure 3.1A,B). LCRF-0006 was identified as a non-peptidyl, small molecular weight molecule with a simple chemical structure which significantly inhibited neurite outgrowth in N-cadherin over-expressing, but not control, NIH/3T3 cells *in vitro*, suggesting LCRF-0006 inhibits N-cadherin-dependent processes.[34] In the current study, we hypothesised that LCRF-0006 would function as a vascular disrupting anti-cancer agent in the haematological malignancy multiple myeloma (MM) which is characterised by the uncontrolled proliferation of clonal antibody-producing plasma cells within the bone marrow (BM). To this end, we evaluated the efficacy of LCRF-0006 as a vascular disrupting agent *in vitro* and *in vivo*, and as an anti-cancer agent using a well-established pre-clinical mouse model of MM. LCRF-0006 was evaluated as a monotherapy and in combination with the proteasome-targeting, anti-MM agent bortezomib.

**Figure 3.1.** The structure of the cyclic pentapeptide ADH-1 (**A**) and the ADH-1 peptidomimetic LCRF-0006 (**B**).

**A**

ADH-1

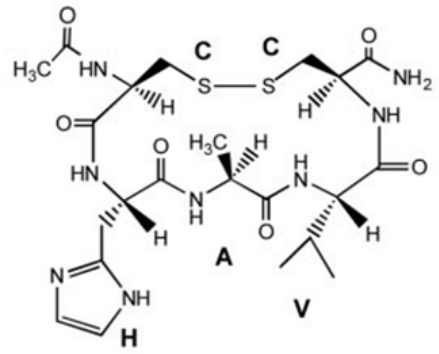


**B**

LCRF-0006

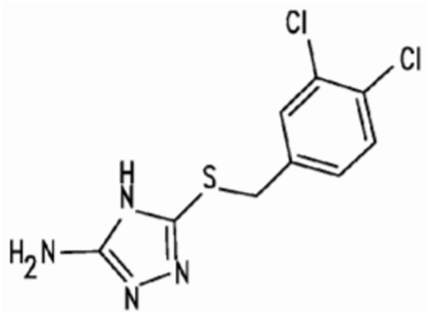

## 3.3 Methods

### 3.3.1 Cell culture

Cell culture reagents were sourced from Sigma-Aldrich (St Louis, MO, USA), unless otherwise specified. All media were supplemented with 2mM L-glutamine, 100U/ml penicillin, 100µg/ml streptomycin, 1mM sodium pyruvate and 10mM HEPES buffer, unless otherwise stated. The mouse MM plasma cell line 5TGM1 (expressing a dual GFP and luciferase reporter construct[35,36]) was maintained in Iscove's modified Dulbecco's medium (IMDM) with 20% foetal calf serum (FCS; Thermo Fisher Scientific, Waltham, MA, USA) and supplements (2mM L-glutamine, 100U/ml penicillin, 100µg/ml streptomycin, 1mM sodium pyruvate and 10mM 4-(2-hydroxyethyl)-1-piperazineethanesulfonic acid [HEPES] buffer). The human MM plasma cell line RPMI-8226 was maintained in Roswell Park Memorial Institute 1640 (RPMI-1640) with 10% FCS and supplements. The human BM EC line TrHBMEC (BMEC)[37] was maintained in M199 medium with 20% FCS and supplements (BMEC medium), as previously described.[38] All cell lines were maintained at 37°C in a humidified atmosphere with 5% $CO_2$.

### 3.3.2 Drugs

For *in vitro* experiments, the N-cadherin antagonist LCRF-0006, kindly provided by Crocus Laboratories, Montreal, Canada, was solubilised in DMSO (Sigma-Aldrich). For *in vivo* experiments, LCRF-0006 was solubilised in saline containing 40% 2-hydroxypropyl-β-cyclodextrin (2-HP-β-CD; Sigma). Bortezomib (Janssen-Cilag Pty Ltd, New Brunswick, NJ, USA) was reconstituted in 0.028% DMSO for *in vitro* studies and 1.33% DMSO for *in vivo* studies.

### 3.3.3 Cell apoptosis assays

To assess the effect of LCRF-0006 on 5TGM1 cell viability *in vitro*, 5TGM1 cells were cultured at $1x10^5$ cells/ml with LCRF-0006, or vehicle alone, in IMDM with 20% FCS and additives in 12-well plates (Corning Life Science, New York, USA). After 3 days, $1x10^5$ cells/test were washed in IMDM with 20% FCS and additives, then washed and resuspended in 20µl annexin V binding buffer (Hank's balanced salt solution with 1% HEPES and 5mM $CaCl_2$) containing 0.075µg/ml annexin V-PE (BioLegend; San Diego, CA, USA) and 10% (v/v) 7-AAD (Beckman Coulter; Brea, CA, USA) and were stained

for 20 minutes in the dark at 4°C. Cells were then diluted with ice-cold 200µl annexin V binding buffer and immediately analysed by flow cytometry using an LSRFortessa™ X-20 flow cytometer (BD; Franklin Lakes, NJ, USA). For single-stained positive controls, 5TGM1 cells were treated with DMSO (early apoptosis control) or 80% ethanol (dead cell control) for 10 minutes. For drug synergy assays, 5TGM1 cells were cultured, as described above, in combinations of various concentrations of LCRF-0006 and bortezomib. After 24 hours, $1x10^5$ cells from each condition were stained and analysed, as described above. Drug synergy was defined as a co-efficient of drug interaction (CDI) value of less than 0.7, where CDI was the actual viability of 5TGM1 cells treated with the drug combination (AB) divided by their predicted viability (calculated as the product of 5TGM1 cell viabilities treated with each drug alone [A*B]).

To assess the effect of LCRF-0006 on BMEC viability *in vitro*, BMECs were seeded at $1.2x10^5$ cells/well ($2.4x10^5$ cells/ml) in BMEC medium in 24-well plates (Corning Life Science) and cultured for 24 hours. Confluent BMEC monolayers were then cultured with LCRF-0006, or vehicle alone, in M199 medium with 15% FCS and supplements (as previously described[38]). After 24 hours, BMECs were trypsinised and $1x10^5$ cells/test were washed in M199 medium with 15% FCS and supplements, and prepared and analysed for cell viability, as described above.

### 3.3.4 Endothelial tube disruption assays

Endothelial tubes were pre-formed on growth factor-reduced Matrigel® matrix in a 96-well plate by seeding $3.5x10^4$ BMECs in a 50:50 mix of BMEC medium and conditioned media from the human MM cell line RPMI-8226 as a stimulant, as described previously.[39] To investigate the effect of LCRF-0006 on endothelial tube integrity, immature (5-hour-old) or established (24-hour-old) endothelial tubes were then treated with up 200µg/ml LCRF-0006. Tubes were then imaged over a 24 hour period using an Olympus CKX41 inverted microscope and DP21 imaging system (Tokyo Japan) and analysed using cellSens Entry 1.11 software (Olympus).

### 3.3.5 Endothelial monolayer retraction and recovery assay

BMECs were seeded into gelatinized 96-well plates ($5x10^4$ cells/well) and grown to confluence over 24 hours. BMECs were then treated with LCRF-0006 in IMDM with 2% FCS and additives for 1 hour and imaged, as described above. After gently washing twice in IMDM with 2% FCS and additives, BMECs were allowed to recover for 1 hour

in M199 with 20% FCS and BMEC supplements and again imaged. BMEC monolayer confluency was assessed using cellSens Entry 1.11 software.

### 3.3.6 Endothelial monolayer permeability assay

BMECs ($5x10^4$ cells/well) were seeded onto gelatinized 0.4µm 6.5mm trans-wells (Corning Life Science) and grown to confluence over 24 hours. BMECs were then treated with LCRF-0006 in IMDM with 2% FCS and additives for 1 hour and gently washed twice in serum-free IMDM with additives. To measure endothelial monolayer permeability, 1 mg/mL 70 kDa FITC-dextran (Sigma) in phenol red-free IMDM with 2% FCS and additives was added to the trans-wells and fluorescence in the bottom chamber (containing phenol red-free IMDM with 2% FCS and additives) was assessed after 1 hour using a FLUOstar® Omega microplate reader (BMG LABTECH; Ortenberg, Germany).

### 3.3.7 Animal studies

C57Bl/KaLwRij mice (aged 6-8 weeks) were used for all *in vivo* studies. For MM tumour studies, mice were inoculated with $5x10^5$ 5TGM1 cells in 100µl phosphate-buffered saline (PBS) by intravenous injection (i.v.) via the tail vein. Total body tumour burden was assessed at days 14, 21 and 28 by bioluminescence imaging (BLI) using a Xenogen IVIS 200 imaging system (Perkin Elmer, Waltham, MA, USA), as previously described.[38]

All animals used for therapy studies were randomised by age, sex and, where appropriate, tumour burden. For monotherapy studies, mice were administered LCRF-0006 (100mg/kg/day) or vehicle alone i.p. (110-150µl volume), commencing 15 minutes prior to 5TGM1 cell injection or at day 14 following establishment of disease until the conclusion of the experiment. For the combination studies, mice with established MM disease were administered LCRF-0006 (100mg/kg) or vehicle alone i.p. on day 14, followed by 6 cycles of LCRF-0006 and bortezomib combination therapy (or relevant vehicle controls) over the remaining 14 days of the experiment. Each treatment cycle consisted of LCRF-0006 (100mg/kg) or 2-HP-β-CD vehicle alone i.p. followed by low-dose bortezomib (0.5mg/kg)[40] or 1.33% DMSO vehicle alone i.p. 1 hour later. At day 28, cardiac blood was collected into tubes containing 50µl 0.5M EDTA (pH 8.0) and complete blood counts were performed using a HEMAVET®950 automated blood analyzer (Drew Scientific; Miami Lakes, FL). Drug synergy was

defined as a co-efficient of drug interaction (CDI) value of less than 0.7, where CDI was the actual proportion of tumour remaining in C57Bl/KaLwRij mice treated with the drug combination (AB) relative to mice treated with vehicles alone (as assessed by BLI), divided by the predicted proportion of tumour remaining (calculated as the product of proportion of tumour remaining in C57Bl/KaLwRij treated with each drug alone [A*B]).

*In vivo* vascular permeability was assessed using an amended version of previously published protocols.[41-43] Mice were injected once with 100mg/kg LCRF-0006 or vehicle alone (as described above). After 1 hour, mice were injected with 250mg/kg 70 kDa FITC-dextran i.v. via the tail vein and humanely killed 30 minutes later. Eyes were immediately enucleated and fixed for 2 hours in 4% PFA. The retinal tissues were then isolated[44], dissected into maltese-cross formation and flat-mounted onto glass slides using Fluoroshield™ mounting medium (Sigma). Extravasated FITC-dextran was immediately assessed by epi-fluorescence microscopy (Olympus).

All animal procedures were performed in accordance with guidelines approved by the South Australian Health and Medical Research Institute (SAHMRI) Animal Ethics Committee (SAM165).

### 3.3.8 Detection of circulating tumour cells

Freshly collected blood was transferred to round-bottom polystyrene tubes and red blood cells were lysed by three rounds of 10 min incubation in 7.5ml red blood cell lysis buffer (0.15M $NH_4Cl$ 10mM $KHCO_3$ 1.1mM di-sodium EDTA in Milli-Q water) at room temperature. Samples were centrifuged for 5 minutes at 1400 rpm, washed once in 10 ml ice-cold PFE buffer (2% FCS 2mM EDTA in PBS), resuspended in 0.5ml PFE buffer and were immediately analysed by flow cytometry using a FACSCanto™ II flow cytometer (BD). For gating purposes, a control sample (from a tumour-naïve mouse) was spiked with *in vitro*-cultured 5TGM1 cells.

### 3.3.9 Cell composition analysis of compact bone

Compact bone was isolated from the long bones (i.e. femora and tibiae) of both hind limbs from humanely killed mice and prepared for analysis of mesenchymal stromal cell (MSC) and osteoblast (OB) numbers, as previously described.[35] Samples were run on a BD LSRFortessa™ X-20 flow cytometer using BD FACSDiva™ software v8.0 (BD) and analysed using FlowJo V.10.0.8 software (FlowJo, LLC; Ashland, Oregon).

Non-haematopoietic cell populations were defined as: $Lin^-CD45^-CD31^+$ (ECs), $Lin^-CD45^-CD31^-Sca\text{-}1^+CD51^-$ (MSCs), $Lin^-CD45^-CD31^-Sca\text{-}1^+CD51^+$ (osteoprogenitors; OPs) and $Lin^-CD45^-CD31^-Sca\text{-}1^-CD51^+$ (OBs).

### 3.3.10 Statistical analyses

For *in vitro* studies, statistical significance was calculated using a one-way ANOVA with Dunnett's multiple comparisons test, or two-way ANOVA with Sidak's multiple comparisons test. For *in vivo* studies, statistical significance was calculated using a Mann-Whitney U test, Kruskal-Wallis test with Dunn's multiple comparisons test, one-way ANOVA with Holm-Sidak's multiple comparisons test or two-way ANOVA with Bonferroni's multiple comparisons test. Tumour burden data were log-transformed prior to conducting statistical analyses. All statistical analyses were performed using GraphPad Prism® v7.02 software (GraphPad Software, Inc.; La Jolla, CA).

## 3.4 Results

### 3.4.1 LCRF-0006 disrupts EC junctions and increases monolayer permeability at sub-cytotoxic doses *in vitro*

Previous studies have shown the ability of N-cadherin antagonists to rapidly compromise the integrity of confluent EC monolayers, resulting in increased vascular permeability *in vitro*.[17,45] In order to assess whether LCRF-0006 can disrupt EC monolayers, we treated confluent BMEC monolayers with LCRF-0006 *in vitro*. Initially, we confirmed that LCRF-0006 did not affect the survival of BMECs *in vitro*, using Annexin V (early apoptosis) and 7-AAD (dead cell) staining. The treatment of confluent BMEC monolayers with LCRF-0006 for 24 hours had no significant effect on BMEC viability in comparison to vehicle-treated monolayers, as assessed by the AnnexinV$^{neg}$ 7-AAD$^{neg}$ cell population, at concentrations up to 200µg/ml (Supplementary Figure 3.1). However, LCRF-0006 induced a dose-dependent dissociation of EC-EC contacts, resulting in increased EC rounding and monolayer retraction, and decreased monolayer confluency after 1 hour of treatment at concentrations of 50µg/ml and greater, when compared with vehicle-treatment ($P < 0.0001$; Figure 3.2A,B). Notably, these effects were reversible, as monolayers treated with up to 100µg/ml LCRF-0006 completely reformed within 1 hour of removal of LCRF-0006 (Figure 3.2A,B). Previous studies have shown that EC retraction, rounding and gap formation is associated with increased vascular permeability to macromolecules *in vitro*.[46-49] To this end, we assessed the effects of LCRF-0006-mediated BMEC monolayer disruption on macromolecular permeability *in vitro*, using a 70 kDa FITC-dextran trans-well flow-through assay. The pre-treatment of confluent BMEC monolayers with LCRF-0006 for 1 hour significantly increased BMEC monolayer permeability to 70 kDa FITC-dextran in a dose-dependent manner, when compared with vehicle-treatment ($P < 0.05$) (Figure 3.2C).

### 3.4.2 LCRF-0006 disrupts endothelial tube integrity at sub-cytotoxic doses *in vitro*

We then assessed the effect of LCRF-0006 on pre-formed three-dimensional endothelial tubes grown on a basement membrane-like Matrigel® matrix *in vitro*. Initially, we assessed the effect of LCRF-0006 on immature (5-hour-old) endothelial tubes. Vehicle-treated tubes matured normally into networks of thick tubes with smooth morphology

**Figure 3.2. LCRF-0006 disrupts BMEC monolayers and increases their permeability to 70 kDa FITC-dextran *in vitro*.** Confluent BMEC monolayers in 96-well plates were treated with LCRF-0006, or vehicle alone, for 1 hour and then imaged. After removing LCRF-0006, monolayers were gently washed, allowed to recover for 1 hour and imaged again. Images shown are representative of 3 independent experiments. Scale bars depict 100µm (**A**). BMEC monolayer confluency quantitated after treatment and recovery. Graph depicts mean ± SEM of 3 independent experiments (**B**). **** $P <$ 0.0001 compared with monolayers treated with vehicle alone (0µg/ml) $^{\#\#\#\#}$ $P < 0.0001$ compared with monolayers after 1 hour of treatment (two-way ANOVA with Sidak's multiple comparisons test). Confluent BMEC monolayers established on 0.4µM trans-well membranes were treated with LCRF-0006, or vehicle alone, for 1 hour. Monolayers were then gently washed, 70 kDa FITC-dextran (1 mg/mL) was added to the upper chamber of trans-wells and FITC-dextran flow-through was assessed 1 hour later by measuring fluorescence in the bottom chamber of triplicate trans-wells. Graph depicts mean ± SEM of 3 independent experiments (**C**). * $P < 0.05$ compared with monolayers treated with vehicle alone (0µg/ml) (one-way ANOVA with Dunnett's multiple comparisons test).

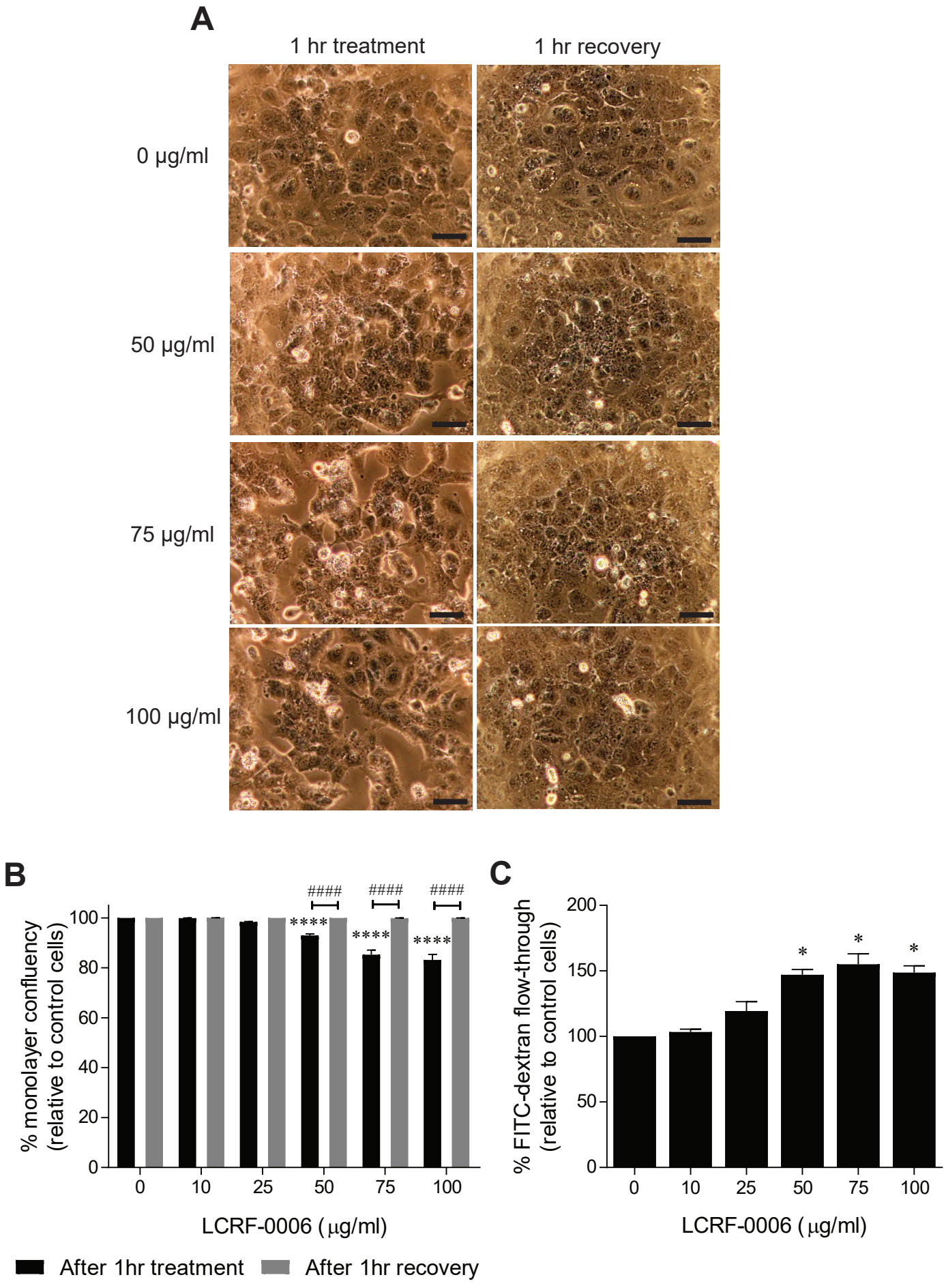
A
1 hr treatment
1 hr recovery
0 µg/ml
50 µg/ml
75 µg/ml
100 µg/ml
B
% monolayer confluency (relative to control cells)
100
80
60
40
20
0
####
####
####
****
****
****
0
10
25
50
75
100
LCRF-0006 (µg/ml)
After 1hr treatment
After 1hr recovery
C
% FITC-dextran flow-through (relative to control cells)
200
150
100
50
0
*
*
*
0
10
25
50
75
100
LCRF-0006 (µg/ml)

over 24 hours (Supplementary Figure 3.2A,B). In contrast, concentrations of 100µg/ml LCRF-0006 and greater compromised tube maturation, with EC rounding and detachment from tubes observed, resulting in a significant reduction in tube thickness after 24 hrs ($P < 0.0001$) (Figure 3.3A and Supplementary Figure 3.2A,B). However, addition of LCRF-0006 to immature tubes did not reduce the total length of EC tubes after 24 hrs (data not shown). Notably, the initial effects of LCRF-0006 treatment were rapid, with BMEC retraction and rounding seen as early as 30 minutes after LCRF-0006 addition (data not shown), consistent with EC gap formation.[46,50,51] LCRF-0006 was then added to established (24-hour-old) networks of endothelial tubes. Similar to the effects on immature tubes, treatment with 100µg/ml LCRF-0006 and greater for 24 hours resulted in a loss of tube smoothness and a significant reduction of tube thickness ($P < 0.0001$) (Figure 3.3B and Supplementary Figure 3.3A,B), without affecting tube length (data not shown).

### 3.4.3 LCRF-0006 is well tolerated and increases blood vessel permeability *in vivo*

As LCRF-0006 disrupted endothelial integrity and increased permeability *in vitro*, we then postulated that LCRF-0006 may have effects on vascular permeability *in vivo*, consistent with previous findings using N-cadherin antagonists.[14,17] Prior to conducting vascular permeability experiments, we assessed whether LCRF-0006 had any toxicities in C57Bl/KaLwRij mice. Mice treated with 100mg/kg/day LCRF-0006 for 28 days tolerated the dosing regimen well with no effects on weight (Supplementary Figure 3.4A) or other adverse effects observed, in comparison with vehicle-treated animals. In addition, complete blood counts in C57Bl/KaLwRij mice were unaffected by 28 days of LCRF-0006 treatment, in comparison with vehicle-treated, or un-treated, mice (Supplementary Table 3.1). Given that N-cadherin plays a role in OB differentiation[52-55], we also assessed whether LCRF-0006 affected the proportion of MSCs, OPs and OBs within the long bones of LCRF-0006-treated C57Bl/KaLwRij mice. The proportion of MSCs, OPs and OBs within the $Lin^-CD45^-CD31^-$ fraction of compact bone isolated from the long bones was unaffected by 28 days of LCRF-0006 treatment, when compared with that of vehicle-treated animals (Supplementary Figure 3.4B-D). In addition, LCRF-0006 did not affect the proportion of $CD31^+$ ECs within the $Lin^-CD45^-$ fraction of compact bone or BM, relative to that of vehicle-treated controls (Supplementary Figure 3.4E,F). In line with these findings, histological analysis

**Figure 3.3. LCRF-0006 disrupts immature and established endothelial tubes *in vitro*.** BMECs were cultured on growth factor-reduced Matrigel® matrix in a 96-well plate and endothelial tube formation was induced using a 50:50 mix of BMEC culture medium and RPMI-8226 conditioned medium. Immature (5-hour-old) (**A**) or established (24-hour-old) (**B**) tubes were treated with LCRF-0006 for 24 hours, imaged and mean tube thickness was quantitated. Images shown are representative of 2 independent experiments. Scale bars depict 250µm. Graphs depict mean ± range of 2 independent experiments. * $P < 0.05$ ** $P < 0.01$ *** $P < 0.001$ **** $P < 0.0001$ compared with tubes treated with vehicle alone (0µg/ml) (one-way ANOVA with Dunnett's multiple comparisons test).

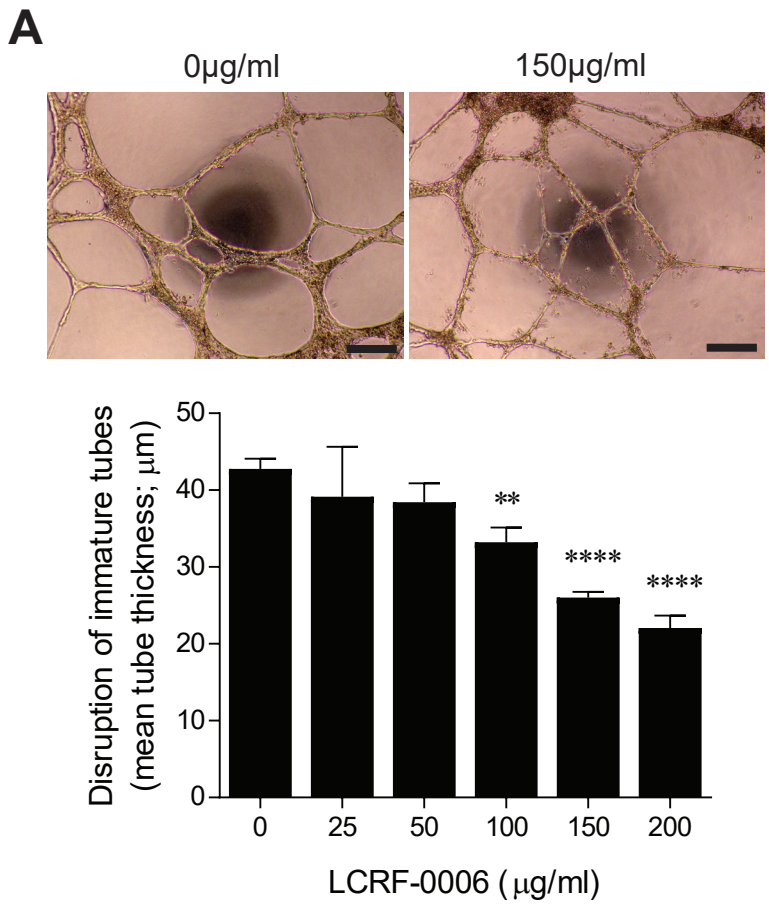
A
0μg/ml
150μg/ml
Disruption of immature tubes
(mean tube thickness; μm)
50
40
30
20
10
0
**
****
****
0
25
50
100
150
200
LCRF-0006 (μg/ml)

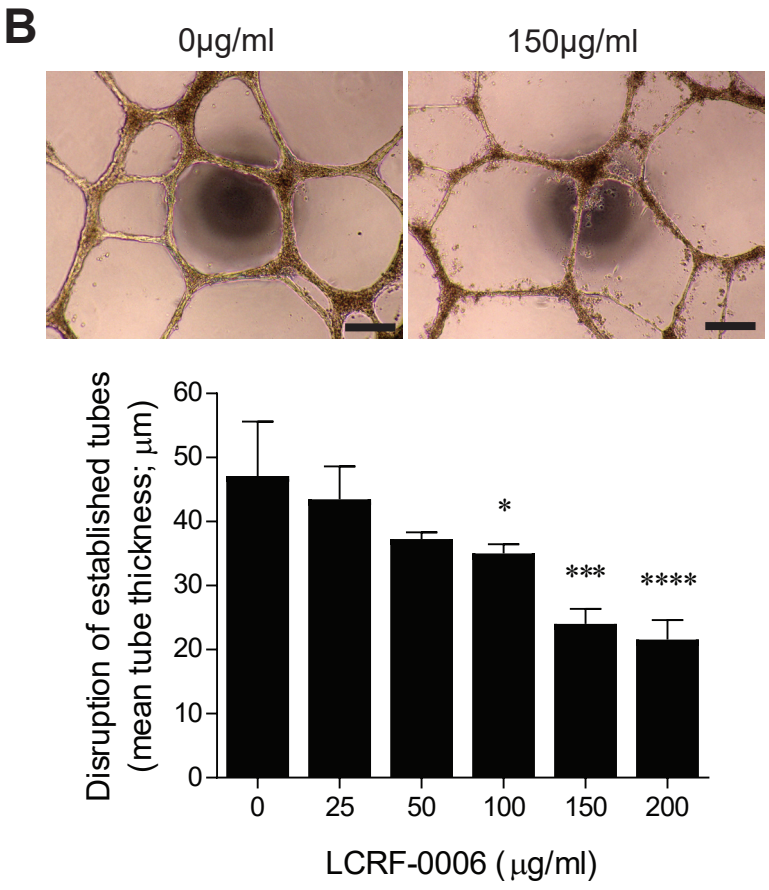
B
0μg/ml
150μg/ml
Disruption of established tubes
(mean tube thickness; μm)
60
50
40
30
20
10
0
*
***
****
0
25
50
100
150
200
LCRF-0006 (μg/ml)

revealed LCRF-0006 had no overt effects on blood vessel number or vascular morphology (data not shown).

Fluorescence angiography of the retina is an established technique used to rapidly investigate vascular perfusion and permeability in response to cytokines and other agents in rodent models.[41,42] To this end, we performed whole-mount retinal fluorescence angiography to assess the effect of LCRF-0006 on FITC-dextran extravasation *in vivo*. C57Bl/KaLwRij mice were infused with 70 kDa FITC-dextran 1 hour after a single treatment with 100mg/kg LCRF-0006 or vehicle alone and, 30 minutes later, whole mounts of the retinas were prepared for fluorescence imaging. Sites of retinal peri-vascular hyper-fluorescence, indicative of blood vessel leakiness, were only observed in mice pre-treated with LCRF-0006 (3/4 LCRF-0006-treated mice vs. 0/4 vehicle-treated mice) (Figure 3.4A-D).

### 3.4.4 LCRF-0006 and low-dose bortezomib combination therapy synergistically induces tumour regression in mice with established MM disease

Previous studies have reported the efficacy of ADH-1 to inhibit tumour establishment and growth in a range of pre-clinical mouse models including pancreatic cancer, lung cancer and MM.[38,56,57] In addition to disrupting tumour-associated vasculature[17,57], ADH-1 has been shown to induce apoptosis in several N-cadherin-expressing cancer cell types *in vitro*[56,58,59] suggesting that N-cadherin antagonism may suppress tumour progression by targeting both tumour cells and the associated vasculature. To this end, we investigated the efficacy of LCRF-0006 as an anti-cancer agent in a pre-clinical mouse model of MM. Initially, we assessed the effect of LCRF-0006 treatment on the viability of the N-cadherin-expressing mouse myeloma cell line 5TGM1 *in vitro*. LCRF-0006 treatment significantly induced 5TGM1 cell apoptosis at concentrations of 25µg/ml and greater after 72 hours ($P < 0.01$; $IC_{50}$= 53.03µg/ml) (Figure 3.5A). However, daily treatment of 5TGM1 tumour-bearing C57Bl/KaLwRij mice with 100mg/kg LCRF-0006 had no effect on tumour burden, as assessed by BLI, compared with vehicle-treated controls (Figure 3.5B). In addition, LCRF-0006 had no significant effect on the proportion of circulating tumour cells within the leukocyte fraction of peripheral blood at day 28 (Supplementary Figure 3.5A). Similar to MM tumour-naïve mice, LCRF-0006 did not affect the proportion of $CD31^+$ ECs within the $Lin^-CD45^-$ fraction of compact bone or BM in mice with established disease, relative to vehicle-treated controls (Supplementary Figure 3.5B,C).

**Figure 3.4. LCRF-0006 increases vascular permeability to 70 kDa FITC-dextran *in vivo.*** C57BL/KaLwRij mice were injected with 250mg/kg 70 kDa FITC-dextran i.v., 1 hour after a single injection of 100mg/kg LCRF-0006 or vehicle (2-HP-β-CD [CD]) alone i.p., and humanely killed 30 minutes later. After fixation of eyes, the retinal tissues were isolated, flat-mounted and immediately assessed for fluorescence using epi-fluorescence microscopy. Representative epi-fluorescence images of vehicle-treated mice (**A,B**) and LCRF-0006-treated mice (**C,D**) are shown. Sites of peri-vascular hyper-fluorescence are indicated (*). Scale bars depict 250μm (**A,C**) and 100μm (**B,D**).

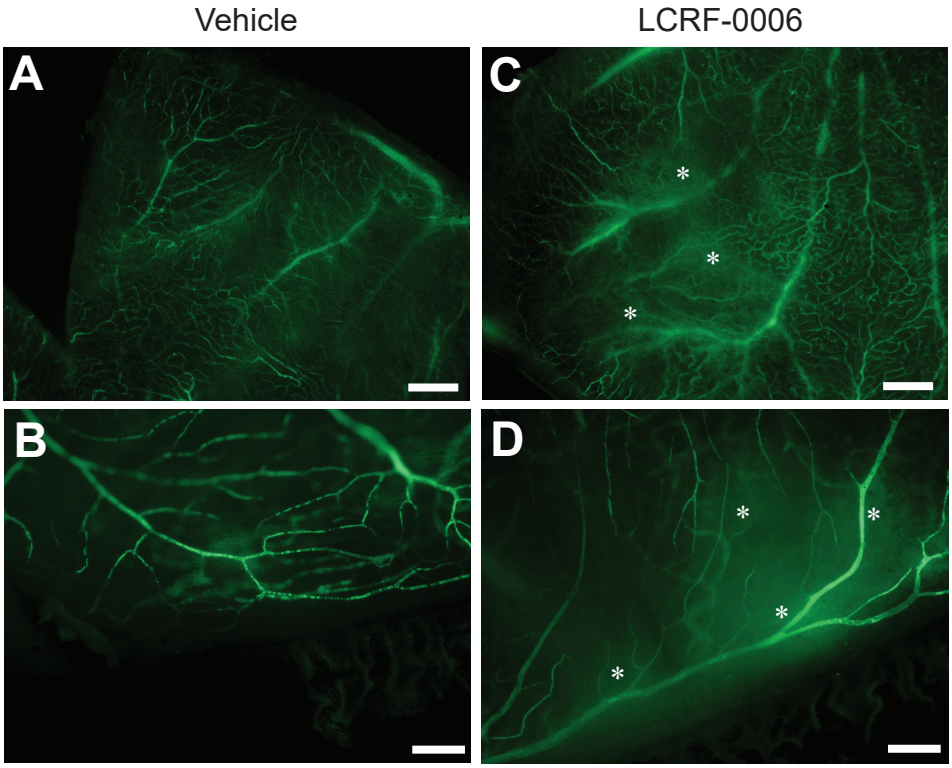
Vehicle
LCRF-0006
A
B
C
D

**Figure 3.5. LCRF-0006 monotherapy induces 5TGM1 MM PC apoptosis *in vitro* but does not inhibit tumour progression *in vivo*.** The viability of 5TGM1 cells following *in vitro* culture in the presence of LCRF-0006 for 72 hours was assessed by flow cytometry following annexin V and 7-AAD staining. Graph depicts mean ± SEM of 3 independent experiments (**A**). * $P < 0.05$ ** $P < 0.01$ *** $P < 0.001$ compared with 5TGM1 cells treated with vehicle alone (0μg/ml) (one-way ANOVA with Dunnett's multiple comparisons test). C57BL/KaLwRij mice with established MM (day 14 post-5TGM1 cell injection) were treated with LCRF-0006 (100mg/kg/day) or vehicle (CD) alone i.p. for 14 days. Tumour burden was assessed at day 14, 21 and 28 by BLI. Graph depicts mean ± SEM. $n$ = 12 mice/treatment group (**B**). Data are not statistically significant (two-way ANOVA).

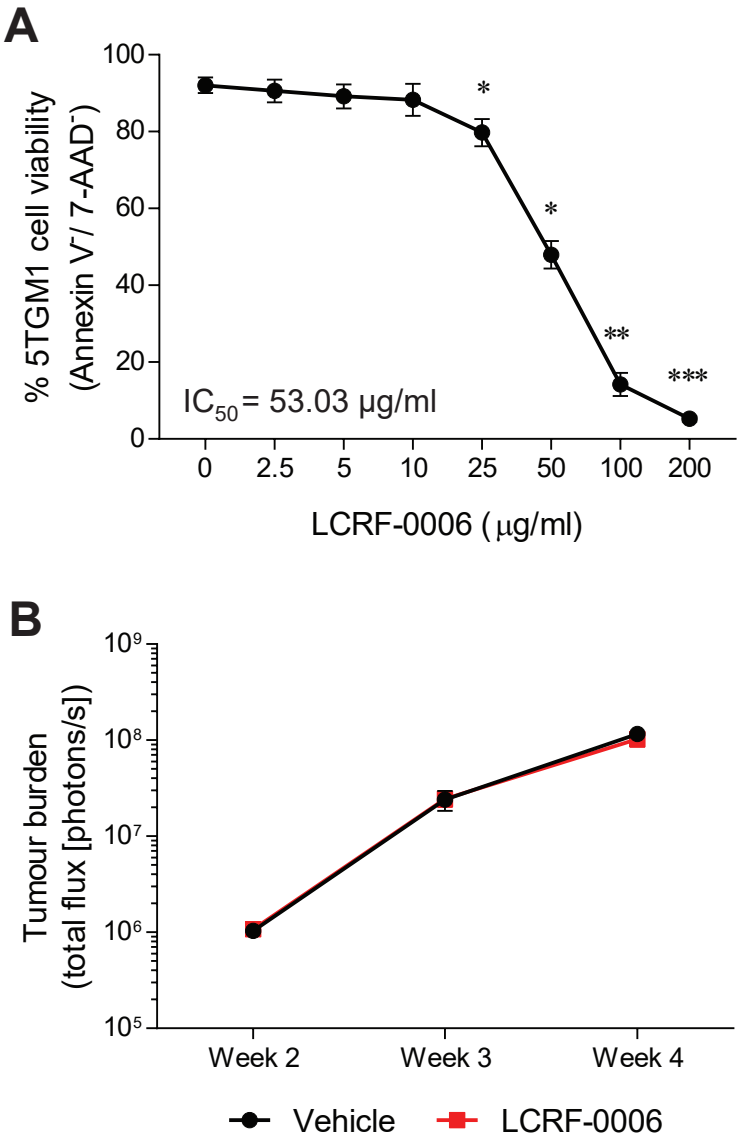
A
% 5TGM1 cell viability
(Annexin V- / 7-AAD-)
100
80
60
40
20
0
IC50 = 53.03 µg/ml
*
*
**
***
0
2.5
5
10
25
50
100
200
LCRF-0006 (µg/ml)
B
Tumour burden
(total flux [photons/s])
10^9
10^8
10^7
10^6
10^5
Week 2
Week 3
Week 4
Vehicle
LCRF-0006

Previous studies have additionally demonstrated that ADH-1 administration increases the delivery of chemotherapeutic drugs and Evans blue dye to tumour sites suggesting that N-cadherin antagonism increases vascular permeability.[17] In light of the increased vascular permeability observed with LCRF-0006 treatment *in vitro* and *in vivo*, we speculated that LCRF-0006 may enhance the delivery of anti-cancer drugs to tumour sites *in vivo*, thereby increasing drug efficacy. To this end, MM tumour-bearing C57Bl/KaLwRij mice were administered 3 cycles of combination therapy per week for 2 weeks, whereby 1 cycle consisted of LCRF-0006 (100mg/kg) followed by a low dose of the anti-MM agent bortezomib (0.5mg/kg) 1 hour later (Figure 3.6A). The combination therapy regimen was well tolerated by mice with no adverse welfare effects. Notably, low-dose bortezomib and the combination of LCRF-0006 and low-dose bortezomib did not affect the proportion of MSCs, OPs and OBs within the $Lin^-CD45^-CD31^-$ fraction of compact bone isolated from the long bones, when compared with vehicle-treated animals (data not shown). Strikingly, while neither low-dose bortezomib nor LCRF-0006 alone significantly affected tumour burden, mice which received the combination of LCRF-0006 and low-dose bortezomib had significantly lower tumour burden at days 21 and 28 compared with mice treated with bortezomib alone, LCRF-0006 alone or vehicles only (all $P < 0.001$) (Figure 3.6B-C). Notably, the combination therapy also resulted in regression of tumour burden in 5/5 mice at day 28, with 2/5 mice administered the combination therapy having no BLI-detectable tumour at the conclusion of the study. Analysis of peripheral blood collected at day 28 revealed that mice administered the combination therapy had significantly fewer residual circulating tumour cells than mice treated with vehicles alone, LCRF-0006 alone or low-dose bortezomib alone (all $P < 0.0001$) (Figure 3.6D). CDI revealed synergism in the anti-MM effects of LCRF-0006 and low-dose bortezomib (at days 21 and 28) (Figure 3.6E).

### 3.4.5 LCRF-0006 and bortezomib synergistically induce 5TGM1 cell apoptosis *in vitro*

While we speculate that the synergistic effects observed *in vivo* may in large part be mediated by LCRF-0006-enhanced tumour delivery of bortezomib, previous studies have also demonstrated the ability of ADH-1 to enhance tumour response to chemotherapeutic agents independently of increasing drug delivery to tumours.[17] To this end, we investigated the effect of LCRF-0006 in combination with bortezomib on

**Figure 3.6. The combination of LCRF-0006 and low-dose bortezomib synergistically increases MM tumour response *in vivo*.** Schematic representation of treatment regimen (**A**). C57BL/KaLwRij mice with established MM (day 14 post-5TGM1 cell injection) were treated with LCRF-0006 (100mg/kg) and low-dose bortezomib (0.5mg/kg) (LCRF-0006 + bortezomib), LCRF-0006 and DMSO vehicle (LCRF-0006), CD vehicle and low-dose bortezomib (bortezomib) or CD and DMSO vehicles (vehicles) i.p., as per treatment regimen. Tumour burden was assessed at day 14, 21 and 28 by BLI. Graph depicts mean ± SEM. $n$ = 5-6 mice/treatment group (**B**). *** $P < 0.001$ **** $P < 0.0001$ compared with mice treated with LCRF-0006, low-dose bortezomib or vehicles (two-way ANOVA with Bonferroni's multiple comparisons test). Images depict tumour burden in individual mice at day 28, as assessed by BLI (**C**). Peripheral blood was collected from mice at day 28 and the proportion of circulating tumour cells within the leukocyte fraction was assessed by flow cytometry. Graph depicts mean ± SEM. $n$ = 5-6 mice/treatment group (**D**). ** $P < 0.01$ **** $P < 0.001$ (one-way ANOVA with Holm-Sidak's multiple comparisons test). The co-efficient of drug interaction (CDI) was calculated using BLI data at day 21 and 28, and the proportion of circulating tumour cells (CTCs) within the leukocyte fraction of peripheral blood at day 28, to assess drug synergy. CDI < 0.7 (shown in shaded text) indicates drug synergy (**E**).

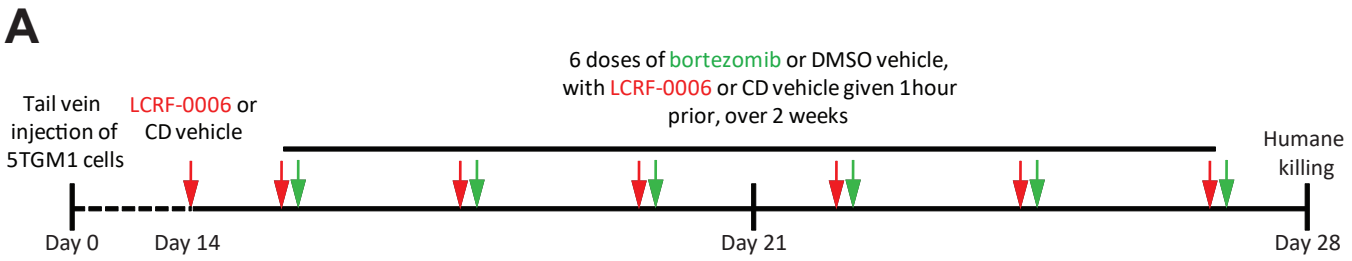


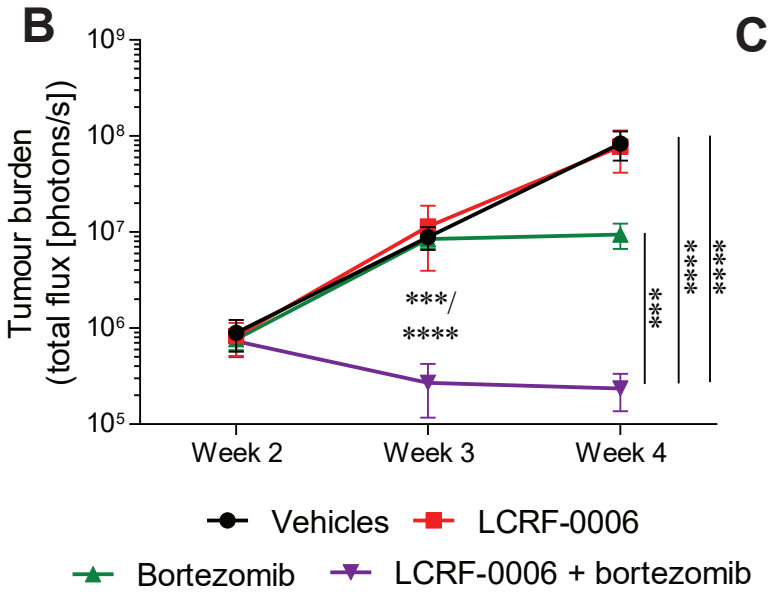


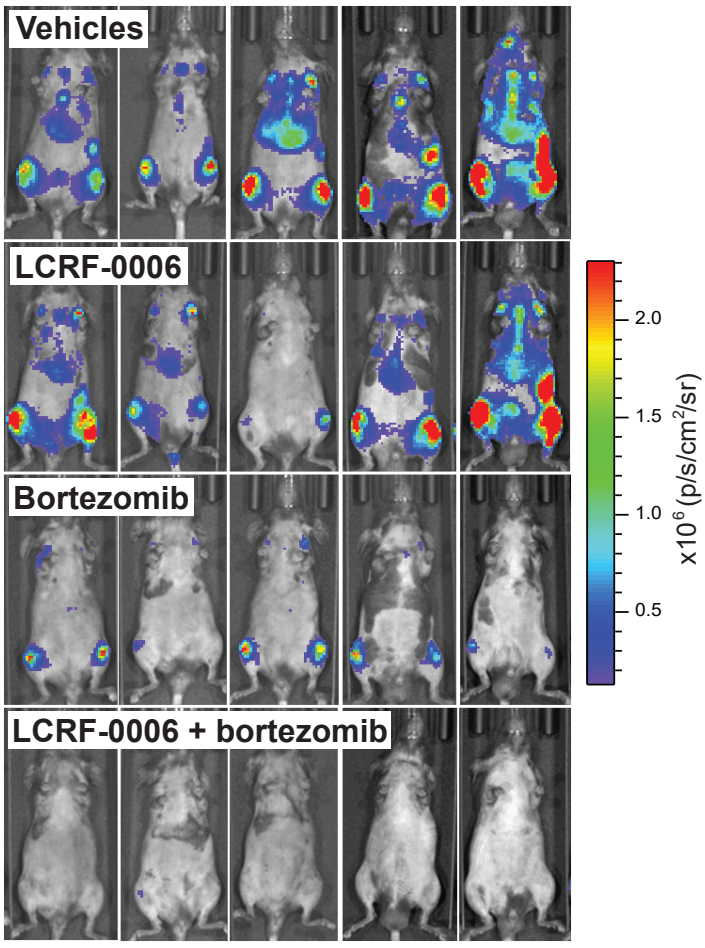


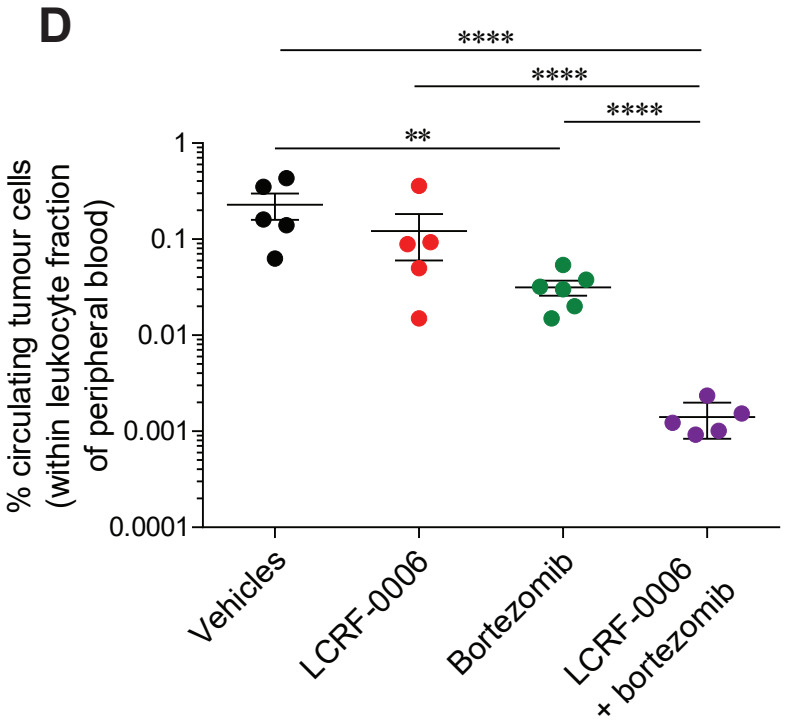


E

CDI

| | Week 3 | Week 4 |
|---|---|---|
| Ventral BLI | 0.025 | 0.029 |
| CTCs | n/a | 0.001 |

induction of 5TGM1 cell apoptosis *in vitro*, as assessed by Annexin V and 7-AAD staining. Initially, we determined the doses of LCRF-0006 (25-150μg/ml) and bortezomib (1-7nM) which individually had minimal to moderate pro-apoptotic effects on 5TGM1 cells, after 24 hrs (Figure 3.7A,B). Significantly, we found that LCRF-0006 and bortezomib had synergistic effects on 5TGM1 cell apoptosis, with LCRF-0006 concentrations of 50μg/ml and above enhancing the sensitivity of 5TGM1 cells to bortezomib, after 24 hrs (CDI < 0.7) (Figure 3.7C,D).

**Figure 3.7. LCRF-0006 synergistically increases bortezomib-induced 5TGM1 MM PC apoptosis *in vitro*.** The viability of 5TGM1 cells following *in vitro* culture in the presence of increasing concentrations of LCRF-0006 (**A**) or bortezomib (**B**) for 24 hours was assessed by flow cytometry following annexin V and 7-AAD staining. Graphs depict mean ± SEM of 3 independent experiments. * $P < 0.05$ ** $P < 0.01$ *** $P < 0.001$ compared with 5TGM1 cells treated with vehicle alone (0µg/ml) (one-way ANOVA with Dunnett's multiple comparisons test). Graphical representation of 5TGM1 cell viability following *in vitro* culture in the presence of bortezomib and increasing concentrations of LCRF-0006 simultaneously for 24 hours (as assessed by flow cytometry following Annexin V and 7-AAD staining), relative to 5TGM1 cells treated with vehicle alone (**C**). Data is representative of 3 independent experiments. The co-efficient of drug interaction (CDI) was calculated using the relative viability of 5TGM1 cells after 24 hours to assess drug synergy. CDI < 0.7 (shown in shaded text) indicates drug synergy (**D**). Data are representative of 3 independent experiments.

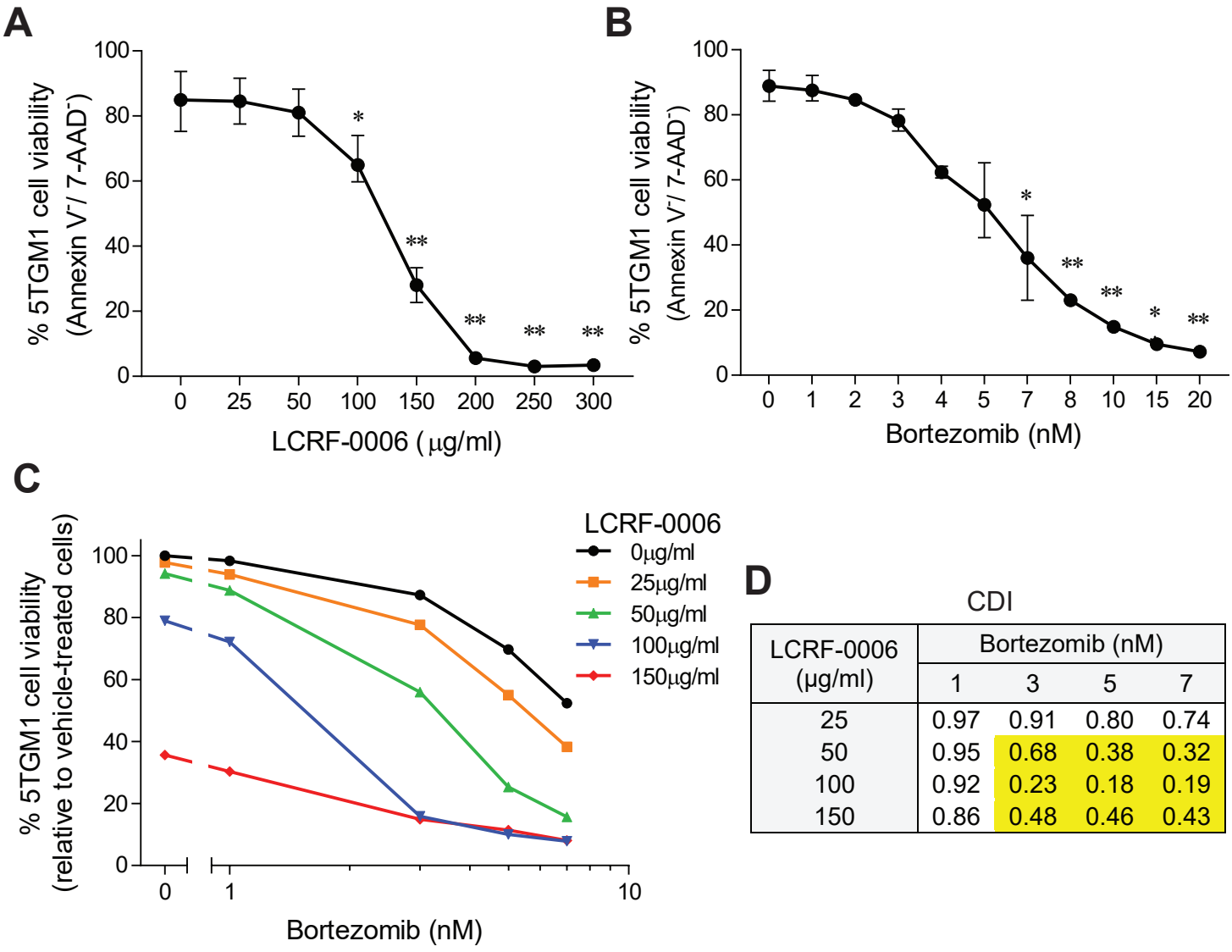


**D**

CDI

| LCRF-0006 (μg/ml) | Bortezomib (nM) | | | |
|---|---|---|---|---|
| | 1 | 3 | 5 | 7 |
| 25 | 0.97 | 0.91 | 0.80 | 0.74 |
| 50 | 0.95 | 0.68 | 0.38 | 0.32 |
| 100 | 0.92 | 0.23 | 0.18 | 0.19 |
| 150 | 0.86 | 0.48 | 0.46 | 0.43 |

## 3.5 Discussion

Tumour-associated vasculature is structurally abnormal, characterised by gaps between adjacent ECs and loosely attached or absent mural cells.[22,28,60] These structural abnormalities, in addition to the disorganised, tortuous nature of tumour-associated vasculature, and the defective lymphatic drainage in tumours, result in abnormal pressure gradients and heterogeneous perfusion which can limit drug delivery to the tumour.[19,60,61] Paradoxically, however, the compromised EC barrier of tumour-associated vasculature is thought to mediate the passive and selective extravasation of macromolecules (> 40 kDa) into interstitial tumour spaces.[23-27,62,63] Furthermore, the paucity of lymphatic drainage is considered to increase the retention of macromolecular drugs at the tumour site.[63,64] Collectively, this phenomenon is known as the enhanced permeability and retention (EPR) effect.[62,63] One hypothesised approach to increase the efficiency of tumour delivery of macromolecular drugs, or drug complexes, is by augmentation of the EPR effect.[62,63,65] Pre-clinical studies have demonstrated that factors such as angiotensin II and nitric oxide can rapidly increase macromolecular extravasation in tumours by increasing tumour blood flow, thereby improving tumour delivery of, and response to, macromolecular drugs and drug complexes.[66-70] Indeed, a nitric oxide delivery system which augments the EPR effect was recently shown to increase the anti-cancer efficacy of nanoparticle albumin-bound paclitaxel (Abraxane®) in several pre-clinical cancer models, including a colon cancer model possessing inherently high vascular permeability and a melanoma model characterised by inherently low vascular permeability.[68,71] Notably, recent studies have demonstrated the efficacy of the N-cadherin antagonist ADH-1 to increase EC permeability *in vitro*, and rapidly enhance tumour blood vessel permeability to macromolecules *in vivo*, as demonstrated by the accumulation of albumin conjugated-Evans blue dye in melanoma tumours of mice treated with ADH-1. Moreover, ADH-1 improved melanoma tumour uptake of, and response to, the chemotherapeutic agent melphalan, which displays high affinity for plasma proteins.[17,72] Taken together, these studies suggest that N-cadherin antagonists may increase the delivery of plasma protein-bound drugs to tumours by increasing the permeability of tumour-associated vasculature, thereby improving tumour response to chemotherapy.[17]

The primary objective of the current study was to evaluate the efficacy of a small molecule peptidomimetic of ADH-1, LCRF-0006, as a novel vascular disrupting

agent and to assess its ability to increase the effectiveness of the anti-MM agent bortezomib[73,74] in a pre-clinical model of MM. We have demonstrated that LCRF-0006 is a vascular disrupting agent which increases blood vessel permeability to macromolecules, as evidenced by LCRF-0006-mediated extravasation of 70 kDa FITC-dextran in retinal tissues. Mechanistically, our *in vitro* studies using BMECs suggest that LCRF-0006 enhances vascular permeability by directly inducing the retraction of endothelial monolayers, thereby facilitating para-cellular macromolecule transport. It is well established that N-cadherin mediates the recruitment and adhesion of mural cells to the abluminal surface of ECs, which stabilises blood vessel integrity and modulates barrier function.[5,6,14,15,18] Indeed, recent studies using three-dimensional bio-engineered microvessels suggest that abrogation of N-cadherin-mediated mural cell attachment to endothelial cells also enhances endothelial barrier permeability to macromolecules.[18] As retinal microvessels have a relatively high pericyte coverage[75], it is possible that LCRF-0006 may also compromise endothelial barrier function by disrupting EC-mural cell interactions.

The observation that disrupted BMEC monolayers recovered *in vitro* following removal of LCRF-0006 suggests that the effects of LCRF-0006 on ECs are transient and reversible, in line with the proposed role of N-cadherin in endothelial barrier closure.[76,77] Moreover, the disruptive effects of LCRF-0006 are not a consequence of EC apoptosis which may eventuate in vessel collapse. This is consistent with our findings that LCRF-0006 did not affect the EC composition of long bones or the overall vascular architecture of the bone marrow, either in the normal or malignant setting. Thus, the effects of LCRF-0006 differ from those of vascular disrupting agents such as microtubule-depolymerizing agents which induce necrosis of tumour-associated vasculature.[28,51,78] Importantly, we also observed that the initial effects of LCRF-0006 on EC retraction and rounding were more rapid in immature endothelial tubes than established tubes. As tumour-associated vasculature is considered to be relatively immature, in comparison to normal blood vessels[28,29], these findings suggest that tumour-associated vasculature may have increased sensitivity to LCRF-0006-mediated disruption, compared with normal blood vessels.

The anti-MM agent bortezomib, used as induction therapy, maintenance therapy, and in the relapse setting[73,74,79,80], is a small, dipeptide boronic acid which becomes highly bound to plasma proteins upon clinical administration.[81] On the basis of previous reports that ADH-1 increased melanoma tumour delivery of, and response to,

melphalan, which similarly has high plasma protein affinity[17,72], we speculated that LCRF-0006 may enhance MM tumour delivery of bortezomib. Although LCRF-0006 did not display single-agent anti-tumour efficacy in the C57Bl/KaLwRij/5TGM1 MM model, LCRF-0006 in combination with a sub-therapeutic dose of bortezomib induced a synergistic response in mice with established tumours, with tumour regression achieved in all animals. Importantly, the combination therapy was well tolerated with no adverse effects observed on animal welfare.

While we speculate that the synergistic effects may, at least in part, be mediated by enhanced tumour delivery of bortezomib facilitated by LCRF-0006, potentially by augmentation of the EPR effect, N-cadherin antagonists may directly enhance tumour response to chemotherapeutic agents. For example, ADH-1 has previously been shown to significantly increase melanoma tumour response to the chemotherapeutic agent temozolamide *in vivo*, without altering tumour up-take of the drug.[17] Consistent with these findings, our *in vitro* drug combination assays provide evidence that LCRF-0006 and bortezomib can synergistically induce apoptosis in 5TGM1 cells, which may further contribute to the synergism observed *in vivo*. One potential mechanism by which LCRF-0006 and bortezomib may synergistically induce MM tumour cell apoptosis is by differential inhibition of the Bcl-2-family pro-survival proteins Bcl-2 and Mcl-1, shown to mediate MM tumour cell survival.[82-85] Proteasome inhibition by bortezomib is thought to induce MM tumour cell apoptosis by increasing the expression of NOXA which neutralizes and degrades Mcl-1.[86-89] In contrast, N-cadherin engagement has been shown to activate Bcl-2 by enhancing PI3K/Akt-mediated phosphorylation of the pro-apoptosis protein Bad.[90-92] Thus, LCRF-0006 may potentially inhibit the phosphorylation of Bad, resulting in inactivation of Bcl-2. Recent studies have also shown that N-cadherin potentiates prostate cancer cell resistance to metformin by activation of NF-κB signalling, which could be inhibited by perturbation of N-cadherin function.[93] In light of this, LCRF-0006 may decrease activation of NF-κB signalling in 5TGM1 cells, a pathway implicated in chemotherapeutic resistance of human MM cells[94-97], thereby increasing sensitivity to bortezomib.

In addition, it is also possible that LCRF-0006 may disrupt the physical engagement of MM cells with the BM microenvironmental niche, known to play critical roles in MM cell growth, proliferation and resistance to chemotherapeutic agents.[98-101] N-cadherin is expressed by numerous cell types within the BM milieu, including MSCs and OBs, and mediates MM tumour cell adhesion to OBs.[52,53,102,103] Moreover, N-

cadherin expression in MM tumour cells is a negative regulator of OB differentiation, which may potentiate tumour growth by maintaining the MSC pool.[52,104] Our analyses revealed that LCRF-0006 treatment did not affect the relative proportion of MSCs, OPs and OBs within the long bones of MM tumour-bearing or tumour-naïve C57Bl/KaLwRij mice, which is consistent with our observed lack of single-agent LCRF-0006 efficacy to inhibit MM tumour growth *in vivo*. However, given the ability of N-cadherin antagonists to overcome BM stromal cell-mediated leukaemic cell resistance to chemotherapeutic agents[105,106], we cannot exclude the possibility that LCRF-0006 treatment may disrupt MM tumour cell interactions with the supportive BM niche *in vivo*, thereby increasing tumour cell sensitivity to bortezomib. Importantly, while bortezomib has known bone anabolic effects in the clinical setting[107,108], low-dose bortezomib did not affect the relative cellular composition of compact bone tissue. Thus, it is unlikely that low-dose bortezomib indirectly alters 5TGM1 cell response to LCRF-0006 therapy by modifying the endosteal BM niche.

Despite significant progress in the development of novel therapeutic agents and effective combination strategies over the past decade, MM is still largely considered to be incurable with most patients relapsing and ultimately succumbing to the disease.[79] Notably, there is increasing evidence, both *in vitro* and in pre-clinical animal models, that N-cadherin antagonism represents a potential approach to increase the efficacy of chemotherapeutic agents.[17,72,105,106] However, these findings have not been fully replicated in Phase I/II clinical trials to date.[30,31] Given synthetic small molecule peptidomimetics may offer increased therapeutic efficacy over their peptide counterparts[32,33], the use of an ADH-1 peptidomimetic is a rational proposition to potentially improve clinical efficacy. In the current study, we report that the small molecule ADH-1 mimetic LCRF-0006 is a novel vascular disrupting agent which increases vascular permeability *in vitro* and *in vivo*. Our findings demonstrate the potential clinical utility of LCRF-0006 in a combinatorial approach to significantly increase bortezomib efficacy and enhance the depth of tumour response in MM patients.

## 3.6 Acknowledgements

The authors would like to acknowledge Dr Randall Grose for assistance with flow cytometry, and Mrs Sharon Paton, Mrs Vicki Wilczek and Ms Jia Ng for assistance with animal experiments. This research was supported by a grant from the Cancer Australia Priority-driven Collaborative Cancer Research Scheme, co-funded by the Leukaemia Foundation. Kate Vandyke was supported by a fellowship from the Multiple Myeloma Research Foundation and by a Mary Overton Early Career Research Fellowship (Royal Adelaide Hospital).

## 3.7 References

1. Komarova Y, Malik AB. Regulation of endothelial permeability via paracellular and transcellular transport pathways. *Annu Rev Physiol*. 2010; 72:463-493.

2. Goddard LM, Iruela-Arispe ML. Cellular and molecular regulation of vascular permeability. *Thromb Haemost*. 2013; 109(3):407-415.

3. Trani M, Dejana E. New insights in the control of vascular permeability: vascular endothelial-cadherin and other players. *Curr Opin Hematol*. 2015; 22(3):267-272.

4. Komarova YA, Kruse K, Mehta D, Malik AB. Protein Interactions at Endothelial Junctions and Signaling Mechanisms Regulating Endothelial Permeability. *Circ Res*. 2017; 120(1):179-206.

5. Paik JH, Skoura A, Chae SS, Cowan AE, Han DK, Proia RL, Hla T. Sphingosine 1-phosphate receptor regulation of N-cadherin mediates vascular stabilization. *Genes Dev*. 2004; 18(19):2392-2403.

6. Tillet E, Vittet D, Feraud O, Moore R, Kemler R, Huber P. N-cadherin deficiency impairs pericyte recruitment, and not endothelial differentiation or sprouting, in embryonic stem cell-derived angiogenesis. *Exp Cell Res*. 2005; 310(2):392-400.

7. Giampietro C, Taddei A, Corada M, Sarra-Ferraris GM, Alcalay M, Cavallaro U, Orsenigo F, Lampugnani MG, Dejana E. Overlapping and divergent signaling pathways of N-cadherin and VE-cadherin in endothelial cells. *Blood*. 2012; 119(9):2159-2170.

8. Erez N, Zamir E, Gour BJ, Blaschuk OW, Geiger B. Induction of apoptosis in cultured endothelial cells by a cadherin antagonist peptide: involvement of fibroblast growth factor receptor-mediated signalling. *Exp Cell Res*. 2004; 294(2):366-378.

9. Salomon D, Ayalon O, Patel-King R, Hynes RO, Geiger B. Extrajunctional distribution of N-cadherin in cultured human endothelial cells. *J Cell Sci*. 1992; 102 ( Pt 1):7-17.

10. Navarro P, Ruco L, Dejana E. Differential localization of VE- and N-cadherins in human endothelial cells: VE-cadherin competes with N-cadherin for junctional localization. *J Cell Biol*. 1998; 140(6):1475-1484.

11. Ferreri DM, Minnear FL, Yin T, Kowalczyk AP, Vincent PA. N-cadherin levels in endothelial cells are regulated by monolayer maturity and p120 availability. *Cell Commun Adhes*. 2008; 15(4):333-349.

12. Amsellem V, Dryden NH, Martinelli R, Gavins F, Almagro LO, Birdsey GM, Haskard DO, Mason JC, Turowski P, Randi AM. ICAM-2 regulates vascular permeability and N-cadherin localization through ezrin-radixin-moesin (ERM) proteins and Rac-1 signalling. *Cell Commun Signal*. 2014; 12:12.

13. Luo Y, Radice GL. N-cadherin acts upstream of VE-cadherin in controlling vascular morphogenesis. *J Cell Biol*. 2005; 169(1):29-34.

14. Gerhardt H, Wolburg H, Redies C. N-cadherin mediates pericytic-endothelial interaction during brain angiogenesis in the chicken. *Dev Dyn*. 2000; 218(3):472-479.

15. Sabatini PJ, Zhang M, Silverman-Gavrila R, Bendeck MP, Langille BL. Homotypic and endothelial cell adhesions via N-cadherin determine polarity and regulate migration of vascular smooth muscle cells. *Circ Res*. 2008; 103(4):405-412.

16. Gerhardt H, Betsholtz C. Endothelial-pericyte interactions in angiogenesis. *Cell Tissue Res*. 2003; 314(1):15-23.

17. Turley RS, Tokuhisa Y, Toshimitsu H, Lidsky ME, Padussis JC, Fontanella A, Deng W, Augustine CK, Beasley GM, Davies MA *et al*. Targeting N-cadherin increases vascular permeability and differentially activates AKT in melanoma. *Ann Surg*. 2015; 261(2):368-377.

18. Alimperti S, Mirabella T, Bajaj V, Polacheck W, Pirone DM, Duffield J, Eyckmans J, Assoian RK, Chen CS. Three-dimensional biomimetic vascular model reveals a RhoA, Rac1, and N-cadherin balance in mural cell-endothelial cell-regulated barrier function. *Proc Natl Acad Sci U S A*. 2017; 114(33):8758-8763.

19. Siemann DW, Horsman MR. Modulation of the tumor vasculature and oxygenation to improve therapy. *Pharmacol Ther*. 2015; 153:107-124.

20. Comunanza V, Bussolino F. Therapy for Cancer: Strategy of Combining Anti-Angiogenic and Target Therapies. *Front Cell Dev Biol*. 2017; 5:101.

21. Blaschuk OW, Rowlands TM. Cadherins as modulators of angiogenesis and the structural integrity of blood vessels. *Cancer Metastasis Rev*. 2000; 19(1-2):1-5.

22. Ribatti D, Nico B, Crivellato E, Vacca A. The structure of the vascular network of tumors. *Cancer Lett*. 2007; 248(1):18-23.

23. Hashizume H, Baluk P, Morikawa S, McLean JW, Thurston G, Roberge S, Jain RK, McDonald DM. Openings between defective endothelial cells explain tumor vessel leakiness. *Am J Pathol*. 2000; 156(4):1363-1380.

24. Gerlowski LE, Jain RK. Microvascular permeability of normal and neoplastic tissues. *Microvasc Res*. 1986; 31(3):288-305.

25. Hobbs SK, Monsky WL, Yuan F, Roberts WG, Griffith L, Torchilin VP, Jain RK. Regulation of transport pathways in tumor vessels: role of tumor type and microenvironment. *Proc Natl Acad Sci U S A*. 1998; 95(8):4607-4612.

26. Damianovich M, Hout Siloni G, Barshack I, Simansky DA, Kidron D, Dar E, Avivi C, Onn A. Structural basis for hyperpermeability of tumor vessels in advanced lung adenocarcinoma complicated by pleural effusion. *Clin Lung Cancer*. 2013; 14(6):688-698.

27. Morikawa S, Baluk P, Kaidoh T, Haskell A, Jain RK, McDonald DM. Abnormalities in pericytes on blood vessels and endothelial sprouts in tumors. *Am J Pathol*. 2002; 160(3):985-1000.

28. Siemann DW. The unique characteristics of tumor vasculature and preclinical evidence for its selective disruption by Tumor-Vascular Disrupting Agents. *Cancer treatment reviews*. 2011; 37(1):63-74.

29. Tozer GM, Kanthou C, Baguley BC. Disrupting tumour blood vessels. *Nat Rev Cancer*. 2005; 5(6):423-435.

30. Beasley GM, Riboh JC, Augustine CK, Zager JS, Hochwald SN, Grobmyer SR, Peterson B, Royal R, Ross MI, Tyler DS. Prospective multicenter phase II trial of systemic ADH-1 in combination with melphalan via isolated limb infusion in patients with advanced extremity melanoma. *J Clin Oncol*. 2011; 29(9):1210-1215.

31. Beasley GM, McMahon N, Sanders G, Augustine CK, Selim MA, Peterson B, Norris R, Peters WP, Ross MI, Tyler DS. A phase 1 study of systemic ADH-1 in combination with melphalan via isolated limb infusion in patients with locally advanced in-transit malignant melanoma. *Cancer*. 2009; 115(20):4766-4774.

32. Scognamiglio PL, Morelli G, Marasco D. Synthetic and structural routes for the rational conversion of peptides into small molecules. *Methods Mol Biol*. 2015; 1268:159-193.

33. Vagner J, Qu H, Hruby VJ. Peptidomimetics, a synthetic tool of drug discovery. *Curr Opin Chem Biol*. 2008; 12(3):292-296.

34. Gour BJ, Blaschuk OW, Ali A, Ni F, Chen Z, Michaud SD, Wang S, Hu Z. Peptidomimetic modulators of cell adhesion. In. United States: Adherex Technologies, Inc.; 2008.

35. Noll JE, Hewett DR, Williams SA, Vandyke K, Kok C, To LB, Zannettino AC. SAMSN1 is a tumor suppressor gene in multiple myeloma. *Neoplasia*. 2014; 16(7):572-585.

36. Cheong CM, Chow AW, Fitter S, Hewett DR, Martin SK, Williams SA, To LB, Zannettino AC, Vandyke K. Tetraspanin 7 (TSPAN7) expression is upregulated in multiple myeloma patients and inhibits myeloma tumour development in vivo. *Exp Cell Res*. 2015; 332(1):24-38.

37. Schweitzer KM, Vicart P, Delouis C, Paulin D, Drager AM, Langenhuijsen MM, Weksler BB. Characterization of a newly established human bone marrow endothelial cell line: distinct adhesive properties for hematopoietic progenitors compared with human umbilical vein endothelial cells. *Lab Invest*. 1997; 76(1):25-36.

38. Mrozik KM, Cheong CM, Hewett D, Chow AW, Blaschuk OW, Zannettino AC, Vandyke K. Therapeutic targeting of N-cadherin is an effective treatment for multiple myeloma. *Br J Haematol*. 2015; 171(3):387-399.

39. Martin SK, Dewar AL, Farrugia AN, Horvath N, Gronthos S, To LB, Zannettino AC. Tumor angiogenesis is associated with plasma levels of stromal-derived factor-1alpha in patients with multiple myeloma. *Clin Cancer Res*. 2006; 12(23):6973-6977.

40. Oyajobi BO, Munoz S, Kakonen R, Williams PJ, Gupta A, Wideman CL, Story B, Grubbs B, Armstrong A, Dougall WC *et al*. Detection of myeloma in skeleton of mice by whole-body optical fluorescence imaging. *Molecular cancer therapeutics*. 2007; 6(6):1701-1708.

41. Scheppke L, Aguilar E, Gariano RF, Jacobson R, Hood J, Doukas J, Cao J, Noronha G, Yee S, Weis S *et al*. Retinal vascular permeability suppression by topical application of a novel VEGFR2/Src kinase inhibitor in mice and rabbits. *J Clin Invest*. 2008; 118(6):2337-2346.

42. Cai J, Wu L, Qi X, Li Calzi S, Caballero S, Shaw L, Ruan Q, Grant MB, Boulton ME. PEDF regulates vascular permeability by a gamma-secretase-mediated pathway. *PLoS One*. 2011; 6(6):e21164.

43. Enis DR, Shepherd BR, Wang Y, Qasim A, Shanahan CM, Weissberg PL, Kashgarian M, Pober JS, Schechner JS. Induction, differentiation, and remodeling of blood vessels after transplantation of Bcl-2-transduced endothelial cells. *Proc Natl Acad Sci U S A*. 2005; 102(2):425-430.

44. Tual-Chalot S, Allinson KR, Fruttiger M, Arthur HM. Whole mount immunofluorescent staining of the neonatal mouse retina to investigate angiogenesis in vivo. *J Vis Exp*. 2013(77):e50546.

45. Devemy E, Blaschuk OW. Identification of a novel N-cadherin antagonist. *Peptides*. 2008; 29(11):1853-1861.

46. Gilmont RR, Dardano A, Engle JS, Adamson BS, Welsh MJ, Li T, Remick DG, Smith DJ, Jr., Rees RS. TNF-alpha potentiates oxidant and reperfusion-induced endothelial cell injury. *J Surg Res*. 1996; 61(1):175-182.

47. Thomas A, Wang S, Sohrabi S, Orr C, He R, Shi W, Liu Y. Characterization of vascular permeability using a biomimetic microfluidic blood vessel model. *Biomicrofluidics*. 2017; 11(2):024102.

48. Siflinger-Birnboim A, Goligorsky MS, Del Vecchio PJ, Malik AB. Activation of protein kinase C pathway contributes to hydrogen peroxide-induced increase in endothelial permeability. *Lab Invest*. 1992; 67(1):24-30.

49. Wong BW, Rahmani M, Luo Z, Yanagawa B, Wong D, Luo H, McManus BM. Vascular endothelial growth factor increases human cardiac microvascular endothelial cell permeability to low-density lipoproteins. *J Heart Lung Transplant*. 2009; 28(9):950-957.

50. Ng CT, Fong LY, Sulaiman MR, Moklas MA, Yong YK, Hakim MN, Ahmad Z. Interferon-Gamma Increases Endothelial Permeability by Causing Activation of p38

MAP Kinase and Actin Cytoskeleton Alteration. *J Interferon Cytokine Res*. 2015; 35(7):513-522.

51. Kanthou C, Tozer GM. Tumour targeting by microtubule-depolymerizing vascular disrupting agents. *Expert Opin Ther Targets*. 2007; 11(11):1443-1457.

52. Groen RW, de Rooij MF, Kocemba KA, Reijmers RM, de Haan-Kramer A, Overdijk MB, Aalders L, Rozemuller H, Martens AC, Bergsagel PL *et al*. N-cadherin-mediated interaction with multiple myeloma cells inhibits osteoblast differentiation. *Haematologica*. 2011; 96(11):1653-1661.

53. Hay E, Laplantine E, Geoffroy V, Frain M, Kohler T, Muller R, Marie PJ. N-cadherin interacts with axin and LRP5 to negatively regulate Wnt/beta-catenin signaling, osteoblast function, and bone formation. *Mol Cell Biol*. 2009; 29(4):953-964.

54. Castro CH, Shin CS, Stains JP, Cheng SL, Sheikh S, Mbalaviele G, Szejnfeld VL, Civitelli R. Targeted expression of a dominant-negative N-cadherin in vivo delays peak bone mass and increases adipogenesis. *J Cell Sci*. 2004; 117(Pt 13):2853-2864.

55. Cheng SL, Shin CS, Towler DA, Civitelli R. A dominant negative cadherin inhibits osteoblast differentiation. *J Bone Miner Res*. 2000; 15(12):2362-2370.

56. Shintani Y, Fukumoto Y, Chaika N, Grandgenett PM, Hollingsworth MA, Wheelock MJ, Johnson KR. ADH-1 suppresses N-cadherin-dependent pancreatic cancer progression. *Int J Cancer*. 2008; 122(1):71-77.

57. Kelland L. Drug evaluation: ADH-1, an N-cadherin antagonist targeting cancer vascularization. *Curr Opin Mol Ther*. 2007; 9(1):86-91.

58. Lammens T, Swerts K, Derycke L, De Craemer A, De Brouwer S, De Preter K, Van Roy N, Vandesompele J, Speleman F, Philippe J *et al*. N-cadherin in neuroblastoma disease: expression and clinical significance. *PLoS One*. 2012; 7(2):e31206.

59. Sadler NM, Harris BR, Metzger BA, Kirshner J. N-cadherin impedes proliferation of the multiple myeloma cancer stem cells. *American journal of blood research*. 2013; 3(4):271-285.

60. Dewhirst MW, Secomb TW. Transport of drugs from blood vessels to tumour tissue. *Nat Rev Cancer*. 2017; 17(12):738-750.

61. Jain RK. Normalizing tumor microenvironment to treat cancer: bench to bedside to biomarkers. *J Clin Oncol*. 2013; 31(17):2205-2218.

62. Maeda H. Tumor-selective delivery of macromolecular drugs via the EPR effect: background and future prospects. *Bioconjug Chem*. 2010; 21(5):797-802.

63. Fang J, Nakamura H, Maeda H. The EPR effect: Unique features of tumor blood vessels for drug delivery, factors involved, and limitations and augmentation of the effect. *Adv Drug Deliv Rev*. 2011; 63(3):136-151.

64. Maeda H, Bharate GY, Daruwalla J. Polymeric drugs for efficient tumor-targeted drug delivery based on EPR-effect. *Eur J Pharm Biopharm*. 2009; 71(3):409-419.

65. Maeda H, Sawa T, Konno T. Mechanism of tumor-targeted delivery of macromolecular drugs, including the EPR effect in solid tumor and clinical overview of the prototype polymeric drug SMANCS. *J Control Release*. 2001; 74(1-3):47-61.

66. Seki T, Fang J, Maeda H. Enhanced delivery of macromolecular antitumor drugs to tumors by nitroglycerin application. *Cancer Sci*. 2009; 100(12):2426-2430.

67. Li CJ, Miyamoto Y, Kojima Y, Maeda H. Augmentation of tumour delivery of macromolecular drugs with reduced bone marrow delivery by elevating blood pressure. *Br J Cancer*. 1993; 67(5):975-980.

68. Kinoshita R, Ishima Y, Chuang VTG, Nakamura H, Fang J, Watanabe H, Shimizu T, Okuhira K, Ishida T, Maeda H *et al*. Improved anticancer effects of albumin-bound paclitaxel nanoparticle via augmentation of EPR effect and albumin-protein interactions using S-nitrosated human serum albumin dimer. *Biomaterials*. 2017; 140:162-169.

69. Maeda H, Noguchi Y, Sato K, Akaike T. Enhanced vascular permeability in solid tumor is mediated by nitric oxide and inhibited by both new nitric oxide scavenger and nitric oxide synthase inhibitor. *Jpn J Cancer Res*. 1994; 85(4):331-334.

70. Wu J, Akaike T, Maeda H. Modulation of enhanced vascular permeability in tumors by a bradykinin antagonist, a cyclooxygenase inhibitor, and a nitric oxide scavenger. *Cancer Res*. 1998; 58(1):159-165.

71. Ishima Y, Chen D, Fang J, Maeda H, Minomo A, Kragh-Hansen U, Kai T, Maruyama T, Otagiri M. S-Nitrosated human serum albumin dimer is not only a novel anti-tumor drug but also a potentiator for anti-tumor drugs with augmented EPR effects. *Bioconjug Chem*. 2012; 23(2):264-271.

72. Augustine CK, Yoshimoto Y, Gupta M, Zipfel PA, Selim MA, Febbo P, Pendergast AM, Peters WP, Tyler DS. Targeting N-cadherin enhances antitumor activity of cytotoxic therapies in melanoma treatment. *Cancer Res*. 2008; 68(10):3777-3784.

73. Rajkumar SV. Multiple myeloma: 2016 update on diagnosis, risk-stratification, and management. *American journal of hematology*. 2016; 91(7):719-734.

74. Mateos MV, Ocio EM, Paiva B, Rosinol L, Martinez-Lopez J, Blade J, Lahuerta JJ, Garcia-Sanz R, San Miguel JF. Treatment for patients with newly diagnosed multiple myeloma in 2015. *Blood reviews*. 2015; 29(6):387-403.

75. Sims DE. Recent advances in pericyte biology--implications for health and disease. *Can J Cardiol*. 1991; 7(10):431-443.

76. Alexander JS, Blaschuk OW, Haselton FR. An N-cadherin-like protein contributes to solute barrier maintenance in cultured endothelium. *J Cell Physiol*. 1993; 156(3):610-618.

77. Qi J, Chen N, Wang J, Siu CH. Transendothelial migration of melanoma cells involves N-cadherin-mediated adhesion and activation of the beta-catenin signaling pathway. *Mol Biol Cell*. 2005; 16(9):4386-4397.

78. Bayless KJ, Davis GE. Microtubule depolymerization rapidly collapses capillary tube networks in vitro and angiogenic vessels in vivo through the small GTPase Rho. *J Biol Chem*. 2004; 279(12):11686-11695.

79. Moreau P, de Wit E. Recent progress in relapsed multiple myeloma therapy: implications for treatment decisions. *Br J Haematol*. 2017; 179(2):198-218.

80. Mohan M, Matin A, Davies FE. Update on the optimal use of bortezomib in the treatment of multiple myeloma. *Cancer Manag Res*. 2017; 9:51-63.

81. www.velcade.com/files/pdfs/velcade_prescribing_information.pdf

82. Bodet L, Gomez-Bougie P, Touzeau C, Dousset C, Descamps G, Maiga S, Avet-Loiseau H, Bataille R, Moreau P, Le Gouill S *et al*. ABT-737 is highly effective against molecular subgroups of multiple myeloma. *Blood*. 2011; 118(14):3901-3910.

83. Punnoose EA, Leverson JD, Peale F, Boghaert ER, Belmont LD, Tan N, Young A, Mitten M, Ingalla E, Darbonne WC *et al*. Expression Profile of BCL-2, BCL-XL, and MCL-1 Predicts Pharmacological Response to the BCL-2 Selective Antagonist Venetoclax in Multiple Myeloma Models. *Molecular cancer therapeutics*. 2016; 15(5):1132-1144.

84. Touzeau C, Ryan J, Guerriero J, Moreau P, Chonghaile TN, Le Gouill S, Richardson P, Anderson K, Amiot M, Letai A. BH3 profiling identifies heterogeneous dependency on Bcl-2 family members in multiple myeloma and predicts sensitivity to BH3 mimetics. *Leukemia*. 2016; 30(3):761-764.

85. Gong JN, Khong T, Segal D, Yao Y, Riffkin CD, Garnier JM, Khaw SL, Lessene G, Spencer A, Herold MJ *et al*. Hierarchy for targeting prosurvival BCL2 family proteins in multiple myeloma: pivotal role of MCL1. *Blood*. 2016; 128(14):1834-1844.

86. Qin JZ, Ziffra J, Stennett L, Bodner B, Bonish BK, Chaturvedi V, Bennett F, Pollock PM, Trent JM, Hendrix MJ *et al*. Proteasome inhibitors trigger NOXA-mediated apoptosis in melanoma and myeloma cells. *Cancer Res*. 2005; 65(14):6282-6293.

87. Gomez-Bougie P, Wuilleme-Toumi S, Menoret E, Trichet V, Robillard N, Philippe M, Bataille R, Amiot M. Noxa up-regulation and Mcl-1 cleavage are associated to apoptosis induction by bortezomib in multiple myeloma. *Cancer Res*. 2007; 67(11):5418-5424.

88. Gomez-Bougie P, Menoret E, Juin P, Dousset C, Pellat-Deceunynck C, Amiot M. Noxa controls Mule-dependent Mcl-1 ubiquitination through the regulation of the Mcl-1/USP9X interaction. *Biochem Biophys Res Commun*. 2011; 413(3):460-464.

89. Wang Q, Mora-Jensen H, Weniger MA, Perez-Galan P, Wolford C, Hai T, Ron D, Chen W, Trenkle W, Wiestner A *et al*. ERAD inhibitors integrate ER stress with an epigenetic mechanism to activate BH3-only protein NOXA in cancer cells. *Proc Natl Acad Sci U S A*. 2009; 106(7):2200-2205.

90. Tran NL, Adams DG, Vaillancourt RR, Heimark RL. Signal transduction from N-cadherin increases Bcl-2. Regulation of the phosphatidylinositol 3-kinase/Akt pathway by homophilic adhesion and actin cytoskeletal organization. *J Biol Chem*. 2002; 277(36):32905-32914.

91. Yamauchi M, Yoshino I, Yamaguchi R, Shimamura T, Nagasaki M, Imoto S, Niida A, Koizumi F, Kohno T, Yokota J *et al*. N-cadherin expression is a potential survival mechanism of gefitinib-resistant lung cancer cells. *Am J Cancer Res*. 2011; 1(7):823-833.

92. Li G, Satyamoorthy K, Herlyn M. N-cadherin-mediated intercellular interactions promote survival and migration of melanoma cells. *Cancer Res*. 2001; 61(9):3819-3825.

93. Ge R, Wang Z, Wu S, Zhuo Y, Otsetov AG, Cai C, Zhong W, Wu CL, Olumi AF. Metformin represses cancer cells via alternate pathways in N-cadherin expressing vs. N-cadherin deficient cells. *Oncotarget*. 2015; 6(30):28973-28987.

94. Landowski TH, Olashaw NE, Agrawal D, Dalton WS. Cell adhesion-mediated drug resistance (CAM-DR) is associated with activation of NF-kappa B (RelB/p50) in myeloma cells. *Oncogene*. 2003; 22(16):2417-2421.

95. Markovina S, Callander NS, O'Connor SL, Xu G, Shi Y, Leith CP, Kim K, Trivedi P, Kim J, Hematti P *et al*. Bone marrow stromal cells from multiple myeloma patients uniquely induce bortezomib resistant NF-kappaB activity in myeloma cells. *Mol Cancer*. 2010; 9:176.

96. Roy P, Mukherjee T, Chatterjee B, Vijayaragavan B, Banoth B, Basak S. Non-canonical NFkappaB mutations reinforce pro-survival TNF response in multiple myeloma through an autoregulatory RelB:p50 NFkappaB pathway. *Oncogene*. 2017; 36(10):1417-1429.

97. Murray MY, Zaitseva L, Auger MJ, Craig JI, MacEwan DJ, Rushworth SA, Bowles KM. Ibrutinib inhibits BTK-driven NF-kappaB p65 activity to overcome bortezomib-resistance in multiple myeloma. *Cell Cycle*. 2015; 14(14):2367-2375.

98. Hazlehurst LA, Landowski TH, Dalton WS. Role of the tumor microenvironment in mediating de novo resistance to drugs and physiological mediators of cell death. *Oncogene*. 2003; 22(47):7396-7402.

99. Hideshima T, Mitsiades C, Tonon G, Richardson PG, Anderson KC. Understanding multiple myeloma pathogenesis in the bone marrow to identify new therapeutic targets. *Nat Rev Cancer*. 2007; 7(8):585-598.

100. Chauhan D, Uchiyama H, Akbarali Y, Urashima M, Yamamoto K, Libermann TA, Anderson KC. Multiple myeloma cell adhesion-induced interleukin-6 expression in bone marrow stromal cells involves activation of NF-kappa B. *Blood*. 1996; 87(3):1104-1112.

101. Noll JE, Williams SA, Purton LE, Zannettino AC. Tug of war in the haematopoietic stem cell niche: do myeloma plasma cells compete for the HSC niche? *Blood Cancer J*. 2012; 2:e91.

102. Dubon MJ, Yu J, Choi S, Park KS. Transforming growth factor beta induces bone marrow mesenchymal stem cell migration via noncanonical signals and N-cadherin. *J Cell Physiol*. 2018; 233(1):201-213.

103. Hay E, Nouraud A, Marie PJ. N-cadherin negatively regulates osteoblast proliferation and survival by antagonizing Wnt, ERK and PI3K/Akt signalling. *PLoS One*. 2009; 4(12):e8284.

104. Noll JE, Williams SA, Tong CM, Wang H, Quach JM, Purton LE, Pilkington K, To LB, Evdokiou A, Gronthos S *et al*. Myeloma plasma cells alter the bone marrow microenvironment by stimulating the proliferation of mesenchymal stromal cells. *Haematologica*. 2014; 99(1):163-171.

105. Eiring AM, Khorashad JS, Anderson DJ, Yu F, Redwine HM, Mason CC, Reynolds KR, Clair PM, Gantz KC, Zhang TY *et al*. beta-Catenin is required for intrinsic but not extrinsic BCR-ABL1 kinase-independent resistance to tyrosine kinase inhibitors in chronic myeloid leukemia. *Leukemia*. 2015; 29(12):2328-2337.

106. Zhang B, Li M, McDonald T, Holyoake TL, Moon RT, Campana D, Shultz L, Bhatia R. Microenvironmental protection of CML stem and progenitor cells from tyrosine kinase inhibitors through N-cadherin and Wnt-beta-catenin signaling. *Blood*. 2013; 121(10):1824-1838.

107. Mohty M, Malard F, Mohty B, Savani B, Moreau P, Terpos E. The effects of bortezomib on bone disease in patients with multiple myeloma. *Cancer*. 2014; 120(5):618-623.

108. Zangari M, Suva LJ. The effects of proteasome inhibitors on bone remodeling in multiple myeloma. *Bone*. 2016; 86:131-138.

**Supplementary Figure 3.1. LCRF-0006 does not affect the viability of BMECs after 24 hours *in vitro*.** Confluent BMEC monolayers grown *in vitro* in 24-well plates were treated with LCRF-0006, or vehicle alone, for 24 hours. BMECs were then trypsinised and cell viability was assessed by flow cytometry using annexin V and 7-AAD staining. Graph depicts mean ± SEM of 3 independent experiments. Data are not statistically significant (one-way ANOVA).

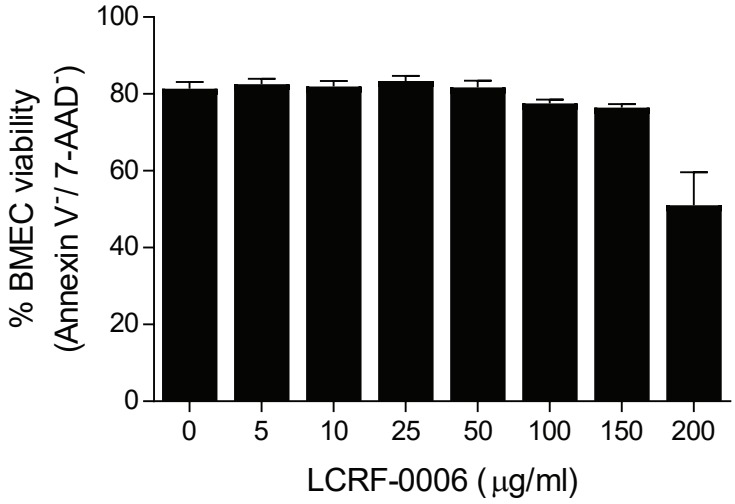
100
80
60
40
20
0
% BMEC viability
(Annexin V- / 7-AAD-)
0
5
10
25
50
100
150
200
LCRF-0006 (μg/ml)

**Supplementary Figure 3.2. Time-course of the effect of LCRF-0006 on immature (5-hour-old) endothelial tubes.** BMECs were cultured on growth factor-reduced Matrigel® matrix supplemented with RPMI-8226 conditioned medium. Tubes were allowed to form for 5 hours and were then treated with LCRF-0006 and imaged after 0, 5 and 24 hours (hrs). Images are representative of 2 independent experiments. Scale bars depict 250µm (**A**) and 100µm (**B**).

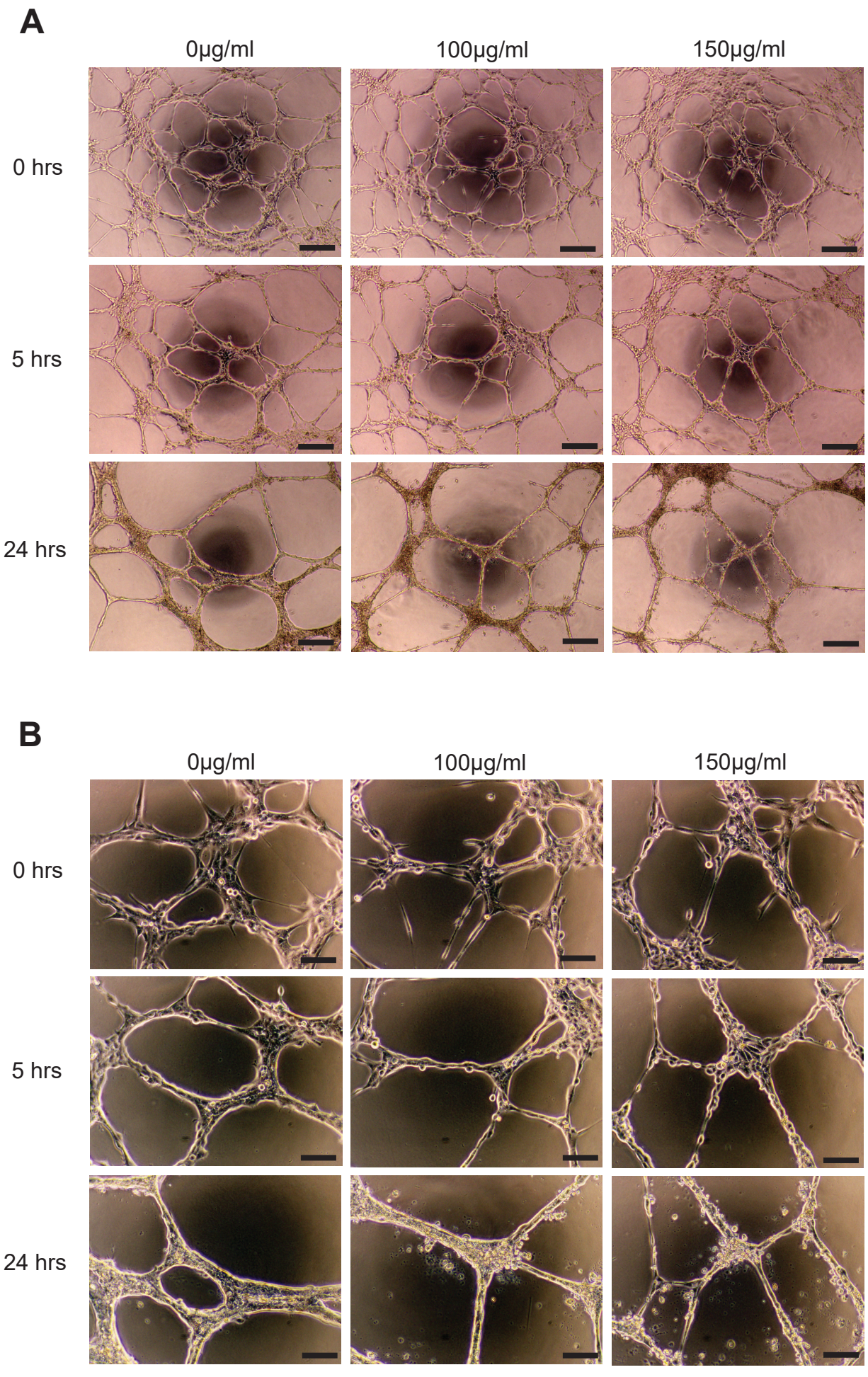
A
0μg/ml
100μg/ml
150μg/ml
0 hrs
5 hrs
24 hrs
B
0μg/ml
100μg/ml
150μg/ml
0 hrs
5 hrs
24 hrs

**Supplementary Figure 3.3. Time-course of the effect of LCRF-0006 on established (24-hour-old) endothelial tubes.** BMECs were cultured on growth factor-reduced Matrigel® matrix supplemented with RPMI-8226 conditioned medium. Tubes were allowed to form for 24 hours and were then treated with LCRF-0006 and imaged after 0, 5 and 24 hours (hrs). Images are representative of 2 independent experiments. Scale bars depict 250µm (**A**) and 100µm (**B**).

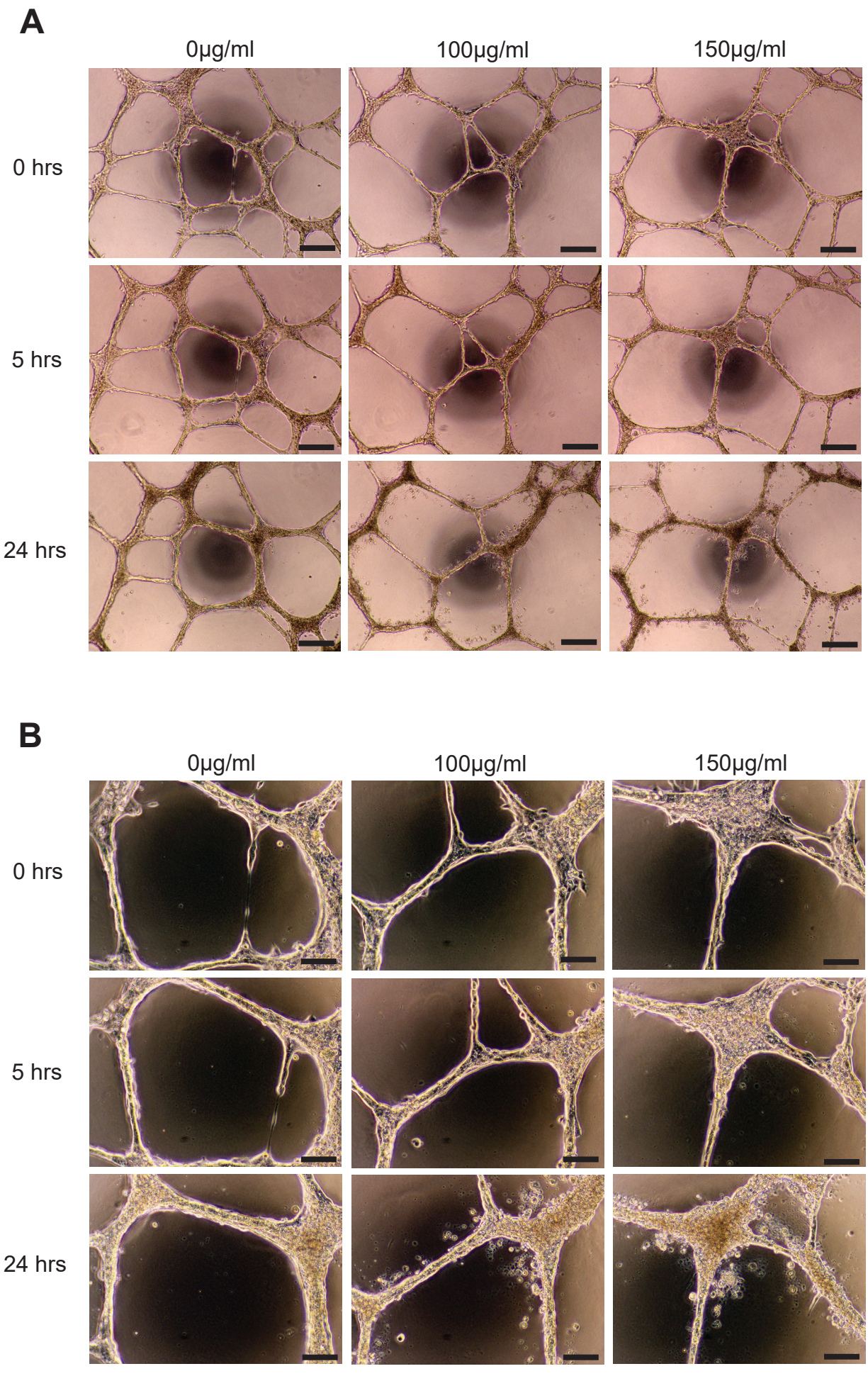
A
0μg/ml
100μg/ml
150μg/ml
0 hrs
5 hrs
24 hrs
B
0μg/ml
100μg/ml
150μg/ml
0 hrs
5 hrs
24 hrs

**Supplementary Figure 3.4. Assessment of LCRF-0006 effects on non-tumour-bearing C57Bl/KaLwRij mice.** C57Bl/KaLwRij mice were treated with 100mg/kg LCRF-0006, or vehicle (CD) alone, by i.p. injection daily for 28 days. Animal weights are shown. Graph depicts mean ± SEM. *n* = 8 mice/treatment group (**A**). Data are not statistically significant (two-way ANOVA). After 28 days, the long bones were isolated and the proportion of MSCs (Sca-$1^{+}$$CD51^{-}$) (**B**), OPs (Sca-$1^{+}$$CD51^{+}$) (**C**) and OBs (Sca-$1^{-}$$CD51^{+}$) (**D**) within the $Lin^{-}$$CD45^{-}$$CD31^{-}$ fraction of compact bone (CB) was quantified. The EC ($CD31^{+}$) composition of the non-haematopoietic ($Lin^{-}$$CD45^{-}$) fraction of CB (**E**) and bone marrow (BM) (**F**) was also quantified. Graphs depict mean ± SEM. *n* = 8 mice/treatment group. Data are not statistically significant (Mann-Whitney U test).

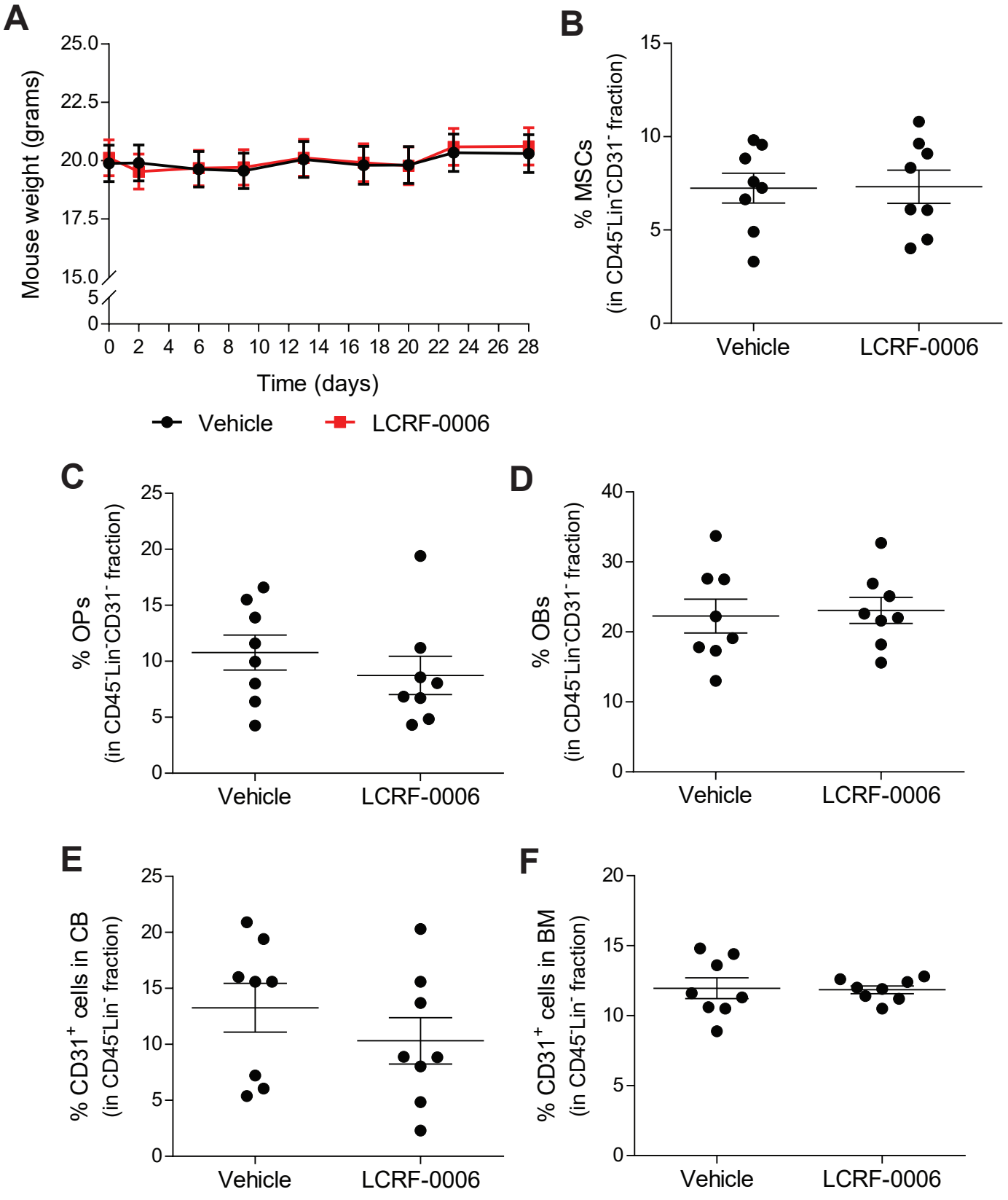
A
Mouse weight (grams)
25.0
22.5
20.0
17.5
15.0
5
0
0 2 4 6 8 10 12 14 16 18 20 22 24 26 28
Time (days)
Vehicle
LCRF-0006
B
% MSCs
(in CD45-Lin-CD31- fraction)
15
10
5
0
Vehicle
LCRF-0006
C
% OPs
(in CD45-Lin-CD31- fraction)
25
20
15
10
5
0
Vehicle
LCRF-0006
D
% OBs
(in CD45-Lin-CD31- fraction)
40
30
20
10
0
Vehicle
LCRF-0006
E
% CD31+ cells in CB
(in CD45-Lin- fraction)
25
20
15
10
5
0
Vehicle
LCRF-0006
F
% CD31+ cells in BM
(in CD45-Lin- fraction)
20
15
10
5
0
Vehicle
LCRF-0006

**Supplementary Figure 3.5. Assessment of LCRF-0006 effects in tumour-bearing C57Bl/KaLwRij mice.** C57BL/KaLwRij mice with established MM (day 14 post-5TGM1 cell injection) were treated with LCRF-0006 (100mg/kg/day) or vehicle (CD) alone i.p. for 14 days. The proportion of circulating tumour cells within the leukocyte fraction of peripheral blood collected from mice at day 28 was assessed by flow cytometry. Graph depicts mean ± SEM. *n* = 12 mice/treatment group (**A**). The EC ($CD31^+$) composition of the non-haematopoietic ($Lin^-CD45^-$) fraction of compact bone (CB) from the long bones (**B**), and bone marrow (BM) (**C**), was quantified. Graphs depict mean ± SEM. *n* = 5-9 mice/treatment group. Data are not statistically significant (Mann-Whitney U test).

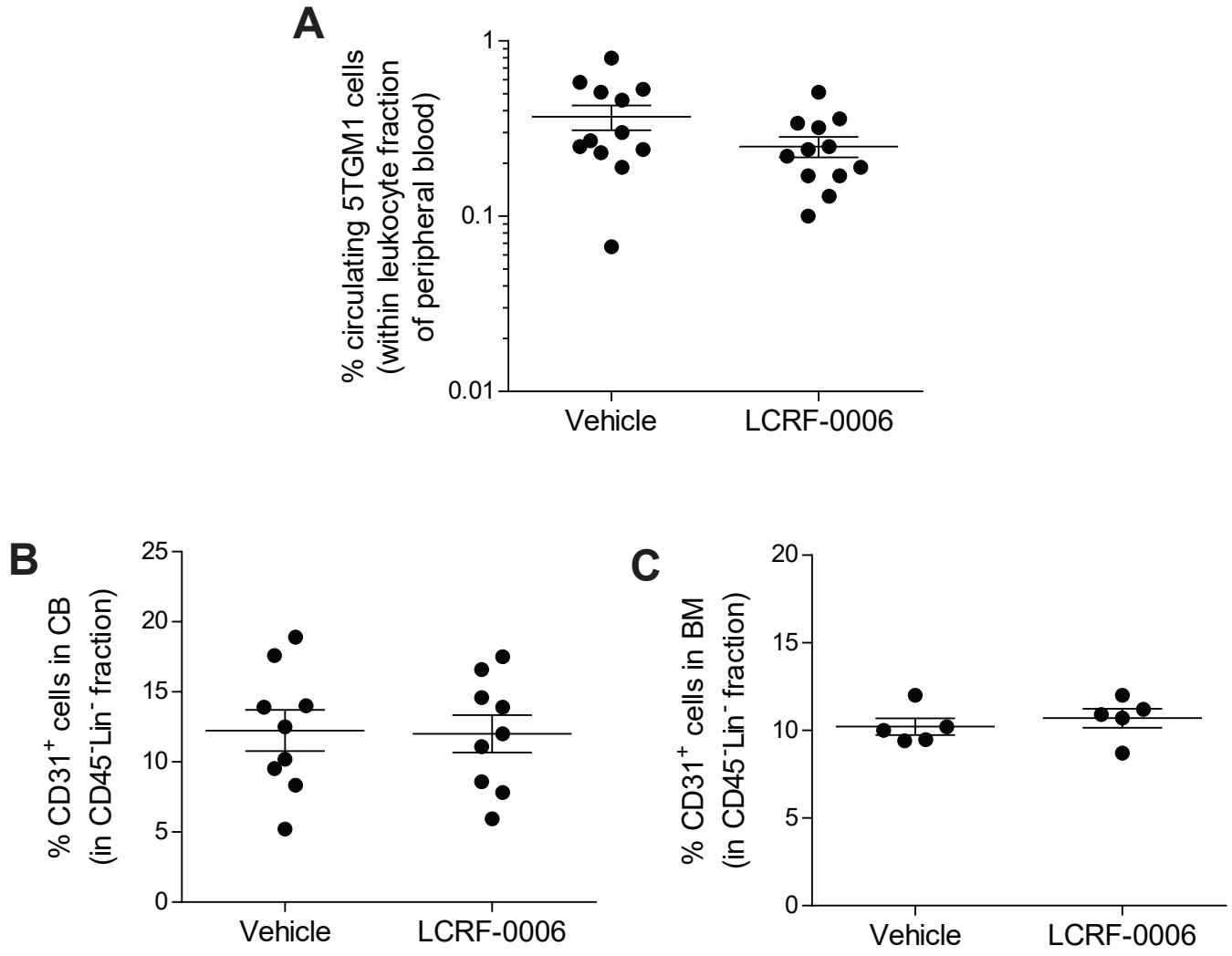
A
% circulating 5TGM1 cells (within leukocyte fraction of peripheral blood)
1
0.1
0.01
Vehicle
LCRF-0006
B
% CD31+ cells in CB (in CD45-Lin- fraction)
25
20
15
10
5
0
Vehicle
LCRF-0006
C
% CD31+ cells in BM (in CD45-Lin- fraction)
20
15
10
5
0
Vehicle
LCRF-0006

**Supplementary Table 3.1 Complete blood counts of C57Bl/KaLwRij mice[1] following 28-day 100mg/kg/day LCRF-0006 treatment**

| Parameter | Treatment | | | p-value[3] |
|---|---|---|---|---|
| | Un-treated[2] | Vehicle[2] | LCRF-0006[2] | |
| | n =8 (5m & 3f) | n =8 (4m & 4f) | n =8 (4m & 4f) | |
| WBCs (K/µl) | 5.92 ± 0.35 | 4.99 ± 0.57 | 5.49 ± 0.61 | n.s. |
| Neutrophils (K/µl) | 1.05 ± 0.18 | 0.68 ± 0.11 | 1.02 ± 0.18 | n.s. |
| Lymphocytes (K/µl) | 4.54 ± 0.18 | 4.05 ± 0.44 | 4.15 ± 0.37 | n.s. |
| Monocytes (K/µl) | 0.25 ± 0.04 | 0.18 ± 0.03 | 0.17 ± 0.04 | n.s. |
| Eosinophils (K/µl) | 0.07 ± 0.03 | 0.06 ± 0.02 | 0.11 ± 0.04 | n.s. |
| Basophils (K/µl) | 0.02 ± 0.01 | 0.02 ± 0.01 | 0.04 ± 0.01 | n.s. |
| RBCs (M/µl) | 7.59 ± 0.20 | 7.97 ± 0.10 | 7.83±0.13 | n.s. |
| Hemoglobin (g/dl) | 9.13 ± 0.14 | 9.55 ± 0.09 | 9.53 ± 0.14 | n.s. |
| Hematocrit (%) | 37.96 ± 0.99 | 39. 2± 0.39 | 39.0 ± 0.63 | n.s. |
| MCV (fl) | 50.08 ± 0.29 | 49.2 ± 0.17 | 49.8 ± 0.21 | n.s. |
| MCH (pg) | 12.05 ± 0.19 | 12.0 ± 0.13 | 12.2 ± 0.14 | n.s. |
| MCHC (g/dl) | 24.09 ± 0.44 | 24.4 ± 0.21 | 24.4 ± 0.33 | n.s. |
| RDW (%) | 16.41 ± 0.22 | 15.9 ± 0.20 | 16.9 ± 0.65 | n.s. |
| Platelets (M/µl) | 0.74 ± 0.06 | 1.05 ± 0.07 | 0.99 ± 0.09 | n.s. |
| MPV (fl) | 4.79 ± 0.16 | 4.95 ± 0.06 | 5.10 ± 0.15 | n.s. |

[1] 11-12 weeks of age at the time of cardiac bleed

[2] mean ± SEM

[3] Kruskal-Wallis test (with Dunn's multiple comparisons test)

WBCs (white blood cells), RBCs (red blood cells), MCV (mean corpuscular volume), MCH (mean corpuscular hemoglobin), MCHC (mean corpuscular hemoglobin concentration), RDW (red blood cell distribution width), MPV (mean platelet volume), n.s. (not significant)

Chapter 4

# The identification of novel mechanisms of N-cadherin regulation in $t(4;14)^+$ and $t(4;14)^-$ multiple myeloma

# Statement of Authorship

| | |
|---|---|
| Title of Paper | The identification of novel mechanisms of N-cadherin regulation in t(4;14)$^{+}$ and t(4;14)$^{-}$ multiple myeloma |
| Publication Status | ☐ Published ☐ Accepted for Publication<br>☐ Submitted for Publication ☑ Unpublished and Unsubmitted work written in manuscript style |
| Publication Details | **Mrozik K.M.**, Cheong C.M., Hewett D.R., Zannettino A.C.W., Vandyke K. Manuscript in preparation. |

## Principal Author

| | | | |
|---|---|---|---|
| Name of Principal Author (Candidate) | Krzysztof Marek Mrozik | | |
| Contribution to the Paper | Primary author of manuscript<br>Designed and performed experiments<br>Data analysis and interpretation | | |
| Overall percentage (%) | 80% | | |
| Certification: | This paper reports on original research I conducted during the period of my Higher Degree by Research candidature and is not subject to any obligations or contractual agreements with a third party that would constrain its inclusion in this thesis. I am the primary author of this paper. | | |
| Signature | | Date | 15/02/18 |

## Co-Author Contributions

By signing the Statement of Authorship, each author certifies that:
the candidate's stated contribution to the publication is accurate (as detailed above);
permission is granted for the candidate in include the publication in the thesis; and
the sum of all co-author contributions is equal to 100% less the candidate's stated contribution.

| | | | |
|---|---|---|---|
| Name of Co-Author | Chee M. Cheong | | |
| Contribution to the Paper | Performed experiments<br>Data analysis | | |
| Signature | | Date | 14/02/18 |

| | | | |
|---|---|---|---|
| Name of Co-Author | Duncan R. Hewett | | |
| Contribution to the Paper | Critical review of manuscript<br>Experimental design | | |
| Signature | | Date | 14/02/18 |

| | | | |
|---|---|---|---|
| Name of Co-Author | Andrew C.W. Zannettino | | |
| Contribution to the Paper | Conceptualisation and critical review of manuscript<br>Experimental design | | |
| Signature | | Date | 14/02/18 |

| | | | |
|---|---|---|---|
| Name of Co-Author | Kate Vandyke | | |
| Contribution to the Paper | Conceptualisation and critical review of manuscript<br>Experimental design<br>Data analysis and interpretation | | |
| Signature | | Date | 15/02/18 |

# The identification of novel mechanisms of N-cadherin regulation in t(4;14)$^{+}$ and t(4;14)$^{-}$ multiple myeloma

Krzysztof M. Mrozik[1,2], Chee M. Cheong[1,2], Duncan R. Hewett[1,2], Andrew C.W. Zannettino[1,2,3*], Kate Vandyke[1,2*]

Author Affiliations:

1. Myeloma Research Laboratory, Adelaide Medical School, Faculty of Health and Medical Sciences, The University of Adelaide, Adelaide, Australia
2. Cancer Theme, South Australian Health and Medical Research Institute, Adelaide, Australia
3. Centre for Cancer Biology, University of South Australia, Adelaide, Australia

* co-senior authors

Running title:

The regulation of N-cadherin in t(4;14)$^{+}$ and t(4;14)$^{-}$ MM

Keywords:

N-cadherin, multiple myeloma, t(4;14), regulation, microarray, MMSET, BTBD3

## 4.1 Abstract

Multiple myeloma (MM) is a largely incurable haematological malignancy characterised by the abnormal proliferation of immunoglobulin-producing plasma cells (PCs) within the bone marrow (BM). We have previously shown that expression of the homophilic cell-cell adhesion molecule N-cadherin (*CDH2*) is up-regulated in MM PCs in approximately 50% of newly-diagnosed MM patients and is associated with inferior patient prognosis. To date, the key drivers of aberrant N-cadherin expression in MM PCs are not fully understood. While 10-15% of *CDH2*-expressing MM cases are associated with the chromosomal translocation t(4;14)$^{+}$, suggesting expression may be driven by the dysregulated oncogenes *MMSET* or *FGFR3*, an additional 35-40% of newly-diagnosed patients also express *CDH2* despite having t(4;14)$^{-}$ status. Here, we combined bioinformatic analyses of publicly available microarray data from newly-diagnosed MM patients with *in vitro* studies in human MM cell lines to confirm that MMSET is a key driver of *CDH2* expression in t(4;14)$^{+}$ MM. Additionally, we performed *in silico* analyses incorporating microarray data from over 900 MM patients to identify potential novel regulators of *CDH2* in t(4:14)$^{-}$ MM. These analyses revealed more than 200 genes which were significantly correlated with *CDH2* in t(4:14)$^{-}$ MM. These included the putative transcriptional regulator *BTBD3*, which positively correlated with *CDH2* levels, and upstream modulators of the JAK/STAT3 signalling cascade (*IL6ST*, *BTF3* and *SGPL1*). Furthermore, these analyses identified 8 miRNAs, including miR-190, which inversely associated with *CDH2* expression and therefore may negatively regulate *CDH2* levels in t(4:14)$^{-}$ MM. *BTBD3* was selected for further investigation as a candidate driver of *CDH2* expression as almost all t(4:14)$^{-}$ *CDH2*$^{high}$ MM patients expressed *BTBD3*, and that *BTBD3* was strongly up-regulated in BM MM PCs, compared with normal BM PCs. While our *BTBD3* over-expression and knock-down studies suggest that BTBD3 is unlikely to be a key driver of *CDH2* expression in t(4:14)$^{-}$ MM, this work provides insight into potential N-cadherin regulatory mechanisms in t(4;14)$^{-}$ MM and reveals a number of regulatory candidates which warrant future investigation. Given that the up-regulation of *BTBD3* expression is associated with a trend towards poorer overall survival in t(4:14)$^{-}$ MM patients, the potential role of BTBD3 in MM pathogenesis also warrants investigation.

## 4.2 Introduction

Multiple myeloma (MM) is the second-most common haematological malignancy after non-Hodgkin lymphoma, with approximately 1,700 new cases diagnosed in Australia each year.[1] MM is characterised by the uncontrolled proliferation of immunoglobulin-producing plasma cells (PCs) within the bone marrow (BM) leading to clinical manifestations such as osteolytic bone lesions, hypercalcaemia, renal insufficiency and anaemia. Chromosomal abnormalities including hyperdiploidy (eg. gain of chromosome 3, 7, 9, 11, 15, 17 and 19) and translocations involving the immunoglobulin heavy chain (*IGH*) switch region on chromosome 14 encompass the primary initiating events of MM disease, leading to the aberrant up-regulation and activation of oncogenes such as *MMSET* (encoding the histone-modifying enzyme MMSET [also known as NSD2 and WHSC1]), the transcription factors *MAF* and *MAFB*, and D-group cyclins. Together with the acquisition of additional genetic lesions, these mutations lead to dysregulated cell signalling and result in aberrant PC growth, survival and behavioural characteristics, thereby driving MM pathogenesis and disease progression.[2,3]

N-cadherin (*CDH2*) is a calcium-dependent, adherens junction-type homophilic cell-cell adhesion and signalling molecule expressed by numerous cell types (e.g. neuronal cells, osteoblasts, endothelial cells and myocytes) which contributes to a variety of cellular processes including polarity establishment, migration and survival.[4-13] In epithelial cancers, the up-regulation or *de novo* expression of N-cadherin is widely associated with tumour invasiveness and metastasis and inferior patient prognosis.[14-24] In addition, there is an emerging body of evidence that N-cadherin is aberrantly expressed in haematological malignancies, particularly playing a role in tumour cell dissemination and chemotherapeutic resistance.[25-33] In MM, N-cadherin gene and protein expression in CD138$^{+}$ BM PCs is up-regulated in approximately 50% of newly-diagnosed patients.[25,26] Studies have also shown that *CDH2* up-regulation in BM MM PCs and increased circulating N-cadherin levels (which correlate with *CDH2* expression in BM MM PCs) at clinical diagnosis are significantly associated with inferior MM patient prognosis.[25] N-cadherin is strongly implicated in the BM-homing capacity of circulating MM PCs, thereby facilitating dissemination.[26] N-cadherin may also contribute to MM-associated bone disease by facilitating MM PC-mediated inhibition of osteoblast differentiation.[26] However, while the deleterious implications of elevated

N-cadherin expression in MM are increasingly apparent, the key drivers of aberrant N-cadherin expression in MM PCs are not fully understood.

Microarray analyses have previously demonstrated that *CDH2* is highly expressed in approximately 90% of MM patients harbouring the chromosomal translocation t(4;14)(p16;q32), a genetic lesion observed in 10-15% of newly-diagnosed patients with intermediate to high-risk disease.[26,34-36] This translocation involves a breakpoint in the *IGH* switch region and a breakpoint region between the genes *MMSET* and *FGFR3* on chromosome 4, resulting in *MMSET* and *FGFR3* being placed under the influence of strong *IGH* gene enhancers.[37] *MMSET* is universally over-expressed in t(4;14)$^{+}$ MM patients, whereas *FGFR3* over-expression is lost in approximately 30% of cases. Notably, t(4;14)$^{+}$ status in MM is an adverse prognostic factor, independent of *FGFR3* expression, suggesting *MMSET* dysregulation is likely to be a primary mediator of oncogenesis in this sub-group of patients.[35] *MMSET* encodes for the histone methyltransferase, MMSET, which is associated with a global H3K36me2/K27me3 switch resulting in a more open chromatin structure favouring gene activation and promoting tumourigenesis.[38-40] Indeed, targeted disruption of the translocated *MMSET* allele in the t(4;14)$^{+}$ human MM cell line (HMCL) KMS-11 has been shown to inhibit MM PC clonogenicity *in vitro* and tumorigenicity *in vivo*.[40,41] Notably, studies have also demonstrated that *MMSET* silencing reduces the expression of several adhesion molecule-encoding genes in KMS-11 cells including *CDH2* [41], suggesting MMSET may be a primary driver of N-cadherin expression in t(4;14)$^{+}$ MM.

In addition to t(4;14)$^{+}$ MM patients, *CDH2* is also up-regulated in approximately 40% of newly-diagnosed t(4;14)$^{-}$ patients.[26] In particular, a distinct population of *CDH2*-overexpressing MM patients is observed in the hyperdiploidy sub-group.[26] Owing to the heterogeneity and lack of known genetic initiators of hyperdiploidy-associated MM disease[3], little is known regarding the potential mechanism(s) responsible for elevated *CDH2* expression in these patients. Interestingly, *CDH2* is also up-regulated at low frequency in other t(4;14)$^{-}$ MM subgroups harbouring a variety of primary genetic lesions.[26] In addition to validating the dysregulated expression of *MMSET* as a key driver of up-regulated *CDH2* in MM, the aim of the study was to reveal potential regulators of *CDH2* expression in t(4;14)$^{-}$ MM by the identification of genes which significantly correlate with *CDH2* expression in t(4;14)$^{-}$ MM patients, using publicly available microarray data. *In silico* analysis was also performed to identify potential microRNAs (miRNAs) which may additionally regulate N-cadherin

levels in t(4;14)$^{-}$ MM. In addition, we investigated the role of a putative transcriptional regulator emanating from our correlative studies, BTB/POZ domain-containing protein 3 (BTBD3), as a potential regulator of *CDH2* expression in t(4;14)$^{-}$ HMCLs *in vitro*.

## 4.3 Methods

### 4.3.1 *In silico* analysis of microarray datasets

For analysis of gene expression in CD138-purified BM PCs from newly-diagnosed MM or monoclonal gammopathy of undetermined significance (MGUS) patients, or normal controls, 5 independent microarray datasets were used: E-MTAB-363 (MM, n = 155; MGUS, n = 5; normal, n = 5)[42], E-GEOD-19784 (MM, n = 368)[43], E-GEOD-26863 (MM, n = 304)[44], E-MTAB-317 (MM, n = 227)[45] and GSE4581 (MM, n = 414)[46]. For gene expression analysis in the HMCL KMS-11 following MMSET silencing, 3 microarray datasets were used: GSE29148[47], GSE50072[40] and GSE24746[39]. For GSE4581, MAS5-normalised data were downloaded from Gene Expression Omnibus (GEO; NCBI) and $\log_2$ normalised prior to analysis. For all other datasets, CEL files from Affymetrix Human Genome U133 Plus 2.0 cDNA microarrays were downloaded from GEO or ArrayExpress (EMBL-EBI), and were processed using RMA as previously described.[48-50] Analysis of overall survival in MM patients stratified on the basis of CD138$^{+}$ BM PC gene expression at diagnosis was performed using the GSE4581 dataset. For analysis of miRNA expression in t(4;14)$^{-}$ MM patients, RMA-processed Human Gene 1.0 ST Array (Affymetrix) mRNA expression data and TaqMan miRNA expression data from CD138$^{+}$ BM PCs in newly-diagnosed MM patients (GSE16558) (n = 60) was analysed, as previously described [51]. Patients were classified as *MMSET*$^{low}$, *MMSET*$^{high}$/*FGFR3*$^{low}$ and *MMSET*$^{high}$/*FGFR3*$^{high}$ using specific cut-offs for *MMSET*/*NSD2* (209053_s_at) and *FGFR3* (204379_s_at) for each dataset, as shown in Supplementary Figure 4.1A-F. Patients were defined as *CDH2*$^{high}$ or *CDH2*$^{low}$ and *BTBD3*$^{high}$ or *BTBD3*$^{low}$ based on the median expression of *CDH2* (203440_at) and BTBD3 (202946_s_at) for the entire MM patient cohort, respectively. Patients were defined as miR-190$^{high}$ or miR-190$^{low}$ using a cut-off of zero. Gene set enrichment analysis (GSEA) was performed using the MSigDB Hallmark gene sets and Curated gene sets collections.[52] Predicted miRNA targets were retrieved from three independent databases (TargetScan, version 7.1 (June 2016), http://targetscan.org[53]; PicTar (March 2007), http://pictar.mdc-berlin.de[54]; miRdb (May 2016), http://mirdb.org[55]).

### 4.3.2 Cell culture

Cell culture reagents were sourced from Sigma-Aldrich (St Louis, MO, USA), unless otherwise specified. The HMCLs MOLP-8, EJM, KMM-1, ANBL6, JJN3, KMS-26,

JIM-1, NCI-H929 and OPM-2 were a kind gift from Prof. Andrew Spencer (Monash University, Melbourne, VIC). The B-cell lines NALM-6 and Balm were kindly provided by Emeritus Prof. Leonie Ashman (University of Newcastle, Newcastle, NSW). The transformed B-cell line ARH-77 and HMCLs KMS-11, LP-1, RPMI-8226 and U266 were obtained from the American Type Culture Collection. EJM cells were maintained in Iscove's Modified Dulbecco's Medium (IMDM) with 10% foetal calf serum (FCS) (Thermo Fisher Scientific, Waltham, MA, USA) and supplements (2mM L-glutamine, 100U/ml penicillin, 100µg/ml streptomycin, 1mM sodium pyruvate and 10mM 4-(2-hydroxyethyl)-1-piperazineethanesulfonic acid [HEPES] buffer) at 37°C in a humidified atmosphere with 5% $CO_2$. All other lines were maintained in Roswell Park Memorial Institute 1640 (RPMI-1640) medium with 10% FCS and supplements.

### 4.3.3 Flow cytometry

For analysis of N-cadherin expression, HMCLs cells were incubated in blocking buffer (2mM EDTA 2% FCS PBS) for 30mins on ice. Cells were then stained with mouse monoclonal anti-N-cadherin antibody (clone GC-4; 30µg/ml; Sigma-Aldrich), or mouse $IgG_1$ isotype control (clone 1B5[56]; a kind gift from Dr Graham Mayrhofer, The University of Adelaide, Adelaide, SA), for 45mins on ice in blocking buffer. After washing in Hank's Balanced Salt Solution with 5% FCS, cells were incubated with PE-conjugated goat anti-mouse IgG (0.2µg/1x$10^6$ cells; SouthernBiotech; Birmingham, AL, USA) for 45 minutes on ice in blocking buffer. Cells were again washed, resuspended in 1% w/v neutral-buffered formalin 2% w/v sucrose 1% sodium azide PBS and analysed using a FACSCanto™ II flow cytometer (BD; Franklin Lakes, NJ, USA). For cell purification, cells were sorted using a FACSAria™ Fusion flow cytometer (BD).

### 4.3.4 Quantitative PCR

All reagents were sourced from Thermo Fisher Scientific, unless otherwise specified. Total RNA was isolated from HMCLs using TRIzol® Reagent. For detection of *MMSET*, *BTBD3*, *CDH2* and *ACTB* mRNA, cDNA was synthesized using SuperScript® IV reverse transcriptase. *MMSET* primers were designed to detect full-length *MMSET* (MMSET II) transcripts (Forward (Fwd) 5'-AGAGGATACAGGACCCTACA-3', Reverse (Rev) 5'-GTGTTTCGTCTGCACTTTCG-3'). For detection of total *BTBD3* transcript levels, *BTBD3*-targeting primers for quantitative real-time PCR (qPCR) were designed to detect all 6 *BTBD3* mRNA transcript variants (Fwd 5'-

GCTGCTTTTCTCGCTATGCT-3', Rev 5'-AGGAGCACACAGGCATTCTT-3'). *CDH2* primers were designed to detect total *CDH2* mRNA transcripts (Fwd 5'-GGCAGTAAAATTGAGCCTGAAG-3', Rev 5'-AGTTTTCTGGCAAGTTGATTGG-3'). qPCR was performed using the RT$^{2}$ SYBR® Green qPCR Mastermix (Qiagen, Hilden, Germany). For miRNA analysis, miRNAs were converted to cDNA using the TaqMan® MicroRNA Reverse Transcription Kit and expression assessed using the TaqMan® Universal Master Mix II, according to the manufacturer's instructions. Pre-designed TaqMan® primers were used to detect hsa-miR-190a-5p (miR-190) (Assay ID 000489; UGAUAUGUUUGAUAUAUUAGGU) and U6 snRNA (Assay ID 001973). Gene and miRNA expression was calculated relative to *ACTB* and U6 snRNA, respectively, using the $2^{-\Delta Ct}$ method.[57]

### 4.3.5 Western blotting

Nuclear protein lysates from HMCLs were prepared using the Nuclear Complex Co-IP Kit (Active Motif, Carlsbad, CA, USA) and polyacrylamide gel electrophoresis was performed as described previously.[58] Following transfer, the PVDF membrane was incubated in blocking buffer (2.5% membrane blocking agent (GE Healthcare; Little Chalfont, UK) in 0.1% Tween 20 Tris-buffered saline) for 2 hours at room temperature. The membrane was then probed overnight at 4°C with a polyclonal rabbit anti-human/mouse BTBD3 antibody (8µg/ml; Sigma, Cat. No. HPA042048) diluted in blocking buffer. After washing, the membrane was incubated with alkaline phosphatase-conjugated donkey anti-rabbit IgG (0.4µg/ml; Merck Millipore, Burlington, MA, USA) diluted in blocking buffer for 1 hour at room temperature. Proteins were visualized with ECL detection reagent (GE Healthcare) on a Gel Doc™ XR+ Imaging System (Bio-Rad; Hercules, CA, USA). The membrane was then stripped using Restore™ PLUS Western Blot Stripping Buffer (Thermo Scientific), re-blocked and probed for 1 hour at room temperature with rabbit anti-histone H3 (Cell Signaling Technology, Danvers, MA; 1:2500) as a nuclear protein-loading control. After washing, the membrane was incubated for 1 hour at room temperature with alkaline phosphatase-conjugated donkey anti-rabbit IgG and protein was visualised, as described above.

### 4.3.6 Over-expression of *MMSET* and *BTBD3* in HMCLs

The pRetroX-MMSET-DsRed vector harbouring full-length *MMSET* cDNA or pRetroX-DsRed empty vector (kind gifts from Prof. Jonathan Licht, University of

Florida Health Cancer Center, Gainsville, FL, USA)[38], were transfected into HEK-293T cells. Supernatant containing viral particles was subsequently used to infect the HMCL RPMI-8226, as previously described.[59] Following expansion, cells over-expressing the DsRed constructs were purified by flow cytometry.

*BTBD3* transcript variants 1 and 6 were amplified from cDNA derived from the t(4;14)$^{-}$ HMCL KMS-26 (primer sets; Fwd 5'-ACACGGATCCACCATGGTAGATGACAAGGAAAA-3' and Rev 5'-AAGTGAATTCTCAAGCATAGAATATAAGTT-3' (transcript variant 1); Fwd 5'-TGTGGGATCCACCATGTTTTACGGAGAACTTGC-3' and Rev 5'-AAGTGAATTCTCAAGCATAGAATATAAGTT-3' (transcript variant 6)) and initially cloned into pGEM®-T Vector System I (Promega; Madison, WI, USA), as per manufacturer's instructions. Each *BTBD3* transcript was subsequently cloned into the pLeGO-iCer2 lentiviral vector[60] (gift from Boris Fehse, Addgene plasmid # 27346) using the *Eco*RI and *Bam*HI restriction sites, and sequence-verified by Sanger sequencing. Constructs were then transfected into HEK293T cells using the psPAX2 (gift from Didier Trono, Addgene plasmid #12260) and pVSV-G (Clontech Laboratories, Inc.; Mountain View, CA, USA) packaging vectors and the viral supernatants were used to infect RPMI-8226 and U266 HMCLs. Following expansion, cerulean-positive cells were purified by flow cytometry.

### 4.3.7 siRNA-mediated *BTBD3* knock-down in HMCLs

All reagents were sourced from Thermo Fisher Scientific, unless otherwise specified. Immediately prior to siRNA transfection at day 0, HMCLs were washed and resuspended in Opti-MEM™ at 2.5x10$^{5}$/ml in 25cm$^{2}$ tissue culture flasks. *Silencer*® Select Negative Control No. 1 siRNA (Cat. 4390843) and pre-designed *BTBD3*-targeting siRNAs (Assay ID s22631, siRNA#1; Assay ID s22632, siRNA#2; Assay ID s22633, siRNA#3) were pre-incubated in Opti-MEM™ at 150nM with 15µl/mL Lipofectamine® RNAiMAX reagent for 15 minutes at room temperature. For no siRNA controls, siRNA was replaced with nuclease-free water. siRNA-lipid complexes (or no siRNA mock complexes) were then added drop-wise to HMCLs for a final concentration of 25nM siRNA and 2.5µl/mL Lipofectamine® RNAiMAX reagent and flasks were gently rocked to mix. After 6 hours at 37°C, cells were diluted 2-fold with antibiotic-free RPMI-1640 containing 10% FCS and supplements, as described above, and cultured for 2 days. At day 2, cells were washed and resuspended in Opti-MEM™

and siRNA transfection was repeated, as described above. At day 4, cells were harvested for RNA isolation.

### 4.3.8 Statistical analyses

For analysis of genes which correlate with *CDH2* expression in t(4;14)$^{-}$ MM patients, Spearman correlation analyses were performed using 4 microarray datasets (E-MTAB-363, E-GEOD-19784, E-GEOD-26863 and E-MTAB-317), using the Benjamini-Hochburg false discovery rate (FDR) correction for multiple testing. Differential expression of gene probesets between groups in microarray experiments was determined using linear models for microarray data analysis (LIMMA;[61]) in MultiExperiment Viewer (MeV;[62]). Survival curves were compared using the log-rank (Mantel-Cox) test with hazard ratios calculated using the Mantel-Haenszel calculation. All other analyses were performed using an ordinary one-way ANOVA with Dunnett's multiple comparisons test, performed using GraphPad Prism® v7.02 software (GraphPad Software, Inc.; La Jolla, CA, USA).

## 4.4 Results

### 4.4.1 The histone methyltransferase MMSET is a key driver of *CDH2* expression in t(4;14)$^{+}$ MM

Previous studies have identified that *CDH2* expression is up-regulated in a high proportion of newly-diagnosed t(4;14)$^{+}$ MM patients.[26,34] Similarly, using qPCR and flow cytometry, we have found that t(4;14)$^{+}$ HMCLs highly express N-cadherin mRNA (Figure 4.1A) and protein (Figure 4.1B), when compared with t(4;14)$^{-}$ MM and B-cell lines. Indeed, the mean expression of *CDH2* is significantly higher in t(4;14)$^{+}$ HMCLs relative to t(4;14)$^{-}$ HMCLs and B-cell lines (data not shown). t(4;14)$^{+}$ MM is characterised by a reciprocal chromosomal translocations that leads to constitutive expression of both *MMSET* and *FGFR3*, although *FGFR3* expression is lost in approximately 30% of these patients.[35] In order to ascertain whether MMSET or FGFR3 is the likely driver of *CDH2* expression in t(4;14)$^{+}$ MM, we analysed *CDH2* expression in publicly available microarray data on CD138$^{+}$ BM PCs from newly-diagnosed MM patients (GSE4581, E-MTAB-363, E-GEOD 19784, E-MTAB-317 and E-GEOD-26863), characterised as *MMSET*$^{high}$ or *MMSET*$^{low}$, and further characterised on the basis of *FGFR3* expression (as shown in Supplementary Figure 4.1A-E). Our analysis revealed that over 82% of *MMSET*$^{high}$ MM patients express high *CDH2* levels (above the median for the entire MM cohort) (GSE4581: 66 *CDH2*$^{high}$ of 74 *MMSET*$^{high}$ patients, 89.2%; E-MTAB-363: 17/19, 89.5%; E-GEOD-19784: 33/35, 94.3%; E-MTAB-317: 30/33, 90.9%; E-GEOD-26863: 28/32, 82.3%), irrespective of their *FGFR3* expression (Figure 4.1C). These data imply that MMSET, and not FGFR3, is responsible for increased *CDH2* expression in t(4;14)$^{+}$ MM patients (Supplementary Figure 4.2A).

To directly investigate whether MMSET regulates *CDH2* in t(4;14)$^{+}$ MM, we then performed *in silico* analysis of publicly available microarray data in which *MMSET* was genetically modified in the t(4;14)$^{+}$ HMCL KMS-11. We found that *CDH2* expression was markedly lower in KMS-11 cells following targeted knockout of the translocated MMSET allele alone (MMSET TKO) (GSE29148 and E-GEOD-50072) (Figure 4.2A,B), consistent with previous findings.[41] Over-expression of full-length MMSET in MMSET-TKO KMS-11 cells also rescued *CDH2* expression (E-GEOD-50072 and GSE24746) (Figure 4.2B,C). Notably, over-expressing MMSET containing a histone-binding domain mutation (MMSET Y1118A) failed to rescue *CDH2* expression

**Figure 4.1. *CDH2* expression is up-regulated in t(4;14)$^{+}$ HMCLs and *MMSET*$^{high}$ MM patients.** *CDH2* expression (normalised to *ACTB* expression) in a panel of HMCLs, stratified based on t(4;14) status, and B-cell lines, as assessed by qPCR. Graph depicts mean ± SEM of 3 independent experiments (**A**). N-cadherin protein expression in representative t(4;14)$^{-}$ and t(4;14)$^{+}$ HMCLs, as assessed by flow cytometry. Black line represents N-cadherin expression and shaded area represents isotype control (**B**). *In silico* analyses of publicly available microarray datasets demonstrating *CDH2* expression in CD138$^{+}$ BM PCs isolated from newly-diagnosed MM patients, segregated into *MMSET*$^{low}$, *MMSET*$^{high}$/*FGFR3*$^{low}$ or *MMSET*$^{high}$/*FGFR3*$^{high}$ subsets (GSE4581, E-MTAB-363, E-GEOD-19784, E-MTAB-317 and E-GEOD-26863). Graphs depict median with inter-quartile range. * $P < 0.05$ ** $P < 0.01$ *** $P < 0.001$ **** $P < 0.0001$ compared with *MMSET*$^{low}$ MM patients (LIMMA) (**C**).

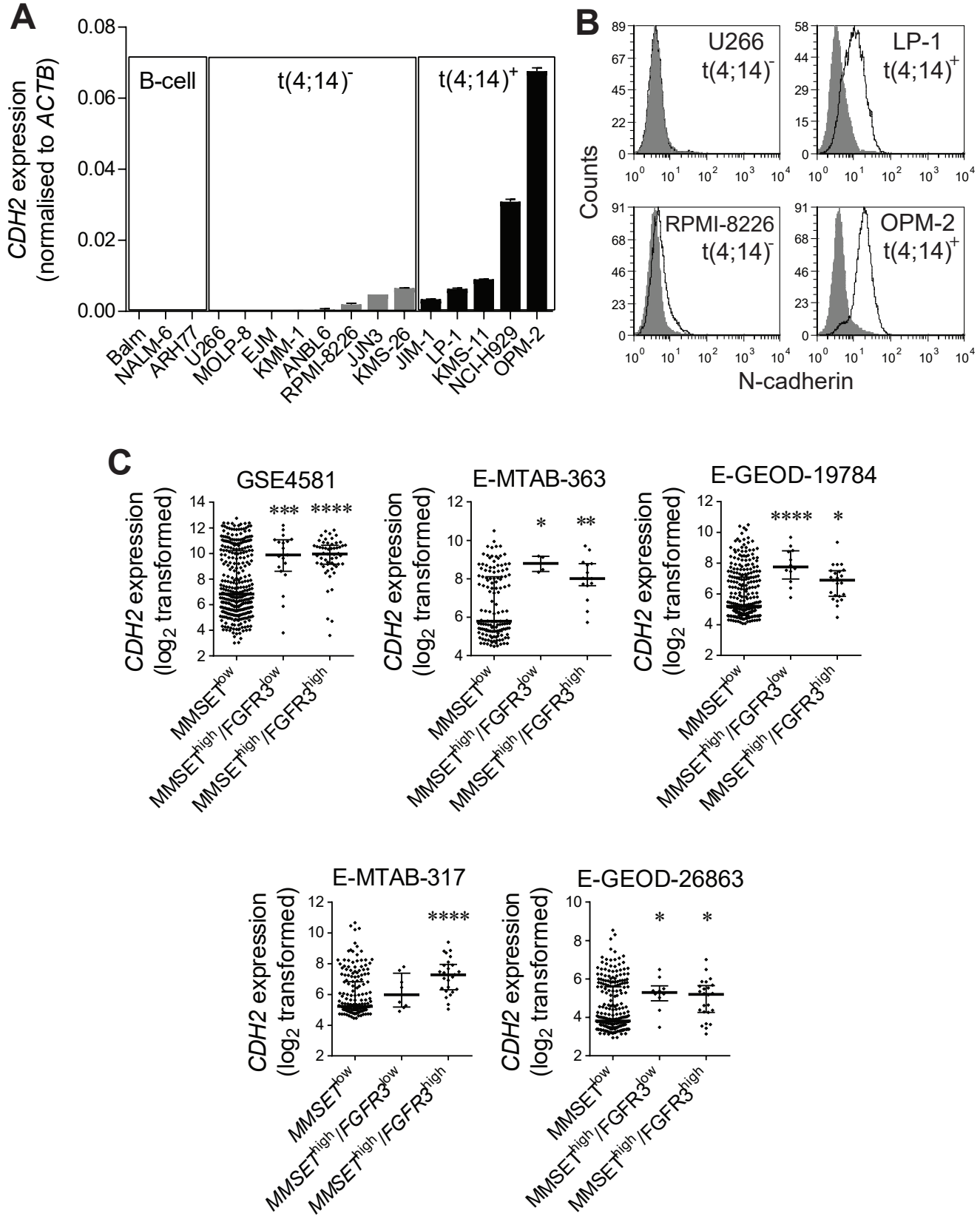
A
CDH2 expression (normalised to ACTB)
0.08
0.06
0.04
0.02
0.00
B-cell
t(4;14)-
t(4;14)+
Balm
NALM-6
ARH77
U266
MOLP-8
EJM
KMM-1
ANBL6
RPMI-8226
JJN3
KMS-26
JIM-1
LP-1
KMS-11
NCI-H929
OPM-2
B
Counts
U266
t(4;14)-
LP-1
t(4;14)+
RPMI-8226
t(4;14)-
OPM-2
t(4;14)+
N-cadherin
C
GSE4581
E-MTAB-363
E-GEOD-19784
E-MTAB-317
E-GEOD-26863
CDH2 expression (log2 transformed)
MMSET low
MMSET high/FGFR3 low
MMSET high/FGFR3 high
MMSET high/FGFR3 high

**Figure 4.2. *CDH2* expression is positively regulated by MMSET in HMCLs.** *In silico* analyses of publicly available microarray datasets demonstrating *CDH2* expression in KMS-11 cells following targeted knockout of the translocated MMSET allele (TKO) (GSE29148, **A**; E-GEOD-50072, **B**) and add-back of full-length MMSET (E-GEOD-50072, **B**; GSE24746, **C**), or MMSET Y1118A mutant (GSE24746, **C**), in TKO KMS-11 cells. Graphs depict mean ± SEM of 3 independent experiments. * $P < 0.05$ *** $P < 0.001$ **** $P < 0.0001$ compared with parental KMS-11 cells (**A**,**B**), or TKO KMS-11 cells (**C**) (one-way ANOVA with Dunnett's multiple comparisons test). *MMSET* and *CDH2* expression (normalised to *ACTB* expression) in RPMI-8226-EV, RPMI-8226-MMSET and RPMI-8226-MMSET Y1118A cells, as assessed by qPCR. Graphs depict mean ± SEM of 3 independent experiments (**D**). **$P < 0.01$ **** $P < 0.0001$ compared with RPMI-8226-EV cells (one-way ANOVA with Dunnett's multiple comparisons test).

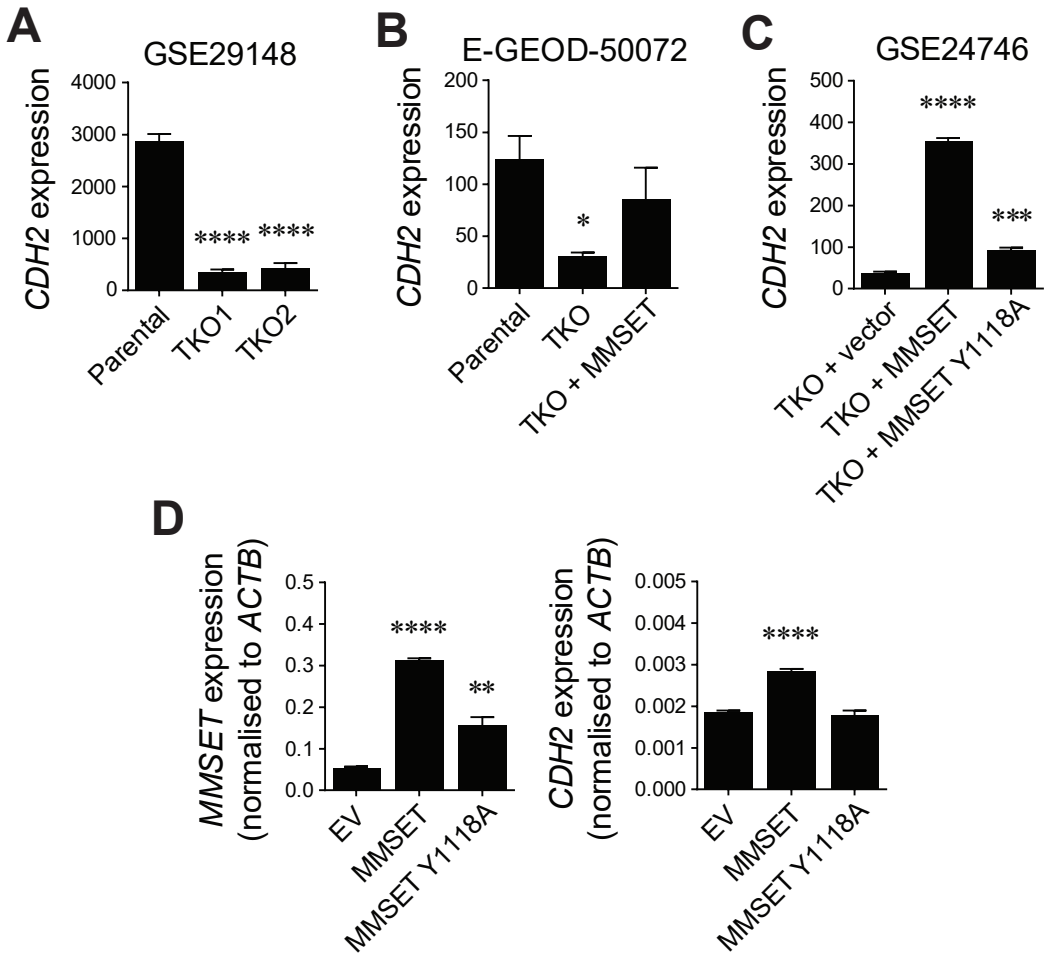
A
GSE29148
CDH2 expression
4000
3000
2000
1000
0
****
****
Parental
TKO1
TKO2
B
E-GEOD-50072
CDH2 expression
200
150
100
50
0
*
Parental
TKO
TKO + MMSET
C
GSE24746
CDH2 expression
500
400
300
200
100
0
****
***
TKO + vector
TKO + MMSET
TKO + MMSET Y1118A
D
MMSET expression (normalised to ACTB)
0.5
0.4
0.3
0.2
0.1
0.0
****
**
EV
MMSET
MMSET Y1118A
CDH2 expression (normalised to ACTB)
0.005
0.004
0.003
0.002
0.001
0.000
****
EV
MMSET
MMSET Y1118A

in MMSET-TKO KMS-11 cells (GSE24746) (Figure 4.2C). To verify these findings, we utilised a t(4;14)$^{-}$ HMCL, RPMI-8226, to independently generate cell lines which over-expressed wild-type or Y1118A mutant MMSET. In concordance with our *in silico* analyses, up-regulation of *CDH2* was observed in RPMI-8226 cells over-expressing full-length MMSET (RPMI-8226-MMSET), but not MMSET Y1118A mutant (RPMI-8226-MMSET Y1118A), relative to empty-vector control RPMI-8226 cells (RPMI-8226-EV) (Figure 4.2D). Taken together, these results demonstrate that MMSET is a key driver of *CDH2* expression in MM and suggest that the ability of MMSET to up-regulate *CDH2* expression in MM PCs is dependent on its functional histone-modifying domain.

### 4.4.2 Identification of genes which significantly correlate with *CDH2* in t(4;14)$^{-}$ MM

While t(4;14)$^{+}$ MM accounts for 15% of newly-diagnosed patients with up-regulated *CDH2* expression in MM PCs, our analysis suggests that a further 41-46% of *MMSET*$^{low}$ patients express high *CDH2* levels (GSE4581: 141 *CDH2*$^{high}$ of 340 *MMSET*$^{low}$ patients, 41.5%; E-MTAB-363: 60/136, 44.1%; E-GEOD-19784: 131/293, 44.7%; E-MTAB-317: 83/192, 43.2%; E-GEOD-26863: 124/270, 45.9%) (Figure 4.1C), in line with previous findings.[26] In order to identify potential regulators of *CDH2* expression in t(4;14)$^{-}$ MM, we identified genes that correlated with *CDH2* expression in BM MM PCs from *MMSET*$^{low}$ MM patients in 4 of the microarray datasets included above (E-MTAB-363, E-GEOD-19784, E-MTAB-317 and E-GEOD-26863). GSE4581 was excluded from this analysis as raw, unprocessed data was not available for this dataset. In total, we identified 186 genes which significantly positively correlated (Table 4.1), and 32 genes which significantly inversely correlated (Table 4.2), with *CDH2* expression in all 4 datasets. Genes which positively correlated with *CDH2* expression included transcriptional regulators (*BTF3*, *E2F5*, *BTBD3*, *GFI1* and *FLI1*), protein kinases (*PAK1* and *PRKD2*), growth factors (*BMP4*), modifiers of chromatin structure (*FBXO22* and *HMGA1*) and ribosomal proteins (*RPS17*, *RPL13A* and *RPL37*). Notably, GSEA revealed an enrichment for genes associated with a hyperdiploidy-related MM gene signature amongst the genes which positively correlated with *CDH2* expression (Supplementary Table 4.1). Genes which inversely correlated with *CDH2* expression included transcriptional regulators (*IRF2BP2* and *TCFL5*) and the kinase inhibitor CDKN1C (*CDKN1C)*. GSEA also identified an enrichment for genes that are down-

**Table 4.1: Genes which positively correlate with *CDH2* expression in t(4;14)$^-$ MM patients**

| Gene | Probeset ID | E-MTAB-317 | | E-MTAB-363 | | E-GEOD-19784 | | E-GEOD-26863 | | Mean correlation co-efficient |
|---|---|---|---|---|---|---|---|---|---|---|
| | | R[1] | FDR[2]-adjusted P-value | R | FDR-adjusted P-value | R | FDR-adjusted P-value | R | FDR-adjusted P-value | |
| XRCC4 | 205071_x_at | 0.328 | 7.53E-04 | 0.478 | 7.71E-05 | 0.353 | 1.08E-06 | 0.492 | 8.91E-14 | 0.413 |
| MGAT4C | 207447_s_at | 0.342 | 4.35E-04 | 0.515 | 8.34E-06 | 0.412 | 1.25E-09 | 0.359 | 6.39E-07 | 0.407 |
| FER | 206412_at | 0.315 | 1.41E-03 | 0.538 | 1.92E-07 | 0.381 | 4.82E-08 | 0.387 | 4.89E-08 | 0.405 |
| C21orf91 | 226109_at | 0.437 | 2.18E-06 | 0.453 | 2.41E-04 | 0.310 | 3.55E-05 | 0.410 | 5.27E-09 | 0.402 |
| MORC1 | 220850_at | 0.303 | 2.21E-03 | 0.486 | 5.16E-05 | 0.398 | 8.17E-09 | 0.390 | 3.64E-08 | 0.394 |
| SCYL2 | 224961_at | 0.403 | 2.66E-05 | 0.398 | 2.91E-03 | 0.402 | 5.77E-09 | 0.374 | 1.57E-07 | 0.394 |
| TNFSF10 | 202688_at | 0.391 | 4.36E-05 | 0.413 | 1.26E-03 | 0.366 | 3.32E-07 | 0.389 | 4.26E-08 | 0.390 |
| EPHB1 | 230425_at | 0.432 | 2.88E-06 | 0.293 | 4.36E-02 | 0.423 | 2.89E-10 | 0.405 | 8.25E-09 | 0.388 |
| CDC42SE2 | 1552612_at | 0.342 | 4.30E-04 | 0.466 | 1.37E-04 | 0.325 | 1.14E-05 | 0.385 | 6.12E-08 | 0.380 |
| **BTBD3** | **202946_s_at** | **0.359** | **1.87E-04** | **0.436** | **5.66E-04** | **0.371** | **1.73E-07** | **0.336** | **4.05E-06** | **0.375** |
| ELOVL7 | 227180_at | 0.315 | 1.40E-03 | 0.403 | 2.31E-03 | 0.382 | 5.74E-08 | 0.401 | 1.26E-08 | 0.375 |
| DLC1 | 210762_s_at | 0.337 | 5.49E-04 | 0.368 | 7.06E-03 | 0.388 | 2.77E-08 | 0.380 | 9.36E-08 | 0.368 |
| LOC346887 | 235205_at | 0.481 | 5.95E-10 | 0.313 | 2.84E-02 | 0.281 | 2.41E-04 | 0.396 | 2.07E-08 | 0.368 |
| COL4A6 | 213992_at | 0.250 | 1.36E-02 | 0.462 | 1.59E-04 | 0.370 | 1.65E-07 | 0.379 | 9.68E-08 | 0.365 |
| PAK1 | 226507_at | 0.424 | 4.99E-06 | 0.292 | 4.44E-02 | 0.341 | 3.29E-06 | 0.403 | 1.01E-08 | 0.365 |
| IDH3A | 202070_s_at | 0.443 | 1.27E-06 | 0.289 | 4.79E-02 | 0.344 | 2.60E-06 | 0.365 | 3.65E-07 | 0.360 |
| ELOVL4 | 219532_at | 0.295 | 3.03E-03 | 0.449 | 2.77E-04 | 0.414 | 1.05E-09 | 0.280 | 2.11E-04 | 0.359 |
| COL4A5 | 213110_s_at | 0.260 | 9.90E-03 | 0.408 | 1.85E-03 | 0.407 | 2.23E-09 | 0.362 | 4.69E-07 | 0.359 |
| SPEF2 | 1552716_at | 0.362 | 1.65E-04 | 0.365 | 7.61E-03 | 0.329 | 6.74E-06 | 0.374 | 1.51E-07 | 0.358 |
| CCRL2 | 211434_s_at | 0.264 | 8.81E-03 | 0.426 | 8.51E-04 | 0.357 | 7.43E-07 | 0.376 | 1.34E-07 | 0.356 |
| PML | 235508_at | 0.425 | 4.66E-06 | 0.382 | 4.75E-03 | 0.310 | 3.16E-05 | 0.296 | 7.03E-05 | 0.353 |
| MMP16 | 223614_at | 0.243 | 1.67E-02 | 0.447 | 2.55E-04 | 0.395 | 8.17E-09 | 0.322 | 1.10E-05 | 0.352 |
| MAB21L1 | 206163_at | 0.311 | 1.63E-03 | 0.490 | 4.52E-05 | 0.318 | 1.86E-05 | 0.283 | 1.68E-04 | 0.351 |
| ISL2 | 232352_at | 0.329 | 7.46E-04 | 0.368 | 7.08E-03 | 0.309 | 3.92E-05 | 0.397 | 1.73E-08 | 0.351 |
| RSL24D1 | 217915_s_at | 0.377 | 7.99E-05 | 0.441 | 4.37E-04 | 0.287 | 1.69E-04 | 0.275 | 2.79E-04 | 0.345 |
| GTPBP8 | 223486_at | 0.388 | 4.97E-05 | 0.344 | 1.35E-02 | 0.330 | 7.77E-06 | 0.316 | 1.70E-05 | 0.344 |
| PCDH9 | 219737_s_at | 0.323 | 1.01E-03 | 0.403 | 2.31E-03 | 0.363 | 4.34E-07 | 0.279 | 2.14E-04 | 0.342 |
| UBA7 | 1294_at | 0.399 | 3.29E-05 | 0.320 | 2.40E-02 | 0.350 | 1.44E-06 | 0.293 | 8.51E-05 | 0.341 |
| NCAM1 | 212843_at | 0.365 | 1.45E-04 | 0.335 | 1.72E-02 | 0.274 | 3.91E-04 | 0.387 | 5.16E-08 | 0.340 |
| SNAPC5 | 1554093_a_at | 0.300 | 2.46E-03 | 0.412 | 1.51E-03 | 0.354 | 9.82E-07 | 0.289 | 1.15E-04 | 0.339 |
| USE1 | 219348_at | 0.369 | 1.22E-04 | 0.364 | 7.99E-03 | 0.283 | 2.09E-04 | 0.330 | 6.01E-06 | 0.337 |
| NT5C3 | 223298_s_at | 0.374 | 9.62E-05 | 0.436 | 5.60E-04 | 0.286 | 1.73E-04 | 0.246 | 1.50E-03 | 0.336 |
| RPL37 | 224767_at | 0.287 | 4.21E-03 | 0.344 | 1.35E-02 | 0.296 | 8.76E-05 | 0.415 | 3.83E-09 | 0.335 |
| TRAT1 | 217147_s_at | 0.295 | 2.97E-03 | 0.370 | 6.62E-03 | 0.371 | 1.73E-07 | 0.295 | 7.47E-05 | 0.333 |
| GTF2F2 | 209595_at | 0.298 | 2.70E-03 | 0.386 | 3.96E-03 | 0.225 | 5.03E-03 | 0.417 | 3.44E-09 | 0.332 |
| SCAMP5 | 212699_at | 0.292 | 3.39E-03 | 0.317 | 2.63E-02 | 0.398 | 8.17E-09 | 0.314 | 2.04E-05 | 0.330 |
| GBA3 | 222943_at | 0.361 | 1.69E-04 | 0.326 | 2.12E-02 | 0.334 | 5.45E-06 | 0.294 | 8.24E-05 | 0.329 |
| CD200 | 209582_s_at | 0.224 | 2.90E-02 | 0.499 | 1.92E-05 | 0.303 | 5.95E-05 | 0.290 | 1.10E-04 | 0.329 |
| CNTN5 | 207452_s_at | 0.281 | 5.16E-03 | 0.331 | 1.78E-02 | 0.358 | 5.00E-07 | 0.343 | 2.38E-06 | 0.328 |
| RPL13A | 200715_x_at | 0.270 | 6.96E-03 | 0.378 | 5.41E-03 | 0.293 | 1.05E-04 | 0.369 | 2.60E-07 | 0.328 |
| EIF2A | 223015_at | 0.267 | 7.91E-03 | 0.427 | 8.11E-04 | 0.283 | 2.07E-04 | 0.332 | 5.45E-06 | 0.327 |
| CMPK2 | 226702_at | 0.390 | 4.55E-05 | 0.347 | 1.24E-02 | 0.308 | 3.95E-05 | 0.262 | 6.14E-04 | 0.327 |

**Table 4.1: Genes which positively correlate with *CDH2* expression in t(4;14)$^-$ MM patients (continued)**

| Gene | Probeset ID | E-MTAB-317 | | E-MTAB-363 | | E-GEOD-19784 | | E-GEOD-26863 | | Mean correlation co-efficient |
|---|---|---|---|---|---|---|---|---|---|---|
| | | R[1] | FDR[2]-adjusted P-value | R | FDR-adjusted P-value | R | FDR-adjusted P-value | R | FDR-adjusted P-value | |
| RSAD2 | 242625_at | 0.381 | 7.05E-05 | 0.356 | 9.49E-03 | 0.311 | 3.26E-05 | 0.255 | 9.23E-04 | 0.326 |
| SAAL1 | 225614_at | 0.389 | 4.63E-05 | 0.356 | 9.30E-03 | 0.309 | 3.83E-05 | 0.248 | 1.35E-03 | 0.326 |
| C3orf17 | 225281_at | 0.289 | 3.86E-03 | 0.372 | 5.85E-03 | 0.308 | 4.05E-05 | 0.334 | 4.68E-06 | 0.326 |
| ISG20 | 204698_at | 0.364 | 1.51E-04 | 0.351 | 1.11E-02 | 0.316 | 1.99E-05 | 0.271 | 3.69E-04 | 0.325 |
| ICAM3 | 204949_at | 0.297 | 2.81E-03 | 0.389 | 3.74E-03 | 0.323 | 1.34E-05 | 0.291 | 1.02E-04 | 0.325 |
| CHSY3 | 242100_at | 0.345 | 3.95E-04 | 0.322 | 2.28E-02 | 0.234 | 3.18E-03 | 0.387 | 5.23E-08 | 0.322 |
| IDH2 | 210046_s_at | 0.365 | 1.46E-04 | 0.314 | 2.74E-02 | 0.337 | 4.25E-06 | 0.264 | 5.45E-04 | 0.320 |
| COPS2 | 202467_s_at | 0.313 | 1.49E-03 | 0.394 | 3.24E-03 | 0.322 | 1.33E-05 | 0.252 | 1.09E-03 | 0.320 |
| CCNDBP1 | 223084_s_at | 0.308 | 1.85E-03 | 0.383 | 4.44E-03 | 0.308 | 3.95E-05 | 0.279 | 2.28E-04 | 0.320 |
| RPL35A | 238026_at | 0.332 | 6.63E-04 | 0.318 | 2.54E-02 | 0.268 | 5.45E-04 | 0.356 | 7.77E-07 | 0.319 |
| TMEM161B | 236227_at | 0.338 | 5.26E-04 | 0.339 | 1.54E-02 | 0.221 | 6.13E-03 | 0.375 | 1.51E-07 | 0.318 |
| TTC9C | 226175_at | 0.363 | 1.58E-04 | 0.353 | 1.01E-02 | 0.258 | 9.89E-04 | 0.298 | 6.35E-05 | 0.318 |
| ARHGAP25 | 204882_at | 0.302 | 2.32E-03 | 0.374 | 5.85E-03 | 0.232 | 3.70E-03 | 0.363 | 4.51E-07 | 0.318 |
| GFI1 | 206589_at | 0.391 | 4.36E-05 | 0.293 | 4.39E-02 | 0.257 | 1.00E-03 | 0.330 | 6.13E-06 | 0.317 |
| UBE2Q2 | 224747_at | 0.335 | 5.96E-04 | 0.309 | 3.09E-02 | 0.310 | 3.55E-05 | 0.315 | 1.92E-05 | 0.317 |
| SMOC1 | 222783_s_at | 0.297 | 2.75E-03 | 0.339 | 1.46E-02 | 0.296 | 9.12E-05 | 0.336 | 3.91E-06 | 0.317 |
| PALM2-AKAP2 | 202760_s_at | 0.283 | 4.86E-03 | 0.303 | 3.53E-02 | 0.293 | 1.05E-04 | 0.382 | 7.19E-08 | 0.315 |
| SQRDL | 217995_at | 0.335 | 5.92E-04 | 0.303 | 3.54E-02 | 0.294 | 9.77E-05 | 0.326 | 8.64E-06 | 0.315 |
| ST8SIA4 | 206925_at | 0.287 | 4.24E-03 | 0.387 | 3.85E-03 | 0.282 | 2.07E-04 | 0.301 | 5.13E-05 | 0.314 |
| MOSC2 | 227417_at | 0.320 | 1.10E-03 | 0.320 | 2.44E-02 | 0.296 | 9.05E-05 | 0.319 | 1.40E-05 | 0.314 |
| GALT | 203179_at | 0.381 | 7.05E-05 | 0.317 | 2.58E-02 | 0.293 | 9.77E-05 | 0.259 | 7.58E-04 | 0.313 |
| HOMER1 | 226651_at | 0.300 | 2.52E-03 | 0.368 | 7.03E-03 | 0.274 | 3.97E-04 | 0.308 | 3.13E-05 | 0.312 |
| ATP5L | 207573_x_at | 0.352 | 2.71E-04 | 0.335 | 1.68E-02 | 0.230 | 4.00E-03 | 0.328 | 7.28E-06 | 0.311 |
| ZDHHC24 | 227549_x_at | 0.278 | 5.66E-03 | 0.353 | 1.01E-02 | 0.294 | 9.98E-05 | 0.318 | 1.49E-05 | 0.311 |
| CDV3 | 213554_s_at | 0.232 | 2.27E-02 | 0.385 | 4.11E-03 | 0.275 | 3.69E-04 | 0.349 | 1.44E-06 | 0.310 |
| C2orf89 | 227867_at | 0.397 | 3.33E-05 | 0.321 | 2.38E-02 | 0.318 | 1.95E-05 | 0.199 | 1.48E-02 | 0.309 |
| GMPR | 204187_at | 0.384 | 6.08E-05 | 0.330 | 1.90E-02 | 0.202 | 1.38E-02 | 0.317 | 1.56E-05 | 0.308 |
| BTLA | 236226_at | 0.238 | 1.92E-02 | 0.365 | 7.68E-03 | 0.310 | 3.55E-05 | 0.319 | 1.38E-05 | 0.308 |
| ST3GAL5 | 203217_s_at | 0.271 | 7.03E-03 | 0.343 | 1.30E-02 | 0.260 | 8.90E-04 | 0.357 | 7.21E-07 | 0.308 |
| PCMTD1 | 244706_at | 0.335 | 5.92E-04 | 0.361 | 8.72E-03 | 0.291 | 1.22E-04 | 0.241 | 2.03E-03 | 0.307 |
| COX7C | 213846_at | 0.281 | 5.17E-03 | 0.342 | 1.42E-02 | 0.244 | 2.05E-03 | 0.357 | 7.18E-07 | 0.306 |
| IFNGR1 | 211676_s_at | 0.243 | 1.64E-02 | 0.433 | 6.51E-04 | 0.281 | 2.40E-04 | 0.267 | 4.78E-04 | 0.306 |
| RPS19 | 202649_x_at | 0.294 | 2.98E-03 | 0.378 | 5.41E-03 | 0.274 | 3.87E-04 | 0.273 | 3.12E-04 | 0.305 |
| MRPS27 | 212145_at | 0.271 | 7.13E-03 | 0.327 | 2.07E-02 | 0.286 | 1.72E-04 | 0.331 | 5.69E-06 | 0.304 |
| C11orf1 | 231530_s_at | 0.290 | 3.84E-03 | 0.345 | 1.31E-02 | 0.247 | 1.72E-03 | 0.333 | 5.19E-06 | 0.304 |
| THG1L | 219122_s_at | 0.311 | 1.67E-03 | 0.321 | 2.33E-02 | 0.243 | 2.17E-03 | 0.337 | 3.56E-06 | 0.303 |
| KIAA1217 | 1554438_at | 0.342 | 4.35E-04 | 0.304 | 3.48E-02 | 0.258 | 9.54E-04 | 0.306 | 3.49E-05 | 0.302 |
| GNB2L1 | 200651_at | 0.252 | 1.27E-02 | 0.346 | 1.27E-02 | 0.250 | 1.52E-03 | 0.361 | 5.18E-07 | 0.302 |
| LOC728052 | 1558795_at | 0.261 | 9.66E-03 | 0.381 | 4.98E-03 | 0.286 | 1.69E-04 | 0.280 | 2.10E-04 | 0.302 |
| IVD | 203682_s_at | 0.338 | 5.26E-04 | 0.376 | 5.76E-03 | 0.231 | 3.93E-03 | 0.263 | 5.96E-04 | 0.302 |
| TAF9 | 202168_at | 0.282 | 4.91E-03 | 0.429 | 7.59E-04 | 0.273 | 4.21E-04 | 0.222 | 5.24E-03 | 0.301 |
| SCN8A | 1561820_at | 0.270 | 7.26E-03 | 0.341 | 1.47E-02 | 0.345 | 1.83E-06 | 0.248 | 1.35E-03 | 0.301 |

**Table 4.1: Genes which positively correlate with *CDH2* expression in t(4;14)$^-$ MM patients (continued)**

| Gene | Probeset ID | E-MTAB-317 | | E-MTAB-363 | | E-GEOD-19784 | | E-GEOD-26863 | | Mean correlation co-efficient |
|---|---|---|---|---|---|---|---|---|---|---|
| | | R[1] | FDR[2]-adjusted P-value | R | FDR-adjusted P-value | R | FDR-adjusted P-value | R | FDR-adjusted P-value | |
| RPL36 | 219762_s_at | 0.299 | 2.58E-03 | 0.376 | 5.78E-03 | 0.238 | 2.65E-03 | 0.291 | 1.02E-04 | 0.301 |
| UBXN1 | 201871_s_at | 0.315 | 1.40E-03 | 0.338 | 1.58E-02 | 0.238 | 2.78E-03 | 0.311 | 2.53E-05 | 0.301 |
| EIF3K | 212716_s_at | 0.271 | 7.13E-03 | 0.348 | 1.23E-02 | 0.260 | 8.89E-04 | 0.322 | 1.14E-05 | 0.300 |
| C19orf42 | 224717_s_at | 0.308 | 1.85E-03 | 0.305 | 3.39E-02 | 0.237 | 2.91E-03 | 0.350 | 1.32E-06 | 0.300 |
| GPR177 | 228949_at | 0.294 | 3.19E-03 | 0.312 | 2.90E-02 | 0.253 | 1.30E-03 | 0.337 | 3.72E-06 | 0.299 |
| C19orf53 | 217926_at | 0.279 | 5.51E-03 | 0.395 | 3.17E-03 | 0.252 | 1.39E-03 | 0.269 | 4.13E-04 | 0.299 |
| COX5A | 203663_s_at | 0.301 | 2.32E-03 | 0.314 | 2.79E-02 | 0.300 | 7.04E-05 | 0.279 | 2.22E-04 | 0.298 |
| SPATA5L1 | 218933_at | 0.321 | 1.06E-03 | 0.344 | 1.34E-02 | 0.293 | 1.08E-04 | 0.232 | 3.19E-03 | 0.298 |
| BMP4 | 211518_s_at | 0.293 | 3.27E-03 | 0.323 | 2.25E-02 | 0.252 | 1.37E-03 | 0.320 | 1.27E-05 | 0.297 |
| PFKFB2 | 226733_at | 0.342 | 4.35E-04 | 0.334 | 1.75E-02 | 0.296 | 9.10E-05 | 0.216 | 6.87E-03 | 0.297 |
| RPL27A | 203034_s_at | 0.227 | 2.65E-02 | 0.346 | 1.30E-02 | 0.229 | 4.17E-03 | 0.384 | 6.63E-08 | 0.296 |
| RPL4 | 200089_s_at | 0.259 | 1.03E-02 | 0.364 | 7.47E-03 | 0.302 | 6.08E-05 | 0.260 | 7.01E-04 | 0.296 |
| NOL6 | 222554_s_at | 0.299 | 2.55E-03 | 0.383 | 3.92E-03 | 0.215 | 7.89E-03 | 0.284 | 1.55E-04 | 0.296 |
| PDLIM2 | 219165_at | 0.300 | 2.52E-03 | 0.293 | 4.36E-02 | 0.303 | 5.95E-05 | 0.286 | 1.34E-04 | 0.296 |
| ERCC1 | 203720_s_at | 0.287 | 4.21E-03 | 0.348 | 1.23E-02 | 0.239 | 2.62E-03 | 0.306 | 3.46E-05 | 0.295 |
| LENG1 | 232018_at | 0.273 | 6.48E-03 | 0.341 | 1.47E-02 | 0.258 | 9.71E-04 | 0.306 | 3.46E-05 | 0.295 |
| RAB8B | 226633_at | 0.214 | 3.67E-02 | 0.356 | 9.53E-03 | 0.300 | 6.64E-05 | 0.307 | 3.17E-05 | 0.294 |
| ZNF622 | 225152_at | 0.358 | 2.04E-04 | 0.289 | 4.83E-02 | 0.238 | 2.72E-03 | 0.293 | 8.42E-05 | 0.294 |
| RBM7 | 218379_at | 0.335 | 5.92E-04 | 0.361 | 8.60E-03 | 0.225 | 4.99E-03 | 0.256 | 8.91E-04 | 0.294 |
| RP3-398D13.1 | 1556366_s_at | 0.260 | 9.85E-03 | 0.357 | 9.04E-03 | 0.318 | 1.75E-05 | 0.241 | 1.94E-03 | 0.294 |
| NCRNA00219 | 225698_at | 0.256 | 1.12E-02 | 0.333 | 1.78E-02 | 0.226 | 4.93E-03 | 0.361 | 5.08E-07 | 0.294 |
| PIP5K1B | 205632_s_at | 0.253 | 1.24E-02 | 0.298 | 3.99E-02 | 0.249 | 1.56E-03 | 0.375 | 1.51E-07 | 0.294 |
| CD48 | 204118_at | 0.277 | 5.72E-03 | 0.391 | 3.57E-03 | 0.235 | 3.15E-03 | 0.267 | 4.75E-04 | 0.293 |
| C19orf43 | 223003_at | 0.275 | 6.26E-03 | 0.315 | 2.69E-02 | 0.213 | 8.57E-03 | 0.367 | 2.95E-07 | 0.292 |
| RPL18 | 200022_at | 0.240 | 1.83E-02 | 0.375 | 5.85E-03 | 0.254 | 1.16E-03 | 0.294 | 8.23E-05 | 0.291 |
| CADM1 | 209031_at | 0.322 | 1.06E-03 | 0.299 | 3.94E-02 | 0.291 | 1.28E-04 | 0.249 | 1.30E-03 | 0.290 |
| GYG1 | 201554_x_at | 0.296 | 2.93E-03 | 0.287 | 4.98E-02 | 0.252 | 1.33E-03 | 0.320 | 1.31E-05 | 0.289 |
| NPM1 | 221691_x_at | 0.314 | 1.44E-03 | 0.372 | 6.19E-03 | 0.240 | 2.33E-03 | 0.228 | 3.85E-03 | 0.289 |
| STOM | 201061_s_at | 0.394 | 3.81E-05 | 0.295 | 4.19E-02 | 0.290 | 1.32E-04 | 0.175 | 3.74E-02 | 0.289 |
| LOC399804 | 216387_x_at | 0.333 | 6.48E-04 | 0.389 | 3.74E-03 | 0.192 | 1.99E-02 | 0.239 | 2.18E-03 | 0.288 |
| PRKD2 | 38269_at | 0.255 | 1.14E-02 | 0.303 | 3.52E-02 | 0.264 | 7.00E-04 | 0.326 | 8.27E-06 | 0.287 |
| FLI1 | 210786_s_at | 0.261 | 9.63E-03 | 0.315 | 2.70E-02 | 0.247 | 1.75E-03 | 0.325 | 9.28E-06 | 0.287 |
| MTX3 | 226528_at | 0.278 | 5.46E-03 | 0.308 | 3.15E-02 | 0.241 | 2.39E-03 | 0.317 | 1.57E-05 | 0.286 |
| FBXO22 | 225737_s_at | 0.299 | 2.61E-03 | 0.308 | 3.13E-02 | 0.245 | 1.96E-03 | 0.288 | 1.18E-04 | 0.285 |
| BAI3 | 205638_at | 0.305 | 2.05E-03 | 0.309 | 3.09E-02 | 0.268 | 5.59E-04 | 0.258 | 8.04E-04 | 0.285 |
| GPM6A | 209469_at | 0.316 | 1.39E-03 | 0.294 | 4.33E-02 | 0.300 | 6.63E-05 | 0.224 | 4.76E-03 | 0.283 |
| C1R | 212067_s_at | 0.217 | 3.43E-02 | 0.299 | 3.85E-02 | 0.344 | 2.54E-06 | 0.272 | 3.50E-04 | 0.283 |
| FAU | 200019_s_at | 0.289 | 3.92E-03 | 0.339 | 1.53E-02 | 0.254 | 1.13E-03 | 0.247 | 1.42E-03 | 0.283 |
| RPS17 | 201665_x_at | 0.216 | 3.48E-02 | 0.355 | 9.90E-03 | 0.306 | 4.52E-05 | 0.251 | 1.15E-03 | 0.282 |
| EAF2 | 219551_at | 0.206 | 4.54E-02 | 0.349 | 1.16E-02 | 0.253 | 1.29E-03 | 0.319 | 1.40E-05 | 0.282 |
| HIST1H2AC | 215071_s_at | 0.298 | 2.73E-03 | 0.340 | 1.51E-02 | 0.305 | 4.54E-05 | 0.183 | 2.81E-02 | 0.281 |
| EIF3G | 208887_at | 0.296 | 2.92E-03 | 0.287 | 4.97E-02 | 0.258 | 9.70E-04 | 0.282 | 1.81E-04 | 0.281 |

**Table 4.1: Genes which positively correlate with *CDH2* expression in t(4;14)$^-$ MM patients (continued)**

| Gene | Probeset ID | E-MTAB-317 | | E-MTAB-363 | | E-GEOD-19784 | | E-GEOD-26863 | | Mean correlation co-efficient |
|---|---|---|---|---|---|---|---|---|---|---|
| | | R[1] | FDR[2]-adjusted P-value | R | FDR-adjusted P-value | R | FDR-adjusted P-value | R | FDR-adjusted P-value | |
| IFIT1 | 203153_at | 0.354 | 2.33E-04 | 0.320 | 2.40E-02 | 0.240 | 2.42E-03 | 0.206 | 1.08E-02 | 0.280 |
| C4orf14 | 223157_at | 0.306 | 2.03E-03 | 0.314 | 2.77E-02 | 0.228 | 4.48E-03 | 0.273 | 3.28E-04 | 0.280 |
| BTF3 | 211939_x_at | 0.280 | 5.22E-03 | 0.344 | 1.30E-02 | 0.241 | 2.30E-03 | 0.250 | 1.26E-03 | 0.279 |
| FHAD1 | 1564635_a_at | 0.208 | 4.30E-02 | 0.314 | 2.66E-02 | 0.329 | 8.41E-06 | 0.263 | 5.80E-04 | 0.279 |
| NOP10 | 217962_at | 0.304 | 2.13E-03 | 0.335 | 1.71E-02 | 0.285 | 1.82E-04 | 0.189 | 2.20E-02 | 0.278 |
| RPS17P5 | 216348_at | 0.251 | 1.30E-02 | 0.292 | 4.52E-02 | 0.320 | 1.71E-05 | 0.250 | 1.23E-03 | 0.278 |
| SOCS2 | 203372_s_at | 0.241 | 1.75E-02 | 0.308 | 3.15E-02 | 0.276 | 3.18E-04 | 0.281 | 1.97E-04 | 0.277 |
| TRPM3 | 216452_at | 0.244 | 1.62E-02 | 0.294 | 4.28E-02 | 0.249 | 1.57E-03 | 0.318 | 1.52E-05 | 0.276 |
| TMEM85 | 223857_x_at | 0.266 | 8.38E-03 | 0.303 | 3.43E-02 | 0.282 | 2.26E-04 | 0.253 | 1.07E-03 | 0.276 |
| RPS13 | 200018_at | 0.247 | 1.47E-02 | 0.323 | 2.25E-02 | 0.254 | 1.14E-03 | 0.278 | 2.28E-04 | 0.276 |
| PLSCR1 | 202430_s_at | 0.344 | 3.95E-04 | 0.289 | 4.80E-02 | 0.239 | 2.49E-03 | 0.227 | 4.01E-03 | 0.275 |
| POLR1D | 224857_s_at | 0.262 | 9.41E-03 | 0.309 | 3.09E-02 | 0.261 | 8.53E-04 | 0.266 | 5.05E-04 | 0.274 |
| RARS | 201330_at | 0.328 | 7.76E-04 | 0.294 | 4.28E-02 | 0.228 | 4.52E-03 | 0.247 | 1.48E-03 | 0.274 |
| CLNS1A | 209143_s_at | 0.313 | 1.49E-03 | 0.377 | 5.52E-03 | 0.207 | 1.12E-02 | 0.192 | 1.99E-02 | 0.272 |
| EID1 | 208669_s_at | 0.265 | 8.64E-03 | 0.292 | 4.51E-02 | 0.295 | 9.40E-05 | 0.237 | 2.46E-03 | 0.272 |
| ZC3H12C | 231899_at | 0.322 | 1.05E-03 | 0.330 | 1.84E-02 | 0.230 | 3.94E-03 | 0.204 | 1.17E-02 | 0.272 |
| RELL2 | 1564031_a_at | 0.211 | 4.01E-02 | 0.293 | 4.36E-02 | 0.287 | 1.51E-04 | 0.293 | 8.51E-05 | 0.271 |
| CCDC85A | 235228_at | 0.271 | 6.95E-03 | 0.305 | 3.39E-02 | 0.298 | 8.05E-05 | 0.207 | 1.04E-02 | 0.270 |
| SSR3 | 217790_s_at | 0.250 | 1.34E-02 | 0.308 | 3.09E-02 | 0.272 | 4.44E-04 | 0.248 | 1.36E-03 | 0.269 |
| C6orf48 | 220755_s_at | 0.247 | 1.45E-02 | 0.310 | 2.96E-02 | 0.229 | 4.17E-03 | 0.284 | 1.55E-04 | 0.268 |
| MFNG | 204153_s_at | 0.237 | 1.97E-02 | 0.397 | 2.97E-03 | 0.264 | 6.88E-04 | 0.168 | 4.81E-02 | 0.267 |
| RPS11 | 200031_s_at | 0.216 | 3.43E-02 | 0.324 | 2.13E-02 | 0.205 | 1.19E-02 | 0.321 | 1.25E-05 | 0.266 |
| EEF1D | 203113_s_at | 0.239 | 1.84E-02 | 0.306 | 3.35E-02 | 0.212 | 8.77E-03 | 0.308 | 3.12E-05 | 0.266 |
| UBLCP1 | 227413_at | 0.315 | 1.44E-03 | 0.287 | 4.94E-02 | 0.225 | 5.17E-03 | 0.236 | 2.57E-03 | 0.266 |
| FBL | 211623_s_at | 0.297 | 2.74E-03 | 0.337 | 1.61E-02 | 0.233 | 3.50E-03 | 0.190 | 2.12E-02 | 0.264 |
| PDCD2L | 224467_s_at | 0.306 | 2.02E-03 | 0.323 | 2.27E-02 | 0.205 | 1.20E-02 | 0.222 | 5.28E-03 | 0.264 |
| KAT5 | 214258_x_at | 0.252 | 1.26E-02 | 0.329 | 1.98E-02 | 0.244 | 2.07E-03 | 0.220 | 5.58E-03 | 0.261 |
| HMGA1 | 206074_s_at | 0.263 | 9.02E-03 | 0.361 | 8.72E-03 | 0.231 | 3.87E-03 | 0.186 | 2.49E-02 | 0.260 |
| RPL35 | 200002_at | 0.226 | 2.67E-02 | 0.290 | 4.66E-02 | 0.203 | 1.33E-02 | 0.317 | 1.58E-05 | 0.259 |
| RPL31 | 221593_s_at | 0.339 | 4.99E-04 | 0.314 | 2.78E-02 | 0.207 | 1.10E-02 | 0.175 | 3.81E-02 | 0.258 |
| GAS5 | 224741_x_at | 0.228 | 2.55E-02 | 0.360 | 8.96E-03 | 0.198 | 1.63E-02 | 0.248 | 1.38E-03 | 0.258 |
| FAM96A | 224779_s_at | 0.243 | 1.66E-02 | 0.306 | 3.30E-02 | 0.290 | 1.32E-04 | 0.190 | 2.09E-02 | 0.257 |
| SIX4 | 229796_at | 0.295 | 2.92E-03 | 0.329 | 1.98E-02 | 0.193 | 1.99E-02 | 0.212 | 8.46E-03 | 0.257 |
| CSNK1A1 | 243338_at | 0.249 | 1.37E-02 | 0.313 | 2.77E-02 | 0.289 | 1.29E-04 | 0.170 | 4.44E-02 | 0.255 |
| NKX6-2 | 235832_at | 0.268 | 7.68E-03 | 0.295 | 4.24E-02 | 0.201 | 1.43E-02 | 0.250 | 1.23E-03 | 0.254 |
| BNIP1 | 37226_at | 0.248 | 1.41E-02 | 0.311 | 2.96E-02 | 0.261 | 8.19E-04 | 0.192 | 1.92E-02 | 0.253 |
| APH1B | 221036_s_at | 0.223 | 2.97E-02 | 0.308 | 3.15E-02 | 0.299 | 7.14E-05 | 0.178 | 3.34E-02 | 0.252 |
| TRIM13 | 203659_s_at | 0.265 | 8.69E-03 | 0.290 | 4.59E-02 | 0.248 | 1.63E-03 | 0.201 | 1.35E-02 | 0.251 |
| MRPS30 | 218398_at | 0.289 | 3.92E-03 | 0.304 | 3.49E-02 | 0.196 | 1.77E-02 | 0.211 | 8.62E-03 | 0.250 |
| CLTA | 204050_s_at | 0.255 | 1.16E-02 | 0.327 | 2.04E-02 | 0.168 | 4.97E-02 | 0.241 | 2.00E-03 | 0.248 |
| TAPBP | 1555565_s_at | 0.252 | 1.27E-02 | 0.337 | 1.63E-02 | 0.204 | 1.26E-02 | 0.194 | 1.76E-02 | 0.247 |
| MGC50722 | 1554681_a_at | 0.267 | 8.11E-03 | 0.343 | 1.41E-02 | 0.207 | 1.13E-02 | 0.171 | 4.35E-02 | 0.247 |

**Table 4.1: Genes which positively correlate with *CDH2* expression in t(4;14)- MM patients (continued)**

| Gene | Probeset ID | E-MTAB-317 | | E-MTAB-363 | | E-GEOD-19784 | | E-GEOD-26863 | | Mean correlation co-efficient |
|---|---|---|---|---|---|---|---|---|---|---|
| | | R[1] | FDR[2]-adjusted P-value | R | FDR-adjusted P-value | R | FDR-adjusted P-value | R | FDR-adjusted P-value | |
| IL6ST | 204864_s_at | 0.283 | 4.88E-03 | 0.328 | 1.94E-02 | 0.189 | 2.26E-02 | 0.187 | 2.40E-02 | 0.247 |
| TOMM70A | 201512_s_at | 0.290 | 3.81E-03 | 0.295 | 4.21E-02 | 0.213 | 8.64E-03 | 0.188 | 2.31E-02 | 0.246 |
| E2F5 | 221586_s_at | 0.247 | 1.47E-02 | 0.295 | 4.19E-02 | 0.222 | 5.97E-03 | 0.215 | 7.10E-03 | 0.245 |
| ANP32A | 201051_at | 0.215 | 3.62E-02 | 0.302 | 3.65E-02 | 0.253 | 1.26E-03 | 0.207 | 1.05E-02 | 0.244 |
| NCK1 | 204725_s_at | 0.226 | 2.71E-02 | 0.321 | 2.33E-02 | 0.176 | 3.71E-02 | 0.253 | 1.07E-03 | 0.244 |
| RPS28 | 208902_s_at | 0.243 | 1.64E-02 | 0.329 | 1.97E-02 | 0.215 | 8.02E-03 | 0.186 | 2.47E-02 | 0.243 |
| TNFAIP8 | 208296_x_at | 0.280 | 5.28E-03 | 0.292 | 4.52E-02 | 0.174 | 4.00E-02 | 0.227 | 4.15E-03 | 0.243 |
| PPP1CC | 200726_at | 0.259 | 1.03E-02 | 0.291 | 4.49E-02 | 0.238 | 2.78E-03 | 0.173 | 4.09E-02 | 0.240 |
| PSMB9 | 204279_at | 0.285 | 4.46E-03 | 0.312 | 2.90E-02 | 0.182 | 2.97E-02 | 0.174 | 3.87E-02 | 0.238 |
| RPS9 | 217747_s_at | 0.247 | 1.47E-02 | 0.294 | 4.33E-02 | 0.171 | 4.39E-02 | 0.236 | 2.64E-03 | 0.237 |
| RPL29 | 200823_x_at | 0.209 | 4.09E-02 | 0.289 | 4.79E-02 | 0.208 | 1.06E-02 | 0.236 | 2.64E-03 | 0.236 |
| SEC11A | 216274_s_at | 0.265 | 8.44E-03 | 0.295 | 4.08E-02 | 0.172 | 4.25E-02 | 0.205 | 1.15E-02 | 0.234 |
| C19orf12 | 225863_s_at | 0.214 | 3.67E-02 | 0.295 | 4.24E-02 | 0.184 | 2.73E-02 | 0.229 | 3.69E-03 | 0.231 |
| RPS5 | 200024_at | 0.234 | 2.15E-02 | 0.321 | 2.33E-02 | 0.186 | 2.53E-02 | 0.181 | 2.99E-02 | 0.231 |
| RPS2 | 217466_x_at | 0.214 | 3.65E-02 | 0.289 | 4.80E-02 | 0.183 | 2.90E-02 | 0.233 | 3.03E-03 | 0.230 |
| RPS3 | 208692_at | 0.203 | 4.85E-02 | 0.292 | 4.36E-02 | 0.208 | 1.09E-02 | 0.215 | 7.06E-03 | 0.230 |
| SCAMP1 | 1552978_a_at | 0.222 | 3.02E-02 | 0.300 | 3.81E-02 | 0.197 | 1.63E-02 | 0.178 | 3.31E-02 | 0.224 |
| CTDSPL2 | 223271_s_at | 0.203 | 4.85E-02 | 0.289 | 4.86E-02 | 0.180 | 3.19E-02 | 0.169 | 4.66E-02 | 0.210 |

[1] Spearman's rank correlation co-efficient

[2] False discovery rate

**Table 4.2: Genes which inversely correlate with *CDH2* expression in t(4;14)$^-$ MM patients**

| Gene | Probeset ID | E-MTAB-317 | | E-MTAB-363 | | E-GEOD-19784 | | E-GEOD-26863 | | Mean correlation co-efficient |
|---|---|---|---|---|---|---|---|---|---|---|
| | | R[1] | FDR[2]-adjusted P-value | R | FDR-adjusted P-value | R | FDR-adjusted P-value | R | FDR-adjusted P-value | |
| PITPNC1 | 219155_at | -0.421 | 6.54E-06 | -0.488 | 4.76E-05 | -0.435 | 0.00E+00 | -0.415 | 3.83E-09 | -0.440 |
| C1orf56 | 223459_s_at | -0.456 | 3.68E-07 | -0.314 | 2.76E-02 | -0.332 | 6.53E-06 | -0.346 | 1.76E-06 | -0.362 |
| TMEM107 | 239824_s_at | -0.307 | 1.91E-03 | -0.401 | 2.20E-03 | -0.355 | 9.06E-07 | -0.287 | 1.33E-04 | -0.337 |
| RAPH1 | 225188_at | -0.355 | 2.30E-04 | -0.390 | 3.57E-03 | -0.310 | 3.55E-05 | -0.277 | 2.51E-04 | -0.333 |
| TCFL5 | 235694_at | -0.236 | 2.03E-02 | -0.433 | 6.47E-04 | -0.336 | 4.25E-06 | -0.283 | 1.74E-04 | -0.322 |
| SEC61A2 | 230215_at | -0.278 | 5.67E-03 | -0.372 | 6.15E-03 | -0.337 | 4.38E-06 | -0.276 | 2.63E-04 | -0.316 |
| HGSNAT | 218017_s_at | -0.275 | 6.16E-03 | -0.331 | 1.90E-02 | -0.273 | 4.22E-04 | -0.384 | 6.50E-08 | -0.316 |
| XPR1 | 226615_at | -0.248 | 1.42E-02 | -0.366 | 7.61E-03 | -0.294 | 1.04E-04 | -0.288 | 1.18E-04 | -0.299 |
| ARF3 | 200734_s_at | -0.301 | 2.37E-03 | -0.326 | 2.05E-02 | -0.206 | 1.19E-02 | -0.357 | 7.49E-07 | -0.297 |
| SFN | 33323_r_at | -0.255 | 1.16E-02 | -0.429 | 7.58E-04 | -0.251 | 1.41E-03 | -0.254 | 1.01E-03 | -0.297 |
| IFNA1 | 208375_at | -0.280 | 5.20E-03 | -0.334 | 1.73E-02 | -0.286 | 1.69E-04 | -0.275 | 2.92E-04 | -0.294 |
| POLA1 | 204835_at | -0.244 | 1.60E-02 | -0.336 | 1.63E-02 | -0.299 | 7.08E-05 | -0.243 | 1.77E-03 | -0.281 |
| ZNRF1 | 225959_s_at | -0.311 | 1.64E-03 | -0.338 | 1.60E-02 | -0.290 | 1.29E-04 | -0.184 | 2.70E-02 | -0.281 |
| PHC1 | 218338_at | -0.302 | 2.33E-03 | -0.311 | 3.01E-02 | -0.226 | 4.82E-03 | -0.272 | 3.41E-04 | -0.278 |
| SGPL1 | 212321_at | -0.235 | 2.07E-02 | -0.388 | 3.77E-03 | -0.216 | 7.50E-03 | -0.262 | 6.30E-04 | -0.275 |
| GSTA4 | 202967_at | -0.263 | 9.10E-03 | -0.312 | 2.93E-02 | -0.168 | 4.84E-02 | -0.332 | 5.49E-06 | -0.269 |
| C1orf93 | 231835_at | -0.241 | 1.79E-02 | -0.310 | 2.98E-02 | -0.232 | 3.58E-03 | -0.280 | 2.10E-04 | -0.266 |
| SLC44A2 | 224609_at | -0.243 | 1.65E-02 | -0.324 | 2.25E-02 | -0.246 | 1.87E-03 | -0.247 | 1.43E-03 | -0.265 |
| CD28 | 206545_at | -0.266 | 8.31E-03 | -0.351 | 1.01E-02 | -0.227 | 4.70E-03 | -0.210 | 9.08E-03 | -0.263 |
| CDKN1C | 213348_at | -0.292 | 3.43E-03 | -0.290 | 4.72E-02 | -0.187 | 2.45E-02 | -0.282 | 1.83E-04 | -0.263 |
| C16orf93 | 231300_at | -0.300 | 2.52E-03 | -0.294 | 4.33E-02 | -0.191 | 2.09E-02 | -0.256 | 8.80E-04 | -0.260 |
| B3GALT6 | 1553959_a_at | -0.223 | 2.90E-02 | -0.396 | 3.07E-03 | -0.195 | 1.85E-02 | -0.224 | 4.63E-03 | -0.260 |
| DHX32 | 218198_at | -0.225 | 2.78E-02 | -0.300 | 3.81E-02 | -0.264 | 6.86E-04 | -0.235 | 2.81E-03 | -0.256 |
| IRF2BP2 | 224570_s_at | -0.219 | 3.27E-02 | -0.288 | 4.89E-02 | -0.236 | 2.89E-03 | -0.277 | 2.51E-04 | -0.255 |
| KCNN3 | 205903_s_at | -0.228 | 2.52E-02 | -0.315 | 2.69E-02 | -0.214 | 8.34E-03 | -0.262 | 6.16E-04 | -0.255 |
| APBB1IP | 1554571_at | -0.323 | 9.78E-04 | -0.291 | 4.59E-02 | -0.197 | 1.63E-02 | -0.204 | 1.18E-02 | -0.254 |
| CDCA7 | 224428_s_at | -0.232 | 2.27E-02 | -0.385 | 3.78E-03 | -0.193 | 1.92E-02 | -0.204 | 1.16E-02 | -0.254 |
| DHTKD1 | 209916_at | -0.280 | 5.24E-03 | -0.297 | 3.95E-02 | -0.214 | 8.31E-03 | -0.214 | 7.50E-03 | -0.251 |
| SLC8A1 | 1556583_a_at | -0.297 | 2.83E-03 | -0.301 | 3.67E-02 | -0.227 | 4.60E-03 | -0.173 | 3.96E-02 | -0.250 |
| RGS5 | 1558785_a_at | -0.258 | 1.03E-02 | -0.315 | 2.69E-02 | -0.180 | 3.19E-02 | -0.186 | 2.51E-02 | -0.235 |
| ETV6 | 235056_at | -0.255 | 1.16E-02 | -0.292 | 4.43E-02 | -0.186 | 2.61E-02 | -0.198 | 1.51E-02 | -0.233 |
| EP400NL | 229892_at | -0.246 | 1.51E-02 | -0.287 | 4.86E-02 | -0.208 | 1.06E-02 | -0.178 | 3.39E-02 | -0.230 |

[1] Spearman's rank correlation co-efficient

[2] False discovery rate

regulated in MM patients with hyperdiploidy amongst the inversely-correlating gene group (Supplementary Table 4.2).

In order to identify potential drivers of *CDH2* expression in t(4;14)$^{-}$ MM patients, genes which significantly positively correlated with *CDH2* expression in *MMSET*$^{low}$ MM patients, and were significantly up-regulated in CD138$^{+}$ BM MM PCs compared with CD138$^{+}$ BM PCs from healthy individuals, were further short-listed. *In silico* analysis of publically-available microarray data (E-MTAB-363) revealed that, of the 186 genes which significantly positively correlated with *CDH2* expression, 13 genes were significantly up-regulated in BM MM PCs compared with normal BM PCs (Table 4.3). *BTBD3,* encoding for the putative transcriptional regulator BTB/POZ domain-containing protein 3 (BTBD3), was the most highly up-regulated gene ($log_2$ 4.61-fold; p = 0.002) which positively correlated with *CDH2* expression in t(4;14)$^{-}$ MM patients (mean correlation co-efficient = 0.375; FDR-adjusted P value < 0.001) (Figure 4.3A,B). Notably, *BTBD3* expression was consistently up-regulated in *MMSET*$^{low}$*CDH2*$^{high}$ MM patients (GSE4581: 100 *BTBD3*$^{high}$ of 141 *MMSET*$^{low}$*CDH2*$^{high}$ patients, 70.9%; E-MTAB-363: 43/60, 71.7%; E-GEOD-19784: 85/131, 64.9%; E-MTAB-317: 54/83, 65.1%; E-GEOD-26863: 78/124, 62.9%), suggesting that it may be responsible for up-regulating *CDH2* expression in t(4;14)$^{-}$ MM patients (Figure 4.3A). In order to determine the clinical significance of *BTBD3* up-regulation in BM MM PCs, we assessed the overall survival of newly-diagnosed MM patients, stratified on the basis of *MMSET* and *BTBD3* expression, in the microarray dataset GSE4581. While overall survival was not significantly affected by *BTBD3* expression in the *MMSET*$^{high}$ patients (p = 0.76), there was a trend towards poorer survival in *MMSET*$^{low}$*BTBD3*$^{high}$ MM patients, when compared with the *MMSET*$^{low}$*BTBD3*$^{low}$ patients (p = 0.064; HR: 1.64 [95% CI: 0.97-2.77]) (Figure 4.3C). Taken together, these findings suggest that BTBD3 may be a potential driver of *CDH2* expression in t(4;14)$^{-}$ MM (Supplementary Figure 4.2B) and may play a role in MM pathogenesis.

### 4.4.3 Identification of miRNAs which may regulate *CDH2* expression in t(4;14)$^{-}$ MM

While *BTBD3* is consistently up-regulated in BM MM PCs from *MMSET*$^{low}$*CDH2*$^{high}$ patients, there are a large proportion of *MMSET*$^{low}$*CDH2*$^{low}$ patients that also express *BTBD3* (GSE4581: 71 *BTBD3*$^{high}$ of 199 *MMSET*$^{low}$*CDH2*$^{low}$ patients, 35.7%; E-MTAB-363: 27/76, 35.5%; E-GEOD-19784: 57/162, 35.2%; E-MTAB-317: 37/109,

**Table 4.3: Genes which positively correlate with *CDH2* expression in t(4;14)$^-$ MM patients and are significantly up-regulated in MM PCs compared with normal PCs**

| | | | normal | | MM | | normal v MM | |
|---|---|---|---|---|---|---|---|---|
| Gene | Full gene name | Probeset ID | $Log_2$ Mean | $Log_2$ SD[1] | $Log_2$ Mean | $Log_2$ SD | Adjusted P-value[2] | $Log_2$ fold change in expression |
| **BTBD3** | **BTB/POZ Domain-Containing Protein 3** | **202946_s_at** | **5.01** | **0.81** | **9.62** | **2.10** | **1.94E-03** | **4.61** |
| HIST1H2AC | Histone Cluster 1 H2A Family Member C | 215071_s_at | 7.94 | 0.74 | 11.70 | 1.27 | 1.94E-03 | 3.76 |
| RPL35A | Ribosomal Protein L35a | 238026_at | 6.68 | 0.55 | 9.83 | 1.07 | 1.94E-03 | 3.14 |
| LOC346887 | LOC346887 | 235205_at | 6.06 | 0.40 | 8.79 | 1.01 | 1.94E-03 | 2.73 |
| ELOVL7 | ELOVL Fatty Acid Elongase 7 | 227180_at | 4.41 | 0.33 | 8.46 | 1.99 | 2.70E-03 | 4.05 |
| STOM | Stomatin | 201061_s_at | 8.24 | 0.54 | 11.23 | 1.16 | 7.50E-03 | 2.99 |
| PLSCR1 | Phospholipid Scramblase 1 | 202430_s_at | 5.21 | 0.93 | 7.70 | 1.29 | 1.29E-02 | 2.49 |
| SSR3 | Signal Sequence Receptor Subunit 3 | 217790_s_at | 7.86 | 0.67 | 10.12 | 0.77 | 1.50E-02 | 2.26 |
| RSAD2 | Radical S-Adenosyl Methionine Domain Containing 2 | 242625_at | 4.68 | 0.40 | 8.06 | 2.04 | 1.91E-02 | 3.38 |
| FBXO22 | F-Box Protein 22 | 225737_s_at | 5.40 | 0.27 | 7.37 | 0.95 | 1.91E-02 | 1.97 |
| SPEF2 | Sperm Flagellar 2 | 1552716_at | 4.67 | 0.23 | 6.17 | 0.64 | 3.62E-02 | 1.50 |
| CMPK2 | Cytidine/Uridine Monophosphate Kinase 2 | 226702_at | 6.40 | 1.09 | 9.52 | 1.92 | 3.95E-02 | 3.11 |
| GMPR | Guanosine Monophosphate Reductase | 204187_at | 6.36 | 0.35 | 8.18 | 0.93 | 4.02E-02 | 1.82 |

[1] Standard deviation

[2] LIMMA

**Figure 4.3. *BTBD3* expression positively correlates with *CDH2* expression in t(4;14)⁻ MM patients, and is significantly up-regulated in MM PCs.** *BTBD3* and *CDH2* correlation in 4 independent, publicly available microarray datasets of CD138-selected BM-derived MM PCs from newly-diagnosed individuals (E-MTAB-363, E-GEOD-19784, E-MTAB-317 and E-GEOD-26863) (Spearman's rank correlation co-efficient (R), FDR-adjusted P value <0.001 for each dataset) (**A**). *BTBD3* expression in CD138-selected BM-derived PCs from normal individuals (n = 5), and newly-diagnosed MGUS (n = 5) and MM (n = 155) patients (E-MTAB-363). ***P* < 0.05 compared with normal individuals (LIMMA) (**B**). Kaplan-Meier plot of overall survival for newly-diagnosed MM patients in GSE4581, stratified on the basis of *MMSET* and *BTBD3* expression (*MMSET*$^{low}$/*BTBD3*$^{low}$ patients, n = 169; *MMSET*$^{low}$/*BTBD3*$^{high}$, n = 171; *MMSET*$^{high}$/*BTBD3*$^{low}$, n = 38; *MMSET*$^{high}$/*BTBD3*$^{high}$, n = 39) (**C**).

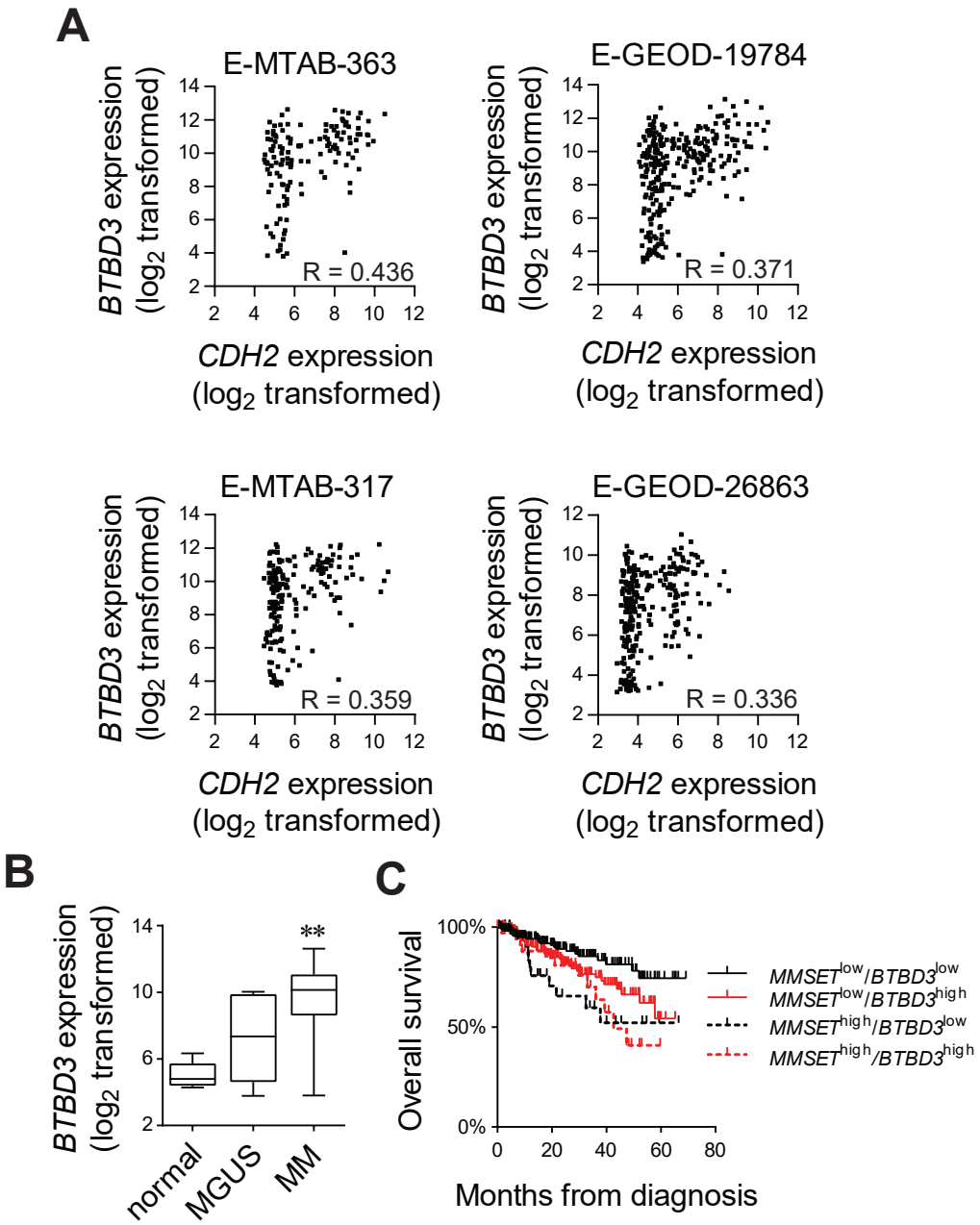
A
E-MTAB-363
R = 0.436
E-GEOD-19784
R = 0.371
E-MTAB-317
R = 0.359
E-GEOD-26863
R = 0.336
BTBD3 expression (log2 transformed)
CDH2 expression (log2 transformed)
B
BTBD3 expression (log2 transformed)
**
normal
MGUS
MM
C
Overall survival
100%
50%
0%
0
20
40
60
80
Months from diagnosis
MMSETlow/BTBD3low
MMSETlow/BTBD3high
MMSEThigh/BTBD3low
MMSEThigh/BTBD3high

33.9%; E-GEOD-26863: 58/146, 39.7%) (Figure 4.3A). Previous studies have demonstrated that N-cadherin gene and protein expression can be regulated by miRNAs, either by directly targeting the 3'-UTR of *CDH2* or genes encoding for proteins which are known regulators of N-cadherin expression in cancer cells.[22,63-73] In order to determine whether miRs may down-regulate *CDH2* expression in t(4;14)$^{-}$ MM, we performed *in silico* analysis of a publicly available microarray dataset which included miRNA expression and mRNA expression in CD138-selected BM PCs from 60 newly-diagnosed MM patients (GSE16558). Of the 60 patients in this dataset, 43 (71.7%) were t(4;14)$^{-}$, as determined by expression of *MMSET* and *FGFR3* (Supplementary Figure 4.1F) and by FISH (data not shown). Consistent with the data shown in Figure 4.3A, a large proportion (24/34, 70.6%) of t(4;14)$^{-}$ MM patients that express *BTBD3* in this dataset do not express *CDH2*. In order to investigate whether the expression of specific miRNAs could be down-regulating *CDH2* in these patients, we compared miRNA expression between the *CDH2*$^{high}$ (n = 14) and *CDH2*$^{low}$ (n = 29) t(4;14)$^{-}$ MM patients in this dataset. We identified 8 miRNAs that were more than two-fold up-regulated in *CDH2*$^{low}$ t(4;14)$^{-}$ MM patients, when compared with *CDH2*$^{high}$ t(4;14)$^{-}$ MM patients (Table 4.4). In order to assess whether these miRNA could potentially directly regulate *CDH2* expression, we examined the predicted targets for these miRNA in three independent databases (TargetScan, PicTar, miRdb) and identified those miRNA that were predicted to target *CDH2* in at least two databases. Collectively, these miRNAs were predicted to target 40 genes identified in our *CDH2* correlative analysis, including *BTBD3*, *IL6ST*, *FBXO22*, *COPS2* and *E2F5* (Table 4.4). miR-190, which is up-regulated 2.26-fold in *CDH2*$^{low}$ t(4;14)$^{-}$ MM patients, is predicted to target *CDH2*. Notably, of the t(4;14)$^{-}$ MM patients that express miR-190, 10 of 11 (91%) expressed low or undetectable levels of *CDH2* (Supplementary Figure 4.3A and Table 4.5). Moreover, of the t(4;14)$^{-}$ MM patients that express *CDH2*, 13 of 14 (93%) expressed low or undetectable levels of miR-190. These data strongly suggest that miR-190 may suppress *CDH2* expression in t(4;14)$^{-}$ MM patients (Supplementary Figure 4.2B).

We further hypothesised that expression of miR-190 may prevent the up-regulation of *CDH2* by BTBD3 in some t(4;14)$^{-}$ MM patients. In support of this, of the t(4;14)$^{-}$ MM patients that express both *BTBD3* and miR-190, 8 of 8 (100%) expressed low or undetectable levels of *CDH2* (Table 4.5). Moreover, of the t(4;14)$^{-}$ *BTBD3*$^{high}$ MM patients that express *CDH2*, 10 of 10 (100%) expressed low or undetectable levels

**Table 4.4: miRNAs that are inversely associated with *CDH2* expression in t(4;14)$^-$ MM patients, and their predicted targets[1]**

| miRNA | $Log_2$ fold change (*CDH2* $^{low}$ vs *CDH2* $^{high}$) | Predicted targets[2] | | | | |
|---|---|---|---|---|---|---|
| hsa-miR-339 | 1.63 | TAPBP | | | | |
| hsa-miR-181a | 1.46 | E2F5 | FHAD1 | BAI3 | MTX3 | ST8SIA4 |
| | | COPS2 | CMPK2 | BTBD3 | | |
| hsa-miR-650[3] | 1.30 | N/A | | | | |
| **hsa-miR-190a** | 1.18 | E2F5 | IL6ST | TRIM13 | SIX4 | CCDC85A |
| | | ZC3H12C | BAI3 | FBXO22 | MTX3 | FLI1 |
| | | CADM1 | SCN8A | PALM2-AKAP2 | SMOC1 | TMEM161B |
| | | COPS2 | CHSY3 | CNTN5 | SCAMP5 | TRAT1 |
| | | RPL37 | COL4A5 | **CDH2** | PCDH9 | |
| hsa-miR-193b | 1.17 | CTDSPL2 | SIX4 | FAM96A | FLI1 | CADM1 |
| | | COPS2 | | | | |
| hsa-miR-17 | 1.14 | SCAMP1 | CCDC85A | ZC3H12C | RAB8B | CMPK2 |
| | | CNTN5 | COL4A5 | E2F5 | | |
| hsa-miR-214 | 1.05 | NOL6 | HOMER1 | SMOC1 | TMEM161B | COL4A5 |
| | | C21orf91 | | | | |
| hsa-miR-545 | 1.04 | NCK1 | ANP32A | E2F5 | MRPS30 | SIX4 |
| | | FBXO22 | MTX3 | CADM1 | PIP5K1B | RBM7 |
| | | ZNF622 | RAB8B | CDV3 | PALM2-AKAP2 | COPS2 |
| | | ELOVL7 | CDC42SE2 | | | |

[1] miRNAs more than two-fold up-regulated in CDH2$^{low}$ t(4;14)$^-$ MM patients, compared with CDH2$^{high}$ t(4;14)$^-$ MM patients, and their predicted targets within the 218 genes which positively or inversely correlate with *CDH2* expression in t(4;14)$^-$ MM patients

[2] Targets predicted in at least 2 of 3 databases (TargenScan; Pictar; MiRdb)

[3] hsa-miR-650 was only anotated in one of 3 databases consulted

**Table 4.5: *CDH2* and miR-190 expression in *BTBD3*$^{low}$ and BTBD3$^{high}$ t(4;14)$^{-}$ MM patients**

| | t(4;14)$^{-}$ | | | | |
|---|---|---|---|---|---|
| | | *BTBD3* $^{low}$ | | *BTBD3* $^{high}$ | |
| | Total | miR-190$^{+}$ | miR-190$^{-}$ | miR-190$^{+}$ | miR-190$^{-}$ |
| *CDH2* $^{low}$ | 29 | 2 | 3 | 8 | 16 |
| *CDH2* $^{high}$ | 14 | 1 | 3 | 0 | 10 |

of miR-190 (Table 4.5). These data suggest that, while *BTBD3* may drive *CDH2* expression in t(4;14)$^{-}$ MM patients, this may be suppressed in some patients by expression of miR-190.

### 4.4.4 Modulation of *BTBD3* expression in HMCLs does not alter *CDH2* expression

To investigate whether BTBD3 is a regulator of *CDH2* expression *in vitro*, we modulated *BTBD3* expression in HMCLs. The *BTBD3* gene encodes for 6 mRNA transcript variants that encode 4 different isoforms of BTBD3 protein (*a* [522 aa], predicted to be translated from transcript variant 1; *b* [461 aa], from transcript variants 3 and 4; *c* [371 aa], from transcript variants 5 and 6; *d* [565 aa] from transcript variant 2). Initially, we assessed total *BTBD3* mRNA expression levels in a panel of t(4;14)$^{-}$ and t(4;14)$^{+}$ HMCLs, using primers to a region common to all 6 *BTBD3* transcript variants (Supplementary Figure 4.4A). Additionally, we screened a panel of *BTBD3*$^{+}$ HMCLs to identify the prominent BTBD3 protein isoforms endogenously expressed in these cells, using an antibody specific for isoforms *a*, *b* and *d* (Supplementary Figure 4.4B). A band corresponding to the predicted molecular weight of isoform *b* (52 kDa) and isoform *a* (58 kDa) was detectable in LP-1 cells, while isoform *b* alone was detectable in RPMI-8226, U266 and OPM2 cells. As the smallest BTBD3 isoform (*c*) (41 kDa) does not contain the epitope recognised by the anti-BTBD3 antibody used, we could not confirm whether this isoform is endogenously expressed in HMCLs.

To investigate whether BTBD3 regulates *CDH2* expression *in vitro*, we over-expressed BTBD3 in t(4;14)$^{-}$ HMCLs which endogenously express low levels of total *BTBD3* (Supplementary Figure 4.4A) and *CDH2* (Figure 4.1A), with high (RPMI-8226) or low (U266) levels of miR-190 (Supplementary Figure 4.3B). To this end, we over-expressed the predominant BTBD3 isoforms detected in HMCLs (*a* and *b*), as well as isoform *c*, in these HMCLs using *BTBD3* transcript variants 1 (for isoforms *a* and *b*) and 6 (for isoform *c*). Over-expression of *BTBD3* transcript variant 1 or 6 in RPMI-8226 (RPMI-8226-BTBD3var.1 and RPMI-8226-BTBD3var.6) and U266 cells (U266-BTBD3var.1 and U266-BTBD3var.6) resulted in more than a 300-fold increase in total *BTBD3* transcript levels, compared with empty vector (EV)-containing cells (RPMI-8226-EV and U266-EV), as shown by qPCR ($P < 0.0001$) (Figure 4.4A,B). At the protein level, RPMI-8226-BTBD3var.1 and U266-BTBD3var.1 cells demonstrated marked up-regulation of BTBD3 protein bands corresponding to isoforms *a* and *b*,

**Figure 4.4. BTBD3 over-expression does not up-regulate N-cadherin mRNA or protein expression in HMCLs.** Total *BTBD3* expression in RPMI-8226 (**A**) and U266 (**B**) cells (normalised to *ACTB* expression), as assessed by qPCR, following over-expression of *BTBD3* transcript variant 1 or 6 (BTBD3var.1 and BTBD3var.6). Graphs depict mean ± SEM of 3 independent experiments. ****$P < 0.0001$ compared with empty vector (EV)-containing cells (EV) (one-way ANOVA with Dunnett's multiple comparisons test) (**A**,**B**). BTBD3 expression in RPMI-8226 (**C**) and U266 (**D**) cells following over-expression of *BTBD3* transcript variant 1 (var.1) or 6 (var.6), relative to EV-containing cells (top panels), as assessed by Western blot. Histone H3 (H3) was utilised as a nuclear protein load control (bottom panels) (**C**,**D**). *CDH2* expression in RPMI-8226 (**E**) and U266 (**F**) cells (normalised to *ACTB* expression), as assessed by qPCR, following over-expression of *BTBD3* transcript variant 1 or 6. Graphs depict mean ± SEM of 3 independent experiments. ****$P < 0.0001$ compared with EV-containing cells (one-way ANOVA with Dunnett's multiple comparisons test) (**E**,**F**). N-cadherin expression in RPMI-8226-EV cells (blue line) and RPMI-8226-BTBD3var.1 cells (orange line), as assessed by flow cytometry. Shaded area represents RPMI-8226-EV cells stained with isotype control antibody (**G**).

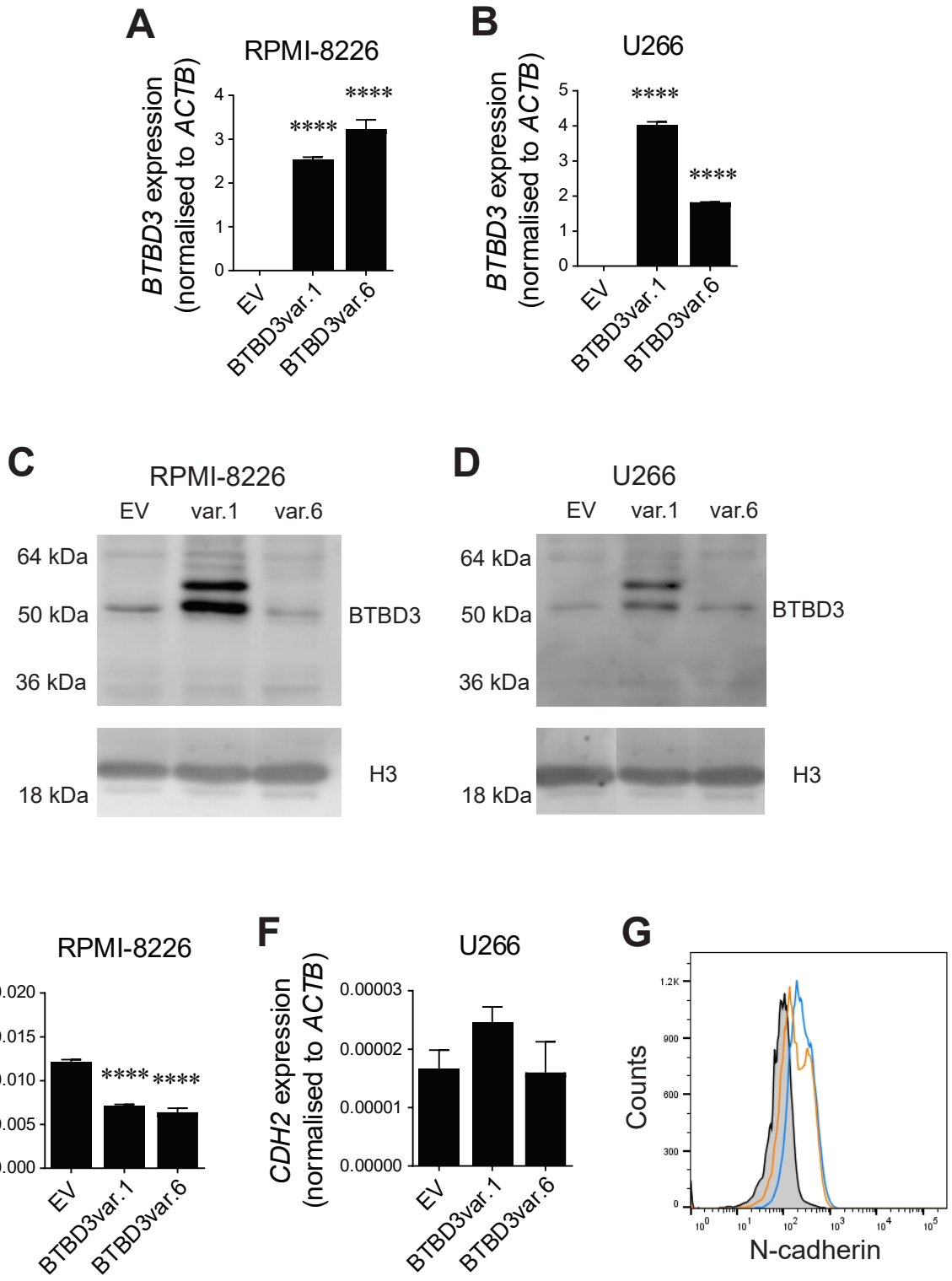
A
RPMI-8226
BTBD3 expression (normalised to ACTB)
****
****
EV
BTBD3var.1
BTBD3var.6
B
U266
BTBD3 expression (normalised to ACTB)
****
****
EV
BTBD3var.1
BTBD3var.6
C
RPMI-8226
EV
var.1
var.6
64 kDa
50 kDa
36 kDa
BTBD3
18 kDa
H3
D
U266
EV
var.1
var.6
64 kDa
50 kDa
36 kDa
BTBD3
18 kDa
H3
E
RPMI-8226
CDH2 expression (normalised to ACTB)
****
****
EV
BTBD3var.1
BTBD3var.6
F
U266
CDH2 expression (normalised to ACTB)
EV
BTBD3var.1
BTBD3var.6
G
Counts
N-cadherin

compared with the corresponding EV-containing cells (Figure 4.4C,D). Due to the limitation of the anti-BTBD3 antibody, we could not confirm over-expression of BTBD3 isoform *c* in RPMI-8226-BTBD3var.6 and U266-BTBD3var.6 cells at the protein level. qPCR revealed that *CDH2* expression was down-regulated in RPMI-8226-BTBD3var.1 and RPMI-8226-BTBD3var.6 cells, compared with RPMI-8226-EV cells (Figure 4.4E), while *CDH2* expression was un-changed in U266-BTBD3var.1 and U266-BTBD3var.6 cells, compared with U266-EV cells (Figure 4.4F). In line with the qPCR data, N-cadherin expression was also reduced in RPMI-8226-BTBD3var.1 cells compared with RPMI-8226-EV cells, as shown by flow cytometry (Figure 4.4G). Taken together, these results suggest that BTBD3 over-expression in t(4;14)$^{-}$ HMCLs does not up-regulate N-cadherin gene or protein expression.

As miR-190 is expressed in both RPMI-8226 and U266 HMCLs, it is possible that miR-190 may be preventing the up-regulation of *CDH2* in BTBD3-overexpressing t(4;14)$^{-}$ HMCLs. In order to independently investigate whether BTBD3 regulates *CDH2* expression in t(4;14)$^{-}$ MM, we performed siRNA-mediated knock-down studies using the t(4;14)$^{-}$ HMCL KMS-26 which co-expresses *BTBD3* (Supplementary Figure 4.4A) and *CDH2* (Figure 4.1A). Treatment of KMS-26 cells with *BTBD3*-targeting siRNA at days 0 and 2 resulted in a 62-68% knock-down of total *BTBD3* mRNA levels at day 4 using *BTBD3* siRNA#1 and siRNA#2, compared with KMS-26 cells treated with negative control siRNA ($P < 0.001$) (Figure 4.5A). However, *CDH2* expression was not significantly reduced at day 4 in KMS-26 cells following treatment with *BTBD3*-targeting siRNA, compared with KMS-26 cells treated with negative control siRNA (Figure 4.5B). These data demonstrate that down-regulation of *BTBD3* does not reduce *CDH2* expression in a t(4;14)$^{-}$ HMCL, suggesting that miR-190 expression is therefore unlikely to account for the inability of BTBD3 over-expression to up-regulate N-cadherin expression in t(4;14)$^{-}$ HMCLs. Taken together, these data demonstrate that BTBD3 is unlikely to be a key regulator of *CDH2* expression in t(4;14)$^{-}$ MM.

**Figure 4.5. *BTBD3* knock-down does not down-regulate *CDH2* expression in the t(4;14)$^-$ HMCL KMS-26.** Total *BTBD3* (**A**) and *CDH2* (**B**) expression in KMS-26 cells (normalised to *ACTB* expression), as assessed by qPCR, following transfection with *BTBD3*-targeting siRNA (siRNA#1, siRNA#2 and siRNA#3). Graphs depict mean ± SEM of 3-6 independent experiments. ***$P < 0.001$ compared with KMS-26 cells transfected with negative control siRNA (NC siRNA) (one-way ANOVA with Dunnett's multiple comparisons test) (**A**,**B**).

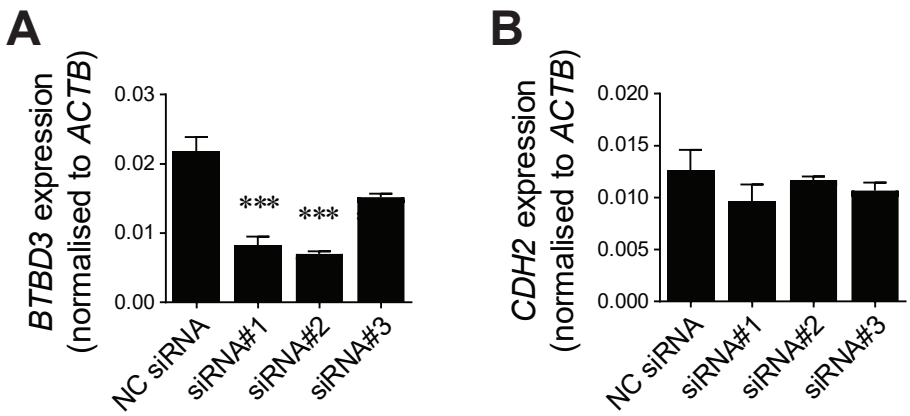
A
BTBD3 expression
(normalised to ACTB)
0.03
0.02
0.01
0.00
***
***
NC siRNA
siRNA#1
siRNA#2
siRNA#3
B
CDH2 expression
(normalised to ACTB)
0.020
0.015
0.010
0.005
0.000
NC siRNA
siRNA#1
siRNA#2
siRNA#3

## 4.5 Discussion

In the solid tumour context, N-cadherin is up-regulated by a range of extracellular stimuli (e.g. TGF-β superfamily, ligands of receptor tyrosine kinases, chemokines and extracellular matrix proteins) and is often associated with the induction of a broader epithelial-to-mesenchymal cellular transition (EMT).[74-84] These stimuli activate a number of intracellular signalling cascades which, in turn, orchestrate the activation of transcription factors Twist1 and Slug, which positively regulate N-cadherin expression.[15,74,75,78,81-83,85-103] Previous studies have also shown that the histone methyltransferase MMSET promotes EMT in prostate cancer cells, including the up-regulation of N-cadherin.[38] Similarly, expression of the N-cadherin gene, *CDH2*, is up-regulated in MM patients with the chromosomal translocation t(4;14), which leads to constitutive over-expression of MMSET and, in approximately 70% of patients, up-regulation of FGFR3.[26,41] In line with these findings, we found that *CDH2* is up-regulated in the majority of *MMSET*$^{high}$ MM patients irrespective of *FGFR3* expression, suggesting that MMSET and not FGFR3 is responsible for up-regulation of *CDH2* in these patients. Furthermore, we have demonstrated that MMSET is a *bona fide* regulator of *CDH2* expression in MM, as evidenced by the up-regulation of *CDH2* following the over-expression of *MMSET* in *MMSET*$^{low}$ MM PCs, supporting previous findings.[41] Consistent with previous studies in human prostate cancer cells[38], we demonstrated that mutation of the MMSET histone-binding domain abrogated MMSET-mediated up-regulation of *CDH2* in MM PCs, suggesting that the histone methyltransferase activity of MMSET is critical in regulating *CDH2* expression in MM. Notably, studies in human prostate cancer cells have shown that Twist1 is a direct target of MMSET. However, while MMSET-over-expression has been shown to up-regulate both Twist1 and N-cadherin expression in prostate cancer cells, siRNA-mediated knock-down of Twist1 cells in MMSET-over-expressing cells did not reduce N-cadherin expression, suggesting that MMSET may directly target the N-cadherin gene, or activate an alternate inducer of N-cadherin expression.[38]

In addition to t(4;14)$^{+}$ MM, our studies demonstrate that *CDH2* is up-regulated in another 40-45% of newly-diagnosed patients despite having *MMSET*$^{low}$ status. Previous studies have shown that *CDH2* is up-regulated in a distinct population of MM patients in the hyperdiploidy-related sub-group.[26] In line with these findings, our GSEA of genes which positively correlated with *CDH2* expression in *MMSET*$^{low}$ MM patients

revealed an enrichment in genes that are associated with a hyperdiploidy-related gene signature. Of the genes which positively correlated with *CDH2* in *MMSET*$^{low}$ MM patients, *BTBD3* was the most strongly up-regulated in MM PCs, suggesting that BTBD3 may be a candidate 'driver' of *CDH2* expression in t(4;14)$^{-}$ MM. Similar to *CDH2* expression, gene expression profiling studies have previously reported an association between *BTBD3* expression and hyperdiploidy-related MM patients subsets.[104,105] Additionally, in MM patients, *BTBD3* expression has previously been associated with elevated expression of *NCAM1*[106], which also positively correlated with *CDH2* expression in our analyses. On the basis of the observation that *BTBD3* was consistently up-regulated in *MMSET*$^{low}$*CDH2*$^{high}$ MM patients and the up-regulation of *BTBD3* in MM PCs, we hypothesized that BTBD3 may positively regulate *CDH2* expression in t(4;14)$^{-}$ MM. Collectively, however, our BTBD3 over-expression and siRNA-mediated *BTBD3* knockdown studies in t(4;14)$^{-}$ HMCLs revealed that BTBD3 is unlikely to be a key driver of *CDH2* expression in t(4;14)$^{-}$ MM patients.

Further examination of our *in silico* analyses revealed other candidates which have previously been implicated in the regulation of *CDH2* expression in other cancers. Janus kinase/signal transducer and activator 3 (JAK/STAT3) signalling is widely implicated in tumourigenesis, and has been shown to positively regulate N-cadherin expression in cancer cells.[75,81,91,93,97,107] Indeed, studies have implicated an IL-6/JAK/STAT3 signalling axis in the up-regulation of N-cadherin expression in melanoma and cancers of the pancreas, stomach, lung and ovary.[75,81,91,93,97] In MM, IL-6-mediated signalling also plays an important role in tumour cell growth and proliferation.[108-112] Notably, our *CDH2* correlative analyses identified several genes which functionally converge to participate in, or regulate, the JAK/STAT3 signalling. These include genes encoding for IL-6 signal transducer (IL6ST/gp130; *IL6ST*) and basic transcription factor 3 (BTF3; *BTF3*) (both positively correlated with *CDH2* expression) and the sphingolipid metabolism enzyme, sphingosine-1-phosphate lyase 1 (S1PL; *SGPL1*) (inversely correlated with *CDH2* expression). IL6ST is a critical signalling-transducer subunit of IL-6-family cytokine receptor complexes and has been shown to promote tumourigenesis in various cancers, including MM.[113,114] The binding of IL-6 to its cognate IL-6 receptor-IL6ST complex activates JAK, which, in turn, activates STAT3-mediated gene transcription.[107,113] BTF3 is an evolutionarily conserved transcription factor which is aberrently expressed in colorectal and prostate cancer.[115-117] In addition to promoting cancer cell proliferation, recent studies have

shown that BTF3 positively regulates expression of *CDH2* in a STAT3 signalling-dependent manner, and promotes metastasis *in vivo*.[118,119] Notably, down-regulation of *CDH2* expression following *BTF3* knock-down in gastric cancer cells was rescued following IL-6-induced activation of STAT3.[119] Studies have also shown that the loss of S1PL, which degrades the cell signalling molecule, sphingosine-1-phosphate, potentiates STAT3 signalling and promotes oncogenesis.[120-122] Thus, whether aberrant JAK/STAT3 signalling up-regulates *CDH2* expression in t(4;14)$^{-}$ MM warrants investigation.

Other genes of interest emanating from our studies include *PAK1* (p21-activated kinase-1; Pak1), *FER* (tyrosine-protein kinase Fer; Fer) and *ZNF622* (zinc finger protein 622; ZNF622) which positively correlate with *CDH2* in t(4;14)$^{-}$ MM. In concordance with our findings, studies have recently reported a positive correlation between Pak1 and N-cadherin levels in clinical samples of non-small cell lung carcinoma.[123] In prostate cancer cells, the Rac1-Pak1 signalling axis has been shown to potentiate TGF-β1-mediated up-regulation of N-cadherin, which can be suppressed by functional inhibition of Pak1.[88] Notably, Fer is an upstream mediator of Rac1-Pak1 signalling[124], suggesting a potential Fer-Rac1-Pak1-N-cadherin signalling axis may exist in MM. KRAS, mutated in approximately 20% of MM patients[3], is another activator of Rac1-Pak1 signalling in epithelial cancers[125], further implicating Rac1-Pak1 in *CDH2* regulation in MM. ZNF622 is also of interest as it binds to and activates the transcription factor B-Myb.[126] Previous studies have shown that B-Myb knock-down reduces N-cadherin expression in both glioma and breast cancer cells[127,128], suggesting that ZNF622-mediated activation of B-Myb may be another mechanism whereby *CDH2* is up-regulated in MM. To date, however, a functional role for these genes in MM has not been investigated.

Our *in silico* analysis of miRNA expression profiles revealed an 8-miRNA expression signature which was inversely associated with *CDH2* levels in newly-diagnosed t(4;14)$^{-}$ MM patients. miR-190, previously implicated in colorectal, breast and pancreatic cancer[129-131], is of particular interest as it is predicted to target the 3'-UTR of *CDH2*. Tellingly, *CDH2* expression was low or undetectable in over 90% (10 of 11) of miR-190-expressing t(4;14)$^{-}$ MM patients in our analysis, suggesting that miR-190 may suppress *CDH2* expression in these patients. *IL6ST* is also a predicted target of miR-190, suggesting miR-190 may negatively regulate IL-6/JAK/STAT3 signalling in MM. Another candidate regulator of *CDH2* expression in t(4;14)$^{-}$ MM is miR-214,

which was recently shown to negatively regulate N-cadherin expression in cervical cancer cells.[132] miR-214 is also down-regulated, and inhibits tumour cell invasion and metastasis, in several cancers including liver, bladder and colon cancer.[132-137] While not predicted to target *CDH2*, miR-339 and miR-193b may also be of interest, as down-regulation of these miRNAs is associated with increased cancer invasivness.[138-143] In addition, miR-545 is predicted to target *ZNF622*, suggesting that a miR-545/ZNF622/B-Myb axis may regulate *CDH2* expression in t(4;14)$^-$ MM. Notably, a number of other genes identified in our *CDH2* correlative analyses are also predicted to be targeted by one or more miRNAs within the 8-miRNA expression signature, including *E2F5* (E2F transcription factor 5) and *FBXO22* (F-box protein 22). While a role for these genes in *CDH2* regulation has not been demonstrated, their functional role as transcriptional regulators[144-148] and their strong correlation with *CDH2* expression in t(4;14)$^-$ MM, suggests that further investigation of their potential regulation of *CDH2* in MM is warranted.

While our studies demonstrated that BTBD3 does not regulate *CDH2* expression in HMCLs, our analyses show, for the first time, that *BTBD3* expression is strongly up-regulated in BM PCs from MM patients, compared with normal controls. Furthermore, we found that elevated *BTBD3* expression in BM MM PCs is associated with a trend towards poorer overall survival in t(4;14)$^-$ patients, suggesting a role for BTBD3 in MM pathogenesis. Structurally, BTBD3 contains an evolutionarily-conserved BTB/POZ (Broad-complex, Tramtrak, Bric-a-brac/poxvirus and zinc finger; BTB) protein-protein interaction domain at the N-terminus, a postulated substrate adaptor for cullin3 E3 ubiquitin ligase which targets proteins for proteasome-mediated degradation.[149,150] Cullin3 E3 ubiquitin ligase complexes are implicated in the destruction of a wide range of substrates including transcriptional regulators and signalling proteins, thereby regulating developmental and cancer-associated signalling pathways.[151-154] BTB domains are also found in 5-10% of $C_2H_2$-type zinc-finger transcription factors (e.g. BCL6 and PLZF) which function as transcriptional repressors by interacting with co-repressor complexes such as histone deacetylases.[155,156] Towards its C-terminus, BTBD3 also contains a BACK domain and a PHR domain which are also speculated to play a role in cullin3 E3 ubiquitin ligase function.[157,158] Thus, it is plausible that BTBD3 also functions as a repressor of gene transcription or cell signalling. While the function of BTBD3 has not been fully elucidated, BTBD3 is highly expressed in the brain[159-161] and has been implicated in dendritic field orientation within the visual cortex[162] and the

barrel cortex[161,162] in mice. In cancer, BTBD3 knock-down has been reported to decrease the migration of hepatocellular carcinoma cells *in vitro*.[163] Given our observation that *BTBD3* is strongly up-regulated in MM patients, and may be associated with poor prognosis in at least some MM patients, further studies investigating the role of BTBD3 in MM are warranted.

In summary, we have demonstrated that *MMSET*, universally dysregulated in t(4;14)$^{+}$ MM patients, is a *bona fide* regulator of *CDH2* expression in MM cells, suggesting it is a key driver of up-regulated N-cadherin in t(4;14)$^{+}$ MM. While our studies suggest that BTBD3 is unlikely to be a key driver of *CDH2* expression in t(4;14)$^{-}$ MM, we have identified several other pathways that may represent previously unknown, MMSET-independent regulators of N-cadherin expression in MM. In addition, we have identified that miR-190 is strongly associated with down-regulation of *CDH2* expression in t(4;14)$^{-}$ MM patients, which may represent an alternative mechanism of N-cadherin regulation in these patients. Finally, our studies have identified BTBD3 as a novel factor that may play a role in the pathogenesis of MM. To this end, future studies are waranted to investigate the effect of this gene on MM disease progression.

## 4.6 Acknowledgements

The authors would like to thank Prof. Jonathan Licht for providing the pRetroX-MMSET-DsRed and pRetroX-DsRed vectors, and Dr Randall Grose for assistance with flow cytometry. This research was supported by a grant from the Cancer Australia Priority-driven Collaborative Cancer Research Scheme, co-funded by the Leukaemia Foundation. Kate Vandyke was supported by a fellowship from the Multiple Myeloma Research Foundation and by a Mary Overton Early Career Research Fellowship (Royal Adelaide Hospital).

## 4.7 References

1. www.myeloma.org.au. Myeloma - a comprehensive guide. Vic, Australia; 2016.

2. Pawlyn C, Morgan GJ. Evolutionary biology of high-risk multiple myeloma. *Nat Rev Cancer*. 2017; 17(9):543-556.

3. Manier S, Salem KZ, Park J, Landau DA, Getz G, Ghobrial IM. Genomic complexity of multiple myeloma and its clinical implications. *Nat Rev Clin Oncol*. 2017; 14(2):100-113.

4. Williams EJ, Furness J, Walsh FS, Doherty P. Activation of the FGF receptor underlies neurite outgrowth stimulated by L1, N-CAM, and N-cadherin. *Neuron*. 1994; 13(3):583-594.

5. Bromberg O, Frisch BJ, Weber JM, Porter RL, Civitelli R, Calvi LM. Osteoblastic N-cadherin is not required for microenvironmental support and regulation of hematopoietic stem and progenitor cells. *Blood*. 2012; 120(2):303-313.

6. Navarro P, Ruco L, Dejana E. Differential localization of VE- and N-cadherins in human endothelial cells: VE-cadherin competes with N-cadherin for junctional localization. *J Cell Biol*. 1998; 140(6):1475-1484.

7. Charrasse S, Meriane M, Comunale F, Blangy A, Gauthier-Rouviere C. N-cadherin-dependent cell-cell contact regulates Rho GTPases and beta-catenin localization in mouse C2C12 myoblasts. *J Cell Biol*. 2002; 158(5):953-965.

8. Sabatini PJ, Zhang M, Silverman-Gavrila R, Bendeck MP, Langille BL. Homotypic and endothelial cell adhesions via N-cadherin determine polarity and regulate migration of vascular smooth muscle cells. *Circ Res*. 2008; 103(4):405-412.

9. Theveneau E, Marchant L, Kuriyama S, Gull M, Moepps B, Parsons M, Mayor R. Collective chemotaxis requires contact-dependent cell polarity. *Dev Cell*. 2010; 19(1):39-53.

10. Ouyang M, Lu S, Kim T, Chen CE, Seong J, Leckband DE, Wang F, Reynolds AB, Schwartz MA, Wang Y. N-cadherin regulates spatially polarized signals through distinct p120ctn and beta-catenin-dependent signalling pathways. *Nat Commun*. 2013; 4:1589.

11. Giampietro C, Taddei A, Corada M, Sarra-Ferraris GM, Alcalay M, Cavallaro U, Orsenigo F, Lampugnani MG, Dejana E. Overlapping and divergent signaling pathways of N-cadherin and VE-cadherin in endothelial cells. *Blood*. 2012; 119(9):2159-2170.

12. Lelievre EC, Plestant C, Boscher C, Wolff E, Mege RM, Birbes H. N-cadherin mediates neuronal cell survival through Bim down-regulation. *PLoS One*. 2012; 7(3):e33206.

13. Hay E, Nouraud A, Marie PJ. N-cadherin negatively regulates osteoblast proliferation and survival by antagonizing Wnt, ERK and PI3K/Akt signalling. *PLoS One*. 2009; 4(12):e8284.

14. Hulit J, Suyama K, Chung S, Keren R, Agiostratidou G, Shan W, Dong X, Williams TM, Lisanti MP, Knudsen K *et al*. N-cadherin signaling potentiates mammary tumor metastasis via enhanced extracellular signal-regulated kinase activation. *Cancer Res*. 2007; 67(7):3106-3116.

15. Shintani Y, Hollingsworth MA, Wheelock MJ, Johnson KR. Collagen I promotes metastasis in pancreatic cancer by activating c-Jun NH(2)-terminal kinase 1 and up-regulating N-cadherin expression. *Cancer Res*. 2006; 66(24):11745-11753.

16. Tanaka H, Kono E, Tran CP, Miyazaki H, Yamashiro J, Shimomura T, Fazli L, Wada R, Huang J, Vessella RL *et al*. Monoclonal antibody targeting of N-cadherin inhibits prostate cancer growth, metastasis and castration resistance. *Nat Med*. 2010; 16(12):1414-1420.

17. Klymenko Y, Kim O, Loughran E, Yang J, Lombard R, Alber M, Stack MS. Cadherin composition and multicellular aggregate invasion in organotypic models of epithelial ovarian cancer intraperitoneal metastasis. *Oncogene*. 2017; 36(42):5840-5851.

18. Saadatmand S, de Kruijf EM, Sajet A, Dekker-Ensink NG, van Nes JG, Putter H, Smit VT, van de Velde CJ, Liefers GJ, Kuppen PJ. Expression of cell adhesion molecules and prognosis in breast cancer. *Br J Surg*. 2013; 100(2):252-260.

19. Gravdal K, Halvorsen OJ, Haukaas SA, Akslen LA. A switch from E-cadherin to N-cadherin expression indicates epithelial to mesenchymal transition and is of strong and independent importance for the progress of prostate cancer. *Clin Cancer Res*. 2007; 13(23):7003-7011.

20. Hui L, Zhang S, Dong X, Tian D, Cui Z, Qiu X. Prognostic significance of twist and N-cadherin expression in NSCLC. *PLoS One*. 2013; 8(4):e62171.

21. Abufaraj M, Haitel A, Moschini M, Gust K, Foerster B, Ozsoy M, D'Andrea D, Karakiewicz PI, Roupret M, Briganti A *et al*. Prognostic Role of N-cadherin Expression in Patients With Invasive Bladder Cancer. *Clin Genitourin Cancer*. 2017.

22. Zhou SJ, Liu FY, Zhang AH, Liang HF, Wang Y, Ma R, Jiang YH, Sun NF. MicroRNA-199b-5p attenuates TGF-beta1-induced epithelial-mesenchymal transition in hepatocellular carcinoma. *Br J Cancer*. 2017; 117(2):233-244.

23. Zhang J, Cheng Q, Zhou Y, Wang Y, Chen X. Slug is a key mediator of hypoxia induced cadherin switch in HNSCC: correlations with poor prognosis. *Oral Oncol*. 2013; 49(11):1043-1050.

24. Okubo K, Uenosono Y, Arigami T, Yanagita S, Matsushita D, Kijima T, Amatatsu M, Uchikado Y, Kijima Y, Maemura K *et al*. Clinical significance of altering epithelial-mesenchymal transition in metastatic lymph nodes of gastric cancer. *Gastric Cancer*. 2017; 20(5):802-810.

25. Vandyke K, Chow AW, Williams SA, To LB, Zannettino AC. Circulating N-cadherin levels are a negative prognostic indicator in patients with multiple myeloma. *Br J Haematol*. 2013; 161(4):499-507.

26. Groen RW, de Rooij MF, Kocemba KA, Reijmers RM, de Haan-Kramer A, Overdijk MB, Aalders L, Rozemuller H, Martens AC, Bergsagel PL *et al*. N-cadherin-mediated interaction with multiple myeloma cells inhibits osteoblast differentiation. *Haematologica*. 2011; 96(11):1653-1661.

27. Sadler NM, Harris BR, Metzger BA, Kirshner J. N-cadherin impedes proliferation of the multiple myeloma cancer stem cells. *American journal of blood research*. 2013; 3(4):271-285.

28. Zhang B, Li M, McDonald T, Holyoake TL, Moon RT, Campana D, Shultz L, Bhatia R. Microenvironmental protection of CML stem and progenitor cells from tyrosine kinase inhibitors through N-cadherin and Wnt-beta-catenin signaling. *Blood*. 2013; 121(10):1824-1838.

29. Zhi L, Wang M, Rao Q, Yu F, Mi Y, Wang J. Enrichment of N-Cadherin and Tie2-bearing CD34+/CD38-/CD123+ leukemic stem cells by chemotherapy-resistance. *Cancer Lett*. 2010; 296(1):65-73.

30. Qiu S, Jia Y, Xing H, Yu T, Yu J, Yu P, Tang K, Tian Z, Wang H, Mi Y *et al*. N-Cadherin and Tie2 positive CD34(+)CD38(-)CD123(+) leukemic stem cell populations can develop acute myeloid leukemia more effectively in NOD/SCID mice. *Leuk Res*. 2014; 38(5):632-637.

31. Zhang B, Groffen J, Heisterkamp N. Increased resistance to a farnesyltransferase inhibitor by N-cadherin expression in Bcr/Abl-P190 lymphoblastic leukemia cells. *Leukemia*. 2007; 21(6):1189-1197.

32. Marjon KD, Termini CM, Karlen KL, Saito-Reis C, Soria CE, Lidke KA, Gillette JM. Tetraspanin CD82 regulates bone marrow homing of acute myeloid leukemia by modulating the molecular organization of N-cadherin. *Oncogene*. 2016; 35(31):4132-4140.

33. Zhi L, Gao Y, Yu C, Zhang Y, Zhang B, Yang J, Yao Z. N-Cadherin Aided in Maintaining the Characteristics of Leukemic Stem Cells. *Anat Rec (Hoboken)*. 2016; 299(7):990-998.

34. Dring AM, Davies FE, Fenton JA, Roddam PL, Scott K, Gonzalez D, Rollinson S, Rawstron AC, Rees-Unwin KS, Li C *et al*. A global expression-based analysis of the consequences of the t(4;14) translocation in myeloma. *Clin Cancer Res*. 2004; 10(17):5692-5701.

35. Keats JJ, Reiman T, Maxwell CA, Taylor BJ, Larratt LM, Mant MJ, Belch AR, Pilarski LM. In multiple myeloma, t(4;14)(p16;q32) is an adverse prognostic factor irrespective of FGFR3 expression. *Blood*. 2003; 101(4):1520-1529.

36. Bergsagel PL, Mateos MV, Gutierrez NC, Rajkumar SV, San Miguel JF. Improving overall survival and overcoming adverse prognosis in the treatment of cytogenetically high-risk multiple myeloma. *Blood*. 2013; 121(6):884-892.

37. Chesi M, Nardini E, Lim RS, Smith KD, Kuehl WM, Bergsagel PL. The t(4;14) translocation in myeloma dysregulates both FGFR3 and a novel gene, MMSET, resulting in IgH/MMSET hybrid transcripts. *Blood*. 1998; 92(9):3025-3034.

38. Ezponda T, Popovic R, Shah MY, Martinez-Garcia E, Zheng Y, Min DJ, Will C, Neri A, Kelleher NL, Yu J *et al*. The histone methyltransferase MMSET/WHSC1 activates TWIST1 to promote an epithelial-mesenchymal transition and invasive properties of prostate cancer. *Oncogene*. 2012; 32(23):2882-2890.

39. Martinez-Garcia E, Popovic R, Min DJ, Sweet SM, Thomas PM, Zamdborg L, Heffner A, Will C, Lamy L, Staudt LM *et al*. The MMSET histone methyl transferase switches global histone methylation and alters gene expression in t(4;14) multiple myeloma cells. *Blood*. 2011; 117(1):211-220.

40. Huang Z, Wu H, Chuai S, Xu F, Yan F, Englund N, Wang Z, Zhang H, Fang M, Wang Y *et al*. NSD2 is recruited through its PHD domain to oncogenic gene loci to drive multiple myeloma. *Cancer Res*. 2013; 73(20):6277-6288.

41. Lauring J, Abukhdeir AM, Konishi H, Garay JP, Gustin JP, Wang Q, Arceci RJ, Matsui W, Park BH. The multiple myeloma associated MMSET gene contributes to cellular adhesion, clonogenic growth, and tumorigenicity. *Blood*. 2008; 111(2):856-864.

42. Reme T, Hose D, Theillet C, Klein B. Modeling risk stratification in human cancer. *Bioinformatics*. 2013; 29(9):1149-1157.

43. Broyl A, Hose D, Lokhorst H, de Knegt Y, Peeters J, Jauch A, Bertsch U, Buijs A, Stevens-Kroef M, Beverloo HB *et al*. Gene expression profiling for molecular classification of multiple myeloma in newly diagnosed patients. *Blood*. 2010; 116(14):2543-2553.

44. Chapman MA, Lawrence MS, Keats JJ, Cibulskis K, Sougnez C, Schinzel AC, Harview CL, Brunet JP, Ahmann GJ, Adli M *et al*. Initial genome sequencing and analysis of multiple myeloma. *Nature*. 2011; 471(7339):467-472.

45. Hose D, Reme T, Hielscher T, Moreaux J, Messner T, Seckinger A, Benner A, Shaughnessy JD, Jr., Barlogie B, Zhou Y *et al*. Proliferation is a central independent prognostic factor and target for personalized and risk-adapted treatment in multiple myeloma. *Haematologica*. 2011; 96(1):87-95.

46. Zhan F, Huang Y, Colla S, Stewart JP, Hanamura I, Gupta S, Epstein J, Yaccoby S, Sawyer J, Burington B *et al*. The molecular classification of multiple myeloma. *Blood*. 2006; 108(6):2020-2028.

47. Kuo AJ, Cheung P, Chen K, Zee BM, Kioi M, Lauring J, Xi Y, Park BH, Shi X, Garcia BA *et al*. NSD2 links dimethylation of histone H3 at lysine 36 to oncogenic programming. *Mol Cell*. 2011; 44(4):609-620.

48. Vandyke K, Zeissig MN, Hewett DR, Martin SK, Mrozik KM, Cheong CM, Diamond P, To LB, Gronthos S, Peet DJ *et al*. HIF-2alpha Promotes Dissemination of Plasma Cells in Multiple Myeloma by Regulating CXCL12/CXCR4 and CCR1. *Cancer Res*. 2017; 77(20):5452-5463.

49. Noll JE, Vandyke K, Hewett DR, Mrozik KM, Bala RJ, Williams SA, Kok CH, Zannettino AC. PTTG1 expression is associated with hyperproliferative disease and poor prognosis in multiple myeloma. *J Hematol Oncol*. 2015; 8:106.

50. Cheong CM, Chow AW, Fitter S, Hewett DR, Martin SK, Williams SA, To LB, Zannettino AC, Vandyke K. Tetraspanin 7 (TSPAN7) expression is upregulated in multiple myeloma patients and inhibits myeloma tumour development in vivo. *Exp Cell Res*. 2015; 332(1):24-38.

51. Gutierrez NC, Sarasquete ME, Misiewicz-Krzeminska I, Delgado M, De Las Rivas J, Ticona FV, Ferminan E, Martin-Jimenez P, Chillon C, Risueno A *et al*. Deregulation of microRNA expression in the different genetic subtypes of multiple myeloma and correlation with gene expression profiling. *Leukemia*. 2010; 24(3):629-637.

52. Liberzon A, Birger C, Thorvaldsdottir H, Ghandi M, Mesirov JP, Tamayo P. The Molecular Signatures Database (MSigDB) hallmark gene set collection. *Cell Syst*. 2015; 1(6):417-425.

53. Agarwal V, Bell GW, Nam JW, Bartel DP. Predicting effective microRNA target sites in mammalian mRNAs. *Elife*. 2015; 4.

54. Krek A, Grun D, Poy MN, Wolf R, Rosenberg L, Epstein EJ, MacMenamin P, da Piedade I, Gunsalus KC, Stoffel M *et al*. Combinatorial microRNA target predictions. *Nat Genet*. 2005; 37(5):495-500.

55. Wong N, Wang X. miRDB: an online resource for microRNA target prediction and functional annotations. *Nucleic Acids Res*. 2015; 43(Database issue):D146-152.

56. Zhang X, Fitzsimmons RL, Cleland LG, Ey PL, Zannettino AC, Farmer EA, Sincock P, Mayrhofer G. CD36/fatty acid translocase in rats: distribution, isolation from hepatocytes, and comparison with the scavenger receptor SR-B1. *Lab Invest*. 2003; 83(3):317-332.

57. Livak KJ, Schmittgen TD. Analysis of relative gene expression data using real-time quantitative PCR and the 2(-Delta Delta C(T)) Method. *Methods*. 2001; 25(4):402-408.

58. Noll JE, Hewett DR, Williams SA, Vandyke K, Kok C, To LB, Zannettino AC. SAMSN1 is a tumor suppressor gene in multiple myeloma. *Neoplasia*. 2014; 16(7):572-585.

59. Isenmann S, Arthur A, Zannettino AC, Turner JL, Shi S, Glackin CA, Gronthos S. TWIST family of basic helix-loop-helix transcription factors mediate human mesenchymal stem cell growth and commitment. *Stem Cells*. 2009; 27(10):2457-2468.

60. Weber K, Bartsch U, Stocking C, Fehse B. A multicolor panel of novel lentiviral "gene ontology" (LeGO) vectors for functional gene analysis. *Mol Ther*. 2008; 16(4):698-706.

61. Smyth GK. Linear models and empirical bayes methods for assessing differential expression in microarray experiments. *Stat Appl Genet Mol Biol*. 2004; 3:Article3.

62. Saeed AI, Sharov V, White J, Li J, Liang W, Bhagabati N, Braisted J, Klapa M, Currier T, Thiagarajan M *et al*. TM4: a free, open-source system for microarray data management and analysis. *Biotechniques*. 2003; 34(2):374-378.

63. Mudduluru G, Abba M, Batliner J, Patil N, Scharp M, Lunavat TR, Leupold JH, Oleksiuk O, Juraeva D, Thiele W *et al*. A Systematic Approach to Defining the microRNA Landscape in Metastasis. *Cancer Res*. 2015; 75(15):3010-3019.

64. Meng Z, Fu X, Chen X, Zeng S, Tian Y, Jove R, Xu R, Huang W. miR-194 is a marker of hepatic epithelial cells and suppresses metastasis of liver cancer cells in mice. *Hepatology*. 2010; 52(6):2148-2157.

65. Suzuki T, Mizutani K, Minami A, Nobutani K, Kurita S, Nagino M, Shimono Y, Takai Y. Suppression of the TGF-beta1-induced protein expression of SNAI1 and N-cadherin by miR-199a. *Genes Cells*. 2014; 19(9):667-675.

66. Mo D, Yang D, Xiao X, Sun R, Huang L, Xu J. MiRNA-145 suppresses lung adenocarcinoma cell invasion and migration by targeting N-cadherin. *Biotechnol Lett*. 2017; 39(5):701-710.

67. Ma T, Zhao Y, Wei K, Yao G, Pan C, Liu B, Xia Y, He Z, Qi X, Li Z *et al*. MicroRNA-124 Functions as a Tumor Suppressor by Regulating CDH2 and Epithelial-Mesenchymal Transition in Non-Small Cell Lung Cancer. *Cell Physiol Biochem*. 2016; 38(4):1563-1574.

68. Dong P, Kaneuchi M, Watari H, Sudo S, Sakuragi N. MicroRNA-106b modulates epithelial-mesenchymal transition by targeting TWIST1 in invasive endometrial cancer cell lines. *Mol Carcinog*. 2014; 53(5):349-359.

69. Li LZ, Zhang CZ, Liu LL, Yi C, Lu SX, Zhou X, Zhang ZJ, Peng YH, Yang YZ, Yun JP. miR-720 inhibits tumor invasion and migration in breast cancer by targeting TWIST1. *Carcinogenesis*. 2014; 35(2):469-478.

70. Li W, Jiang G, Zhou J, Wang H, Gong Z, Zhang Z, Min K, Zhu H, Tan Y. Down-regulation of miR-140 induces EMT and promotes invasion by targeting Slug in esophageal cancer. *Cell Physiol Biochem*. 2014; 34(5):1466-1476.

71. Zhou JN, Zeng Q, Wang HY, Zhang B, Li ST, Nan X, Cao N, Fu CJ, Yan XL, Jia YL *et al*. MicroRNA-125b attenuates epithelial-mesenchymal transitions and targets stem-like liver cancer cells through small mothers against decapentaplegic 2 and 4. *Hepatology*. 2015; 62(3):801-815.

72. Qiao P, Li G, Bi W, Yang L, Yao L, Wu D. microRNA-34a inhibits epithelial mesenchymal transition in human cholangiocarcinoma by targeting Smad4 through transforming growth factor-beta/Smad pathway. *BMC Cancer*. 2015; 15:469.

73. Yang Y, Liu L, Cai J, Wu J, Guan H, Zhu X, Yuan J, Chen S, Li M. Targeting Smad2 and Smad3 by miR-136 suppresses metastasis-associated traits of lung adenocarcinoma cells. *Oncol Res*. 2013; 21(6):345-352.

74. Shiota M, Zardan A, Takeuchi A, Kumano M, Beraldi E, Naito S, Zoubeidi A, Gleave ME. Clusterin mediates TGF-beta-induced epithelial-mesenchymal transition and metastasis via Twist1 in prostate cancer cells. *Cancer Res*. 2012; 72(20):5261-5272.

75. Colomiere M, Ward AC, Riley C, Trenerry MK, Cameron-Smith D, Findlay J, Ackland L, Ahmed N. Cross talk of signals between EGFR and IL-6R through JAK2/STAT3 mediate epithelial-mesenchymal transition in ovarian carcinomas. *Br J Cancer*. 2009; 100(1):134-144.

76. Liao G, Wang M, Ou Y, Zhao Y. IGF-1-induced epithelial-mesenchymal transition in MCF-7 cells is mediated by MUC1. *Cell Signal*. 2014; 26(10):2131-2137.

77. Nagai T, Arao T, Furuta K, Sakai K, Kudo K, Kaneda H, Tamura D, Aomatsu K, Kimura H, Fujita Y *et al*. Sorafenib inhibits the hepatocyte growth factor-mediated epithelial mesenchymal transition in hepatocellular carcinoma. *Molecular cancer therapeutics*. 2011; 10(1):169-177.

78. Hu TH, Yao Y, Yu S, Han LL, Wang WJ, Guo H, Tian T, Ruan ZP, Kang XM, Wang J *et al*. SDF-1/CXCR4 promotes epithelial-mesenchymal transition and progression of colorectal cancer by activation of the Wnt/beta-catenin signaling pathway. *Cancer Lett*. 2014; 354(2):417-426.

79. Zhang L, Wang D, Li Y, Liu Y, Xie X, Wu Y, Zhou Y, Ren J, Zhang J, Zhu H *et al*. CCL21/CCR7 Axis Contributed to CD133+ Pancreatic Cancer Stem-Like Cell Metastasis via EMT and Erk/NF-kappaB Pathway. *PLoS One*. 2016; 11(8):e0158529.

80. Song FN, Duan M, Liu LZ, Wang ZC, Shi JY, Yang LX, Zhou J, Fan J, Gao Q, Wang XY. RANKL promotes migration and invasion of hepatocellular carcinoma cells via NF-kappaB-mediated epithelial-mesenchymal transition. *PLoS One*. 2014; 9(9):e108507.

81. Na YR, Lee JS, Lee SJ, Seok SH. Interleukin-6-induced Twist and N-cadherin enhance melanoma cell metastasis. *Melanoma Res*. 2013; 23(6):434-443.

82. Wu Y, Ginther C, Kim J, Mosher N, Chung S, Slamon D, Vadgama JV. Expression of Wnt3 activates Wnt/beta-catenin pathway and promotes EMT-like phenotype in trastuzumab-resistant HER2-overexpressing breast cancer cells. *Mol Cancer Res*. 2012; 10(12):1597-1606.

83. Shintani Y, Fukumoto Y, Chaika N, Svoboda R, Wheelock MJ, Johnson KR. Collagen I-mediated up-regulation of N-cadherin requires cooperative signals from integrins and discoidin domain receptor 1. *J Cell Biol*. 2008; 180(6):1277-1289.

84. Zhang L, Huang G, Li X, Zhang Y, Jiang Y, Shen J, Liu J, Wang Q, Zhu J, Feng X *et al*. Hypoxia induces epithelial-mesenchymal transition via activation of SNAI1 by hypoxia-inducible factor -1alpha in hepatocellular carcinoma. *BMC Cancer*. 2013; 13:108.

85. Yang H, Wang L, Zhao J, Chen Y, Lei Z, Liu X, Xia W, Guo L, Zhang HT. TGF-beta-activated SMAD3/4 complex transcriptionally upregulates N-cadherin expression in non-small cell lung cancer. *Lung Cancer*. 2015; 87(3):249-257.

86. Park MK, You HJ, Lee HJ, Kang JH, Oh SH, Kim SY, Lee CH. Transglutaminase-2 induces N-cadherin expression in TGF-beta1-induced epithelial mesenchymal transition via c-Jun-N-terminal kinase activation by protein phosphatase 2A down-regulation. *Eur J Cancer*. 2013; 49(7):1692-1705.

87. Brandl M, Seidler B, Haller F, Adamski J, Schmid RM, Saur D, Schneider G. IKK(alpha) controls canonical TGF(ss)-SMAD signaling to regulate genes expressing SNAIL and SLUG during EMT in panc1 cells. *J Cell Sci*. 2010; 123(Pt 24):4231-4239.

88. Al-Azayzih A, Gao F, Somanath PR. P21 activated kinase-1 mediates transforming growth factor beta1-induced prostate cancer cell epithelial to mesenchymal transition. *Biochim Biophys Acta*. 2015; 1853(5):1229-1239.

89. Zhao JH, Luo Y, Jiang YG, He DL, Wu CT. Knockdown of beta-Catenin through shRNA cause a reversal of EMT and metastatic phenotypes induced by HIF-1alpha. *Cancer investigation*. 2011; 29(6):377-382.

90. Shin S, Im HJ, Kwon YJ, Ye DJ, Baek HS, Kim D, Choi HK, Chun YJ. Human steroid sulfatase induces Wnt/beta-catenin signaling and epithelial-mesenchymal transition by upregulating Twist1 and HIF-1alpha in human prostate and cervical cancer cells. *Oncotarget*. 2017; 8(37):61604-61617.

91. Liu XL, Zhang XT, Meng J, Zhang HF, Zhao Y, Li C, Sun Y, Mei QB, Zhang F, Zhang T. ING5 knockdown enhances migration and invasion of lung cancer cells by inducing EMT via EGFR/PI3K/Akt and IL-6/STAT3 signaling pathways. *Oncotarget*. 2017; 8(33):54265-54276.

92. Li B, Xu WW, Lam AKY, Wang Y, Hu HF, Guan XY, Qin YR, Saremi N, Tsao SW, He QY *et al*. Significance of PI3K/AKT signaling pathway in metastasis of esophageal squamous cell carcinoma and its potential as a target for anti-metastasis therapy. *Oncotarget*. 2017; 8(24):38755-38766.

93. Meng J, Zhang XT, Liu XL, Fan L, Li C, Sun Y, Liang XH, Wang JB, Mei QB, Zhang F *et al*. WSTF promotes proliferation and invasion of lung cancer cells by inducing EMT via PI3K/Akt and IL-6/STAT3 signaling pathways. *Cell Signal*. 2016; 28(11):1673-1682.

94. Tsubaki M, Komai M, Fujimoto S, Itoh T, Imano M, Sakamoto K, Shimaoka H, Takeda T, Ogawa N, Mashimo K *et al*. Activation of NF-kappaB by the RANKL/RANK system up-regulates snail and twist expressions and induces epithelial-

to-mesenchymal transition in mammary tumor cell lines. *J Exp Clin Cancer Res*. 2013; 32:62.

95. Cheng ZX, Sun B, Wang SJ, Gao Y, Zhang YM, Zhou HX, Jia G, Wang YW, Kong R, Pan SH *et al*. Nuclear factor-kappaB-dependent epithelial to mesenchymal transition induced by HIF-1alpha activation in pancreatic cancer cells under hypoxic conditions. *PLoS One*. 2011; 6(8):e23752.

96. Takeuchi A, Shiota M, Beraldi E, Thaper D, Takahara K, Ibuki N, Pollak M, Cox ME, Naito S, Gleave ME *et al*. Insulin-like growth factor-I induces CLU expression through Twist1 to promote prostate cancer growth. *Mol Cell Endocrinol*. 2014; 384(1-2):117-125.

97. Wu YS, Chung I, Wong WF, Masamune A, Sim MS, Looi CY. Paracrine IL-6 signaling mediates the effects of pancreatic stellate cells on epithelial-mesenchymal transition via Stat3/Nrf2 pathway in pancreatic cancer cells. *Biochim Biophys Acta*. 2017; 1861(2):296-306.

98. Yoon C, Cho SJ, Chang KK, Park DJ, Ryeom SW, Yoon SS. Role of Rac1 Pathway in Epithelial-to-Mesenchymal Transition and Cancer Stem-like Cell Phenotypes in Gastric Adenocarcinoma. *Mol Cancer Res*. 2017; 15(8):1106-1116.

99. Mody HR, Hung SW, Naidu K, Lee H, Gilbert CA, Hoang TT, Pathak RK, Manoharan R, Muruganandan S, Govindarajan R. SET contributes to the epithelial-mesenchymal transition of pancreatic cancer. *Oncotarget*. 2017; 8(40):67966-67979.

100. Cho KH, Choi MJ, Jeong KJ, Kim JJ, Hwang MH, Shin SC, Park CG, Lee HY. A ROS/STAT3/HIF-1alpha signaling cascade mediates EGF-induced TWIST1 expression and prostate cancer cell invasion. *Prostate*. 2014; 74(5):528-536.

101. Alexander NR, Tran NL, Rekapally H, Summers CE, Glackin C, Heimark RL. N-cadherin gene expression in prostate carcinoma is modulated by integrin-dependent nuclear translocation of Twist1. *Cancer Res*. 2006; 66(7):3365-3369.

102. Qi Y, Wang N, He Y, Zhang J, Zou H, Zhang W, Gu W, Huang Y, Lian X, Hu J *et al*. Transforming growth factor-beta1 signaling promotes epithelial-mesenchymal transition-like phenomena, cell motility, and cell invasion in synovial sarcoma cells. *PLoS One*. 2017; 12(8):e0182680.

103. Liu CC, Cai DL, Sun F, Wu ZH, Yue B, Zhao SL, Wu XS, Zhang M, Zhu XW, Peng ZH *et al*. FERMT1 mediates epithelial-mesenchymal transition to promote colon cancer metastasis via modulation of beta-catenin transcriptional activity. *Oncogene*. 2017; 36(13):1779-1792.

104. Agnelli L, Bicciato S, Mattioli M, Fabris S, Intini D, Verdelli D, Baldini L, Morabito F, Callea V, Lombardi L *et al*. Molecular classification of multiple myeloma: a distinct transcriptional profile characterizes patients expressing CCND1 and negative for 14q32 translocations. *J Clin Oncol*. 2005; 23(29):7296-7306.

105. Li Y, Wang X, Zheng H, Wang C, Minvielle S, Magrangeas F, Avet-Loiseau H, Shah PK, Zhang Y, Munshi NC *et al*. Classify hyperdiploidy status of multiple myeloma patients using gene expression profiles. *PLoS One*. 2013; 8(3):e58809.

106. Damgaard T, Knudsen LM, Dahl IM, Gimsing P, Lodahl M, Rasmussen T. Regulation of the CD56 promoter and its association with proliferation, anti-apoptosis and clinical factors in multiple myeloma. *Leuk Lymphoma*. 2009; 50(2):236-246.

107. Yu H, Lee H, Herrmann A, Buettner R, Jove R. Revisiting STAT3 signalling in cancer: new and unexpected biological functions. *Nat Rev Cancer*. 2014; 14(11):736-746.

108. Zhang XG, Klein B, Bataille R. Interleukin-6 is a potent myeloma-cell growth factor in patients with aggressive multiple myeloma. *Blood*. 1989; 74(1):11-13.

109. Ogata A, Chauhan D, Urashima M, Teoh G, Treon SP, Anderson KC. Blockade of mitogen-activated protein kinase cascade signaling in interleukin 6-independent multiple myeloma cells. *Clin Cancer Res*. 1997; 3(6):1017-1022.

110. Chauhan D, Uchiyama H, Akbarali Y, Urashima M, Yamamoto K, Libermann TA, Anderson KC. Multiple myeloma cell adhesion-induced interleukin-6 expression in bone marrow stromal cells involves activation of NF-kappa B. *Blood*. 1996; 87(3):1104-1112.

111. Puthier D, Bataille R, Amiot M. IL-6 up-regulates mcl-1 in human myeloma cells through JAK / STAT rather than ras / MAP kinase pathway. *Eur J Immunol*. 1999; 29(12):3945-3950.

112. Klein B, Zhang XG, Lu ZY, Bataille R. Interleukin-6 in human multiple myeloma. *Blood*. 1995; 85(4):863-872.

113. Xu S, Neamati N. gp130: a promising drug target for cancer therapy. *Expert Opin Ther Targets*. 2013; 17(11):1303-1328.

114. Dechow T, Steidle S, Gotze KS, Rudelius M, Behnke K, Pechloff K, Kratzat S, Bullinger L, Fend F, Soberon V *et al*. GP130 activation induces myeloma and collaborates with MYC. *J Clin Invest*. 2014; 124(12):5263-5274.

115. Zheng XM, Black D, Chambon P, Egly JM. Sequencing and expression of complementary DNA for the general transcription factor BTF3. *Nature*. 1990; 344(6266):556-559.

116. Wang CJ, Franbergh-Karlson H, Wang DW, Arbman G, Zhang H, Sun XF. Clinicopathological significance of BTF3 expression in colorectal cancer. *Tumour Biol*. 2013; 34(4):2141-2146.

117. Symes AJ, Eilertsen M, Millar M, Nariculam J, Freeman A, Notara M, Feneley MR, Patel HR, Masters JR, Ahmed A. Quantitative analysis of BTF3, HINT1, NDRG1 and ODC1 protein over-expression in human prostate cancer tissue. *PLoS One*. 2013; 8(12):e84295.

118. Liu Q, Zhou JP, Li B, Huang ZC, Dong HY, Li GY, Zhou K, Nie SL. Basic transcription factor 3 is involved in gastric cancer development and progression. *World J Gastroenterol*. 2013; 19(28):4495-4503.

119. Zhang DZ, Chen BH, Zhang LF, Cheng MK, Fang XJ, Wu XJ. Basic Transcription Factor 3 Is Required for Proliferation and Epithelial-Mesenchymal Transition via Regulation of FOXM1 and JAK2/STAT3 Signaling in Gastric Cancer. *Oncol Res*. 2017; 25(9):1453-1462.

120. Degagne E, Pandurangan A, Bandhuvula P, Kumar A, Eltanawy A, Zhang M, Yoshinaga Y, Nefedov M, de Jong PJ, Fong LG *et al*. Sphingosine-1-phosphate lyase downregulation promotes colon carcinogenesis through STAT3-activated microRNAs. *J Clin Invest*. 2014; 124(12):5368-5384.

121. Brizuela L, Ader I, Mazerolles C, Bocquet M, Malavaud B, Cuvillier O. First evidence of sphingosine 1-phosphate lyase protein expression and activity downregulation in human neoplasm: implication for resistance to therapeutics in prostate cancer. *Molecular cancer therapeutics*. 2012; 11(9):1841-1851.

122. Colie S, Van Veldhoven PP, Kedjouar B, Bedia C, Albinet V, Sorli SC, Garcia V, Djavaheri-Mergny M, Bauvy C, Codogno P *et al*. Disruption of sphingosine 1-phosphate lyase confers resistance to chemotherapy and promotes oncogenesis through Bcl-2/Bcl-xL upregulation. *Cancer Res*. 2009; 69(24):9346-9353.

123. Yang Z, Wang H, Xia L, Oyang L, Zhou Y, Zhang B, Chen X, Luo X, Liao Q, Liang J. Overexpression of PAK1 Correlates with Aberrant Expression of EMT Markers and Poor Prognosis in Non-Small Cell Lung Cancer. *J Cancer*. 2017; 8(8):1484-1491.

124. Fan G, Nicholas N. FER mediated HGF-independent regulation of HGFR/MET activates RAC1-PAK1 pathway to potentiate metastasis in ovarian cancer. *Small GTPases*. 2017:0.

125. Mortazavi F, Lu J, Phan R, Lewis M, Trinidad K, Aljilani A, Pezeshkpour G, Tamanoi F. Significance of KRAS/PAK1/Crk pathway in non-small cell lung cancer oncogenesis. *BMC Cancer*. 2015; 15:381.

126. Seong HA, Kim KT, Ha H. Enhancement of B-MYB transcriptional activity by ZPR9, a novel zinc finger protein. *J Biol Chem*. 2003; 278(11):9655-9662.

127. Zhang X, Lv QL, Huang YT, Zhang LH, Zhou HH. Akt/FoxM1 signaling pathway-mediated upregulation of MYBL2 promotes progression of human glioma. *J Exp Clin Cancer Res*. 2017; 36(1):105.

128. Tao D, Pan Y, Jiang G, Lu H, Zheng S, Lin H, Cao F. B-Myb regulates snail expression to promote epithelial-to-mesenchymal transition and invasion of breast cancer cell. *Med Oncol*. 2015; 32(1):412.

129. Gaedcke J, Grade M, Camps J, Sokilde R, Kaczkowski B, Schetter AJ, Difilippantonio MJ, Harris CC, Ghadimi BM, Moller S *et al*. The rectal cancer

microRNAome--microRNA expression in rectal cancer and matched normal mucosa. *Clin Cancer Res*. 2012; 18(18):4919-4930.

130. Lowery AJ, Miller N, Devaney A, McNeill RE, Davoren PA, Lemetre C, Benes V, Schmidt S, Blake J, Ball G *et al*. MicroRNA signatures predict oestrogen receptor, progesterone receptor and HER2/neu receptor status in breast cancer. *Breast Cancer Res*. 2009; 11(3):R27.

131. Zhang Y, Li M, Wang H, Fisher WE, Lin PH, Yao Q, Chen C. Profiling of 95 microRNAs in pancreatic cancer cell lines and surgical specimens by real-time PCR analysis. *World J Surg*. 2009; 33(4):698-709.

132. Wang JM, Ju BH, Pan CJ, Gu Y, Li MQ, Sun L, Xu YY, Yin LR. MiR-214 inhibits cell migration, invasion and promotes the drug sensitivity in human cervical cancer by targeting FOXM1. *Am J Transl Res*. 2017; 9(8):3541-3557.

133. Wang P, Chen S, Fang H, Wu X, Chen D, Peng L, Gao Z, Xie C. miR-214/199a/199a* cluster levels predict poor survival in hepatocellular carcinoma through interference with cell-cycle regulators. *Oncotarget*. 2016; 7(1):929-945.

134. Wang J, Zhang X, Wang L, Yang Y, Dong Z, Wang H, Du L, Wang C. MicroRNA-214 suppresses oncogenesis and exerts impact on prognosis by targeting PDRG1 in bladder cancer. *PLoS One*. 2015; 10(2):e0118086.

135. Long LM, He BF, Huang GQ, Guo YH, Liu YS, Huo JR. microRNA-214 functions as a tumor suppressor in human colon cancer via the suppression of ADP-ribosylation factor-like protein 2. *Oncol Lett*. 2015; 9(2):645-650.

136. He GY, Hu JL, Zhou L, Zhu XH, Xin SN, Zhang D, Lu GF, Liao WT, Ding YQ, Liang L. The FOXD3/miR-214/MED19 axis suppresses tumour growth and metastasis in human colorectal cancer. *Br J Cancer*. 2016; 115(11):1367-1378.

137. Li B, Han Q, Zhu Y, Yu Y, Wang J, Jiang X. Down-regulation of miR-214 contributes to intrahepatic cholangiocarcinoma metastasis by targeting Twist. *FEBS J*. 2012; 279(13):2393-2398.

138. Zhou C, Liu G, Wang L, Lu Y, Yuan L, Zheng L, Chen F, Peng F, Li X. MiR-339-5p regulates the growth, colony formation and metastasis of colorectal cancer cells by targeting PRL-1. *PLoS One*. 2013; 8(5):e63142.

139. Wu ZS, Wu Q, Wang CQ, Wang XN, Wang Y, Zhao JJ, Mao SS, Zhang GH, Zhang N, Xu XC. MiR-339-5p inhibits breast cancer cell migration and invasion in vitro and may be a potential biomarker for breast cancer prognosis. *BMC Cancer*. 2010; 10:542.

140. Li Y, Zhao W, Bao P, Li C, Ma XQ, Li Y, Chen LA. miR-339-5p inhibits cell migration and invasion in vitro and may be associated with the tumor-node-metastasis staging and lymph node metastasis of non-small cell lung cancer. *Oncol Lett*. 2014; 8(2):719-725.

141. Li XF, Yan PJ, Shao ZM. Downregulation of miR-193b contributes to enhance urokinase-type plasminogen activator (uPA) expression and tumor progression and invasion in human breast cancer. *Oncogene*. 2009; 28(44):3937-3948.

142. Xu C, Liu S, Fu H, Li S, Tie Y, Zhu J, Xing R, Jin Y, Sun Z, Zheng X. MicroRNA-193b regulates proliferation, migration and invasion in human hepatocellular carcinoma cells. *Eur J Cancer*. 2010; 46(15):2828-2836.

143. Li J, Kong F, Wu K, Song K, He J, Sun W. miR-193b directly targets STMN1 and uPA genes and suppresses tumor growth and metastasis in pancreatic cancer. *Mol Med Rep*. 2014; 10(5):2613-2620.

144. Donzelli S, Fontemaggi G, Fazi F, Di Agostino S, Padula F, Biagioni F, Muti P, Strano S, Blandino G. MicroRNA-128-2 targets the transcriptional repressor E2F5 enhancing mutant p53 gain of function. *Cell Death Differ*. 2012; 19(6):1038-1048.

145. Chen CR, Kang Y, Siegel PM, Massague J. E2F4/5 and p107 as Smad cofactors linking the TGFbeta receptor to c-myc repression. *Cell*. 2002; 110(1):19-32.

146. Pierce AM, Schneider-Broussard R, Philhower JL, Johnson DG. Differential activities of E2F family members: unique functions in regulating transcription. *Mol Carcinog*. 1998; 22(3):190-198.

147. Tan MK, Lim HJ, Harper JW. SCF(FBXO22) regulates histone H3 lysine 9 and 36 methylation levels by targeting histone demethylase KDM4A for ubiquitin-mediated proteasomal degradation. *Mol Cell Biol*. 2011; 31(18):3687-3699.

148. Tian X, Dai S, Sun J, Jin G, Jiang S, Meng F, Li Y, Wu D, Jiang Y. F-box protein FBXO22 mediates polyubiquitination and degradation of KLF4 to promote hepatocellular carcinoma progression. *Oncotarget*. 2015; 6(26):22767-22775.

149. Geyer R, Wee S, Anderson S, Yates J, Wolf DA. BTB/POZ domain proteins are putative substrate adaptors for cullin 3 ubiquitin ligases. *Mol Cell*. 2003; 12(3):783-790.

150. Xu L, Wei Y, Reboul J, Vaglio P, Shin TH, Vidal M, Elledge SJ, Harper JW. BTB proteins are substrate-specific adaptors in an SCF-like modular ubiquitin ligase containing CUL-3. *Nature*. 2003; 425(6955):316-321.

151. Genschik P, Sumara I, Lechner E. The emerging family of CULLIN3-RING ubiquitin ligases (CRL3s): cellular functions and disease implications. *Embo J*. 2013; 32(17):2307-2320.

152. Pae J, Cinalli RM, Marzio A, Pagano M, Lehmann R. GCL and CUL3 Control the Switch between Cell Lineages by Mediating Localized Degradation of an RTK. *Dev Cell*. 2017; 42(2):130-142 e137.

153. Pintard L, Willems A, Peter M. Cullin-based ubiquitin ligases: Cul3-BTB complexes join the family. *Embo J*. 2004; 23(8):1681-1687.

154. Chen HY, Chen RH. Cullin 3 Ubiquitin Ligases in Cancer Biology: Functions and Therapeutic Implications. *Front Oncol*. 2016; 6:113.

155. Collins T, Stone JR, Williams AJ. All in the family: the BTB/POZ, KRAB, and SCAN domains. *Mol Cell Biol*. 2001; 21(11):3609-3615.

156. Wong CW, Privalsky ML. Components of the SMRT corepressor complex exhibit distinctive interactions with the POZ domain oncoproteins PLZF, PLZF-RARalpha, and BCL-6. *J Biol Chem*. 1998; 273(42):27695-27702.

157. Stogios PJ, Prive GG. The BACK domain in BTB-kelch proteins. *Trends Biochem Sci*. 2004; 29(12):634-637.

158. Sampathkumar P, Ozyurt SA, Miller SA, Bain KT, Rutter ME, Gheyi T, Abrams B, Wang Y, Atwell S, Luz JG *et al*. Structures of PHR domains from Mus musculus Phr1 (Mycbp2) explain the loss-of-function mutation (Gly1092-->Glu) of the C. elegans ortholog RPM-1. *J Mol Biol*. 2010; 397(4):883-892.

159. Schonrock N, Humphreys DT, Preiss T, Gotz J. Target gene repression mediated by miRNAs miR-181c and miR-9 both of which are down-regulated by amyloid-beta. *J Mol Neurosci*. 2012; 46(2):324-335.

160. Mashiko H, Yoshida AC, Kikuchi SS, Niimi K, Takahashi E, Aruga J, Okano H, Shimogori T. Comparative anatomy of marmoset and mouse cortex from genomic expression. *J Neurosci*. 2012; 32(15):5039-5053.

161. Wang CF, Hsing HW, Zhuang ZH, Wen MH, Chang WJ, Briz CG, Nieto M, Shyu BC, Chou SJ. Lhx2 Expression in Postmitotic Cortical Neurons Initiates Assembly of the Thalamocortical Somatosensory Circuit. *Cell Rep*. 2017; 18(4):849-856.

162. Matsui A, Tran M, Yoshida AC, Kikuchi SS, U M, Ogawa M, Shimogori T. BTBD3 controls dendrite orientation toward active axons in mammalian neocortex. *Science*. 2013; 342(6162):1114-1118.

163. Xiao W, Zhao W, Li L, Wu Q, Zhu L, Zhang Q, Dai W, Wang Y, Zhang B. Preliminary investigation of the role of BTB domain-containing 3 gene in the proliferation and metastasis of hepatocellular carcinoma. *Oncol Lett*. 2017; 14(2):2505-2510.

**Supplementary Figure 4.1. *MMSET* and *FGFR3* expression in MM patients**. Newly-diagnosed MM patients were categorised as *MMSET*$^{low}$ or *MMSET*$^{high}$, and *FGFR3*$^{low}$ or *FGFR3*$^{high}$, based on their expression of *MMSET*/*NSD2* (209053_s_at) and *FGFR3* (204379_s_at) in CD138-selected BM MM PCs, as determined by microarray analysis. The cut-off (grey line) used to delineate high and low *MMSET* and *FGFR3* expression is shown for microarray datasets GSE4581 (*MMSET*$^{high}$/*FGFR3*$^{high}$, n = 55 patients; *MMSET*$^{high}$/*FGFR3*$^{low}$, n = 19; *MMSET*$^{low}$, n = 340), E-MTAB-363 (*MMSET*$^{high}$/*FGFR3*$^{high}$, n = 15; *MMSET*$^{high}$/*FGFR3*$^{low}$, n = 4; *MMSET*$^{low}$, n = 136), E-GEOD-19784 (*MMSET*$^{high}$/*FGFR3*$^{high}$, n = 23; *MMSET*$^{high}$/*FGFR3*$^{low}$, n = 12; *MMSET*$^{low}$, n = 293), E-MTAB-317 (*MMSET*$^{high}$/*FGFR3*$^{high}$, n = 26; *MMSET*$^{high}$/*FGFR3*$^{low}$, n = 8; *MMSET*$^{low}$, n = 192), E-GEOD-26863 (*MMSET*$^{high}$/*FGFR3*$^{high}$, n = 24; *MMSET*$^{high}$/*FGFR3*$^{low}$, n = 10; *MMSET*$^{low}$, n = 270) and GSE16558 (*MMSET*$^{high}$/*FGFR3*$^{high}$, n = 14; *MMSET*$^{high}$/*FGFR3*$^{low}$, n = 3; *MMSET*$^{low}$, n = 43).

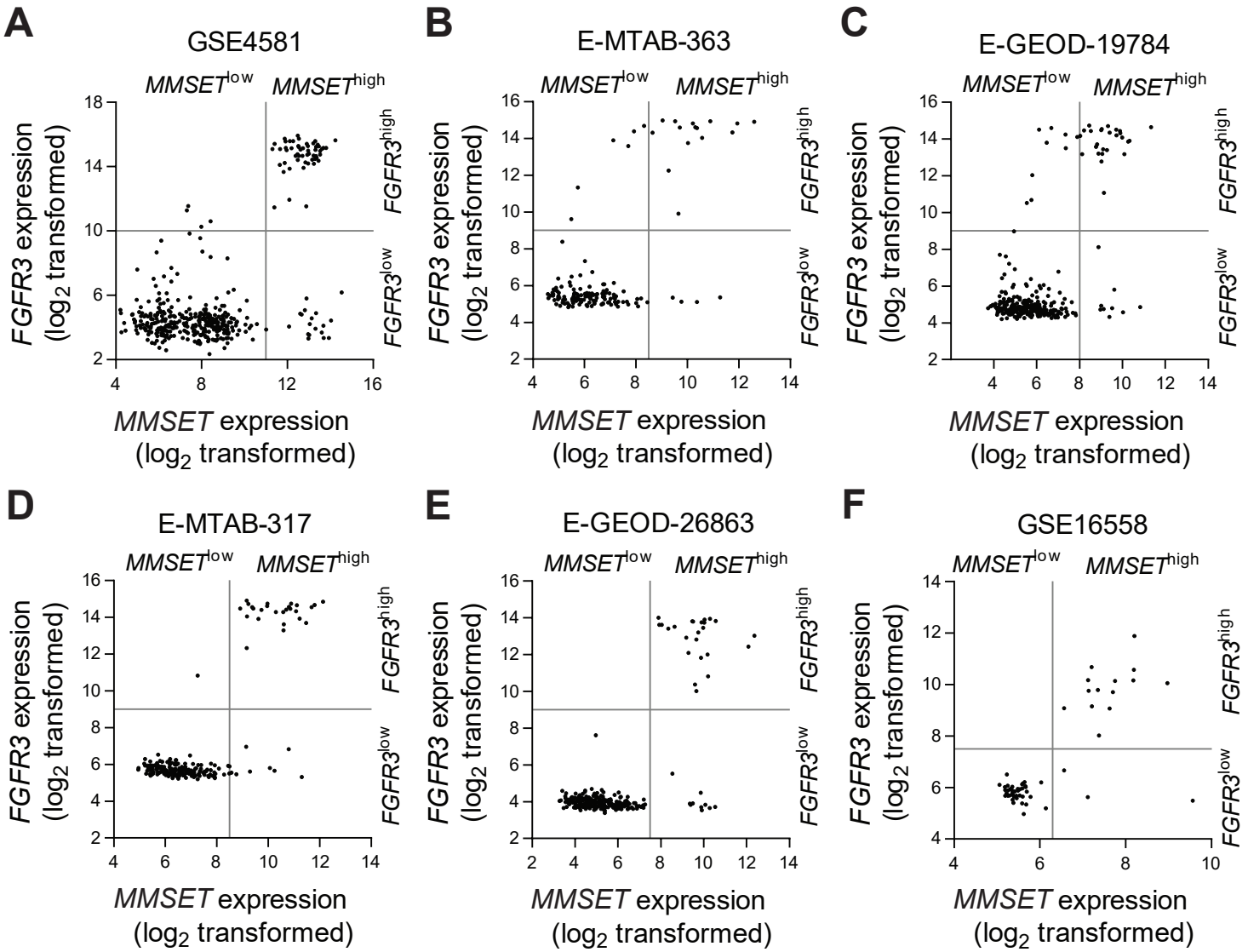
A
GSE4581
MMSET low
MMSET high
FGFR3 high
FGFR3 low
FGFR3 expression (log2 transformed)
MMSET expression (log2 transformed)
B
E-MTAB-363
C
E-GEOD-19784
D
E-MTAB-317
E
E-GEOD-26863
F
GSE16558

**Supplementary Figure 4.2. A schematic overview of the hypothesised *CDH2* regulatory mechanisms in MM based on *in silico* analysis of publicly available microarray data of CD138$^{+}$ BM PCs from newly-diagnosed MM patients.** MMSET is hypothesised to be a key positive regulator of *CDH2* expression in t(4;14)$^{+}$ MM (**A**). In t(4;14)$^{-}$ MM, BTBD3 is hypothesised to be a potential driver of *CDH2* expression, while miR-190 may suppress *CDH2* expression (**B**).

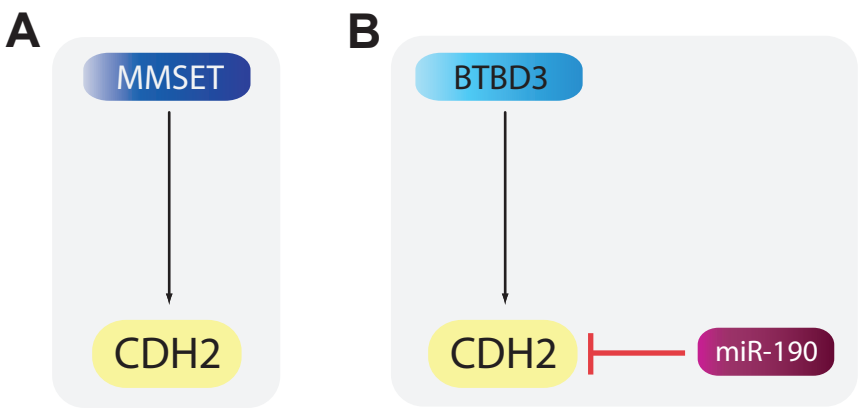
A
MMSET
CDH2
B
BTBD3
CDH2
miR-190

**Supplementary Figure 4.3. miR-190 and *CDH2* expression in t(4;14)$^{-}$ MM patients, and expression of miR-190 in a panel of t(4;14)$^{-}$ HMCLs.** Newly-diagnosed MM patients were categorised as miR-190$^{low}$ or miR-190$^{high}$, and *CDH2*$^{low}$ or *CDH2*$^{high}$, based on their expression of miR-190 and *CDH2* (203440_at) in CD138-selected BM MM PCs, as determined by microarray analysis. The cut-off (grey line) used to delineate high and low miR-190 and *CDH2* expression is shown for the microarray dataset GSE16558 (**A**). miR-190 expression levels (normalised to the U6 snRNA reference gene), as assessed by qPCR, in a panel of t(4;14)$^{-}$ HMCLs. Graph depicts mean ± SEM of 3 independent experiments (**B**).

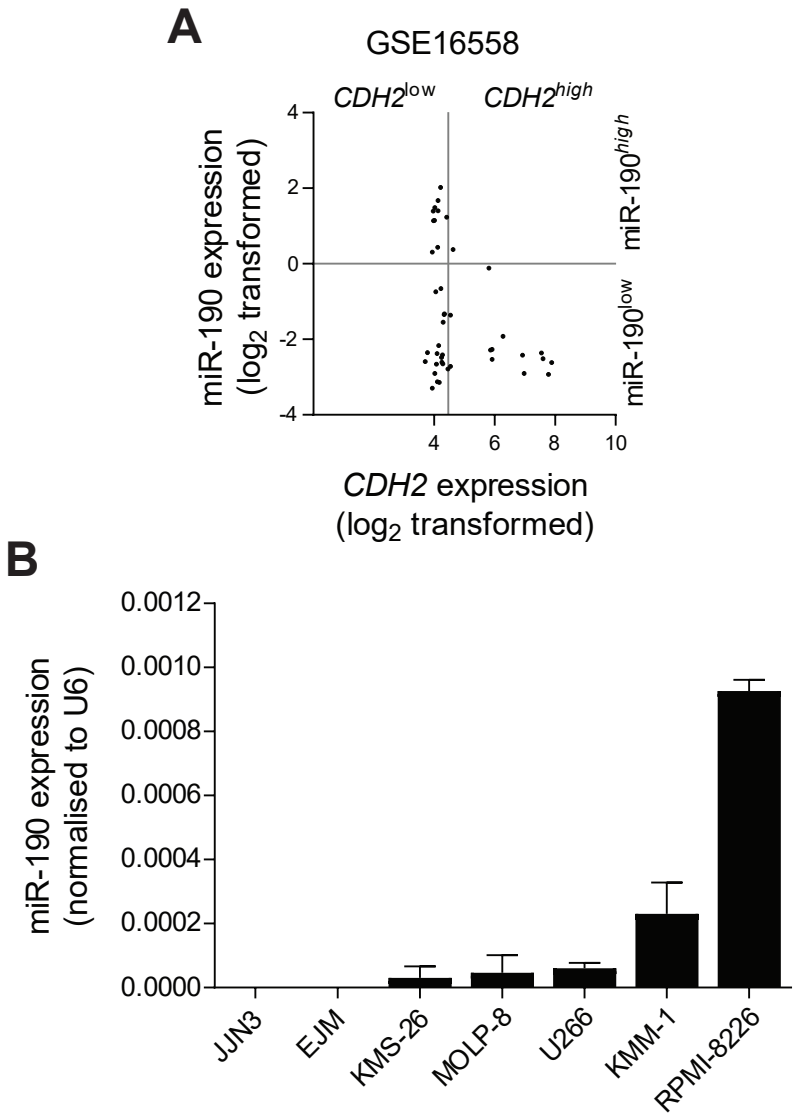
A
GSE16558
CDH2low
CDH2high
miR-190high
miR-190low
miR-190 expression
(log2 transformed)
CDH2 expression
(log2 transformed)
4
2
0
-2
-4
4
6
8
10
B
miR-190 expression
(nomalised to U6)
0.0012
0.0010
0.0008
0.0006
0.0004
0.0002
0.0000
JJN3
EJM
KMS-26
MOLP-8
U266
KMM-1
RPMI-8226

**Supplementary Figure 4.4. Expression of BTBD3 mRNA and protein in a panel of HMCLs.** *BTBD3* expression (normalised to *ACTB* expression), as assessed by qPCR, in a panel of HMCLs, stratified based on t(4;14) status. Graph depicts mean ± SEM of 3 independent experiments (**A**). Expression of BTBD3 isoforms in representative HMCLs (top panel), as assessed by Western blot. Histone H3 was utilised as a nuclear protein load control (bottom panel) (**B**).

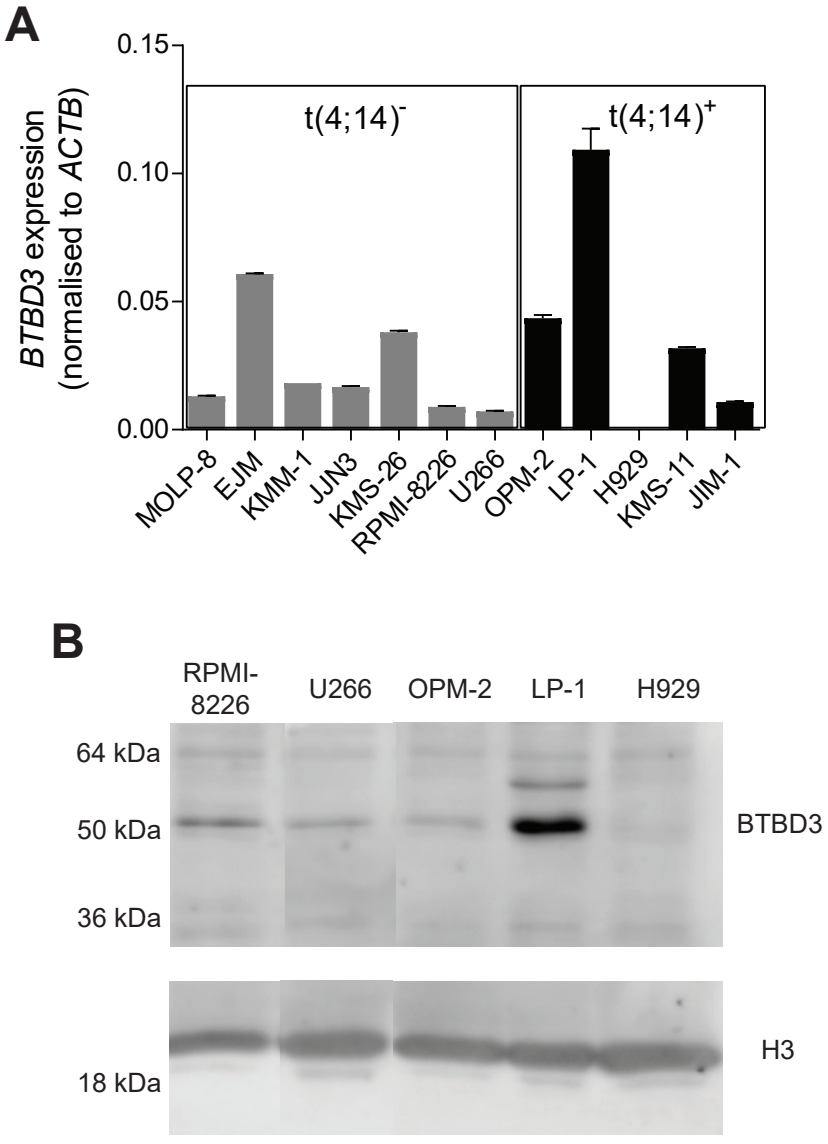
A
BTBD3 expression (normalised to ACTB)
0.15
0.10
0.05
0.00
t(4;14)-
t(4;14)+
MOLP-8
EJM
KMM-1
JJN3
KMS-26
RPMI-8226
U266
OPM-2
LP-1
H929
KMS-11
JIM-1
B
RPMI-8226
U266
OPM-2
LP-1
H929
64 kDa
50 kDa
36 kDa
BTBD3
18 kDa
H3

**Supplementary Table 4.1: GSEA of genes which positively correlate with *CDH2* expression in t(4;14)$^-$ MM patients**

| Gene set name | # Genes in overlap | k/K | FDR q-value | Genes | | | |
|---|---|---|---|---|---|---|---|
| ZHAN_MULTIPLE_MYELOMA HP_UP[1] | 24 | 0.49 | 1.92E-41 | GTF2F2 | CDV3 | EPB41L4A-AS1 | |
| | | | | POLR1D | ATP5L | FLI1 | PAK1 |
| | | | | RSAD2 | TNFSF10 | THG1L | XRCC4 |
| | | | | ELOVL7 | CCRL2 | PIP5K1B | EPHB1 |
| | | | | SCYL2 | ISL2 | C2orf89 | CNTN5 |
| | | | | CCDC85A | GBA3 | RPS17 | RPL13A |
| | | | | RPL37 | | | |
| CHNG_MULTIPLE_MYELOMA HYPERPLOID_UP [2] | 22 | 0.42 | 3.23E-36 | EIF3K | EIF3G | CLTA | FBL |
| | | | | NPM1 | UBA7 | SCAMP5 | RPS17 |
| | | | | RPL13A | RPL37 | RPS3 | RPL29 |
| | | | | RPL4 | RPS19 | RPS9 | RPL27A |
| | | | | RPL18 | RPL35 | RPL35A | RPS13 |
| | | | | RPL36 | RSL24D1 | | |
| KEGG_RIBOSOME[3] | 21 | 0.24 | 1.96E-28 | RPS17 | RPL13A | RPL37 | RPS3 |
| | | | | RPL29 | RPL4 | RPS19 | RPS9 |
| | | | | RPL27A | RPL18 | RPL35 | RPL35A |
| | | | | RPS13 | RPL36 | RSL24D1 | RPS5 |
| | | | | RPS11 | RPL31 | RPS28 | RPS2 |
| | | | | FAU | | | |
| REACTOME_TRANSLATION[4] | 25 | 0.11 | 1.08E-25 | RPS17 | RPL13A | RPL37 | RPS3 |
| | | | | RPL29 | RPL4 | RPS19 | RPS9 |
| | | | | RPL27A | RPL18 | RPL35 | RPL35A |
| | | | | RPS13 | RPL36 | EIF3K | EIF3G |
| | | | | RPS5 | RPS11 | RPL31 | RPS28 |
| | | | | RPS2 | FAU | SEC11A | SSR3 |
| | | | | EEF1D | | | |
| REACTOME_3_UTR_MEDIATED TRANSLATIONAL REGULATION[5] | 22 | 0.13 | 1.79E-23 | RPS17 | RPL13A | RPL37 | RPS3 |
| | | | | RPL29 | RPL4 | RPS19 | RPS9 |
| | | | | RPL27A | RPL18 | RPL35 | RPL35A |
| | | | | RPS13 | RPL36 | EIF3K | EIF3G |
| | | | | RPS5 | RPS11 | RPL31 | RPS28 |
| | | | | RPS2 | FAU | | |
| REACTOME_SRP_DEPENDENT COTRANSLATIONAL PROTEIN TARGETING TO MEMBRANE[6] | 22 | 0.12 | 2.19E-23 | RPS17 | RPL13A | RPL37 | RPS3 |
| | | | | RPL29 | RPL4 | RPS19 | RPS9 |
| | | | | RPL27A | RPL18 | RPL35 | RPL35A |
| | | | | RPS13 | RPL36 | RPS5 | RPS11 |
| | | | | RPL31 | RPS28 | RPS2 | FAU |
| | | | | SEC11A | SSR3 | | |
| REACTOME_INFLUENZA VIRAL RNA TRANSCRIPTION AND REPLICATION[7] | 21 | 0.12 | 2.09E-22 | RPS17 | RPL13A | RPL37 | GTF2F2 |
| | | | | RPS3 | RPL29 | RPL4 | RPS19 |
| | | | | RPS9 | RPL27A | RPL18 | RPL35 |
| | | | | RPL35A | RPS13 | RPL36 | RPS5 |
| | | | | RPS11 | RPL31 | RPS28 | RPS2 |
| | | | | RPS2 | FAU | | |

**Supplementary Table 4.1: GSEA of genes which positively correlate with *CDH2* expression in t(4;14)$^{-}$ MM patients (continued)**

| Gene set name | # Genes in overlap | k/K | FDR q-value | Genes | | | |
|---|---|---|---|---|---|---|---|
| REACTOME_INFLUENZA LIFE CYCLE[8] | 22 | 0.11 | 2.84E-22 | RPS17 | RPL13A | RPL37 | GTF2F2 |
| | | | | RPS3 | RPL29 | RPL4 | RPS19 |
| | | | | RPS9 | RPL27A | RPL18 | RPL35 |
| | | | | RPL35A | RPS13 | RPL36 | CLTA |
| | | | | RPS5 | RPS11 | RPL31 | RPS28 |
| | | | | RPS2 | FAU | | |
| REACTOME PEPTIDE CHAIN ELONGATION[9] | 20 | 0.13 | 8.06E-22 | RPS17 | RPL13A | RPL37 | RPS3 |
| | | | | RPL29 | RPL4 | RPS19 | RPS9 |
| | | | | RPL27A | RPL18 | RPL35 | RPL35A |
| | | | | RPS13 | RPL36 | RPS5 | RPS11 |
| | | | | RPL31 | RPS28 | RPS2 | FAU |
| REACTOME NONSENSE MEDIATED DECAY ENHANCED BY THE EXON JUNCTION COMPLEX[10] | 20 | 0.11 | 1.32E-20 | RPS17 | RPL13A | RPL37 | RPS3 |
| | | | | RPL29 | RPL4 | RPS19 | RPS9 |
| | | | | RPL27A | RPL18 | RPL35 | RPL35A |
| | | | | RPS13 | RPL36 | RPS5 | RPS11 |
| | | | | RPL31 | RPS28 | RPS2 | FAU |

1. Top 50 up-regulated genes in cluster HP of multiple myeloma samples characterized by a hyperploid signature.
2. Protein biosynthesis, transport or catabolism genes up-regulated in hyperploid multiple myeloma (MM) compared to the non-hyperploid MM samples.
3. Ribosome
4. Genes involved in Translation
5. Genes involved in 3' -UTR-mediated translational regulation
6. Genes involved in SRP-dependent cotranslational protein targeting to membrane
7. Genes involved in Influenza Viral RNA Transcription and Replication
8. Genes involved in Influenza Life Cycle
9. Genes involved in Peptide chain elongation
10. Genes involved in Nonsense Mediated Decay Enhanced by the Exon Junction Complex

**Supplementary Table 4.2: GSEA of genes which inversely correlate with *CDH2* expression in t(4;14)$^-$ MM patients**

| Gene set name | # Genes in overlap | k/K | FDR q-value | Genes | | | |
|---|---|---|---|---|---|---|---|
| ZHAN_MULTIPLE_MYELOMA_HP_DN[1] | 7 | 0.15 | 1.16E-11 | IRF2BP2 | SGPL1 | RAPH1 | TMEM107 |
| | | | | KCNN3 | TCFL5 | APBB1IP | |
| PATIL_LIVER_CANCER[2] | 7 | 0.01 | 1.64E-03 | IRF2BP2 | CDCA7 | GSTA4 | RGS5 |
| | | | | ARF3 | POLA1 | XPR1 | |
| MILI_PSEUDOPODIA_HAPTOTAXIS_DN[3] | 6 | 0.01 | 9.64E-03 | SGPL1 | CDCA7 | HGSNAT | B3GALT6 |
| | | | | SEC61A2 | SLC44A2 | | |
| RODRIGUES_THYROID_CARCINOMA_ ANAPLASTIC_DN[4] | 5 | 0.01 | 3.53E-02 | RAPH1 | GSTA4 | RGS5 | HGSNAT |
| | | | | PITPNC1 | | | |
| DODD_NASOPHARYNGEAL_ CARCINOMA_DN[5] | 7 | 0.01 | 3.53E-02 | CDCA7 | ARF3 | POLA1 | B3GALT6 |
| | | | | SEC61A2 | DHTKD1 | ETV6 | |

1. Top 50 down-regulated genes in cluster HP of multiple myeloma samples characterized by a hyperploid signature.

2. Genes up-regulated in hepatocellular carcinoma (HCC) compared to normal liver samples.

3. Transcripts depleted from pseudopodia of NIH/3T3 cells (fibroblast) in response to haptotactic migratory stimulus by fibronectin, FN1.

4. Genes down-regulated in anaplastic thyroid carcinoma (ATC) compared to normal thyroid tissue.

5. Genes down-regulated in nasopharyngeal carcinoma (NPC) compared to the normal tissue.

Chapter 5

# Discussion

## 5.1 General discussion

In Australia alone, approximately 10,000 individuals are living with MM, with approximately 1,700 new cases of MM diagnosed each year.[1] The advent of so-called 'novel' anti-MM agents, including the immunomodulatory drugs thalidomide and lenalidomide, and the proteasome inhibitor bortezomib, has significantly changed the therapeutic landscape of MM patient management over the past 15-20 years.[2,3] The use of bortezomib, the first-in-class proteasome inhibitor approved by the US FDA in 2003, is considered to be a major breakthrough in the treatment of patients with MM. Currently, bortezomib forms an integral backbone of many chemotherapeutic regimens in MM, used as induction therapy in both autologous stem cell transplantation (ASCT)-eligible and -ineligible patients, as a maintenance therapy and in the relapse setting.[4-7] Notably, the use of bortezomib-based treatment regimens in newly diagnosed MM patients appears to overcome the poor prognosis associated with high-risk cytogenetic features (e.g. t(4;14)$^{+}$ status or deletion of chromosome 17p) and improves overall survival (OS) rates in both ASCT-eligible and -ineligible patients, in comparison to non-bortezomib-based therapies.[8-12] Importantly, such advancements in the therapeutic management of MM continue to improve the OS prospects of individuals diagnosed with the disease.[13-15] Currently, the median overall survival (OS) of newly diagnosed MM patients is approximately 6-10 years.[4,15]

While some patients achieve long-term disease remission, with OS of greater than 15 years, approximately 15-20% of patients experience rapid disease relapse, or respond poorly to induction therapy, resulting in early death.[15-17] The identification of MM patients who are likely to do poorly, namely those with 'high-risk' disease, is paramount to the success of therapeutically managing these patients in order to maximise their survival prospects.[15] A combination of determinants are used to clinically define high-risk MM including advanced disease stage (ISS stage III), poor genetic profile (e.g. t(4;14), t(14;16), del(17p), 1q21 amplification) and the presence of extramedullary disease.[15] Other features associated with high-risk disease include high numbers of circulating tumour cells (CTCs) and failure to respond to an induction therapy containing a proteasome inhibitor or immunomodulatory agent.[18] Notably, studies emanating from our laboratory have shown that stratification of newly diagnosed MM patients based on plasma N-cadherin levels identify a subset of individuals (> 6ng/ml plasma N-cadherin) with increased risk of earlier death,

irrespective of ISS stage, tumour burden or poor cytogenetic features.[19] N-cadherin gene (*CDH2*) expression in $CD138^+$ PCs is also up-regulated in approximately 50% of newly diagnosed MM patients, compared with *CDH2* levels in normal individuals.[19,20] Collectively, these findings raise several important issues, including how N-cadherin expression is dysregulated in MM, what functional role(s) N-cadherin plays in MM pathogenesis and whether N-cadherin represents a potential therapeutic target in MM.

## 5.2 The regulation of N-cadherin expression in $t(4;14)^+$ and $t(4;14)^-$ MM

A key aim of this thesis research was to determine how N-cadherin expression is dysregulated in both $t(4;14)^+$ and $t(4;14)^-$ MM (Chapter 4). *CDH2* is highly expressed in approximately 85% of patients featuring the reciprocal chromosomal translocation t(4;14), observed in 10-15% of MM cases, whereby the genes *MMSET* (encoding for the histone methyltrasferase MMSET) and *FGFR3* (encoding for fibroblast growth factor receptor 3) are placed under the control of strong enhancers.[20-22] This translocation universally results in the over-expression of *MMSET* and, in 70% of cases, the over-expression of *FGFR3*.[23,24] Given $t(4;14)^+$ status in MM is an adverse prognostic factor, independent of *FGFR3* expression, *MMSET* dysregulation is considered to be the primary mediator of oncogenesis and aberrant gene expression in this subset of MM patients.[25-27] Using a combination of *in silico* and *in vitro* analyses, we have confirmed that MMSET is a key regulator of *CDH2* expression in MM cells, suggesting it is an important driver of up-regulated N-cadherin in $t(4;14)^+$ MM.

In addition to $t(4;14)^+$ MM patients, *CDH2* up-regulation is a feature in another 35-40% of newly diagnosed patients despite having $t(4;14)^-$ status.[20] In particular, a distinct population of *CDH2*-overexpressing MM patients is observed in the hyperdiploidy subset, accounting for approximately 50% of patients in the subset.[20,28] Owing to the genetic heterogeneity between $CDH2^+$ patients in the $t(4;14)^-$ MM subsets[29], little is currently known regarding the mechanism(s) by which *CDH2* expression is up-regulated in these patients. To this end, we performed *in silico* analysis of newly diagnosed $t(4;14)^-$ MM patients to reveal potential regulators of *CDH2* expression in $t(4;14)^-$ MM PCs. While *in vitro* studies in HMCLs did not validate our leading candidate, BTBD3, as a critical regulator of *CDH2* expression in MM, our studies revealed several other mechanisms by which *CDH2* expression may be

regulated in t(4;14)$^-$ MM. For example, several genes identified as being significantly associated with *CDH2* expression in t(4;14)$^-$ MM patients (*IL6ST*, *BTF3* and *SGPL1*) functionally converge to regulate the JAK/STAT3 signalling cascade[30-32], which is implicated in MM PC growth and survival[33-35], and has previously been shown to positively regulate N-cadherin expression in solid tumours.[36-39] Other potential mechanisms of *CDH2* up-regulation in t(4;14)$^-$ MM include the Fer/Rac1/Pak1 and ZNF622/B-myb signalling axes, which have previously been implicated in positively regulating N-cadherin expression in other cancers.[40-44] miR-190 is also of particular interest, as the majority of t(4;14)$^-$ MM patients which express miR-190 have low or undetectable *CDH2* expression. Moreover, miR-190 is predicted to target the *CDH2* 3'-UTR. Further studies are required to investigate whether these pathways and molecules regulate N-cadherin expression in t(4;14)$^-$ MM.

While BTBD3, a putative transcriptional regulator[45-52], is unlikely to be a critical regulator of *CDH2* expression in MM, our analyses show, for the first time, that *BTBD3* expression is strongly up-regulated in bone marrow (BM) PCs from MM patients, compared with normal controls. Moreover, the up-regulation of *BTBD3* in MM PCs is associated with a trend towards poorer overall survival in t(4;14)$^-$ MM patients, suggesting a role for BTBD3 in MM pathogenesis. Thus, future studies investigating the functional role of BTBD3 in MM are also warranted.

## 5.3 The therapeutic utility of ADH-1 in the prevention of MM PC dissemination

The development and progression of MM is underpinned by the continuous trafficking, or dissemination, of MM PCs from one tumour site to distant BM sites via the circulation. For instance, MM PCs egress from a primary BM site and disseminate to multiple skeletal sites to form micrometastases, leading to the asymptomatic precursor stage of MM, called monoclonal gammopathy of undermined significance (MGUS). The subsequent growth of these metastases results in the transition to symptomatic MM[53], which occurs at a relatively slow rate in individuals with MGUS (1% per annum).[54] Elevated numbers of CTCs are also associated with more rapid progression from MGUS, or the pre-malignant stage of MM called smouldering MM, to overt MM.[55,56] Further growth and dissemination of MM PCs promotes disease progression and, in advanced cases, the development of plasma cell leukaemia and extramedullary

disease.[53,57-61] The dissemination of MM PCs is also likely to facilitate the re-population and growth of therapy-resistant MM PCs within the BM, thereby promoting disease relapse. Indeed, elevated numbers of CTCs in previously treated MM patients are associated with inferior prognosis.[62]

Therapeutic targeting of tumour cell adhesion to endothelium has been suggested as a modality to prevent the extravasation and dissemination of MM PCs. For example, functional inhibition of PSGL-1-mediated MM PC interaction with P-selectin, important in leukocyte tethering to endothelial cells (ECs), inhibits MM PC adhesion to ECs and reduces MM PC extravasation and BM homing *in vivo*.[63] In addition, studies have shown that blocking MM PC adhesion to ECs with an anti-CD44v10 antibody inhibits the homing of circulating MM PCs to the BM and reduces tumour development.[64] In line with the aforementioned studies, we found that pre-treatment of C57Bl/KaLwRij mice with the N-cadherin antagonist ADH-1 (N-Ac-CHAVC-$NH_2$) inhibited tumour development following intravenous injection of 5TGM1 MM PCs. This effect was not seen in mice treated with ADH-1 1 week after injection of tumour cells, suggesting that N-cadherin plays a role in the initial BM homing or establishment of the tumour cells within the BM. While our *in vivo* studies did not specifically investigate the role of N-cadherin in extravasation and BM homing, we have shown that N-cadherin mediates the adhesion of MM PCs to ECs, which is likely to play a role in the extravasation and intravasation of MM PCs (Chapter 2).[65] In support of this, pre-clinical studies have previously demonstrated that N-cadherin knock-down in MM PCs decreases the capacity of CTCs to home to the BM *in vivo*, resulting in increased residual cells within the peripheral blood.[20] As well as preventing the establishment of MM PCs within the BM, the inability of circulating MM PCs to rapidly extravasate and home to the BM is likely to increase their vulnerability to anoikis (a form of programmed cell death induced by the lack of integrin-mediated cell adhesion), shear stress and attack by immune cells[66,67], thereby potentially inhibiting MM disease progression.

Although we found that ADH-1 treatment did not decrease tumour development in C57Bl/KaLwRij mice with established MM, the limited sensitivity of bioluminescence imaging (BLI) prevented the assessment of the effects of ADH-1 on MM PC dissemination and the formation of micro-metastases in this model. In addition, recent bar-coding studies conducted in our laboratory have demonstrated that while the systemic dissemination of individual 5TGM1 cell clones is a feature of the

C57Bl/KaLwRij model, it does not contribute to the bulk of the tumour burden observed at the conclusion of the study.[68] Thus, any inhibitory effects of ADH-1 on the ability of 5TGM1 cells to disseminate in C57Bl/KaLwRij mice with established disease is unlikely to result in decreased BLI signal at the conclusion of the study. In addition to ECs, ADH-1 may also antagonise N-cadherin function in other host-derived cell types, including BM stromal cells that support MM PC proliferation and survival.[69-72] However, our *in vitro* co-culture studies suggest that N-cadherin-mediated adhesion between 5TGM1 cells and BM stromal cells is unlikely to play a critical role in 5TGM1 cell proliferation. Moreover, in the context of MM pathogenesis, the inability of ADH-1 treatment to inhibit MM progression in C57Bl/KaLwRij mice with established disease suggests that N-cadherin-mediated adhesion between 5TGM1 cells and BM stromal cells in the BM microenvironment is less important than N-cadherin-mediated 5TGM1 cell-EC interactions.

Further studies are warranted to determine whether therapeutic targeting of N-cadherin may be useful as a maintenance therapy in the clinical MM setting. To this end, ADH-1 could be used to prevent the dissemination of residual therapy-resistant MM PCs, thereby inhibiting or delaying tumour re-population of the BM and limiting disease relapse. Theoretically, the introduction of ADH-1 as a maintenance therapy could be particularly useful for those 50% of MM patients in which N-cadherin expression in MM PCs is elevated. In addition to MM, the extravasation of CTCs plays a critical role in dissemination and metastasis formation in many solid tumours.[73-76] Notably, N-cadherin has been implicated in the adhesion of breast cancer cells and melanoma cells to ECs and in the formation of lung metastases following intravenous injection of melanoma cells in mice.[77-80] Thus, it is possible that ADH-1 may be therapeutically useful in the context of preventing tumour cell dissemination and metastasis formation in solid tumours.

## 5.4 The use of LCRF-0006 as a novel vascular disrupting agent

Unlike normal blood vessels, which consist of a layer of tightly associated ECs that are structurally supported by mural cells (e.g. pericytes and smooth muscle cells), tumour-associated vasculature is structurally abnormal, characterised by gaps between adjacent ECs and loosely attached or absent mural cells.[81-83] These structural abnormalities, in addition to the disorganised, tortuous nature of tumour-associated vasculature, and the

defective lymphatic drainage in tumours, result in abnormal pressure gradients and heterogeneous perfusion which can limit drug delivery to the tumour.[81,84,85]

Paradoxically, however, these structural abnormalities can lead to increased permeability of tumour-associated vasculature which, combined with the paucity of lymphatic drainage in tumours, is thought to contribute to the passive and selective accumulation of macromolecules (> 40 kDa) in sites of tumour, known as the enhanced permeability and retention (EPR) effect.[81,86,87] Notably, augmentation of the EPR effect is widely recognised, and increasingly investigated, as a potential therapeutic strategy to increase tumour delivery, and therefore efficacy, of macromolecular drugs or drug complexes.[87-93] To this end, augmentation of the EPR effect may be therapeutically useful for tumour delivery of large drugs such as monoclonal antibodies (e.g. rituximab, daratumamab and elotuzamab)[94-96], or drugs with high affinity (> 80%) for large plasma proteins (e.g. albumin), including tyrosine kinase inhibitors (e.g. imatinib and nilotinib), proteosome inhibitors (e.g. bortezomib and carfilzomib) and melphalan.[97-101] Additionally, augmentation of the EPR effect may also increase tumour delivery of drugs in nanoparticle delivery systems.[91,102] Importantly, pre-clinical studies suggest that agents which augment the EPR effect may improve the efficacy of anti-cancer agents in tumours characterised by either inherently low, or high, vascular permeability.[90,103] Notably, recent studies have demonstrated the ability of vascular disrupting agents to increase tumour accumulation, and anti-cancer efficacy, of macromolecular drugs and drug complexes *in vivo*, suggesting that such agents can augment the EPR effect.[91,104]

LCRF-0006 is a synthetic, metabolically stable compound which structurally mimics the HAV domain of ADH-1.[105] Synthetic small molecule mimetics of peptide drugs are thought to offer increased therapeutic efficacy in comparison to their peptide counterparts, due to enhanced proteolytic stability, bio-availability and potency.[106,107] Indeed, LCRF-0006 has been found to inhibit N-cadherin-dependent processes four-fold more potently than ADH-1 (Orest Blaschuk; personal communication). N-cadherin is expressed by both ECs and mural cells and is a critical regulator of vascular integrity and endothelial barrier function.[104,108-111] To this end, *in vitro* studies have demonstrated that endothelial barrier permeability to macromolecules can be enhanced by functional perturbation of N-cadherin in blood vessels.[104,111] Moreover, ADH-1 has been shown to rapidly enhance tumour blood vessel permeability to macromolecules *in vivo*.[104] Notably, we found that LCRF-0006 acts as a vascular disrupting agent which increases

blood vessel permeability to macromolecules, as evidenced by LCRF-0006-mediated extravasation of 70 kDa FITC-dextran in mouse retinal tissues (Chapter 3). In contrast to vascular disrupting agents such as microtubule-depolymerizing agents which induce necrosis of tumour vasculature[84,112,113], the disruptive effects of LCRF-0006 on ECs are transient and reversible, which is consistent with the proposed role of N-cadherin in endothelial barrier closure.[79,114] Thus, the effects of LCRF-0006 may be more comparable to the transient effects of inflammatory mediators (e.g. histamine and thrombin) which induce reversible cell retraction and inter-endothelial gap formation.[115-117]

In line with the ability of ADH-1 to increase the efficacy of melphalan[104], the data presented here shows that LCRF-0006 synergistically increased the depth of MM tumour response in C57Bl/KaLwRij mice to the anti-MM agent bortezomib. We speculate that these synergistic effects may, at least in part, be mediated by LCRF-0006-enhanced tumour delivery of bortezomib, potentially by augmentation of the EPR effect. As bortezomib is highly bound to plasma proteins *in vivo*[99], we hypothesise that an increase in the permeability of tumour-associated vasculature caused by pre-treatment with LCRF-0006 may enhance accumulation of plasma protein-bound bortezomib in sites of tumour, consistent with the ADH-1-mediated increase in delivery of melphalan in a pre-clinical model of melanoma.[104] Given LCRF-0006 synergistically increased MM tumour response to a sub-therapeutic dose of bortezomib, these findings may also be clinically relevant in increasing MM patient depth of response to low doses of bortezomib, thereby potentially alleviating detrimental side-effects such as peripheral neuropathy. In support of this, recent studies using a pre-clinical mouse model of colon cancer demonstrated the ability of an EPR-augmenting agent to increase the anti-tumour efficacy of albumin-bound paclitaxel, without increasing the myelosuppressive effects of paclitaxel treatment.[90] An important observation emanating from our endothelial tube disruption assays was that the initial effects of LCRF-0006 on EC retraction and rounding were more rapid in immature (5-hour-old) endothelial tubes than established (24-hour-old) tubes, suggesting that tumour-associated vasculature may have increased propensity to LCRF-0006-mediated disruption. However, given our findings that LCRF-0006 increased the permeability of normal micro-vessels to macromolecules, further studies are warranted to determine whether LCRF-0006 may selectively enhance the delivery of anti-cancer agents such as bortezomib to tumour sites while minimising side-effects on healthy tissues.

## 5.5 The use of LCRF-0006 to increase MM PC sensitivity to anti-cancer agents

In addition to increasing vascular permeability, LCRF-0006 acted synergistically with bortezomib to directly induce 5TGM1 MM PC apoptosis *in vitro*, which may further contribute to the synergism observed *in vivo*. In line with these findings, ADH-1 has previously been shown to significantly increase melanoma tumour response to the chemotherapeutic agent temozolamide *in vivo*, without altering tumour up-take of the drug.[104] To date, a role for N-cadherin in MM PC resistance to chemotherapeutics has not been demonstrated. One potential mechanism by which LCRF-0006 and bortezomib may synergistically induce MM tumour cell apoptosis is by differential inhibition of the Bcl-2-family pro-survival proteins Bcl-2 and Mcl-1, shown to mediate MM PC survival.[118-121] In other cancer cell types, N-cadherin engagement has been shown to activate Bcl-2 by enhancing PI3K/Akt-mediated phosphorylation of the pro-apoptosis protein Bad.[78,122,123] Interestingly, the combination of the Bcl-2 inhibitor venetoclax and bortezomib has recently shown promising efficacy in relapsed/refractory MM and is now being evaluated in Phase III clinical trials.[124] These studies were conducted on the basis of encouraging pre-clinical findings which demonstrated that venetoclax increased MM tumour sensitivity to bortezomib, despite having limited single-agent efficacy.[119] Further studies are required to assess the mechanisms whereby LCRF-0006 synergises with bortezomib and induces apoptosis in MM cells.

N-cadherin has also been implicated in the resistance of other cancer cell types to anti-cancer agents. For example, studies have shown that N-cadherin potentiates prostate cancer cell resistance to metformin *in vitro* and *in vivo*, by activation of NF-κB signalling.[125] In addition, studies have demonstrated the ability of N-cadherin antagonists, including ADH-1, to decrease micro-environmental protection of chronic myeloid leukaemia cells to the tyrosine kinase inhibitor imatinib.[126,127] In line with these findings, N-cadherin silencing has been shown to induce apoptosis in lung cancer cell lines resistant to the tyrosine kinase inhibitor gefitinib.[123] To this end, further studies are warranted to determine whether LCRF-0006-mediated inhibition of N-cadherin function can increase tumour cell sensitivity to tyrosine kinase inhibitors.

## 5.6 Future directions and concluding remarks

MM is still largely considered to be incurable with most patients relapsing and ultimately succumbing to the disease.[6] However, it is evident that deeper tumour responsiveness to induction therapy results in more durable responses and improved long-term prospects for MM patients.[128-132] Thus, an important goal of modern combination therapy regimens in the management of MM patients is to achieve the maximum possible depth of tumour response to induction therapy.[6] To this end, our finding that a significantly deeper tumour response was achieved in mice which received the LCRF-0006-bortezomib combination therapy, suggests that the addition of LCRF-0006 to current chemotherapeutic regimens incorporating bortezomib may represent a novel strategy to increase the depth of MM patient response to bortezomib therapy. To this end, LCRF-0006 may therapeutically be useful in newly diagnosed patients, during maintenance therapy and in the relapse setting. Furthermore, the potential ability of LCRF-0006 to augment the EPR effect, increasing extravasation of macromolecular drugs and drug complexes (e.g. plasma protein-bound drugs), suggests that it could also improve the efficacy of 75% of the pharmaceutical industry's current 20 top-selling anti-cancer drugs.[133]

In addition to initial response to treatment, the subsequent rapidity of the outgrowth and spread of resistant clones is an important determinant of the outcomes for myeloma patients.[134-137] Treatment relapse is likely to be dependent upon the ability of therapy-resistant MM PC to re-enter the circulation, disseminate and repopulate sites throughout the BM.[62] Therefore, limiting the dissemination of MM PCs presents a promising opportunity to prevent overt relapse and improve overall survival. Our findings demonstrate that N-cadherin is likely to facilitate the adhesion of circulating MM PCs to ECs during extravasation, a critical step in the BM homing cascade.[65] To this end, ADH-1 could be utilised to prevent the dissemination of MM PCs via the circulation, thereby inhibiting MM disease relapse in those 50% of MM patients that express up-regulated levels of N-cadherin.

This thesis research demonstrates that MMSET, universally dysregulated in $t(4;14)^+$ MM patients, is a critical regulator of *CDH2* expression in MM PCs, suggesting it is the key driver of up-regulated N-cadherin in $t(4;14)^+$ MM. This thesis has also identified several potential molecules and pathways which may represent previously

unknown, MMSET-independent regulators of N-cadherin expression in t(4;14)$^-$ MM. While BTBD3 is unlikely to be a critical regulator of *CDH2* in t(4;14)$^-$ MM, this thesis suggests that BTBD3 is potentially important in MM pathogenesis, which warrants future investigation. In addition, this thesis research suggests that therapeutic targeting of N-cadherin using the antagonist ADH-1 could potentially be utilised to prevent the dissemination of PCs, thereby delaying MM progression and relapse.[65] Finally, this thesis research has identified a small molecule peptidomimetic of ADH-1, LCRF-0006, as a novel vascular disrupting agent which enhances vascular permeability and synergistically increases the efficacy of the anti-MM agent bortezomib in a pre-clinical mouse model of established MM disease. To this end, LCRF-0006 may be clinically useful in increasing the depth of MM tumour response to bortezomib, which is currently used in MM patients as induction therapy, maintenance therapy, and in the relapsed setting. In addition, we speculate that the potential ability of LCRF-0006 to augment the EPR effect could be utilised to increase the delivery, and anti-cancer efficacy, of various chemotherapeutic agents in MM and other cancers in the clinical setting. Together with our collaborators, we are currently developing next-generation small molecules which inhibit N-cadherin-dependent processes more potently than LCRF-0006 or ADH-1. These will be explored more extensively in the context of dissemination and chemotherapy combination therapies in MM and other pre-clinical cancer models.

## 5.7 References

1. www.myeloma.org.au. Myeloma - a comprehensive guide. Vic, Australia; 2016.

2. Fonseca R, Abouzaid S, Bonafede M, Cai Q, Parikh K, Cosler L, Richardson P. Trends in overall survival and costs of multiple myeloma, 2000-2014. *Leukemia*. 2017; 31(9):1915-1921.

3. Laubach J, Richardson P, Anderson K. Multiple myeloma. *Annu Rev Med*. 2011; 62:249-264.

4. Rajkumar SV. Multiple myeloma: 2016 update on diagnosis, risk-stratification, and management. *American journal of hematology*. 2016; 91(7):719-734.

5. Mateos MV, Ocio EM, Paiva B, Rosinol L, Martinez-Lopez J, Blade J, Lahuerta JJ, Garcia-Sanz R, San Miguel JF. Treatment for patients with newly diagnosed multiple myeloma in 2015. *Blood reviews*. 2015; 29(6):387-403.

6. Moreau P, de Wit E. Recent progress in relapsed multiple myeloma therapy: implications for treatment decisions. *Br J Haematol*. 2017; 179(2):198-218.

7. Mohan M, Matin A, Davies FE. Update on the optimal use of bortezomib in the treatment of multiple myeloma. *Cancer Manag Res*. 2017; 9:51-63.

8. Bergsagel PL, Mateos MV, Gutierrez NC, Rajkumar SV, San Miguel JF. Improving overall survival and overcoming adverse prognosis in the treatment of cytogenetically high-risk multiple myeloma. *Blood*. 2013; 121(6):884-892.

9. Sonneveld P, Schmidt-Wolf IG, van der Holt B, El Jarari L, Bertsch U, Salwender H, Zweegman S, Vellenga E, Broyl A, Blau IW *et al*. Bortezomib induction and maintenance treatment in patients with newly diagnosed multiple myeloma: results of the randomized phase III HOVON-65/ GMMG-HD4 trial. *J Clin Oncol*. 2012; 30(24):2946-2955.

10. Sonneveld P, Goldschmidt H, Rosinol L, Blade J, Lahuerta JJ, Cavo M, Tacchetti P, Zamagni E, Attal M, Lokhorst HM *et al*. Bortezomib-based versus nonbortezomib-based induction treatment before autologous stem-cell transplantation in patients with previously untreated multiple myeloma: a meta-analysis of phase III randomized, controlled trials. *J Clin Oncol*. 2013; 31(26):3279-3287.

11. Durie BG, Hoering A, Abidi MH, Rajkumar SV, Epstein J, Kahanic SP, Thakuri M, Reu F, Reynolds CM, Sexton R *et al*. Bortezomib with lenalidomide and dexamethasone versus lenalidomide and dexamethasone alone in patients with newly diagnosed myeloma without intent for immediate autologous stem-cell transplant (SWOG S0777): a randomised, open-label, phase 3 trial. *Lancet*. 2017; 389(10068):519-527.

12. Gentile M, Magarotto V, Offidani M, Musto P, Bringhen S, Teresa Petrucci M, Gay F, Larocca A, Uccello G, Petrungaro A *et al*. Lenalidomide and low-dose dexamethasone (Rd) versus bortezomib, melphalan, prednisone (VMP) in elderly newly

diagnosed multiple myeloma patients: A comparison of two prospective trials. *American journal of hematology*. 2017; 92(3):244-250.

13. Kumar SK, Dispenzieri A, Lacy MQ, Gertz MA, Buadi FK, Pandey S, Kapoor P, Dingli D, Hayman SR, Leung N *et al*. Continued improvement in survival in multiple myeloma: changes in early mortality and outcomes in older patients. *Leukemia*. 2014; 28(5):1122-1128.

14. Blimark CH, Turesson I, Genell A, Ahlberg L, Bjorkstrand B, Carlson K, Forsberg K, Juliusson G, Linder O, Mellqvist UH *et al*. Outcome and survival of myeloma patients diagnosed 2008-2015. Real world data on 4904 patients from the Swedish Myeloma Registry (SMR). *Haematologica*. 2017.

15. Lonial S, Boise LH, Kaufman J. How I treat high-risk myeloma. *Blood*. 2015; 126(13):1536-1543.

16. Usmani SZ, Crowley J, Hoering A, Mitchell A, Waheed S, Nair B, AlSayed Y, Vanrhee F, Barlogie B. Improvement in long-term outcomes with successive Total Therapy trials for multiple myeloma: are patients now being cured? *Leukemia*. 2013; 27(1):226-232.

17. Avet-Loiseau H. Ultra high-risk myeloma. *Hematology Am Soc Hematol Educ Program*. 2010; 2010:489-493.

18. Usmani SZ, Rodriguez-Otero P, Bhutani M, Mateos MV, Miguel JS. Defining and treating high-risk multiple myeloma. *Leukemia*. 2015; 29(11):2119-2125.

19. Vandyke K, Chow AW, Williams SA, To LB, Zannettino AC. Circulating N-cadherin levels are a negative prognostic indicator in patients with multiple myeloma. *Br J Haematol*. 2013; 161(4):499-507.

20. Groen RW, de Rooij MF, Kocemba KA, Reijmers RM, de Haan-Kramer A, Overdijk MB, Aalders L, Rozemuller H, Martens AC, Bergsagel PL *et al*. N-cadherin-mediated interaction with multiple myeloma cells inhibits osteoblast differentiation. *Haematologica*. 2011; 96(11):1653-1661.

21. Dring AM, Davies FE, Fenton JA, Roddam PL, Scott K, Gonzalez D, Rollinson S, Rawstron AC, Rees-Unwin KS, Li C *et al*. A global expression-based analysis of the consequences of the t(4;14) translocation in myeloma. *Clin Cancer Res*. 2004; 10(17):5692-5701.

22. Chesi M, Nardini E, Lim RS, Smith KD, Kuehl WM, Bergsagel PL. The t(4;14) translocation in myeloma dysregulates both FGFR3 and a novel gene, MMSET, resulting in IgH/MMSET hybrid transcripts. *Blood*. 1998; 92(9):3025-3034.

23. Keats JJ, Maxwell CA, Taylor BJ, Hendzel MJ, Chesi M, Bergsagel PL, Larratt LM, Mant MJ, Reiman T, Belch AR *et al*. Overexpression of transcripts originating from the MMSET locus characterizes all t(4;14)(p16;q32)-positive multiple myeloma patients. *Blood*. 2005; 105(10):4060-4069.

24. Santra M, Zhan F, Tian E, Barlogie B, Shaughnessy J, Jr. A subset of multiple myeloma harboring the t(4;14)(p16;q32) translocation lacks FGFR3 expression but maintains an IGH/MMSET fusion transcript. *Blood*. 2003; 101(6):2374-2376.

25. Keats JJ, Reiman T, Maxwell CA, Taylor BJ, Larratt LM, Mant MJ, Belch AR, Pilarski LM. In multiple myeloma, t(4;14)(p16;q32) is an adverse prognostic factor irrespective of FGFR3 expression. *Blood*. 2003; 101(4):1520-1529.

26. Lauring J, Abukhdeir AM, Konishi H, Garay JP, Gustin JP, Wang Q, Arceci RJ, Matsui W, Park BH. The multiple myeloma associated MMSET gene contributes to cellular adhesion, clonogenic growth, and tumorigenicity. *Blood*. 2008; 111(2):856-864.

27. Martinez-Garcia E, Popovic R, Min DJ, Sweet SM, Thomas PM, Zamdborg L, Heffner A, Will C, Lamy L, Staudt LM *et al*. The MMSET histone methyl transferase switches global histone methylation and alters gene expression in t(4;14) multiple myeloma cells. *Blood*. 2011; 117(1):211-220.

28. Zhan F, Huang Y, Colla S, Stewart JP, Hanamura I, Gupta S, Epstein J, Yaccoby S, Sawyer J, Burington B *et al*. The molecular classification of multiple myeloma. *Blood*. 2006; 108(6):2020-2028.

29. Manier S, Salem KZ, Park J, Landau DA, Getz G, Ghobrial IM. Genomic complexity of multiple myeloma and its clinical implications. *Nat Rev Clin Oncol*. 2017; 14(2):100-113.

30. Dechow T, Steidle S, Gotze KS, Rudelius M, Behnke K, Pechloff K, Kratzat S, Bullinger L, Fend F, Soberon V *et al*. GP130 activation induces myeloma and collaborates with MYC. *J Clin Invest*. 2014; 124(12):5263-5274.

31. Zhang DZ, Chen BH, Zhang LF, Cheng MK, Fang XJ, Wu XJ. Basic Transcription Factor 3 Is Required for Proliferation and Epithelial-Mesenchymal Transition via Regulation of FOXM1 and JAK2/STAT3 Signaling in Gastric Cancer. *Oncol Res*. 2017; 25(9):1453-1462.

32. Degagne E, Pandurangan A, Bandhuvula P, Kumar A, Eltanawy A, Zhang M, Yoshinaga Y, Nefedov M, de Jong PJ, Fong LG *et al*. Sphingosine-1-phosphate lyase downregulation promotes colon carcinogenesis through STAT3-activated microRNAs. *J Clin Invest*. 2014; 124(12):5368-5384.

33. Scuto A, Krejci P, Popplewell L, Wu J, Wang Y, Kujawski M, Kowolik C, Xin H, Chen L, Wang Y *et al*. The novel JAK inhibitor AZD1480 blocks STAT3 and FGFR3 signaling, resulting in suppression of human myeloma cell growth and survival. *Leukemia*. 2011; 25(3):538-550.

34. Tsuyama N, Danjoh I, Otsuyama K, Obata M, Tahara H, Ohta T, Ishikawa H. IL-6-induced Bcl6 variant 2 supports IL-6-dependent myeloma cell proliferation and survival through STAT3. *Biochem Biophys Res Commun*. 2005; 337(1):201-208.

35. Puthier D, Bataille R, Amiot M. IL-6 up-regulates mcl-1 in human myeloma cells through JAK / STAT rather than ras / MAP kinase pathway. *Eur J Immunol*. 1999; 29(12):3945-3950.

36. Colomiere M, Ward AC, Riley C, Trenerry MK, Cameron-Smith D, Findlay J, Ackland L, Ahmed N. Cross talk of signals between EGFR and IL-6R through JAK2/STAT3 mediate epithelial-mesenchymal transition in ovarian carcinomas. *Br J Cancer*. 2009; 100(1):134-144.

37. Liu XL, Zhang XT, Meng J, Zhang HF, Zhao Y, Li C, Sun Y, Mei QB, Zhang F, Zhang T. ING5 knockdown enhances migration and invasion of lung cancer cells by inducing EMT via EGFR/PI3K/Akt and IL-6/STAT3 signaling pathways. *Oncotarget*. 2017; 8(33):54265-54276.

38. Meng J, Zhang XT, Liu XL, Fan L, Li C, Sun Y, Liang XH, Wang JB, Mei QB, Zhang F *et al*. WSTF promotes proliferation and invasion of lung cancer cells by inducing EMT via PI3K/Akt and IL-6/STAT3 signaling pathways. *Cell Signal*. 2016; 28(11):1673-1682.

39. Wu YS, Chung I, Wong WF, Masamune A, Sim MS, Looi CY. Paracrine IL-6 signaling mediates the effects of pancreatic stellate cells on epithelial-mesenchymal transition via Stat3/Nrf2 pathway in pancreatic cancer cells. *Biochim Biophys Acta*. 2017; 1861(2):296-306.

40. Al-Azayzih A, Gao F, Somanath PR. P21 activated kinase-1 mediates transforming growth factor beta1-induced prostate cancer cell epithelial to mesenchymal transition. *Biochim Biophys Acta*. 2015; 1853(5):1229-1239.

41. Fan G, Nicholas N. FER mediated HGF-independent regulation of HGFR/MET activates RAC1-PAK1 pathway to potentiate metastasis in ovarian cancer. *Small GTPases*. 2017:0.

42. Seong HA, Kim KT, Ha H. Enhancement of B-MYB transcriptional activity by ZPR9, a novel zinc finger protein. *J Biol Chem*. 2003; 278(11):9655-9662.

43. Zhang X, Lv QL, Huang YT, Zhang LH, Zhou HH. Akt/FoxM1 signaling pathway-mediated upregulation of MYBL2 promotes progression of human glioma. *J Exp Clin Cancer Res*. 2017; 36(1):105.

44. Tao D, Pan Y, Jiang G, Lu H, Zheng S, Lin H, Cao F. B-Myb regulates snail expression to promote epithelial-to-mesenchymal transition and invasion of breast cancer cell. *Med Oncol*. 2015; 32(1):412.

45. Geyer R, Wee S, Anderson S, Yates J, Wolf DA. BTB/POZ domain proteins are putative substrate adaptors for cullin 3 ubiquitin ligases. *Mol Cell*. 2003; 12(3):783-790.

46. Xu L, Wei Y, Reboul J, Vaglio P, Shin TH, Vidal M, Elledge SJ, Harper JW. BTB proteins are substrate-specific adaptors in an SCF-like modular ubiquitin ligase containing CUL-3. *Nature*. 2003; 425(6955):316-321.

47. Genschik P, Sumara I, Lechner E. The emerging family of CULLIN3-RING ubiquitin ligases (CRL3s): cellular functions and disease implications. *Embo J*. 2013; 32(17):2307-2320.

48. Pae J, Cinalli RM, Marzio A, Pagano M, Lehmann R. GCL and CUL3 Control the Switch between Cell Lineages by Mediating Localized Degradation of an RTK. *Dev Cell*. 2017; 42(2):130-142 e137.

49. Pintard L, Willems A, Peter M. Cullin-based ubiquitin ligases: Cul3-BTB complexes join the family. *Embo J*. 2004; 23(8):1681-1687.

50. Chen HY, Chen RH. Cullin 3 Ubiquitin Ligases in Cancer Biology: Functions and Therapeutic Implications. *Front Oncol*. 2016; 6:113.

51. Collins T, Stone JR, Williams AJ. All in the family: the BTB/POZ, KRAB, and SCAN domains. *Mol Cell Biol*. 2001; 21(11):3609-3615.

52. Wong CW, Privalsky ML. Components of the SMRT corepressor complex exhibit distinctive interactions with the POZ domain oncoproteins PLZF, PLZF-RARalpha, and BCL-6. *J Biol Chem*. 1998; 273(42):27695-27702.

53. Ghobrial IM. Myeloma as a model for the process of metastasis: implications for therapy. *Blood*. 2012; 120(1):20-30.

54. Kyle RA, Larson DR, Therneau TM, Dispenzieri A, Kumar S, Cerhan JR, Rajkumar SV. Long-Term Follow-up of Monoclonal Gammopathy of Undetermined Significance. *N Engl J Med*. 2018; 378(3):241-249.

55. Kumar S, Rajkumar SV, Kyle RA, Lacy MQ, Dispenzieri A, Fonseca R, Lust JA, Gertz MA, Greipp PR, Witzig TE. Prognostic value of circulating plasma cells in monoclonal gammopathy of undetermined significance. *J Clin Oncol*. 2005; 23(24):5668-5674.

56. Bianchi G, Kyle RA, Larson DR, Witzig TE, Kumar S, Dispenzieri A, Morice WG, Rajkumar SV. High levels of peripheral blood circulating plasma cells as a specific risk factor for progression of smoldering multiple myeloma. *Leukemia*. 2013; 27(3):680-685.

57. Dingli D, Nowakowski GS, Dispenzieri A, Lacy MQ, Hayman SR, Rajkumar SV, Greipp PR, Litzow MR, Gastineau DA, Witzig TE *et al*. Flow cytometric detection of circulating myeloma cells before transplantation in patients with multiple myeloma: a simple risk stratification system. *Blood*. 2006; 107(8):3384-3388.

58. Nowakowski GS, Witzig TE, Dingli D, Tracz MJ, Gertz MA, Lacy MQ, Lust JA, Dispenzieri A, Greipp PR, Kyle RA *et al*. Circulating plasma cells detected by flow cytometry as a predictor of survival in 302 patients with newly diagnosed multiple myeloma. *Blood*. 2005; 106(7):2276-2279.

59. Witzig TE, Gertz MA, Lust JA, Kyle RA, O'Fallon WM, Greipp PR. Peripheral blood monoclonal plasma cells as a predictor of survival in patients with multiple myeloma. *Blood*. 1996; 88(5):1780-1787.

60. Vagnoni D, Travaglini F, Pezzoni V, Ruggieri M, Bigazzi C, Dalsass A, Mestichelli F, Troiani E, Falcioni S, Mazzotta S *et al*. Circulating plasma cells in newly diagnosed symptomatic multiple myeloma as a possible prognostic marker for patients with standard-risk cytogenetics. *Br J Haematol*. 2015; 170(4):523-531.

61. Gonsalves WI, Rajkumar SV, Gupta V, Morice WG, Timm MM, Singh PP, Dispenzieri A, Buadi FK, Lacy MQ, Kapoor P *et al*. Quantification of clonal circulating plasma cells in newly diagnosed multiple myeloma: implications for redefining high-risk myeloma. *Leukemia*. 2014; 28(10):2060-2065.

62. Gonsalves WI, Morice WG, Rajkumar V, Gupta V, Timm MM, Dispenzieri A, Buadi FK, Lacy MQ, Singh PP, Kapoor P *et al*. Quantification of clonal circulating plasma cells in relapsed multiple myeloma. *Br J Haematol*. 2014; 167(4):500-505.

63. Muz B, Azab F, de la Puente P, Rollins S, Alvarez R, Kawar Z, Azab AK. Inhibition of P-Selectin and PSGL-1 Using Humanized Monoclonal Antibodies Increases the Sensitivity of Multiple Myeloma Cells to Bortezomib. *Biomed Res Int*. 2015; 2015:417586.

64. Asosingh K, Gunthert U, De Raeve H, Van Riet I, Van Camp B, Vanderkerken K. A unique pathway in the homing of murine multiple myeloma cells: CD44v10 mediates binding to bone marrow endothelium. *Cancer Res*. 2001; 61(7):2862-2865.

65. Mrozik KM, Cheong CM, Hewett D, Chow AW, Blaschuk OW, Zannettino AC, Vandyke K. Therapeutic targeting of N-cadherin is an effective treatment for multiple myeloma. *Br J Haematol*. 2015; 171(3):387-399.

66. Strilic B, Offermanns S. Intravascular Survival and Extravasation of Tumor Cells. *Cancer Cell*. 2017; 32(3):282-293.

67. Valastyan S, Weinberg RA. Tumor metastasis: molecular insights and evolving paradigms. *Cell*. 2011; 147(2):275-292.

68. Hewett DR, Vandyke K, Lawrence DM, Friend N, Noll JE, Geoghegan JM, Croucher PI, Zannettino ACW. DNA Barcoding Reveals Habitual Clonal Dominance of Myeloma Plasma Cells in the Bone Marrow Microenvironment. *Neoplasia*. 2017; 19(12):972-981.

69. Noll JE, Williams SA, Purton LE, Zannettino AC. Tug of war in the haematopoietic stem cell niche: do myeloma plasma cells compete for the HSC niche? *Blood Cancer J*. 2012; 2:e91.

70. Katz BZ. Adhesion molecules--The lifelines of multiple myeloma cells. *Seminars in cancer biology*. 2010; 20(3):186-195.

71. Hideshima T, Mitsiades C, Tonon G, Richardson PG, Anderson KC. Understanding multiple myeloma pathogenesis in the bone marrow to identify new therapeutic targets. *Nat Rev Cancer*. 2007; 7(8):585-598.

72. Mitsiades CS, Mitsiades NS, Munshi NC, Richardson PG, Anderson KC. The role of the bone microenvironment in the pathophysiology and therapeutic management of multiple myeloma: interplay of growth factors, their receptors and stromal interactions. *Eur J Cancer*. 2006; 42(11):1564-1573.

73. Reymond N, d'Agua BB, Ridley AJ. Crossing the endothelial barrier during metastasis. *Nat Rev Cancer*. 2013; 13(12):858-870.

74. Custodio-Santos T, Videira M, Brito MA. Brain metastasization of breast cancer. *Biochim Biophys Acta*. 2017; 1868(1):132-147.

75. Popper HH. Progression and metastasis of lung cancer. *Cancer Metastasis Rev*. 2016; 35(1):75-91.

76. Laubli H, Borsig L. Selectins promote tumor metastasis. *Seminars in cancer biology*. 2010; 20(3):169-177.

77. Hazan RB, Phillips GR, Qiao RF, Norton L, Aaronson SA. Exogenous expression of N-cadherin in breast cancer cells induces cell migration, invasion, and metastasis. *J Cell Biol*. 2000; 148(4):779-790.

78. Li G, Satyamoorthy K, Herlyn M. N-cadherin-mediated intercellular interactions promote survival and migration of melanoma cells. *Cancer Res*. 2001; 61(9):3819-3825.

79. Qi J, Chen N, Wang J, Siu CH. Transendothelial migration of melanoma cells involves N-cadherin-mediated adhesion and activation of the beta-catenin signaling pathway. *Mol Biol Cell*. 2005; 16(9):4386-4397.

80. Na YR, Lee JS, Lee SJ, Seok SH. Interleukin-6-induced Twist and N-cadherin enhance melanoma cell metastasis. *Melanoma Res*. 2013; 23(6):434-443.

81. Dewhirst MW, Secomb TW. Transport of drugs from blood vessels to tumour tissue. *Nat Rev Cancer*. 2017; 17(12):738-750.

82. Siemann DW. The unique characteristics of tumor vasculature and preclinical evidence for its selective disruption by Tumor-Vascular Disrupting Agents. *Cancer treatment reviews*. 2011; 37(1):63-74.

83. Ribatti D, Nico B, Crivellato E, Vacca A. The structure of the vascular network of tumors. *Cancer Lett*. 2007; 248(1):18-23.

84. Siemann DW, Horsman MR. Modulation of the tumor vasculature and oxygenation to improve therapy. *Pharmacol Ther*. 2015; 153:107-124.

85. Jain RK. Normalizing tumor microenvironment to treat cancer: bench to bedside to biomarkers. *J Clin Oncol*. 2013; 31(17):2205-2218.

86. Fang J, Nakamura H, Maeda H. The EPR effect: Unique features of tumor blood vessels for drug delivery, factors involved, and limitations and augmentation of the effect. *Adv Drug Deliv Rev*. 2011; 63(3):136-151.

87. Maeda H. Tumor-selective delivery of macromolecular drugs via the EPR effect: background and future prospects. *Bioconjug Chem*. 2010; 21(5):797-802.

88. Seki T, Fang J, Maeda H. Enhanced delivery of macromolecular antitumor drugs to tumors by nitroglycerin application. *Cancer Sci*. 2009; 100(12):2426-2430.

89. Li CJ, Miyamoto Y, Kojima Y, Maeda H. Augmentation of tumour delivery of macromolecular drugs with reduced bone marrow delivery by elevating blood pressure. *Br J Cancer*. 1993; 67(5):975-980.

90. Kinoshita R, Ishima Y, Chuang VTG, Nakamura H, Fang J, Watanabe H, Shimizu T, Okuhira K, Ishida T, Maeda H *et al*. Improved anticancer effects of albumin-bound paclitaxel nanoparticle via augmentation of EPR effect and albumin-protein interactions using S-nitrosated human serum albumin dimer. *Biomaterials*. 2017; 140:162-169.

91. Satterlee AB, Rojas JD, Dayton PA, Huang L. Enhancing Nanoparticle Accumulation and Retention in Desmoplastic Tumors via Vascular Disruption for Internal Radiation Therapy. *Theranostics*. 2017; 7(2):253-269.

92. Blocker SJ, Douglas KA, Polin LA, Lee H, Hendriks BS, Lalo E, Chen W, Shields AF. Liposomal (64)Cu-PET Imaging of Anti-VEGF Drug Effects on Liposomal Delivery to Colon Cancer Xenografts. *Theranostics*. 2017; 7(17):4229-4239.

93. Berke S, Kampmann AL, Wuest M, Bailey JJ, Glowacki B, Wuest F, Jurkschat K, Weberskirch R, Schirrmacher R. (18)F-Radiolabeling and In Vivo Analysis of SiFA-Derivatized Polymeric Core-Shell Nanoparticles. *Bioconjug Chem*. 2018; 29(1):89-95.

94. https://www.accessdata.fda.gov/drugsatfda_docs/label/2010/103705s5311lbl.pdf

95. https://www.janssenmd.com/pdf/darzalex/darzalex_pi.pdf

96. https://www.accessdata.fda.gov/drugsatfda_docs/label/2015/761035s000lbl.pdf

97.https://www.pharma.us.novartis.com/sites/www.pharma.us.novartis.com/files/gleevec_tabs.pdf

98. https://www.accessdata.fda.gov/drugsatfda_docs/label/2007/022068lbl.pdf

99. www.velcade.com/files/pdfs/velcade_prescribing_information.pdf

100. https://pi.amgen.com/~/media/amgen/repositorysites/pi-amgen-com/kyprolis/kyprolis_pi.pdf

101. https://www.accessdata.fda.gov/drugsatfda_docs/label/2016/207155s000lbl.pdf

102. Maeda H, Bharate GY, Daruwalla J. Polymeric drugs for efficient tumor-targeted drug delivery based on EPR-effect. *Eur J Pharm Biopharm*. 2009; 71(3):409-419.

103. Ishima Y, Chen D, Fang J, Maeda H, Minomo A, Kragh-Hansen U, Kai T, Maruyama T, Otagiri M. S-Nitrosated human serum albumin dimer is not only a novel anti-tumor drug but also a potentiator for anti-tumor drugs with augmented EPR effects. *Bioconjug Chem*. 2012; 23(2):264-271.

104. Turley RS, Tokuhisa Y, Toshimitsu H, Lidsky ME, Padussis JC, Fontanella A, Deng W, Augustine CK, Beasley GM, Davies MA *et al*. Targeting N-cadherin increases vascular permeability and differentially activates AKT in melanoma. *Ann Surg*. 2015; 261(2):368-377.

105. Gour BJ, Blaschuk OW, Ali A, Ni F, Chen Z, Michaud SD, Wang S, Hu Z. Peptidomimetic modulators of cell adhesion. In. United States: Adherex Technologies, Inc.; 2008.

106. Scognamiglio PL, Morelli G, Marasco D. Synthetic and structural routes for the rational conversion of peptides into small molecules. *Methods Mol Biol*. 2015; 1268:159-193.

107. Vagner J, Qu H, Hruby VJ. Peptidomimetics, a synthetic tool of drug discovery. *Curr Opin Chem Biol*. 2008; 12(3):292-296.

108. Gerhardt H, Wolburg H, Redies C. N-cadherin mediates pericytic-endothelial interaction during brain angiogenesis in the chicken. *Dev Dyn*. 2000; 218(3):472-479.

109. Paik JH, Skoura A, Chae SS, Cowan AE, Han DK, Proia RL, Hla T. Sphingosine 1-phosphate receptor regulation of N-cadherin mediates vascular stabilization. *Genes Dev*. 2004; 18(19):2392-2403.

110. Tillet E, Vittet D, Feraud O, Moore R, Kemler R, Huber P. N-cadherin deficiency impairs pericyte recruitment, and not endothelial differentiation or sprouting, in embryonic stem cell-derived angiogenesis. *Exp Cell Res*. 2005; 310(2):392-400.

111. Alimperti S, Mirabella T, Bajaj V, Polacheck W, Pirone DM, Duffield J, Eyckmans J, Assoian RK, Chen CS. Three-dimensional biomimetic vascular model reveals a RhoA, Rac1, and N-cadherin balance in mural cell-endothelial cell-regulated barrier function. *Proc Natl Acad Sci U S A*. 2017; 114(33):8758-8763.

112. Kanthou C, Tozer GM. Tumour targeting by microtubule-depolymerizing vascular disrupting agents. *Expert Opin Ther Targets*. 2007; 11(11):1443-1457.

113. Bayless KJ, Davis GE. Microtubule depolymerization rapidly collapses capillary tube networks in vitro and angiogenic vessels in vivo through the small GTPase Rho. *J Biol Chem*. 2004; 279(12):11686-11695.

114. Alexander JS, Blaschuk OW, Haselton FR. An N-cadherin-like protein contributes to solute barrier maintenance in cultured endothelium. *J Cell Physiol*. 1993; 156(3):610-618.

115. Lum H, Malik AB. Mechanisms of increased endothelial permeability. *Can J Physiol Pharmacol*. 1996; 74(7):787-800.

116. Budworth RA, Anderson M, Clothier RH, Leach L. Histamine-induced Changes in the Actin Cytoskeleton of the Human Microvascular Endothelial Cell line HMEC-1. *Toxicol In Vitro*. 1999; 13(4-5):789-795.

117. van Nieuw Amerongen GP, Natarajan K, Yin G, Hoefen RJ, Osawa M, Haendeler J, Ridley AJ, Fujiwara K, van Hinsbergh VW, Berk BC. GIT1 mediates thrombin signaling in endothelial cells: role in turnover of RhoA-type focal adhesions. *Circ Res*. 2004; 94(8):1041-1049.

118. Bodet L, Gomez-Bougie P, Touzeau C, Dousset C, Descamps G, Maiga S, Avet-Loiseau H, Bataille R, Moreau P, Le Gouill S *et al*. ABT-737 is highly effective against molecular subgroups of multiple myeloma. *Blood*. 2011; 118(14):3901-3910.

119. Punnoose EA, Leverson JD, Peale F, Boghaert ER, Belmont LD, Tan N, Young A, Mitten M, Ingalla E, Darbonne WC *et al*. Expression Profile of BCL-2, BCL-XL, and MCL-1 Predicts Pharmacological Response to the BCL-2 Selective Antagonist Venetoclax in Multiple Myeloma Models. *Molecular cancer therapeutics*. 2016; 15(5):1132-1144.

120. Touzeau C, Ryan J, Guerriero J, Moreau P, Chonghaile TN, Le Gouill S, Richardson P, Anderson K, Amiot M, Letai A. BH3 profiling identifies heterogeneous dependency on Bcl-2 family members in multiple myeloma and predicts sensitivity to BH3 mimetics. *Leukemia*. 2016; 30(3):761-764.

121. Gong JN, Khong T, Segal D, Yao Y, Riffkin CD, Garnier JM, Khaw SL, Lessene G, Spencer A, Herold MJ *et al*. Hierarchy for targeting prosurvival BCL2 family proteins in multiple myeloma: pivotal role of MCL1. *Blood*. 2016; 128(14):1834-1844.

122. Tran NL, Adams DG, Vaillancourt RR, Heimark RL. Signal transduction from N-cadherin increases Bcl-2. Regulation of the phosphatidylinositol 3-kinase/Akt pathway by homophilic adhesion and actin cytoskeletal organization. *J Biol Chem*. 2002; 277(36):32905-32914.

123. Yamauchi M, Yoshino I, Yamaguchi R, Shimamura T, Nagasaki M, Imoto S, Niida A, Koizumi F, Kohno T, Yokota J *et al*. N-cadherin expression is a potential survival mechanism of gefitinib-resistant lung cancer cells. *Am J Cancer Res*. 2011; 1(7):823-833.

124. Moreau P, Chanan-Khan A, Roberts AW, Agarwal AB, Facon T, Kumar S, Touzeau C, Punnoose EA, Cordero J, Munasinghe W *et al*. Promising efficacy and acceptable safety of venetoclax plus bortezomib and dexamethasone in relapsed/refractory MM. *Blood*. 2017; 130(22):2392-2400.

125. Ge R, Wang Z, Wu S, Zhuo Y, Otsetov AG, Cai C, Zhong W, Wu CL, Olumi AF. Metformin represses cancer cells via alternate pathways in N-cadherin expressing vs. N-cadherin deficient cells. *Oncotarget*. 2015; 6(30):28973-28987.

126. Zhang B, Li M, McDonald T, Holyoake TL, Moon RT, Campana D, Shultz L, Bhatia R. Microenvironmental protection of CML stem and progenitor cells from tyrosine kinase inhibitors through N-cadherin and Wnt-beta-catenin signaling. *Blood*. 2013; 121(10):1824-1838.

127. Eiring AM, Khorashad JS, Anderson DJ, Yu F, Redwine HM, Mason CC, Reynolds KR, Clair PM, Gantz KC, Zhang TY *et al*. beta-Catenin is required for intrinsic but not extrinsic BCR-ABL1 kinase-independent resistance to tyrosine kinase inhibitors in chronic myeloid leukemia. *Leukemia*. 2015; 29(12):2328-2337.

128. Paiva B, Cedena MT, Puig N, Arana P, Vidriales MB, Cordon L, Flores-Montero J, Gutierrez NC, Martin-Ramos ML, Martinez-Lopez J *et al*. Minimal residual disease monitoring and immune profiling in multiple myeloma in elderly patients. *Blood*. 2016; 127(25):3165-3174.

129. Lahuerta JJ, Paiva B, Vidriales MB, Cordon L, Cedena MT, Puig N, Martinez-Lopez J, Rosinol L, Gutierrez NC, Martin-Ramos ML *et al*. Depth of Response in Multiple Myeloma: A Pooled Analysis of Three PETHEMA/GEM Clinical Trials. *J Clin Oncol*. 2017; 35(25):2900-2910.

130. Munshi NC, Avet-Loiseau H, Rawstron AC, Owen RG, Child JA, Thakurta A, Sherrington P, Samur MK, Georgieva A, Anderson KC *et al*. Association of Minimal Residual Disease With Superior Survival Outcomes in Patients With Multiple Myeloma: A Meta-analysis. *JAMA Oncol*. 2017; 3(1):28-35.

131. Rawstron AC, Gregory WM, de Tute RM, Davies FE, Bell SE, Drayson MT, Cook G, Jackson GH, Morgan GJ, Child JA *et al*. Minimal residual disease in myeloma by flow cytometry: independent prediction of survival benefit per log reduction. *Blood*. 2015; 125(12):1932-1935.

132. Martinez-Lopez J, Lahuerta JJ, Pepin F, Gonzalez M, Barrio S, Ayala R, Puig N, Montalban MA, Paiva B, Weng L *et al*. Prognostic value of deep sequencing method for minimal residual disease detection in multiple myeloma. *Blood*. 2014; 123(20):3073-3079.

133. https://www.thebalance.com/top-cancer-drugs-2663234

134. Kumar SK, Dispenzieri A, Fraser R, Mingwei F, Akpek G, Cornell R, Kharfan-Dabaja M, Freytes C, Hashmi S, Hildebrand G *et al*. Early relapse after autologous hematopoietic cell transplantation remains a poor prognostic factor in multiple myeloma but outcomes have improved over time. *Leukemia*. 2017; doi: 10.1038/leu.2017.331. [Epub ahead of print]:1-10.

135. Majithia N, Rajkumar SV, Lacy MQ, Buadi FK, Dispenzieri A, Gertz MA, Hayman SR, Dingli D, Kapoor P, Hwa L *et al*. Early relapse following initial therapy

for multiple myeloma predicts poor outcomes in the era of novel agents. *Leukemia*. 2016; 30(11):2208-2213.

136. Ong SY, de Mel S, Chen YX, Ooi MG, Surendran S, Lin A, Koh LP, Linn YC, Ho AY, Hwang WY *et al*. Early relapse post autologous transplant is a stronger predictor of survival compared with pretreatment patient factors in the novel agent era: analysis of the Singapore Multiple Myeloma Working Group. *Bone Marrow Transplant*. 2016; 51(7):933-937.

137. Jimenez-Zepeda VH, Reece DE, Trudel S, Chen C, Tiedemann R, Kukreti V. Early relapse after single auto-SCT for multiple myeloma is a major predictor of survival in the era of novel agents. *Bone Marrow Transplant*. 2015; 50(2):204-208.